

**Vulnerability Assessment of Modern Power Systems
Voltage Stability and System Strength Perspectives**

Boricic, Aleksandar

DOI

[10.4233/uuid:41f3b03d-12c6-4000-b668-b764f0146d4a](https://doi.org/10.4233/uuid:41f3b03d-12c6-4000-b668-b764f0146d4a)

Publication date

2024

Document Version

Final published version

Citation (APA)

Boricic, A. (2024). *Vulnerability Assessment of Modern Power Systems: Voltage Stability and System Strength Perspectives*. [Dissertation (TU Delft), Delft University of Technology].
<https://doi.org/10.4233/uuid:41f3b03d-12c6-4000-b668-b764f0146d4a>

Important note

To cite this publication, please use the final published version (if applicable).
Please check the document version above.

Copyright

Other than for strictly personal use, it is not permitted to download, forward or distribute the text or part of it, without the consent of the author(s) and/or copyright holder(s), unless the work is under an open content license such as Creative Commons.

Takedown policy

Please contact us and provide details if you believe this document breaches copyrights.
We will remove access to the work immediately and investigate your claim.

VULNERABILITY ASSESSMENT OF MODERN POWER SYSTEMS

VOLTAGE STABILITY AND SYSTEM STRENGTH PERSPECTIVES

VULNERABILITY ASSESSMENT OF MODERN POWER SYSTEMS

VOLTAGE STABILITY AND SYSTEM STRENGTH PERSPECTIVES

Dissertation

for the purpose of obtaining the degree of doctor
at Delft University of Technology
by the authority of the Rector Magnificus, prof. dr. ir. T.H.J.J. van der Hagen,
chair of the Board for Doctorates
to be defended publicly on
Tuesday 30 April 2024 at 15:00 o'clock

by

Aleksandar BORIČIĆ

Master of Science in Electric Power Systems Engineering,
Eindhoven University of Technology, Eindhoven, the Netherlands
Master of Science in Technology,
KTH Royal Institute of Technology, Stockholm, Sweden
born in Podgorica, Montenegro

This dissertation has been approved by the promotor.

Composition of the doctoral committee:

Rector Magnificus

Chairperson

Prof. dr. ir. M. Popov

Delft University of Technology, *promotor*

em. Prof. ir. M. van der Meijden

Delft University of Technology, *promotor*

Independent members:

Prof. dr. D. Westermann

Ilmenau University of Technology, Germany

Prof. dr. M. Paolone

Swiss Federal Institute of Technology Lausanne

Prof. dr. V. Terzija

Newcastle University, England

Prof. dr. P. Palensky

Delft University of Technology

Ir. D. Klaar

TenneT TSO B.V., the Netherlands

Prof. dr. A. Smets

Delft University of Technology, reserve member

This research project was supported by a large consortium consisting of TenneT TSO, Alliander DSO, Stedin DSO, General Electric, Dutch National Metrology Institute (VSL), and The Dutch Research Council (NWO).



Keywords: Energy transition, power systems, vulnerability, system strength, weak grids, voltage stability, short-term stability, oscillations, PMUs

Printed by: ProefschriftMaken

Cover by: Aleksandar Boričić / GPT-4

Copyright © 2024 by A. Boričić

ISBN 978-94-6384-572-4

An electronic copy of this dissertation is available at
<https://repository.tudelft.nl/>.

Neka budućnost kaže istinu i procijeni svakoga u skladu s njegovim radom i zaslugama. Sadašnjost je njihova; a budućnost, za koju sam zaista radio, je moja.

Let the future tell the truth and evaluate each one according to his work and accomplishments. The present is theirs; the future, for which I really worked, is mine.

- **Nikola Tesla**, Electrical Engineer, Innovator, Futurist
(10/07/1856 - 07/01/1943)

CONTENTS

Summary	ix
Samenvatting	xi
1. Introduction	3
1.1. Evolution of Electric Power Systems	3
1.2. Grid Vulnerability and Stability Challenges	9
1.3. Real-Grid Disturbances and Research Gaps	12
1.4. Research Questions	14
1.5. Research Project Structure	14
1.6. Thesis Outline	16
2. Voltage Stability of Modern Power Systems	25
2.1. Power System Stability: Definition and Classification	25
2.2. Voltage Stability: Fundamentals and Trends	28
2.3. Maximum Power Transfer and Voltage Stability	30
2.4. Short-Term Instability: Evaluation Methods	35
2.5. Concluding Remarks	40
3. System Strength and Grid Weakness	45
3.1. System Strength Fundamentals	45
3.1.1. System strength definition	48
3.1.2. System strength classification	49
3.2. Steady-State System Strength	49
3.2.1. Existing evaluation methods	52
3.2.2. Summary of the existing methods and their limitations	56
3.3. Excess System Strength (ESS) method	60
3.4. Dynamic-State System Strength	72
3.5. Concluding Remarks	74
4. Short-Term Stability with DER and Dynamic Loads	81
4.1. Modern Distribution Networks	82
4.2. Impact Analysis on Short-Term Stability	84
4.2.1. Test system description	84
4.2.2. Methodology	88
4.3. Results and Discussion	90
4.3.1. Impact of dynamic loads on short-term stability	90
4.3.2. Impact of dynamic loads and DER on short-term stability	94
4.4. Concluding Remarks	99

5. Data-Driven Stability and Strength Evaluation Methods	107
5.1. Data Opportunities in Modern Power Systems	108
5.2. Quantification: Cumulative Voltage Deviation (CVD) Method	110
5.2.1. Methodology	110
5.2.2. Numerical simulations	112
5.3. Short-Term Instability Classification Algorithm	120
5.3.1. Methodology and implementation	121
5.3.2. Classification accuracy	126
5.4. Voltage Vulnerability Curves and Dynamic-state System Strength	127
5.4.1. Short-circuit capacity and voltage deviations	128
5.4.2. VVC methodology	131
5.4.3. Numerical simulations and results	132
5.4.4. VVC with parameter uncertainty	139
5.5. Concluding Remarks	144
6. Conclusions	149
6.1. Scientific Contributions	149
6.2. Practical Recommendations	157
6.3. Future Research Recommendations	160
A. IEEE Test System Description	165
B. DER and Load Models	167
List of Abbreviations	171
List of Publications	173
Acknowledgements	175
Biography	177

SUMMARY

Climate change is one of the most dangerous and simultaneously most complex threats humanity has ever faced. The key response to this threat has been an unprecedented strategic shift in the energy sector, known as the *energy transition*. Electricity powers the modern world and is at the very centre of the energy transition. The shift to sustainable electricity production, transmission, distribution, and consumption is therefore vital. However, such a change brings significant technical challenges that should be addressed. The objective of this research is to uncover and investigate some of the key challenges in this regard and propose solutions for their mitigation.

This thesis largely focuses on two technical aspects and related challenges: power system vulnerability and stability. The emphasis lies on *modern power systems*, where conventional synchronous generation is increasingly replaced by inverter-based resources (IBRs). The first research objective is to improve the understanding of both system vulnerability and stability, particularly in the context of voltage stability and system strength and their intricate relationship. Relying on this improved understanding, the second objective is to develop advanced and novel evaluation methods and algorithms.

The main contributions of the thesis can be grouped into three themes.

Firstly, the comprehensive fundamental analysis of both theoretical and numerical nature uncovers the increasing importance of voltage stability and system strength as the main grid vulnerability aspects. While conventional power systems have a dominant electromechanical dimension, with frequency being the key parameter of interest, modern power systems increasingly rely on IBRs. These resources largely operate in the electromagnetic domain and often require stable voltages and sufficient system strength. This results in a natural degradation of power system stability, where generation typically no longer *provides*, but rather *requires*, system resilience. The implications of this are hereby extensively explored and discussed, proposing a necessary paradigm shift in the way we understand and analyze power system stability and resilience.

Secondly, the thesis critically investigates some of the existing stability and strength evaluation methods from various quantitative and qualitative perspectives. The results indicate that the often-applied methods lose relevance in modern power systems. This occurs as their underlying mathematical equations are typically designed for conventional synchronous-based systems and their physical behaviour, which no longer dictates the dynamics of modern grids. Furthermore, improved definitions and classifications of system stability and strength are proposed. These findings indicate that novel and fundamentally different evaluation methods for voltage stability and system strength need to be developed to accurately analyze evolving power system dynamics.

The third main contribution of the thesis is precisely in this direction. In terms of steady-state voltage stability limits and system strength, a new method termed Effective System Strength (ESS) is developed. The method analytically bridges the two concepts

together, showing high accuracy for system strength evaluation and static voltage stability margins in modern power systems. Furthermore, a novel quantitative method for short-term instability analysis is developed, with Cumulative Voltage Deviation (CVD) as the key dynamic performance parameter of interest. Unlike most methods which result in a binary stability evaluation, this method quantifies the disturbance by its severity, which can be used for probabilistic and risk-based stability and dynamic security analysis. This is particularly important for modern power systems where the uncertainty of dynamic response is rising. In parallel to the quantification, a data-based classification method is proposed to distinguish between various instability mechanisms of interest. Lastly, the quantification approach is expanded further to Voltage Vulnerability Curves (VVC), a data-driven method for uncovering not only steady-state system strength aspects but also dynamic vulnerability in the light of faster and more intricate IBR and demand dynamic responses.

The developed methods form a basis for advanced voltage stability and system strength evaluation of modern power systems. Such an evaluation can play an important role in the overall stability and dynamic security assessment performed by power system operators, with the goal of cutting through the complexity of numerous possible contingencies and operating scenarios. The evaluation automatically identifies the most vulnerable weak grid sections and dangerous operating scenarios that may lead to cascading faults and possible instability. Consequently, once such grid sections and scenarios are observed, more detailed simulations and analyses can be performed by power system stability experts in a much more time-efficient and targeted manner. Subsequently, proactive mitigation measures can be taken to avoid the risk of instability and blackouts.

The thesis concludes with a summary of the main scientific findings. Additionally, several practical recommendations for the analysis and operation of modern power systems are provided. As more technical challenges remain that are out of the scope of this research, further research directions are proposed.

SAMENVATTING

Klimaatverandering is een van de gevaarlijkste en tegelijkertijd meest complexe bedreigingen waar de mensheid ooit mee te maken heeft gehad. De belangrijkste reactie op deze bedreiging is een ongekende strategische verschuiving in de energiesector, bekend als de energietransitie. Elektriciteit voorziet de moderne wereld van energie en staat centraal in de energietransitie. De verschuiving naar duurzame productie, transmissie, distributie en consumptie van elektriciteit is daarom van vitaal belang. Dergelijke verandering brengt echter aanzienlijke technische uitdagingen met zich mee die moeten worden aangepakt. Het doel van dit onderzoek is om enkele van de belangrijkste uitdagingen in dit opzicht bloot te leggen, te onderzoeken, en oplossingen voor te stellen om ze te beperken.

Dit proefschrift richt zich voornamelijk op twee technische aspecten en gerelateerde uitdagingen: de kwetsbaarheid en de stabiliteit van het elektriciteitssysteem. De nadruk ligt op moderne elektriciteitssystemen, waar conventionele synchrone opwekking steeds vaker wordt vervangen door invertergebaseerde bronnen (IBRs). De eerste onderzoeksdoelstelling is het verbeteren van het begrip van zowel kwetsbaarheid als stabiliteit van het systeem, met name in de context van spanningsstabiliteit, systeemsterkte en hun gecompliceerde relatie. Op basis van dit verbeterde begrip is de tweede doelstelling het ontwikkelen van nieuwe en geavanceerde evaluatiemethoden en algoritmen.

De belangrijkste bijdragen van dit proefschrift kunnen worden gegroepeerd in drie thema's.

Ten eerste onthult de uitgebreide fundamentele analyse, van zowel theoretische als numerieke aard, het toenemende belang van spanningsstabiliteit en systeemsterkte als de belangrijkste aspecten van netkwetsbaarheid. Terwijl conventionele elektriciteitssystemen een dominante elektromechanische dimensie hebben, waarbij frequentie een van de belangrijkste parameters is, vertrouwen moderne elektriciteitssystemen steeds meer op IBRs. Deze energiebronnen werken grotendeels in het elektromagnetische domein en vereisen vaak stabiele spanning en voldoende systeemsterkte. Dit resulteert in een degradatie van de stabiliteit in het elektriciteitssysteem, waarbij de opwekking niet langer de veerkracht naar het systeem levert, maar deze juist vereist. De implicaties hiervan worden uitgebreid onderzocht en besproken, waarbij een noodzakelijke paradigmaverschuiving wordt voorgesteld in de manier waarop we stabiliteit en veerkracht van elektriciteitssystemen begrijpen en analyseren.

Ten tweede worden enkele van de bestaande stabiliteit en systeemsterkte evaluatiemethoden kritisch onderzocht vanuit verschillende kwantitatieve en kwalitatieve perspectieven. De resultaten geven aan dat de vaak toegepaste methoden hun relevantie verliezen in moderne energiesystemen. Dit komt doordat hun onderliggende wiskundige vergelijkingen vaak ontworpen zijn voor conventionele synchrone systemen en hun natuurkundige gedrag, dat niet langer de dynamiek van moderne systemen domineert.

Verder worden verbeterde definities en classificaties van stabiliteit en systeemsterkte voorgesteld. Deze inzichten geven aan dat er nieuwe en fundamenteel andere evaluatiemethoden voor spanningsstabiliteit en systeemsterkte moeten worden ontwikkeld om de veranderende dynamica van elektriciteitssystemen nauwkeuriger te analyseren.

De derde belangrijke bijdrage van dit proefschrift zijn meerdere nieuwe evaluatiemethoden. Met betrekking tot spanningsstabiliteitsgrenzen en systeemsterkte in stationaire toestand wordt een nieuwe methode ontwikkeld die Effective System Strength (ESS) wordt genoemd. De methode slaat een analytische brug tussen de twee concepten en toont een hoge nauwkeurigheid voor de evaluatie van systeemsterkte en statische spanningsstabiliteitsmarges in moderne elektriciteitssystemen. Verder is er een nieuwe kwantitatieve methode voor de analyse van kortetermijninstabiliteit ontwikkeld, met Cumulative Voltage Deviation (CVD) als belangrijkste dynamische prestatieparameter. In tegenstelling tot de meeste methoden die resulteren in een binaire stabiliteitsbeoordeling, kwantificeert deze methode de verstoring aan de hand van de ernst ervan, wat kan worden gebruikt voor probabilistische en risicogebaseerde stabiliteit en dynamische veiligheidsanalyse. Dit is vooral belangrijk voor moderne elektriciteitssystemen waar de onzekerheid van de dynamische respons toeneemt. Parallel aan de kwantificering wordt een op datagedreven classificatiemethode voorgesteld om onderscheid te maken tussen verschillende instabiliteitsmechanismen. Ten slotte wordt de kwantificeringsaanpak verder uitgebreid tot Voltage Vulnerability Curves (VVC), een datagedreven methode om niet alleen de systeemsterkte aspecten van het stationaire systeem bloot te leggen, maar ook de dynamische kwetsbaarheid door snellere en meer ingewikkelde IBR en vraagdynamische respons.

De ontwikkelde methoden vormen een basis voor geavanceerde evaluatie van de spanningsstabiliteit en systeemsterkte van moderne elektriciteitssystemen. Een dergelijke evaluatie kan een belangrijke rol spelen in de algehele beoordeling van de stabiliteit en dynamische veiligheid die door netbeheerders wordt uitgevoerd, met als doel de complexiteit van talloze mogelijke onvoorziene gebeurtenissen en bedrijfsscenario's te verminderen. De evaluatie identificeert automatisch de meest kwetsbare netwerksecties en gevaarlijke bedrijfsscenario's die kunnen leiden tot opeenvolgende storingen en mogelijke instabiliteit. Zodra dergelijke netwerksecties en scenario's zijn waargenomen, kunnen experts op het gebied van stabiliteit van het elektriciteitssysteem op een veel tijds-efficiëntere en gerichtere manier gedetailleerdere simulaties en analyses uitvoeren. Vervolgens kunnen proactieve maatregelen worden genomen om het risico op instabiliteit en blackouts te voorkomen.

Het proefschrift eindigt met een beschrijving van de belangrijkste wetenschappelijke bevindingen van dit onderzoek. Daarnaast worden verschillende praktische aanbevelingen gegeven voor het analyseren en de bedrijfsvoering van moderne elektriciteitssystemen. Aangezien er verdere technische uitdagingen zijn die niet binnen de omvang van dit onderzoek vallen, worden mogelijke onderzoeksrichtingen voorgesteld.

1

INTRODUCTION

The only constant in life is change.

- Heraclitus, Ancient Greek Philosopher, 5th century B.C.

1.1. EVOLUTION OF ELECTRIC POWER SYSTEMS

THE history of electric power systems dates back to the late 19th century. What started as short-distance electrification of street lighting has evolved into thousands of kilometres of meshed grids bringing electricity from power plants to the end consumers seamlessly. This technological advance concurred with the explosive growth in population size and welfare, as access to electricity broadened.

The century-long evolution of power systems had two primary goals: to provide *secure* and *affordable* supply of electricity. In the ever-growing demand for electricity in society, the economy dictated that abundant and cheap sources were to prevail as dominant ones. Hydropower potential quickly reached its natural limits, while nuclear power faces societal opposition due to its perceived risks. Therefore, power systems turned to a seemingly unlimited energy source - *fossil fuels*. Power plants with massive turbines and synchronous generators started forming the core of modern power systems. This provided society with plentiful electricity, system flexibility, and operational robustness. Powered by this cheap and vastly abundant resource with no significant downsides (known at the time), power systems expanded in size following the growing electricity demand. Cross-border interconnections also emerged, leading to what is often referred to as the largest and most complex machines ever built. The resulting systems can be described as conventional electric power systems, defined in this thesis as follows and illustrated in [Figure 1.1](#).

Conventional electric power system is a large network of electrical components designed to provide high-reliability and low-cost electricity supply. Large, often fossil-powered, synchronous generators centralized in power plants provide the supply unidirectionally. The plants tend to be located near partly-electrified residential, commercial, and industrial demand clusters. The static and dynamic characteristics of this demand are relatively simple, well-understood, and predictable.

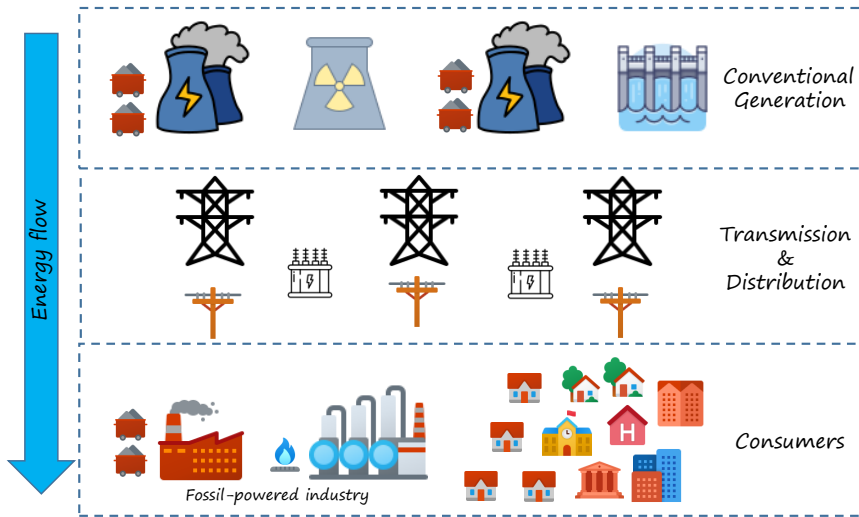
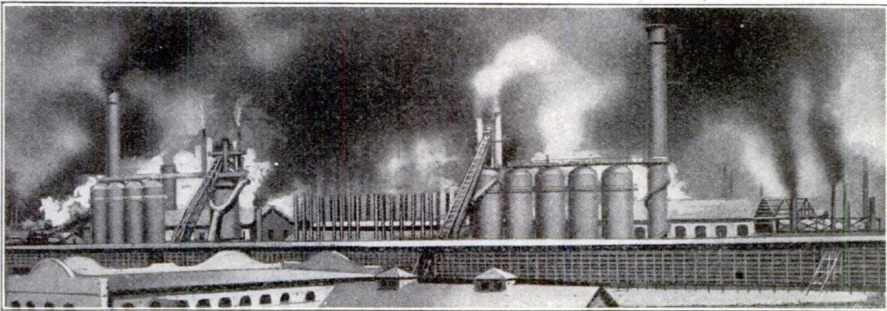


Figure 1.1.: Simple illustration of a conventional power system and its parts.

Science did not take long to discover a significant problem in this trend. Burning fossil fuels results in significant carbon dioxide (CO_2) emissions into the atmosphere, among other polluting gases and particles. As the levels of CO_2 increased in the atmosphere, the average temperature rose, initiating what we refer to today as *climate change*. Many believe we only became aware of this in the last few decades. Contrary to that belief, some scientists warned about the potential consequences more than a century ago, as excerpted¹ in [Figure 1.2.](#)



The furnaces of the world are now burning about 2,000,000,000 tons of coal a year. When this is burned, uniting with oxygen, it adds about 7,000,000,000 tons of carbon dioxide to the atmosphere yearly. This tends to make the air a more effective blanket for the earth and to raise its temperature. The effect may be considerable in a few centuries.

Figure 1.2.: Predictions of climate change due to the burning of coal (1912) [1].

The first traces of climate change awareness date back to even before 1912, to at

¹In hindsight, "...a few centuries" turned out to be a severe understatement of our polluting capacity.

least the 1896 article published by a Swedish scientist and one of the first Nobel laureates in Chemistry, Svante Arrhenius [2].

If the quantity of carbonic acid increases in geometric progression, the augmentation of the temperature will increase nearly in arithmetic progression.

- Svante Arrhenius, 1896

Even several decades before this article, scientists such as John Tyndall and Eunice Newton Foote² theoreticized and experimented with the impact of CO₂ concentration on the atmospheric temperature [4]. Their work followed up on the hypothesis of the French scientist Joseph Fourier that something in the Earth's atmosphere acts like an insulating blanket [5].

An atmosphere of that gas [CO₂] would give to our earth a high temperature; and if as some suppose, at one period of its history the air had mixed with it a larger proportion than at present, an increased temperature...must have necessarily resulted.

- Eunice Newton Foote, 1856

However, these predictions and observations remained dormant for several decades, particularly in the midst of two world wars where potential climate change concerns were easily overlooked. Nevertheless, in the 1950s, government funding for scientific climate studies became less scarce, resulting in a clear confirmation of what was predicted more than half a century earlier. Mankind was on a path to cause global warming of unprecedented speed and magnitude, with potentially disastrous consequences. Actions became necessary.

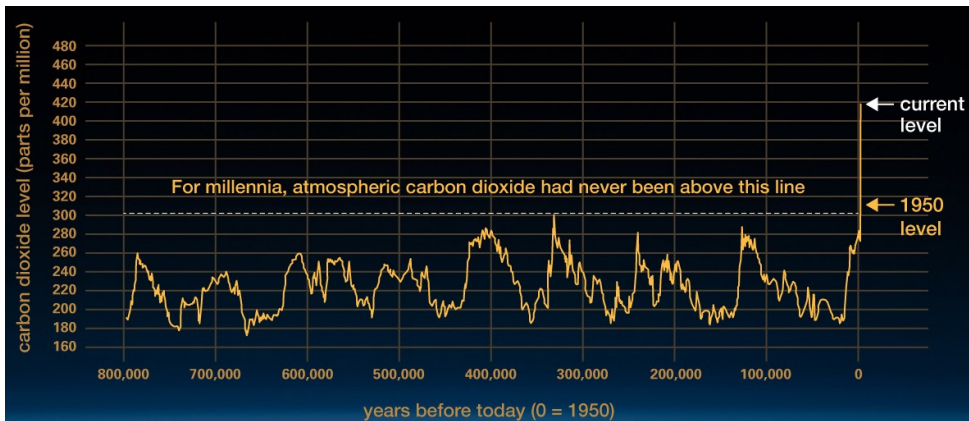


Figure 1.3.: Impact of the Industrial Revolution on the CO₂ level rise based on the NASA comparison of atmospheric samples in ice cores [6].

²Despite her remarkable insights, her work went unnoticed in climate science history until recently [3]. Mid-19th century male-dominated science was unfortunately not always fair to female scientists.

It took several decades, but the continuous growth of dominantly fossil-based power systems has been disrupted. The third goal, besides security and affordability of supply, became increasingly important – *sustainability*. The original dilemma suddenly became a trilemma [7]. This fundamental change that will unprecedentedly reshape power systems is illustrated in Figure 1.4.

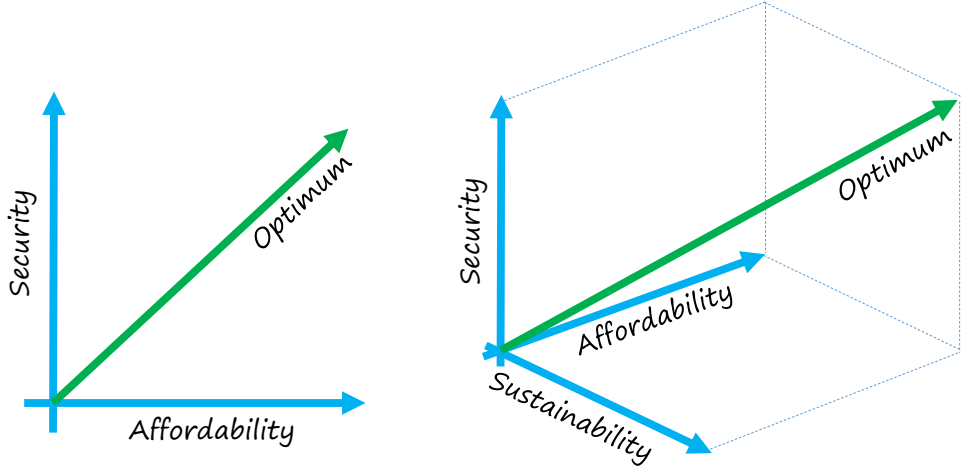


Figure 1.4.: Optimization goal evolution from the electricity supply perspective; Conventional (left) and modern (right) power systems.

As the awareness of climate change grew worldwide³, the electricity sector started to research and develop innovative and more sustainable ways for electricity generation. Many technologies were developed, two of which were the main drivers of the ongoing revolution – *solar* and *wind* energy.

This newly appreciated goal of sustainability did not only affect the electricity supply. Other energy-intensive sectors such as heating, transportation, and industry, also faced the need to rapidly introduce sustainability goals into their physical and financial equations. The result is an unprecedented electrification of demand, accelerating the need for renewable electricity supply further.

The conventional electric power systems have started a transformation that is still ongoing toward what is referred to in this thesis as modern electric power systems. Such systems are illustrated in Figure 1.5, and defined as follows.

Modern electric power system is a large network of electrical components designed to provide a low-cost, reliable, and sustainable electricity supply in a decentralized manner with bidirectional power flows. Generating units are dominantly renewable inverter-based resources scattered across the grid, often far from residential, commercial, and industrial demand clusters. The demand is highly electrified, with a large number of motors and complex inverter-based loads. Green hydrogen, coupled with the grid and renewable electricity supply, partly powers heavier industries.

³Despite remarkably strong fossil industry lobbying [8–10].

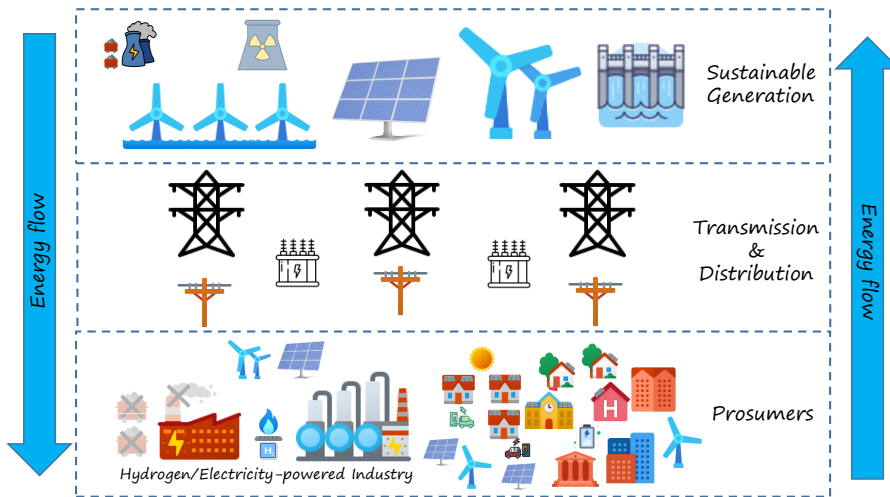


Figure 1.5.: Illustration of a modern power system.

Global emission reduction plans and climate agreements such as the United Nations Framework Convention on Climate Change [11], The Kyoto Protocol [12], and The Paris Agreement [13] established international plans and treaties to combat climate change and limit the mean global temperature rise below 1.5°C by the end of the 21st century⁴. While 1.5°C may not sound like a lot, it is important to understand the sensitivity of the climate to even slight changes in the mean temperature. Even a small long-term temperature increase could initiate the so-called climate tipping points, such as the collapse of ice sheets, loss of the Amazon rainforest, or the disappearance of tropical coral reefs [15]. As a consequence, the process of climate change can quickly become self-sustaining and largely irreversible.

To limit CO_2 emissions and reach the mentioned climate goals, the electricity sector started the rapid shift to a sustainable supply. Modern power systems began to see an unprecedented proliferation of renewable energy sources (RES), especially small and large-scale wind and solar generation. The global growth in renewable energy production is expected to not only continue but to *accelerate* further, as shown in Figure 1.6. As electrification continues, a clean electricity supply is a key pre-condition for achieving a climate-neutral society. Therefore, power systems need to decarbonize much sooner than 2050, with recent plans in G7 countries to reach net zero electricity supply emissions by as early as 2035 [16].

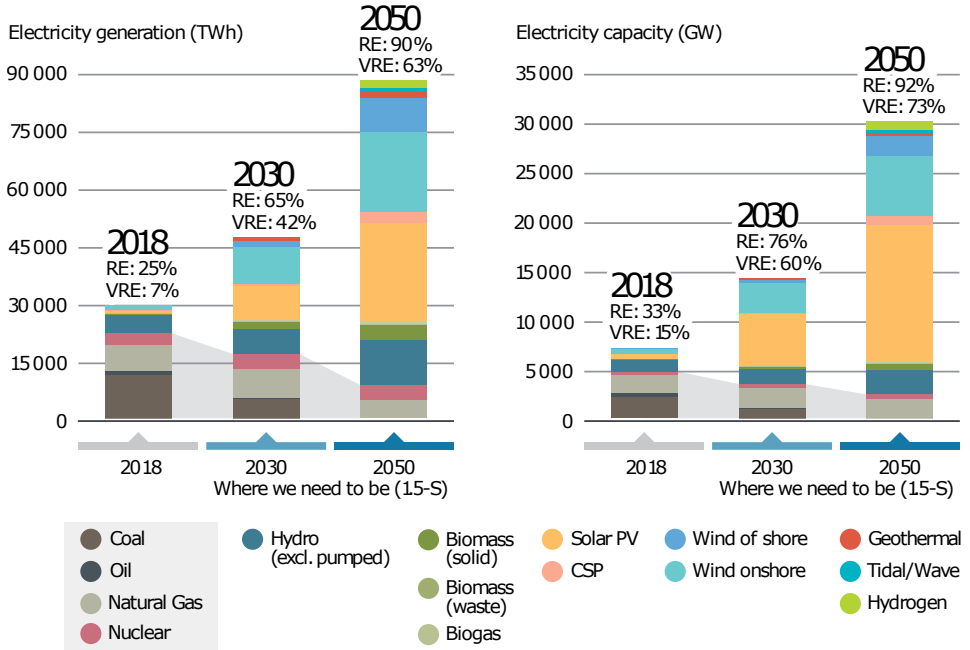
Deployment of renewables has been increasing exponentially, owing to the rising concerns about climate change, energy security, and fossil fuel prices...Over the coming decades, solar PV and wind will dominate the growth of renewables.

- International Renewable Energy Agency (2022) [17]

⁴This goal has in the meantime become increasingly unlikely to be met, with current projections at $2.2\text{--}3.5^{\circ}\text{C}$ by the year 2100 unless the government policies are significantly strengthened [14].

Renewables become the largest source of global electricity generation by early 2025, surpassing coal...Electricity from wind and solar PV more than doubles in the next five years, providing almost 20 percent of global power generation in 2027.

- International Energy Agency (2022) [18]



Note: 1.5-S = 1.5°C Scenario; CSP = concentrated solar power; GW = gigawatts; PV = photovoltaic; RE = renewable energy; TWh/yr = terawatt hours per year; VRE = variable renewable energy.

Figure 1.6.: Global total power generation and the installed capacity of power generation sources in 1.5°C scenario in 2018, 2030 and 2050 [17].

While necessary for the sustainability goal, the described trends lead to an unprecedented evolution in power system development with several key challenges that need to be overcome for a successful energy transition. The main challenges come with the balancing act of optimizing security, affordability, and sustainability (Figure 1.4). Designing and operating a power system that scores high on all three dimensions is an intricate task. While renewable energy sources are convenient in terms of sustainability, fossil-based supply has had a massive technological head start regarding affordability and security of supply.

After a century of fossil-fuel dominance, further enabled by government subsidies, the fossil-based electricity supply became very mature and affordable. However, renewables become less expensive as the technology becomes more mature. In fact, they are already surpassing fossil-based generation on many affordability metrics

[19]. As carbon taxes inevitably become widely present in energy policies, any remaining financial benefits of fossil fuels are expected to vanish quickly and turn negative.

Regarding the security of supply, synchronous generators (SGs), primarily used in fossil-based power plants, are a very mature and optimized technology with a high level of robustness. Meanwhile, renewables are, in comparison, relatively new technologies and largely rely on power electronic equipment for grid integration and operation. This brings many previously unknown technical challenges regarding power system security and resilience. As the penetration of renewables rises, these challenges will likely become a bottleneck in achieving fully sustainable and secure power systems. Therefore, it becomes crucial to better understand and address these technical challenges. A few key ones will be extensively discussed in this thesis.

1.2. GRID VULNERABILITY AND STABILITY CHALLENGES

In contrast to conventional power systems, modern power systems dominantly rely on RES to supply electricity. Besides their variable nature, RES are also integrated into a power system in a fundamentally different manner. This significantly affects the technical foundations of grid vulnerability and power system stability. To understand these differences, illustrated in Figure 1.7, it is necessary to briefly go back to the technical fundamentals of electric power generation.

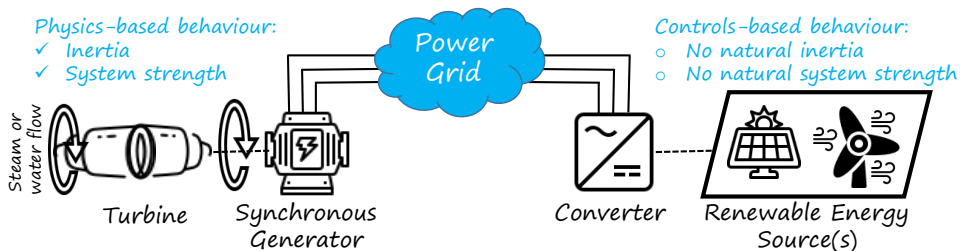


Figure 1.7.: An illustration of some fundamental differences between synchronous and renewable inverter-based generation.

Synchronous generators, illustrated on the left side of Figure 1.7, form the core of conventional power systems. They are massive turbine-powered machines spinning at hundreds to thousands of revolutions per minute. With a carefully designed combination of the right rotation speed and spatially distributed energized copper windings, a great amount of mechanical energy applied by water or steam on the turbine is transformed into electrical energy.

A particularly convenient aspect of such machines is that they naturally oppose disturbances. Two main parameters describe the operation of a synchronous generator and, consequently, a power system as a whole. Those two parameters are the *frequency* and *voltage*. The electricity supply frequency is directly proportional to the rotational speed of the synchronous generators. It is a profound balancing act of the active power supply (generation) and system demand (consumption). If

a disturbance occurs in the system (e.g. a partial loss of the supply or demand), synchronous generators will experience a force that tries to accelerate (or decelerate) their rotors. As that occurs, frequency is increased (or reduced).

Nevertheless, these massive rotating machines comprised of mechanically coupled synchronous generators and turbines are robust and not easily influenced. Instead, the large amount of energy stored in the rotating masses, known as the rotational kinetic energy, is quickly dissipated to counter the external force attempting to change the state of motion. This is known as *inertia* and is a fundamental concept of conventional power systems. We all experience similar inertia, either while riding a bike or simply standing still – objects and bodies tend to stay in their current state or motion and oppose changes. In a similar way, synchronous generators actively help stabilize the system by providing frequency resilience in terms of inertia.

The other aspect of robustness the synchronous generators provide is related to voltage and is a bit more intricate – *system strength*. At a high level, system strength is a generator's natural ability to counter voltage changes. In that sense, it can be thought of as the inertia-like effect of voltage, rather than frequency. This effect, however, has nothing to do with the rotational mass, but is electromagnetic by nature and is related to the opposition to the change of the magnetic flux between the stator and the rotor of a generator. System strength will be discussed much more comprehensively in [Chapter 3](#).

Unlike synchronous machines, RES, depicted on the right side of [Figure 1.7](#), do not have massive rotating machinery with stored kinetic energy, strong electromagnetic coupling to the grid, or the ability to temporarily provide high reactive currents to support the voltage during disturbances. Instead, they are mechanically decoupled from the system and are integrated through converters (i.e., inverters⁵). This means RES, often referred to as *inverter-based resources* (IBRs), interact with a system through fast-operating power electronics components, making their response more control-based than physics-based. Therefore, the behaviour of RES is fundamentally different in both steady-state and (particularly) dynamic-state operations, which reflects on the vulnerability and stability of modern power systems.

The two main topics of this thesis, power system vulnerability and power system stability, are here introduced and defined.

Power system vulnerability is a susceptibility measure of a power system regarding cascading events and potential system collapse. A vulnerable system can be characterized as a low-resilience (robustness) system that experiences relatively high impact from disturbances.

Vulnerability is therefore related to power system security. Still, it goes beyond traditional N-1 (N-2) criteria and deals with the susceptibility to significant disturbances, particularly low-probability high-impact (chain of) events⁶.

In this thesis, two major indicators of system vulnerability in terms of cascading

⁵Inverter is a converter that transforms (inverts) DC signals to AC. The two terms are used interchangeably in this thesis.

⁶Other standard dimensions of power system vulnerability and resilience not discussed explicitly in this thesis are related to cybersecurity, natural disasters, extreme weather events, communication failure, and even sabotage considering the rising geopolitical tensions [20–24].

faults and instability risks are inertia and system strength. As introduced previously, the level of inertia describes a power system's vulnerability to frequency dynamics and related instability. Similarly, system strength tells us how vulnerable the power system is to voltage disturbances and related instabilities. In other words, system strength (inertia) is a quantifiable measure of vulnerability regarding voltage (frequency) behaviour. Inertia and frequency are largely out of the scope of this thesis, whilst system strength and voltage stability will be explored extensively.

When discussing the security of the electricity supply, it is crucial to understand power system stability, which is another essential concept for this research [25].

Power system stability is the ability of an electric power system, for a given initial operating condition, to regain a state of operating equilibrium after being subjected to a physical disturbance, with most system variables bounded so that practically the entire system remains intact.

Power system stability and its evolution from conventional to modern power systems, mainly related to voltage stability and short-term stability, is discussed extensively in [Chapter 2](#).

Besides the discussed challenges addressed in this thesis, modern power systems face many other technical challenges as well [26–29]. Some of the main ones are visualized in [Figure 1.8](#), with the highlighted focus of this thesis defined further.

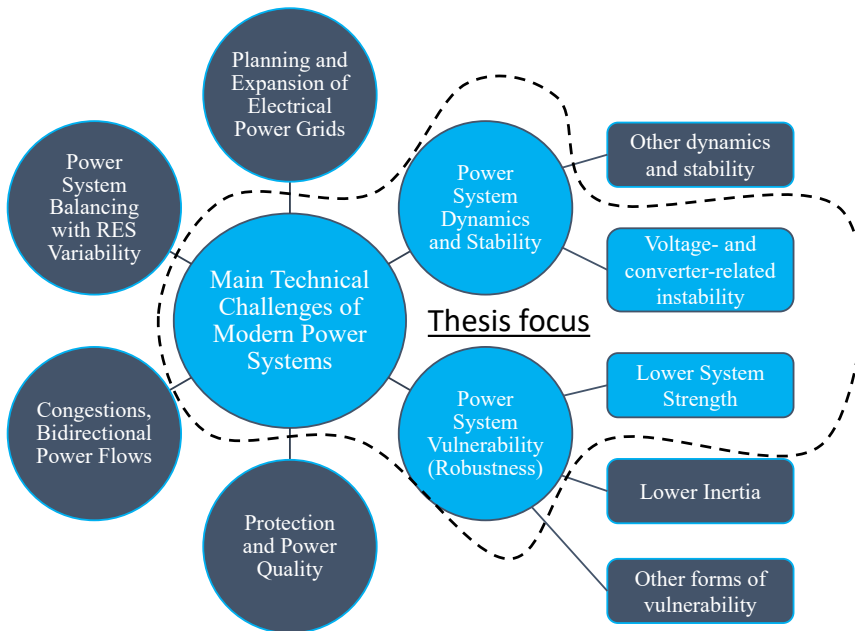


Figure 1.8.: Main technical challenges present and expected in modern power systems, with the highlighted focus of this thesis.

The way the power system evolution, its vulnerability aspects, and its effects

relate to each other within the scope of this thesis is discussed and summarized in [Figure 1.9](#). Power systems evolve as the energy transition progresses and synchronous generation is replaced by inverter-based generation. This introduces novel vulnerability aspects regarding system resilience and increased risks of cascading events. Finally, these vulnerability aspects manifest as various technical effects on power systems and their operation, particularly related to system dynamics and stability. These three associated trends, illustrated with blue arrows in [Figure 1.9](#), are all comprehensively explored and addressed in this thesis.

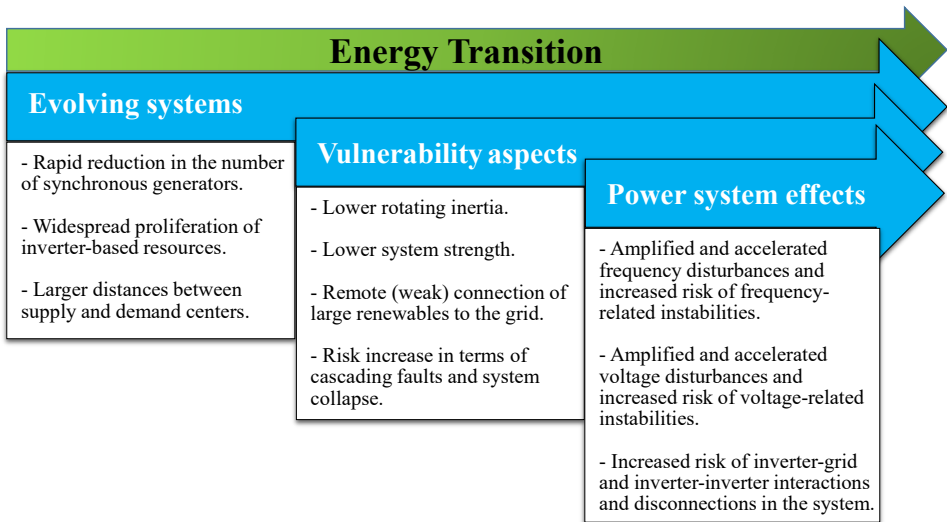


Figure 1.9.: Relation of key concepts relevant for this thesis.

The following section extensively describes how these concepts and changes translate into tangible technical challenges. Furthermore, essential research gaps in this regard are discussed.

1.3. REAL-GRID DISTURBANCES AND RESEARCH GAPS

The extensive proliferation of RES and concurrent decommissioning of fossil-based synchronous generation results in an increased likelihood of severe disturbances in the grid. These structural changes are visible worldwide as the number of cascading faults, oscillations, system separation events, and even blackouts rises. Some of the notable and well-documented examples specifically relevant to modern power system challenges discussed in the scope of this thesis are listed in [Table 1.1](#).

What most of these events have in common is the intertwined series of complex events and causes that are often closely related to the level of vulnerability and the increase (reduction) in the amount of RES (SG). This is not to say that RES themselves are directly causing more instability events, but they do bring the increase in complexity and higher probability of dangerous dynamics occurring. In

other words, the reduction in SG (and thus in inertia and system strength) weakens the natural resilience of the grid, creating a more vulnerable environment in power grids. Meanwhile, the higher proliferation of inverter-based RES tends to increase the number of complex voltage and frequency dynamics in the grid. Combining these two trends results in a rising number of intricate, faster, often novel, and potentially severe system events as exemplified in [Table 1.1](#).

Table 1.1.: Some of the recent large disturbances in modern power systems.

Events	Main Causes	Consequences	Sources
RES tripping (2016-2022)	Loss of synchronism, over(under)voltages, momentary cessation, phase jump, control issues	Minor to major RES loss, local supply disruptions, power quality degradation, minor financial costs	[30–40]
Oscillations (2007-2022)	Inverter-grid interactions, weak grid operation, high power transfers, control issues, resonance	Minor to major RES loss, (inter)connection disruptions, equipment damage risks, minor financial costs	[41–47]
System separation (2006-2021)	Reduced system resilience, angle and voltage instability, cascading, ride-through issues, phase jump, control issues	Large power deficit/surplus, localized demand shedding, amplified blackout risk, limited financial costs	[48–53]
System blackouts (2009-2021)	Low system resilience, severe weather events, high (low) RES (SG) share, ride-through issues, cascading, (emergency) protection failure, frequency and voltage collapse	Large-scale blackout, millions without power, public infrastructure issues, communication disruptions, (severe) equipment damage, substantial financial costs	[54–57]

These trends become increasingly important in terms of system strength and voltage stability, as most inverter-based RES inherently rely on stable voltages and strong grids to preserve synchronism and the desired steady- and dynamic-state operation. To deal with this fundamental resilience reduction in power systems, modern power systems' complex dynamics and stability need to be understood better, and suitable evaluation and mitigation measures need to be developed. Some of the main research gaps related to the decrease in vulnerability and the rising number of discussed disturbances are identified and listed below.

- *Better understanding of vulnerability and stability in modern power systems.*
- *Better understanding of grid weakening and its consequences for cascading faults and system collapse risks.*
- *Evaluating impacts of widespread proliferation of distributed energy resources on system vulnerability and stability.*
- *Improved methods for evaluating system vulnerability, particularly related to short-term (voltage) stability and system strength.*

- *The ability to effectively detect, quantify, and classify disturbances in the grid.*
- *Better utilization of modern measurements and advanced data-driven approaches for system vulnerability assessment.*

To address these research gaps, the main research questions of this thesis are defined and introduced in the following section.

1.4. RESEARCH QUESTIONS

The scope of this thesis comprises the essential challenges in modern power systems, primarily in the field of voltage stability and system strength. The five main research questions and consequential thesis objectives are derived and listed below.

1. *How does the energy transition lead to a higher vulnerability of electric power systems? What are the possible consequences? (Chapter 1)*
2. *Why is securing voltage stability (particularly short-term) a progressively more critical and challenging task in modern power systems? Why are the existing evaluation methods insufficient? (Chapter 2)*
3. *How should system strength be understood and evaluated in modern power systems, and how does it relate to vulnerability and stability? (Chapter 3)*
4. *What kind of effects do dynamic loads and distributed generation have on the short-term stability and resilience of modern power systems? (Chapter 4)*
5. *How can novel data- and simulation-driven approaches and methods help in alleviating the challenges highlighted in this thesis? (Chapter 5)*

Each chapter of this thesis primarily deals with one of the main research questions, as highlighted. The findings in this thesis concerning these five main research questions are once again concisely discussed and summarized in the final chapter.

The research presented in this thesis is also part of a broader research framework on the resilience of modern power systems. This is briefly introduced in the following subsection.

1.5. RESEARCH PROJECT STRUCTURE

The research presented in this thesis is part of a joint industry-academia research project *Resilient Synchroreasurement-based Grid Protection Platform (ReSident)*⁷.

ReSident is motivated by the challenges in the control of future electric power grids, such as reduced system resilience and increased operational uncertainty due to the large-scale integration of renewable energy sources. With advanced algorithms and a comprehensive real-time monitoring platform, the classification of disturbances

⁷This research project was supported by a large industry consortium consisting of TenneT TSO, Alliander DSO, Stedin DSO, General Electric, Dutch National Metrology Institute (VSL), and The Dutch Research Council (NWO).

and assessment of their impact is aimed to be realized to take preventive operating actions and real-time remedial actions for anticipating and preventing large system failures under increased vulnerability and operational uncertainty.

The visualized overview of the ReSident project is given in Figure 1.10. The research scope of the entire project consists of four work packages (WPs), each dealing with one dimension of the resilience of modern power systems. The four WPs and their respective research objectives are briefly listed below.

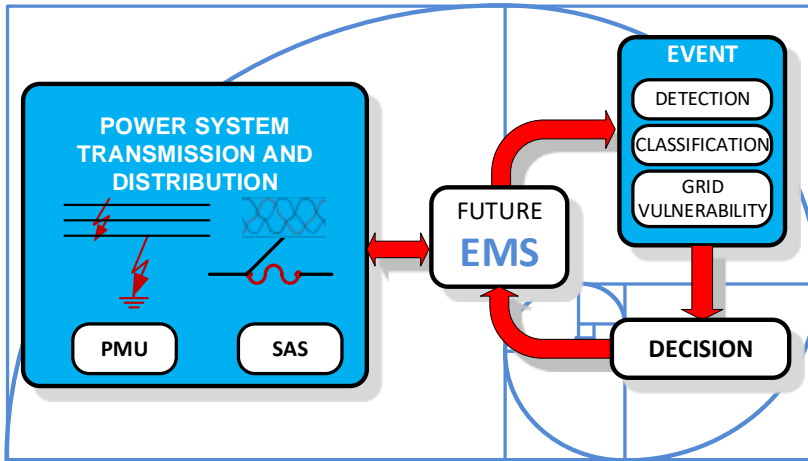


Figure 1.10.: Resident project overview.

- **WP1–Next-generation Energy Management System (EMS) Platform:** To create a real-time communication platform for the simulation of power systems based on real-time data and to test/validate WAMPAC applications.
- **WP2–Event Detection, Localization and Classification:** To achieve situational awareness in the grid by utilizing advanced AI and machine learning methods for real-time detection, localization, and classification of disturbances.
- **WP3–Stability-aware Controlled Network Separation:** To derive a method for early detection and prevention of out-of-step system conditions by controlled system separation and re-stabilization.
- **WP4–Grid Vulnerability and Cascading Failures Prevention:** To develop offline and online algorithms and tools for the vulnerability assessment of renewables-dominated grids to quantify, anticipate, and prevent risks of cascading failures and system collapse.

Extensive work on WP1 and WP3 is completed and can be found in [58, 59], respectively, while the research in terms of WP2 is planned to be completed in 2024. This thesis primarily focuses on WP4, particularly from the perspective of voltage stability and system strength, as introduced in previous sections.

The thesis outline is hereby introduced further.

1.6. THESIS OUTLINE

The thesis is divided into six main chapters. The structure of the thesis and its chapters are shown in [Figure 1.11](#). The remainder of this subsection briefly introduces the content of each chapter.

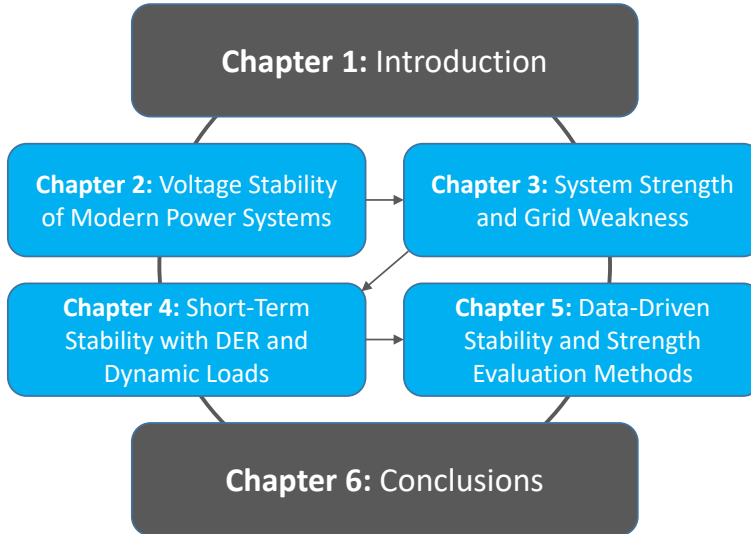


Figure 1.11.: Structure of the thesis.

[Chapter 1](#) starts by describing the structural changes the power systems face worldwide as climate change awareness grows. The changes and trends toward sustainable power supply introduce vulnerability and stability challenges, which are described further. Moreover, the key challenges addressed in this thesis are described. Finally, the research structure in the scope of a larger project is presented, followed by the research objectives and thesis structure.

[Chapter 2](#) deals with power system stability matters. In light of the evolving power systems, stability is redefined and reclassified to reflect the emerging challenges in maintaining a stable operation. The chapter dives deeper into the issue of voltage stability, its link to maximum power transfer, the rising relevance of short-term voltage stability, and its relation to other instability mechanisms. Finally, extensive literature research on these topics addresses the challenges of modern power systems and open research questions.

[Chapter 3](#) tackles the increasingly important topic of system strength and grid weakness. The chapter begins with a comprehensive overview of the system strength concept in conventional and modern power systems, followed by an introduction of a novel classification. The second part of the chapter deals with the evaluation of system strength. The existing methods for steady-state system strength are analyzed and compared, showing their notable limitations when applied in modern grids. A new approach is introduced in an attempt to overcome the existing limitations.

Finally, a discussion on dynamic system strength and its challenges is presented.

In [Chapter 4](#), the ever-increasing impact of distributed energy resources (DER) and dynamic loads on bulk power system stability is analyzed. The focus is on short-term forms of instability, particularly voltage instability. A comprehensive analysis of the impacts is presented, followed by key findings and a discussion on the necessity for better evaluation in future grids.

[Chapter 5](#) discusses new data-driven opportunities for power system analysis arising from improved grid observability and enhanced computational power. Novel quantification and classification techniques are derived to provide vulnerability assessment of modern power systems. A comprehensive numerical analysis is presented, showcasing the efficacy of the methods. Finally, to deal with the remaining challenges described in the previous chapters, a new method for dynamic system strength evaluation considering DER and dynamic loads is introduced and tested.

Finally, [Chapter 6](#) summarizes the overall research achievements and outlines the main scientific findings. The research questions are comprehensively answered, followed by practical recommendations for designing, analyzing, and operating modern power systems. Lastly, several crucial future research directions are introduced and discussed related to the vulnerability and resilience of modern power systems.

REFERENCES

- [1] “Remarkable Weather of 1911: The Effect of the Combustion of Coal on the Climate”. In: *Popular Mechanics* (Mar. 1912), pp. 339–342.
- [2] Svante Arrhenius. “On the Influence of Carbonic Acid in the Air upon the Temperature of the Ground”. In: *Philosophical Magazine and Journal of Science* 41 (Apr. 1896), pp. 237–276. URL: https://www.rsc.org/images/Arrhenius1896_tcm18-173546.pdf.
- [3] *Eunice Newton Foote Medal For Earth-Life Science*. URL: <https://www.agu.org/honor-and-recognize/honors/union-medals/eunice-newton-foote-medal>.
- [4] E. Foote. “Circumstances affecting the heat of the Sun’s rays”. In: *The American Journal of Science and Arts* 2 (Nov. 1856), pp. 382–383. URL: https://static1.squarespace.com/static/5a2614102278e77e59a04f26/t/5aa1c3cf419202b500c3b388/1520550865302/foote_circumstances-affecting-heat-suns-rays_1856.pdf.
- [5] J. Fourier. “Remarques Générales Sur Les Températures Du Globe Terrestre Et Des Espaces Planétaires [On the Temperatures of the Terrestrial Sphere and Interplanetary Space]”. In: *Annales de Chimie et de Physique* 27 (1924), pp. 136–167. URL: <https://geosci.uchicago.edu/~rtp1/papers/Fourier1827Trans.pdf>.
- [6] NASA. *Evidence - How Do We Know Climate Change Is Real?* URL: <https://climate.nasa.gov/evidence/>.
- [7] DNV. *Trilemma and Transition*. Tech. rep. DNV, Energy Industry Insights, 2023. URL: <https://www.dnv.com/power-renewables/energy-industry-insights/trilemma-transition-receipt.html>.
- [8] The Guardian. *IPCC: We can tackle climate change if big oil gets out of the way*. Apr. 2022. URL: <https://www.theguardian.com/environment/2022/apr/05/ipcc-report-scientists-climate-crisis-fossil-fuels>.
- [9] *Big Oil’s Real Agenda on Climate Change*. Tech. rep. InfluenceMap, Mar. 2019. URL: <https://influencemap.org/report/How-Big-Oil-Continues-to-Oppose-the-Paris-Agreement-38212275958aa21196dae3b76220bdbc>.
- [10] The Guardian. *Shell and Exxon’s secret 1980s climate change warnings*. Sept. 2018. URL: <https://www.theguardian.com/environment/climate-consensus-97-per-cent/2018/sep/19/shell-and-exxons-secret-1980s-climate-change-warnings>.
- [11] *United Nations Framework Convention on Climate Change*. 1992. URL: <https://unfccc.int/resource/docs/convkp/conveng.pdf>.
- [12] *Kyoto Protocol to the United Nations Framework Convention on Climate Change*. 1998. URL: <https://unfccc.int/resource/docs/convkp/kpeng.pdf>.
- [13] *The Paris Agreement (Paris Climate Accords)*. 2016. URL: https://unfccc.int/sites/default/files/english_paris_agreement.pdf.
- [14] IPCC. *AR6 Synthesis Report Climate Change 2023*. Tech. rep. Mar. 2023. URL: https://report.ipcc.ch/ar6syrr/pdf/IPCC_AR6_SYR_LongerReport.pdf.
- [15] *Climate Tipping Points*. OECD, Dec. 2022. ISBN: 9789264858763. DOI: 10.1787/abc5a69e-en. URL: <https://www.oecd.org/environment/climate-tipping-points-abc5a69e-en.htm>.
- [16] IEA. *Achieving Net Zero Electricity Sectors in G7 Members*. Tech. rep. International Energy Agency, Oct. 2021. URL: <https://www.iea.org/reports/achieving-net-zero-electricity-sectors-in-g7-members>.

- [17] IRENA. *World Energy Transitions Outlook 2022: 1.5°C Pathway*. Tech. rep. Abu Dhabi: International Renewable Energy Agency, 2022. URL: <https://www.irena.org/publications/2022/mar/world-energy-transitions-outlook-2022>.
- [18] IEA. *Renewables*. Tech. rep. Paris: International Energy Agency, 2022. URL: <https://www.iea.org/reports/renewables-2022>.
- [19] IRENA. *Renewable Power Generation Costs in 2021*. Tech. rep. International Renewable Energy Agency, 2021. URL: <https://www.irena.org/publications/2022/Jul/Renewable-Power-Generation-Costs-in-2021>.
- [20] IEA. *Power Systems in Transition*. Paris, 2020. URL: <https://www.iea.org/reports/power-systems-in-transition>.
- [21] T. J. Bekkers Frank. *The High Value of The North Sea*. Sept. 2021. URL: <https://hcss.nl/wp-content/uploads/2021/10/Value-of-the-North-Sea-HR.pdf>.
- [22] A. Younesi, H. Shayeghi, Z. Wang, P. Siano, A. Mehrizi-Sani, and A. Safari. “Trends in modern power systems resilience: State-of-the-art review”. In: *Renewable and Sustainable Energy Reviews* 162 (July 2022), p. 112397. ISSN: 13640321. DOI: [10.1016/j.rser.2022.112397](https://doi.org/10.1016/j.rser.2022.112397).
- [23] EPRI. *Power System Supply Resilience: The Need for Definitions and Metrics in Decision-Making*. Tech. rep. Electric Power Research Institute, Aug. 2020. URL: <https://www.epri.com/research/programs/OTIZ12/results/3002014963>.
- [24] IEEE PES TR-83. *Resilience Framework, Methods, and Metrics for the Electricity Sector*. Tech. rep. IEEE Power & Energy Society, Oct. 2020. URL: https://resourcecenter.ieee-pes.org/publications/technical-reports/PES_TP_TR83_ITSLC_102920.html.
- [25] N. Hatzigiargyriou, J. Milanovic, C. Rahmann, V. Ajarapu, C. Canizares, I. Erlich, D. Hill, I. Hiskens, I. Kamwa, B. Pal, P. Pourbeik, J. Sanchez-Gasca, A. Stankovic, T. Van Cutsem, V. Vittal, and C. Vournas. “Definition and Classification of Power System Stability – Revisited & Extended”. In: *IEEE Transactions on Power Systems* 36.4 (July 2021), pp. 3271–3281. ISSN: 0885-8950. DOI: [10.1109/TPWRS.2020.3041774](https://doi.org/10.1109/TPWRS.2020.3041774).
- [26] F. Milano, F. Dorfler, G. Hug, D. J. Hill, and G. Verbic. “Foundations and Challenges of Low-Inertia Systems (Invited Paper)”. In: *2018 Power Systems Computation Conference (PSCC)*. IEEE, June 2018, pp. 1–25. ISBN: 978-1-910963-10-4. DOI: [10.23919/PSCC.2018.8450880](https://doi.org/10.23919/PSCC.2018.8450880).
- [27] F. Capitanescu. “Are We Prepared Against Blackouts During the Energy Transition?: Probabilistic Risk-Based Decision Making Encompassing Jointly Security and Resilience”. In: *IEEE Power and Energy Magazine* 21.3 (May 2023), pp. 77–86. ISSN: 1540-7977. DOI: [10.1109/MPE.2023.3247053](https://doi.org/10.1109/MPE.2023.3247053).
- [28] R. W. Kenyon, M. Bossart, M. Marković, K. Doubleday, R. Matsuda-Dunn, S. Mitova, S. A. Julien, E. T. Hale, and B.-M. Hodge. “Stability and control of power systems with high penetrations of inverter-based resources: An accessible review of current knowledge and open questions”. In: *Solar Energy* 210 (Nov. 2020), pp. 149–168. ISSN: 0038092X. DOI: [10.1016/j.solener.2020.05.053](https://doi.org/10.1016/j.solener.2020.05.053).
- [29] J. Shair, H. Li, J. Hu, and X. Xie. “Power system stability issues, classifications and research prospects in the context of high-penetration of renewables and power electronics”. In: *Renewable and Sustainable Energy Reviews* 145 (July 2021), p. 111111. ISSN: 13640321. DOI: [10.1016/j.rser.2021.111111](https://doi.org/10.1016/j.rser.2021.111111).
- [30] NERC. *1200 MW Fault Induced Solar Photovoltaic Resource Interruption Disturbance Report*. Tech. rep. North American Electric Reliability Corporation, June 2017.
- [31] N. Stringer, N. Haghdadi, A. Bruce, J. Riesz, and I. MacGill. “Observed behavior of distributed photovoltaic systems during major voltage disturbances and implications for power system security”. In: *Applied Energy* 260 (Feb. 2020), p. 114283. ISSN: 03062619. DOI: [10.1016/j.apenergy.2019.114283](https://doi.org/10.1016/j.apenergy.2019.114283).
- [32] National Grid. *2019 Hornsea Offshore Windfarm Incident Report*. Tech. rep. Sept. 2019. URL: <https://www.nationalgrideso.com/document/152346/download>.
- [33] NERC. *April and May 2018 Fault Induced Solar Photovoltaic Resource Interruption Disturbances Report*. Tech. rep. North American Electric Reliability Corporation, Jan. 2019.

- [34] NERC. *San Fernando Disturbance*. Tech. rep. North American Electric Reliability Corporation, Nov. 2020.
- [35] NERC. *2021 Odessa Disturbance*. Tech. rep. North American Electric Reliability Corporation, Sept. 2021.
- [36] NERC. *Multiple Solar PV Disturbances in CAISO*. Tech. rep. North American Electric Reliability Corporation, Apr. 2022.
- [37] NERC. *Panhandle Wind Disturbance*. Tech. rep. North American Electric Reliability Corporation, Aug. 2022.
- [38] NERC. *2022 Odessa Disturbance*. Tech. rep. North American Electric Reliability Corporation, Dec. 2022.
- [39] NERC. *Major Event Analysis Reports*. URL: <https://www.nerc.com/pa/rrm/ea/Pages/Major-Event-Reports.aspx>.
- [40] AEMO. *Behaviour of distributed resources during power system disturbances: Overview of key findings*. Tech. rep. Australian Energy Market Operator, May 2021.
- [41] Y. Cheng, L. Fan, J. Rose, S.-H. Huang, J. Schmall, X. Wang, X. Xie, J. Shair, J. R. Ramamurthy, N. Modi, C. Li, C. Wang, S. Shah, B. Pal, Z. Miao, A. Isaacs, J. Mahseredjian, and J. Zhou. “Real-World Subsynchronous Oscillation Events in Power Grids With High Penetrations of Inverter-Based Resources”. In: *IEEE Transactions on Power Systems* 38.1 (Jan. 2023), pp. 316–330. ISSN: 0885-8950. DOI: [10.1109/TPWRS.2022.3161418](https://doi.org/10.1109/TPWRS.2022.3161418).
- [42] IEEE PES-TR80. *Wind Energy Systems Sub-Synchronous Oscillations: Events and Modeling*. Tech. rep. IEEE Power & Energy Society, July 2020. URL: https://resourcecenter.ieee-pes.org/publications/technical-reports/PES_TP_TR80_AMPS_WSSO_070920.html.
- [43] L. Fan, Z. Miao, D. Piper, D. Ramasubramanian, L. Zhu, and P. Mitra. “Analysis of 0.1-Hz Var Oscillations in Solar Photovoltaic Power Plants”. In: *IEEE Transactions on Sustainable Energy* 14.1 (Jan. 2023), pp. 734–737. ISSN: 1949-3029. DOI: [10.1109/TSTE.2022.3220083](https://doi.org/10.1109/TSTE.2022.3220083).
- [44] J. Matevosyan. *ERCOT’s Experience Integrating High Shares of IBR*. June 2021. URL: <https://www.wingrid.org/wp-content/uploads/2021/08/13-Julia-Matevosyan-ERCOT-Integrating-high-shares-of-IBR.pdf>.
- [45] J. Leslie. *G-PST/ESIG Webinar Series: Managing Grid Stability in a High IBR Network*. Jan. 2022. URL: <https://www.esig.energy/event/webinar-managing-grid-stability-in-a-high-ibr-network/>.
- [46] ENTSO-E. *Analysis of Central Europe Inter-area Oscillations of 19 and 24 February 2011*. Tech. rep. European Network of Transmission System Operators for Electricity, Aug. 2011. URL: https://eepublicdownloads.entsoe.eu/clean-documents/pre2015/publications/entsoe/RG_SOC_CE/Top7_110913_CE_inter-area-oscil_feb_19th_24th_final.pdf.
- [47] ENTSO-E. *Analysis of Central Europe Inter-area Oscillations of 1 December 2016*. Tech. rep. European Network of Transmission System Operators for Electricity, July 2017. URL: https://eepublicdownloads.entsoe.eu/clean-documents/SOC%20documents/Regional_Groups_Continental_Europe/2017/CE_inter-area_oscillations_Dec_1st_2016_PUBLIC_V7.pdf.
- [48] AEMO. *Final Report – Queensland and South Australia system separation on 25 August 2018*. Tech. rep. Australian Energy Market Operator, Jan. 2019. URL: https://www.aemo.com.au/-/media/Files/Electricity/NEM/Market_Notices_and_Events/Power_System_Incident_Reports/2018/Qld---SA-Separation-25-August-2018-Incident-Report.pdf.
- [49] UCTE. *Final Report: System Disturbance on 4 November 2006*. Tech. rep. Union for the co-ordination of Transmission of Electricity, Nov. 2006. URL: <https://eepublicdownloads.entsoe.eu/clean-documents/pre2015/publications/ce/otherreports/Final-Report-20070130.pdf>.
- [50] ENTSO-E. *Continental Europe Synchronous Area Separation on 08 January 2021*. Tech. rep. European Network of Transmission System Operators for Electricity, July 2021. URL: https://eepublicdownloads.azureedge.net/clean-documents/SOC%20documents/SOC%20Reports/entso-e_CESysSep_Final_Report_210715.pdf.

- [51] ENTSO-E. *Continental Europe Synchronous Area Separation on 24 July 2021*. Tech. rep. European Network of Transmission System Operators for Electricity, Mar. 2022. URL: https://eepublicdownloads.azureedge.net/clean-documents/Publications/2022/entso-e_CESysSep_210724_02_Final_Report_220325.pdf.
- [52] AEMO. *Final Report – New South Wales and Victoria Separation Event on 4 January 2020*. Tech. rep. A, Sept. 2020. URL: https://aemo.com.au/-/media/files/electricity/nem/market_notices_and_events/power_system_incident_reports/2020/final-report-nsw-and-victoria-separation-event-4-jan-2020.pdf?la=en#:~:text=This%20is%20AEMO's%20final%20report,in%20the%20Snowy%20Mountains%20area..
- [53] AEMO. *Final Report –Victoria and South Australia Separation Event on 31 January 2020*. Tech. rep. Australian Energy Market Operator, Nov. 2020. URL: https://aemo.com.au/-/media/files/electricity/nem/market_notices_and_events/power_system_incident_reports/2020/final-report-vic-sa-separation-31-jan--2020.pdf.
- [54] A. Martins, P. Gomes, F. Alves, D. Falcao, C. Ribeiro, A. Guarini, N. Martins, and G. Taranto. “Lessons Learned in Restoration from Recent Blackout Incidents in Brazilian Power System”. In: *CIGRE Session*. CIGRE, 2012. URL: https://e-cigre.org/publication/C2-214_2012-lessons-learned-in-restoration-from-recent-blackout-incidents-in-brazilian-power-system.
- [55] V. Rampurkar, P. Pentayya, H. A. Mangalvedekar, and F. Kazi. “Cascading Failure Analysis for Indian Power Grid”. In: *IEEE Transactions on Smart Grid* 7.4 (July 2016), pp. 1951–1960. ISSN: 1949-3053. DOI: [10.1109/TSG.2016.2530679](https://doi.org/10.1109/TSG.2016.2530679).
- [56] ENTSO-E. *Report on Blackout in Turkey on 31st March 2015*. Tech. rep. European Network of Transmission System Operators for Electricity, Sept. 2015. URL: https://eepublicdownloads.entsoe.eu/clean-documents/SOC%20documents/Regional_Groups_Continental_Europe/20150921_Black_Out_Report_v10_w.pdf.
- [57] R. Yan, N.-A. -Masood, T. Kumar Saha, F. Bai, and H. Gu. “The Anatomy of the 2016 South Australia Blackout: A Catastrophic Event in a High Renewable Network”. In: *IEEE Transactions on Power Systems* 33.5 (Sept. 2018), pp. 5374–5388. ISSN: 0885-8950. DOI: [10.1109/TPWRS.2018.2820150](https://doi.org/10.1109/TPWRS.2018.2820150).
- [58] M. Naglič. “On power system automation: Synchronised measurement technology supported power system situational awareness”. PhD thesis. Delft University of Technology, 2020. URL: <https://research.tudelft.nl/en/publications/on-power-system-automation-synchronised-measurement-technology-su>.
- [59] I. Tyuryukanov. “Graph Partitioning Algorithms for Control of AC Transmission Networks: Generator Slow Coherency, Intentional Controlled Islanding, and Secondary Voltage Control”. PhD thesis. Delft University of Technology, Mar. 2020. URL: <https://research.tudelft.nl/en/publications/graph-partitioning-algorithms-for-control-of-ac-transmission-netw>.

2

VOLTAGE STABILITY OF MODERN POWER SYSTEMS

A chain is only as strong as its weakest link.

- English/Dutch proverb¹

To accurately evaluate voltage stability margins in modern power systems, it is crucial to understand the concept of voltage stability well. While voltage stability in conventional systems is a well-understood topic, the same cannot be said for renewable-driven modern power systems. This chapter introduces the topic of stability of modern power systems, after which a more detailed focus on voltage stability fundamentals and its evaluation in modern systems is presented.

2.1. POWER SYSTEM STABILITY: DEFINITION AND CLASSIFICATION

As introduced in [Chapter 1](#), stability is the ability of a system to remain operational after being subjected to a disturbance. Power systems should be able to successfully cope with various dynamics of different origins, occurring in a wide range of timescales, and maintain stability. In the energy transition, power systems evolve, and the system dynamics change accordingly, generally becoming faster, more complex, and potentially more dangerous. An overview of typical dynamic phenomena and their corresponding timescales is shown in [Figure 2.1](#). They are divided into four types: wave, electromagnetic, electromechanical, and thermodynamic phenomena. Time scales of dynamics range from microseconds to hours.

This thesis primarily focuses on the intersection of electromagnetic and electromechanical phenomena in the range of 100 ms (10^{-1} s) to 10 seconds.

Parts of this chapter have been published in peer-reviewed articles and/or conference proceedings.

See the [List of Publications](#) section for more details.

¹In Dutch commonly known as *Een ketting is zo sterk als zijn zwakste schakel*.

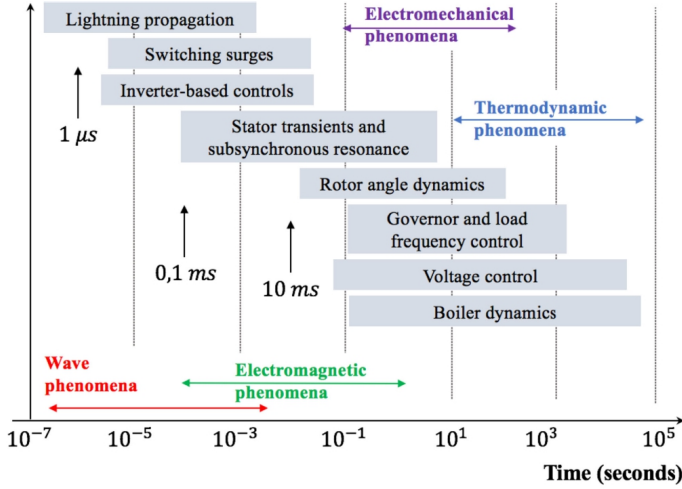


Figure 2.1.: Time scales of various dynamics in power systems [1].

Power system stability classification has also evolved with the large variety of dynamic phenomena occurring in the system. As systems progress from conventional to modern, new classes of instability emerge. Figure 2.2 illustrates the evolution of power system stability classification over the past couple of decades. Each of these stability classes is hereby briefly introduced. For a more extensive overview of different types of instability, the readers are referred to [1, 2]².

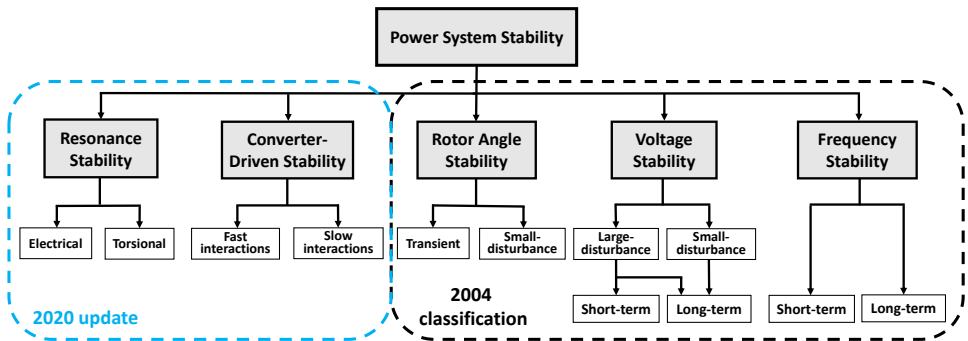


Figure 2.2.: Widely-used classification of power system stability (adapted from [2]).

Frequency stability is the ability of a power system to maintain the active power balance and stable frequency in the safe bands around 50 (60) Hz³. It is divided into short-term and long-term frequency stability, dealing with a different timescale of dynamics that may cause instability. To manage active power system-wide and to

²A slightly different yet interesting perspective on stability classification can be found in [3].

³Nominal frequency values differ per country. A clear overview can be found in [4].

maintain production-consumption balance over the short- and long-term timescales is the key task for avoiding frequency instability.

Voltage stability is generally described as the ability of a power system to maintain steady voltages at all buses in a system while being able to deliver power requested by loads. Voltage instability can occur due to large or small disturbances over the short- or long-term, depending on the type of dynamics taking place. Reactive power coordination is central to maintaining voltage stability, particularly in transmission systems. Voltage stability is one of the main topics of this thesis and is thereby extensively discussed further. Voltage stability is also closely related to the concept of system strength, which will be elaborated on in [Chapter 3](#).

Rotor angle stability describes the ability of a (group of) synchronous generator(s) to remain in synchronism with the rest of the system during normal operation or after being subjected to a disturbance. It is generally divided into transient and small-disturbance rotor angle stability. Key variables that describe rotor angle stability are rotor angles and their value difference between generators.

These three classes (rotor angle, voltage, and frequency stability) are at the essence of conventional power systems as they directly relate to the operation of synchronous generators (SGs). However, as inverter-based resources (IBRs) take over as a dominant generation source, new dynamics appear in the system. This leads to new classes of power system stability: resonance and converter-driven stability. The two classes are inherently related to the operation of modern power systems, often involving IBRs and their interactions with each other and other grid elements.

Converter-driven stability is related to the operation of IBRs and their interactions with the rest of the grid. It can manifest itself in terms of fast interactions (hundreds to thousands of Hz), and slow interactions (typically sub-synchronous, e.g. around 10Hz). The former interacts with wave and electromagnetic phenomena in the grid, while the latter with electromagnetic and electromechanical phenomena (see [Figure 2.1](#)). An important aspect of converter-driven instability is related to system strength and weak grid operation, which will be discussed in [Chapter 3](#).

Resonance stability deals with the resonance phenomena that occur when energy exchange periodically takes place in an oscillatory manner. Events such as sub-synchronous resonance fall under this class, occurring due to resonance between series compensation and i) torsional frequencies of the turbine-generator shaft, ii) electrical characteristics of an SG, or iii) double-fed induction generators present in type-III wind farms. Resonance instability should not be confused with other types of electromagnetic sub-synchronous oscillations occurring between multiple IBRs or between IBR(s) and the grid [5]. These are generally considered to be converter-driven instabilities instead.

Besides these two newly introduced stability classes, the three original classes have also evolved. For instance, rotor angle stability, while fundamentally related to synchronous generators, is increasingly affected by the operation of IBRs during and after disturbances. This is a consequence of both lower system inertia and a different response of IBRs compared to SGs. Therefore, rotor angle stability, particularly the transient sub-type, is becoming a faster and more intricate phenomenon. A similar applies to frequency stability, where power imbalances lead to much faster and

amplified frequency deviations in modern systems, threatening frequency stability.

Nonetheless, the largest changes are arguably occurring in the voltage stability aspects, which are the main topic of this thesis and will be discussed in more detail in the next section. Finally, another aspect that will be discussed is the rising interaction between different short-term stability classes as dynamics inevitably become more intertwined in modern power systems.

2.2. VOLTAGE STABILITY: FUNDAMENTALS AND TRENDS

Voltage stability is divided considering two aspects: the timescale of events and the severity of disturbances. In terms of the timescale, short-term and long-term voltage stability are differentiated. Furthermore, small- and large-disturbance instability phenomena are often distinguished [6].

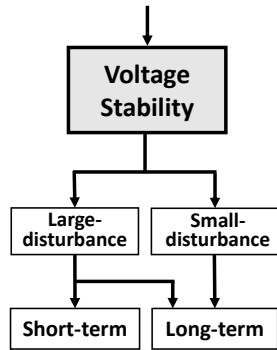


Figure 2.3.: Classification of voltage stability.

A system has high *voltage security* if it is able to maintain stable voltages following credible contingencies or load changes [6, 7]. Expanding on this further, a system can be considered *voltage resilient/robust* (vulnerable) if it exhibits a relatively low (high) risk of cascading faults and voltage instability and collapse.

Observing the systems worldwide, both frequency vulnerability and voltage vulnerability have been steadily increasing over the past decades. This is visualized in [Figure 2.4](#) for power systems with a (relatively) high share of renewable energy, such as in Australia (AU), Texas (TX), Ireland (IR), Hawaii (HI), and to some extent Great Britain (GB), and Central Europe (CE). Furthermore, the risks of control instability (converter-driven instability) have also appeared and are increasing.

In general, smaller more isolated systems with a higher IBR penetration have increased stability risks, while larger interconnected systems are still relatively resilient. This can be seen by comparing, for instance, the Australian to the Central European power system. Nevertheless, the scarcity of inertia and system strength will become a broader concern, with effects felt throughout the systems. Therefore, even the larger systems could see the stability risks increase, and neighbouring systems may be unable to assist as they simultaneously face the very same challenges.

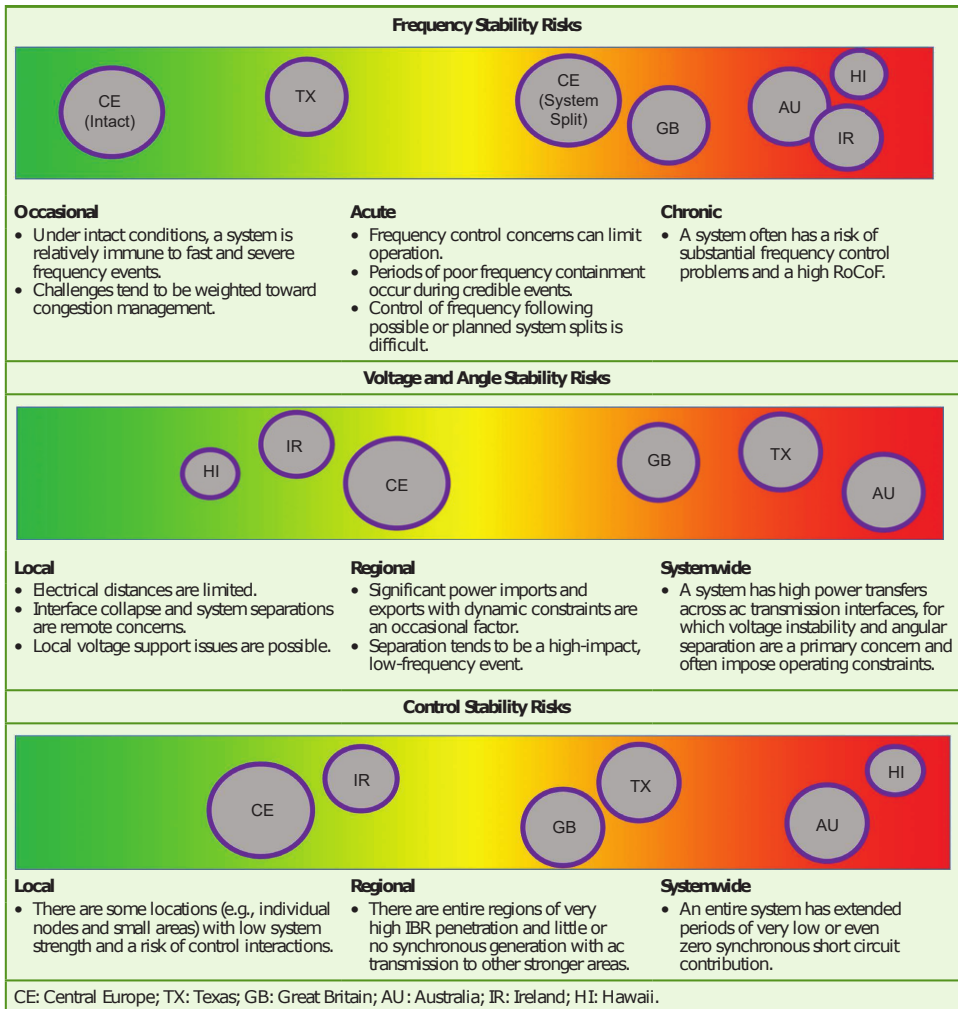


Figure 2.4.: Stability risks in power systems with various IBR penetration [8].

Zooming in on the Central European (CE) system, it is generally considered to be rather resilient to frequency stability risks. Nevertheless, if the CE system runs into system splits (as seen in 2021, see Table 1.1), the separated sections experience a high risk of frequency instability. Voltage and angle stability risks are also elevated in CE and worldwide [6]. As introduced in Chapter 1 and Table 1.1, many large disturbance events in modern systems were related to voltage stability and vulnerability. From the perspective of the CE system, as renewables rapidly replace synchronous generation continent-wide, system dynamics will evolve. Additionally, available reactive power support and system strength are expected to become more scarce. Furthermore, renewable sources will be installed at new and more remote

locations (e.g. offshore wind in the North Sea), often far from the consumption centres (major cities and industrial clusters) or existing electrical infrastructure. Consequently, large power transfers over relatively weak grid corridors shall become more common. Therefore, these two trends, illustrated in Figure 2.5, play a major role in reshaping voltage stability and system strength and their importance in modern power systems.

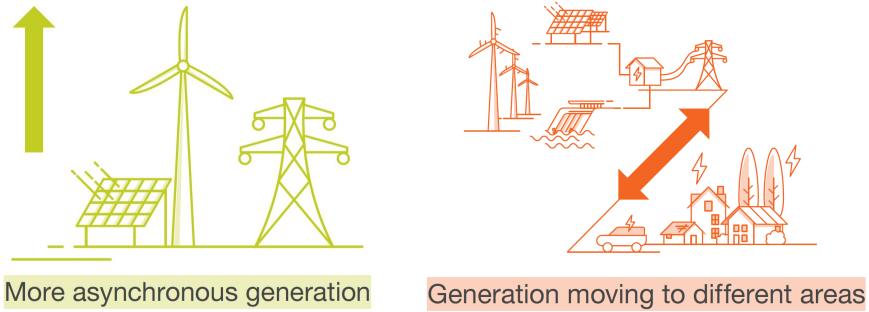


Figure 2.5.: Power system changes that impact voltage stability (adapted from [9]).

All of these developments lead to the premise of this thesis that voltage resilience will be one of the larger bottlenecks in present and especially future modern power systems worldwide. While relatively smaller systems with ambitious climate and renewables plans already experience some of the technical consequences, it is unlikely to take long until such consequences are also frequently seen in systems considered to be more robust, such as the CE power system. It is therefore vital to understand the impact on voltage stability to make sure systems' operational resilience and security are guaranteed for the challenging decades to come.

2.3. MAXIMUM POWER TRANSFER AND VOLTAGE STABILITY

Voltage instability typically takes the form of a progressive reduction of voltage in (a part of) the grid, potentially leading to voltage collapse. The time frame of interest for long-term voltage stability varies from tens of seconds to (tens of) minutes. It involves slower-acting equipment in the system such as thermostatically controlled loads, on-load tap-changers, and generator excitation limiters.

Voltage instability often occurs when a high active power transfer is present with limited reactive power support. If a (small or large) disturbance occurs in such a situation, the system becomes stressed further, as dynamic loads and tap changers attempt to restore the power consumption. However, the attempt to restore active power may also lead to higher (reactive) power demand. If such active and reactive power demands cannot be met by the system anymore, the equilibrium is lost, and progressive voltage degradation takes place. To illustrate this phenomenon, angle and voltage stability limits will be mathematically introduced first by exploring the maximum power transfer over a transmission corridor.

Let us assume a simple power system with two synchronous machines⁴ connected by a reactance X which represents the equivalent transfer impedance of the grid⁵. The single-line diagram of such a system is exemplified in Figure 2.6.

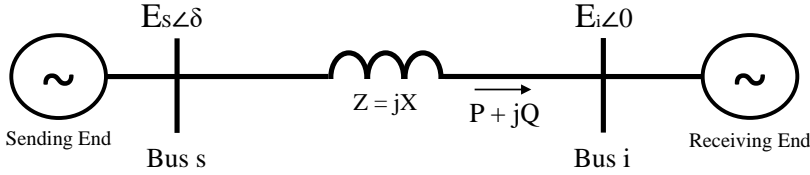


Figure 2.6.: A simple two-machine power system.

The total apparent power \underline{S} can be expressed as a function of bus voltages and the transfer impedance, as shown in Equation (2.1):

$$\underline{S} = P + jQ = E_i \underline{I}^* = E_i \left[\frac{E_s - E_i}{jX} \right]^* \quad (2.1)$$

By expressing the voltages in the Euler form, the following can be derived:

$$P + jQ = E_i \left[\frac{E_s \cos \delta + jE_s \sin \delta - E_i}{jX} \right]^* = \frac{E_s E_i}{X} \sin \delta + j \left[\frac{E_s E_i \cos \delta - E_i^2}{X} \right] \quad (2.2)$$

Active and reactive power (P and Q) can be expressed as:

$$P = \frac{E_s E_i}{X} \sin \delta = P_{max} \sin \delta \quad (2.3)$$

$$Q = \frac{E_s E_i \cos \delta - E_i^2}{X} \quad (2.4)$$

The relation in Equation (2.3) can be graphically represented as shown in Figure 2.7. As seen from the figure and equation, maximum active power is reached for angle $\delta = 90^\circ$, termed as P_{max} .

If a load $P = 0.8 < P_{max}$ is assumed, as illustrated with the blue dashed line, the operating point on the left part of the curve ($\delta < 90^\circ$) is the only steady-state stable point of the two. If the angle grows above 90° , mechanical power input would be higher than what can be transferred across the system. The resulting difference would accelerate the generator and cause the angle difference to grow even further. However, as per the concave shape of the curve shown in Figure 2.7, the power transfer would shrink, resulting in an even faster generator acceleration and angle instability. Note that the angle can exceed the 90° limit for a short (transient) amount of time, as long as its final settling value remains below it.

⁴The same applies for two connected power systems represented using the Thevenin's equivalent.

⁵Grid resistance is assumed to be zero ($R \approx 0$). This assumption is discussed further in Chapter 3.

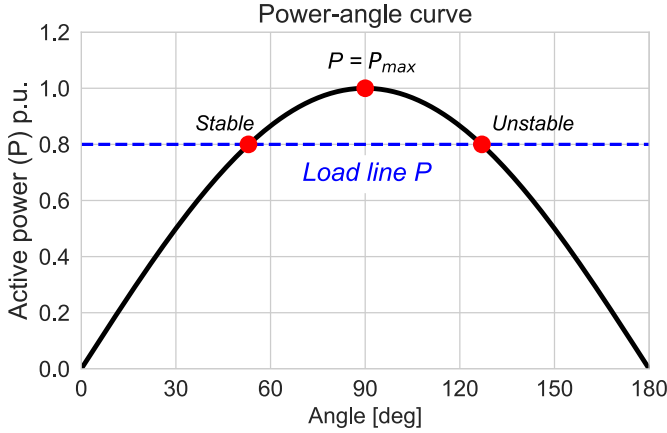


Figure 2.7.: An example of a power-angle curve for a simple 2-machine system.

However, this limitation, known as the angle stability limit, is not the only condition for stable operation. The other condition is known as the voltage stability limit, which can be understood as follows. If Equation (2.3) and Equation (2.4) are combined to eliminate angle δ , the following relationship can be derived.

$$(E_i^2)^2 + (2QX - E_s^2)E_i^2 + X^2(P^2 + Q^2) = 0 \quad (2.5)$$

If short-circuit capacity (S_{sc}) at bus i is defined as in Equation (2.6),

$$S_{sc} = \frac{E_i^2}{X} \quad (2.6)$$

Solving for the voltage E_i , the following equation can be obtained:

$$E_i^2 = X \left[(0.5S_{sc} - Q) \pm \sqrt{(0.5S_{sc})^2 - (P^2 + QS_{sc})} \right] \quad (2.7)$$

This relationship can be visualized in the so-called PV curves, as shown in Figure 2.8. The Equation (2.7) has two solutions depicted in the figure's full and dashed lines. If a constant system load of 0.4 per unit (40% of S_{sc}) is assumed, there are two possible operating points on the curve, indicated by red dots. However, the lower point has a very low operating voltage. To transfer this active power with such a low voltage would require very high currents and would consequently result in high losses. Furthermore, the operation on the lower part of the PV curve would imply that any additional demand leads to both drop in voltage *and* power, eventually leading to instability [10]. Therefore, a stable and viable operation can only take place on the upper part (full line) of the PV curve in Figure 2.8, limited by the point at $P_{max} < 0.5S_{sc}$ for the given case.

In case of a disturbance in the grid, a loss of a part of the transmission capacity can occur. This may result in reduced post-disturbance power transfer limits, as

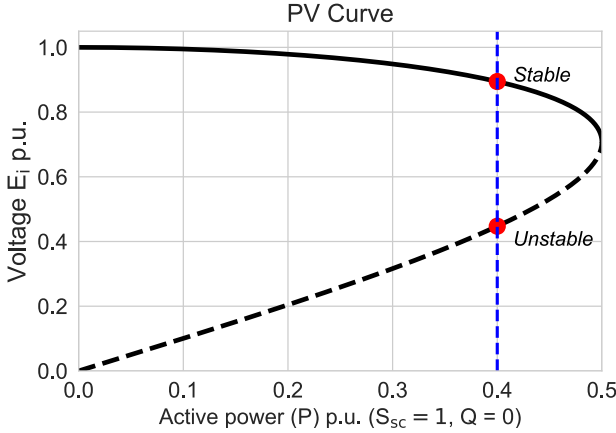


Figure 2.8.: Example of a PV curve for a simple 2-machine system.

shown by the red PV curve in Figure 2.9. To illustrate this, it is assumed that a 33% increase in the grid reactance X occurs (e.g. a loss of a parallel line or a transformer). Since there is no intersection between the system load and the new PV curve (shown in red), there is no stable operating point, and voltage collapse would occur.

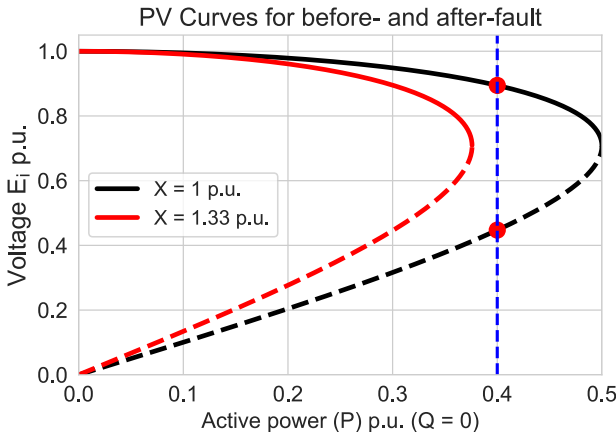


Figure 2.9.: Example of PV curves before and after a fault.

One approach to increase the maximum power transfer is by providing reactive power at the receiving bus (e.g. by using shunt capacitors). This can effectively stretch the PV curve to the right, allowing for a higher active power transfer (above 50% of S_{sc}). However, there is also a theoretical as well as a practical limit to reactive power compensation and consequent operating voltage range.

Figure 2.10 illustrates the stable and unstable active and reactive power regions when reactive power would be provided locally at the receiving bus.

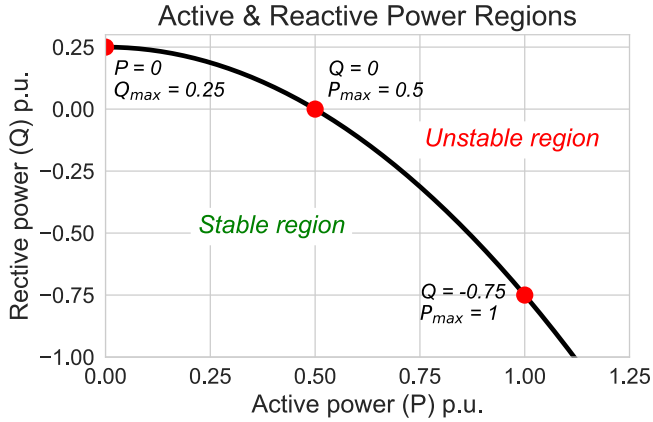


Figure 2.10.: Active and reactive power regions of stable and unstable operation.

For the case of $Q = 0$ (as plotted in Figure 2.8), maximum power transfer is equal to half of the S_{sc} . This corresponds to the middle red dot in Figure 2.10. As more reactive power is provided locally, more active power can be transferred over the transmission corridor⁶. If one would, for instance, want to transfer $P = 1$ per unit, it would require $Q = 0.75$ per unit of reactive power support. Theoretically, even higher active power could be transferred. However, the voltage should also be within the technically feasible limits, often defined as $0.9 \leq U \leq 1.1$ per unit. Interestingly, for $P = 0$, the maximum reactive power that can be transferred is only a quarter of the S_{sc} . This is a consequence of a dominantly reactive (rather than resistive) transmission system. The reactance of transmission systems is generally much higher than resistance⁷, due to the larger presence of overhead lines versus cables, as well as dominantly reactive equipment such as transformers and synchronous generators. Therefore, transferring reactive power across the transmission grid is generally difficult. It should be instead provided locally as much as possible, by strategically placing static and dynamic reactive power sources across the grid.

Some aspects of voltage stability, such as the maximum power transfer, will be explored more extensively in Chapter 3, as they become very relevant for system strength in modern power systems. Furthermore, the effects of inverter-based generation on maximum power transfer and voltage stability will be notably expanded on. The other main focus of this chapter and thesis is on *short-term* voltage (in)stability, discussed extensively in the following subsection.

⁶A common way to provide reactive power locally is by connecting shunt capacitors. This is explored in Chapter 3.

⁷In modern systems with more IBRs (fewer SGs) and more HV cables, this assumption may not be that reasonable anymore. The effects of growing resistance are explored further in Chapter 3.

2.4. SHORT-TERM INSTABILITY: EVALUATION METHODS

Short-term voltage instability⁸ (STVI) involves dynamics of fast-acting demand such as induction motors, electronically-controlled loads, and more recently, HVDC links, inverter-based resources (IBRs) and distributed energy resources (DERs) [2, 6]. STVI is, therefore, more likely to occur in grid sections with more of these elements present. For this reason, to appropriately analyze and simulate dynamics that lead to STVI, a detailed representation of dynamic loads and nearby (inverter-based) elements is necessary.

Unlike long-term voltage stability, short-term voltage instability deals with dynamics within a much shorter time frame, i.e., up to 10 seconds. In this sense, it is important to recognize that STVI manifests itself in a very similar time frame as several other types of short-term dynamics and instabilities in modern power systems. These four distinct types of short-term instability mechanisms are listed in Figure 2.11 and discussed further in more detail.

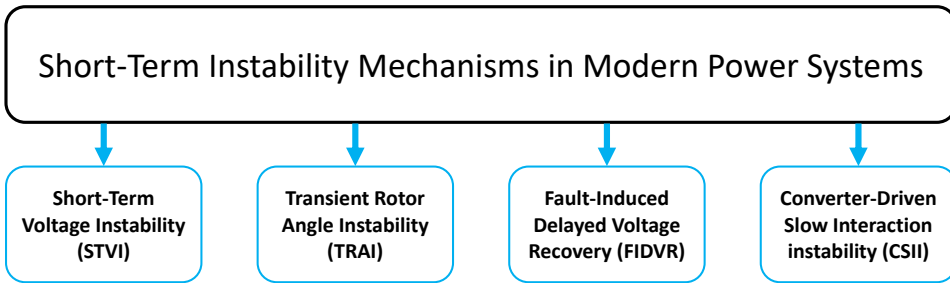


Figure 2.11.: Mechanisms of short-term instability in modern power systems [2, 11]

In conventional power systems, short-term instability was understood as either Short-Term Voltage Instability (STVI) or Transient Rotor Angle Instability (TRAI) [10].

Transient Rotor Angle Instability (TRAI), unlike STVI, is an event related to synchronous generators (SG), briefly introduced in Section 2.1. A disturbance, typically a short circuit in tie lines and/or near SGs, could cause the rotor angles of the generators (or generator groups) to drift sufficiently far from each other to lose synchronism. The instability can be either a first swing instability or instability occurring after a few cycles of oscillations. The former (latter) is more common for smaller (larger) systems with a few (many) SGs. The typical frequency range of these electromechanical oscillations is up to 2.5 Hz, depending on the size and the number of SGs involved [2].

These two forms of instability, STVI, and TRAI, are still present in modern systems, however, they become more intertwined with each other and with new IBRs' and load dynamics. Furthermore, new subtypes of short-term instability are emerging to describe the full scope of short-term stability of modern systems.

⁸Sometimes also referred to as transient voltage instability, although this term is discouraged.

One of them is **Fault-Induced Delayed Voltage Recovery** (FIDVR). FIDVR is characterized as a post-fault depressed voltage, typically lasting from several seconds to tens of seconds, jeopardizing the system's ability to recover. This is often attributed to the stalling of large amounts of induction motors, particularly A/C units [12], however, it can be also related to other dynamic or electronically-controlled loads. With the rising electrification of sectors such as heating/cooling, transportation, and small/large industries, demand will likely play a more active role in short-term voltage dynamics in the future. This is particularly relevant as many of these loads will have an inverter-based interface to the grid. In the case of stalled motors, an overvoltage situation may arise after they get disconnected by the overcurrent or thermal protection. FIDVR is not an instability on its own, as the system may succeed in recovering in some cases, but the voltage consequences of FIDVR present a significant threat to cascading. Conceptually, FIDVR can also be described as a specific type of STVI, as it is fundamentally related to dynamic load response. In that sense, it would also occasionally appear in conventional power systems. However, FIDVR can be affected and possibly exacerbated by DER operation, particularly inverter blocking or disconnection [13, 14]. Besides the voltage effects, FIDVR can also cause a voltage dip-induced frequency event. This is elaborated further in [Chapter 4](#). FIDVR is, therefore, an essential and distinctive short-term instability mechanism in modern power systems.

Another newly introduced form of short-term instability is converter-driven instability. It can manifest in terms of fast interactions (hundreds to thousands of Hz), and slow interactions (typically⁹ around 10 Hz) [2]. The latter, **Converter-driven Slow-Interactions Instability** (CSII), is of further interest for this thesis, while the former is out of scope. CSII usually emerges in weak system sections, where voltage is very sensitive to changes in active and reactive current or power¹⁰. After a disturbance, inverter controls may not be able to “lock” onto the grid voltage and frequency correctly, resulting in voltage oscillations. Additionally, as more inverters are introduced in the systems, there is more chance of undesired interactions, sometimes leading to oscillatory behaviour and possible voltage collapse if undamped. The post-fault converter-related instabilities have been an increasingly relevant subject worldwide, particularly (but not exclusively) in the systems with already high (local) IBR penetration and with consequent system strength reduction [15]. The most common CSII events seen in modern power systems are different types of sub-synchronous oscillations, with some already exemplified in [Table 1.1](#).

The four described phenomena (STVI, TRAI, FIDVR, and CSII) and their most important characteristics are concisely summarized in [Figure 2.12](#), with their typical location of emergence, dynamical causes and effects that describe it, and an illustration of typical voltage deviations they result in.

⁹See [Table 1.1](#) for various events of this type.

¹⁰This will be discussed more extensively in [Chapter 3](#).

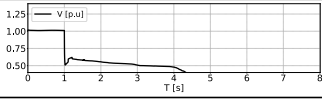
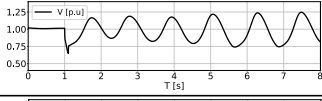
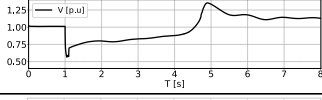
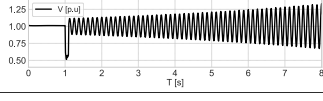
Instability Mechanism	Distinctive Characteristics of Each Short-Term Instability Phenomenon		
	Typical Location	Typical Dynamical Causes and Effects	Typical Post-Fault Voltage Deviation
Short-Term Voltage Instability (STVI)	Grid sections with high amounts of (dynamic) load and DER;	Motors dynamics and stalling; HVDC links dynamics; IBR and DER dynamics; Combination of any of the above;	
Transient Rotor Angle Instability (TRAI)	Tie-lines; Near-SG buses;	Large rotor angle deviations; Low CCT - loss of synchronism; Electromechanical oscillations (<2.5Hz);	
Fault-Induced Delayed Voltage Recovery (FIDVR)	Areas with a high share of dynamic load (particularly A/C units) and DER;	Massive induction motors stalling (mostly A/C) and disconnection; Massive DER disconnection and/or blocking;	
Converter-driven Slow Interactions Instability (CSII)	Remote or "weak" grid sections (low strength); Areas with many IBRs; High IBR control gains;	Interactions between IBR/DER controls, grid, and SG controls; Interactions with dynamic load; Oscillations (typically 7-10Hz range);	

Figure 2.12.: Overview of the four distinctive short-term instability phenomena, their characteristics, and illustrative voltage deviations [16].

As described, all four phenomena are distinctive in terms of the location where they typically emerge, the origin of instability, the way of manifesting itself, and ultimately the control actions that can be taken to prevent them. However, they also have many common characteristics:

- Manifestation in a similar time scale (usually <10s),
- Lead to significantly disturbed (but distinctive) post-fault voltage deviations,
- Often interact with each other when a system instability takes place,
- Become more common and more severe due to the introduction of more inverter-based resources and system strength reduction,
- May lead to rapid cascading events and system blackouts.

As the instability phenomena become more entangled, the risks of cascading events increase accordingly [13]. This ultimately translates into higher system vulnerability, particularly in terms of voltage resilience, as discussed in Chapter 1. It is therefore important to evaluate the existing short-term instability evaluation methods and determine whether they are effective in modern power systems where dynamics become faster, more complex, and increasingly intertwined.

The most common existing methods designed to evaluate short-term (voltage) instability are explored and summarized in Table 2.1.

Table 2.1.: Overview of the existing ST stability evaluation methods [11].

Method	Abbreviation	Year	Sources
Lyapunov Exponent	LE	2013	[17–22]
Transient Voltage Deviation Index	TVDI	2014	[23, 24]
Trajectory Violation Integral	TVI	2015	[25]
Voltage Instability Predictor	VIP	2012	[26–30]
Contingency Severity Index	CSI	2011	[31]
Voltage Stability Risk Index	VSRI	2007	[32, 33]
Data-Driven Methods	DDM	2015–2020	[34–43]

It is necessary to pinpoint the relevant qualitative indicators to evaluate the efficacy of the existing methods. There are several important conditions that a short-term instability evaluation method needs to meet in modern power systems to be both effective and practically applicable. The main ones are listed below:

- Able to detect and quantify the severity of various post-fault short-term voltage deviations,
- Useful in both conventional and modern power systems,
- Intuitive for practical on- and off-line applications,
- Adaptable to any system and operational scenario,
- As simple and computationally efficient as possible,
- Can provide real-time stability insights, for instance by relying on PMU data.

The methods presented in [Table 2.1](#) are qualitatively analyzed and extensively evaluated on these conditions in [11]. The summary of the results for each method is presented in [Figure 2.13](#).

Based on the analysis and results shown in [Figure 2.13](#), none of the methods is (very) good on all the relevant qualitative factors. Where more advanced methods like LE excel, the more straightforward linear methods are less applicable. However, these improvements are often accompanied by increased complexity and parameter sensitivity, which negatively reflects on the method's robustness.

Most of the methods, except for the VIP and data-driven methods, are generally model-free and are hence simple regarding the necessary inputs. The VIP and DDM require more research to evaluate whether they can be used for short-term instability evaluation without any model inputs. The situation is similar for real-time applicability, where most methods are (very) good. The VIP and VSRI methods were initially developed for long-term voltage stability monitoring and are, therefore, relatively less suitable for faster real-time stability evaluations. DDMs require more research in this regard, as it is questionable whether they can be sufficiently fast and cost-effective with the available solutions and computational possibilities.

Method	Model-free	Real-Time applicability	Applicable to various ST phenomena	Useful in IBG-rich systems	Computational complexity	Parameter sensitivity
LE	✓✓	✓✓	✓✓	✓✓	X	X
TVDI	✓✓	✓✓	X	?	✓✓	✓
TVI	✓✓	✓✓	✓	✓✓	X	?
VIP	?	✓	X	X	✓	✓
CSI	✓✓	✓✓	?	?	✓✓	✓
VSRI	✓✓	✓	?	✓	✓	?
DDM	?	?	✓✓	✓✓	X	X

✓✓: Very good, ✓: Good, X: Bad, ?: More research needed.

Figure 2.13.: Qualitative evaluation of the analyzed methods [11].

Nonetheless, the major challenge for most methods is the applicability to modern systems with a high penetration of inverter-based generation and to other short-term instability phenomena. These are arguably the two most essential factors in the analysis. The best-suited methods for these concerns are computationally more complex, such as LE, TVI, and potentially VSRI and DDM. LE was already shown to apply to other short-term phenomena, such as transient rotor angle stability. Furthermore, the LE concept of evaluating if a dynamical system is chaotic does not lose its predicting power if a system integrates more IBR and becomes more complex overall. TVI was not explicitly tested on other phenomena. Still, the method is practically intuitive with a time-adjustable instability threshold, and it is likely possible to utilize it for various short-term instability mechanisms, irrespective of the IBR penetration. Computationally simpler methods (i.e., TVDI and CSI) are likely to be less useful in modern systems, and their applicability to various short-term phenomena is limited. This is mainly the consequence of simplistic instability thresholds, which are not adaptable enough and potentially misleading in systems with a high share of IBR. Nevertheless, more research is required in this regard. On the other hand, VSRI applies moving average calculations, which can offer some insights even for IBR-rich systems. However, it is unclear if the method can detect other short-term instabilities or if its efficacy is limited to voltage stability. This necessitates further research. The VIP method becomes less effective with the increase in systems' complexity and is therefore not very suitable for either of these two challenges. Thevenin's equivalence on such fast dynamical phenomena is unlikely to yield accurate and useful results. Advanced DDM might overcome these difficulties completely as they are widely applicable for complex dynamical systems in general, but they bring other challenges for real-time assessments.

In terms of complexity and parameter sensitivity, simpler linear methods without too many parameters (i.e., TVDI, CSI, and VIP) are always preferred. The methods that use derivatives or integrals (i.e., LE and TVI) compensate for their dominance in efficacy for the increased complexity and parameter sensitivity. This seems to be particularly true for LE, where it was shown that parametrization could be very challenging. VSRI is not exceptionally complex to compute, but its parametrization

challenges have not been explored extensively yet. Data-driven methods are generally neither simple to calculate nor easy to parameterize. All the methods also differ in the speed of instability detection, which is not explicitly considered here. Some information can be found in [33].

The general conclusion is that no single existing method can successfully evaluate short-term instability for various systems and events in modern power systems. Most of the currently available methods are designed for conventional power systems and conventional power system dynamics. Therefore, they largely fall short in evaluating the short-term instabilities of modern power systems where dynamics are much more complex. Some methods are promising, however, they still require additional improvements. Furthermore, computational complexity should be carefully addressed, as every second used to evaluate the system stability is a second less for potential emergency control strategies to be deployed. Finally, broadly implementable methods without extensive case-by-case parametrization are more desirable.

2.5. CONCLUDING REMARKS

As power systems evolve from conventional to modern, so does the manner in which power system instability manifests itself. This is particularly true for voltage stability, which is directly affected by an increase in (often remotely located) renewable generation and displacement of robust synchronous generation. Therefore, how we understand and evaluate voltage stability needs to evolve accordingly, to accurately evaluate and preserve system resilience.

This also applies to short-term voltage stability, which becomes increasingly complex, faster, and more intricate to analyze. Furthermore, other system dynamics in a similar time frame often intertwine with short-term voltage stability. These two trends are explored further in [Chapter 4](#). The findings generally indicate that a more holistic evaluation approach is preferable. However, the present experience in short-term stability evaluation typically focuses on the analysis, quantification, and prediction of instability mechanisms individually. This may not be optimal, considering intertwined voltage dynamics seen more commonly in modern power systems. The quantification of various types of short-term instabilities is preferred and necessary to preserve the stability of renewables-driven power grids in different operational scenarios. The effects should be quantified and accurately predicted before any intelligent preventive and corrective strategies can be introduced. A method that fulfils all these conditions would provide enormous benefits to the modern power grid dynamic vulnerability assessment, and it is an interesting advancement consideration. This topic is tackled further in [Chapter 5](#).

Furthermore, voltage resilience and system strength are directly related to the likelihood of voltage instability. Therefore, it becomes important to understand the relation between voltage stability and system strength and how the two can be accurately evaluated in conventional and modern power systems. This will be discussed in the following chapter.

REFERENCES

- [1] N. Hatziaargyriou, J. Milanovic, C. Rahmann, V. Ajarapu, C. Canizares, I. Erlich, D. Hill, I. Hiskens, I. Kamwa, B. Pal, P. Pourbeik, J. Sanchez-Gasca, A. Stankovic, T. Van Cutsem, V. Vittal, and C. Vournas. “Definition and Classification of Power System Stability – Revisited & Extended”. In: *IEEE Transactions on Power Systems* 36.4 (July 2021), pp. 3271–3281. ISSN: 0885-8950. DOI: [10.1109/TPWRS.2020.3041774](https://doi.org/10.1109/TPWRS.2020.3041774).
- [2] IEEE PES-TR77. *Stability definitions and characterization of dynamic behavior in systems with high penetration of power electronic interfaced technologies*. Tech. rep. IEEE Power & Energy Society, May 2020. URL: https://resourcecenter.ieee-pes.org/publications/technical-reports/PES_TP_TR77_PSDP_STABILITY_051320.html.
- [3] J. Shair, H. Li, J. Hu, and X. Xie. “Power system stability issues, classifications and research prospects in the context of high-penetration of renewables and power electronics”. In: *Renewable and Sustainable Energy Reviews* 145 (July 2021), p. 111111. ISSN: 13640321. DOI: [10.1016/j.rser.2021.111111](https://doi.org/10.1016/j.rser.2021.111111).
- [4] *Guide To International Power Frequencies*. URL: <https://powersystemsinternational.com/guide-to-international-power-frequencies/>.
- [5] V. Sewdien. “Sub synchronous oscillations in modern transmission grids Design and validation of novel concepts for mitigating adverse dfig-ssr interactions”. PhD thesis. Delft: Delft University of Technology, June 2021. URL: <https://doi.org/10.4233/uuid:8b23ce5e-fd8c-4475-972d-bc50d7a2df1a>.
- [6] *IEEE PES-TR109: Evaluation of Voltage Stability Assessment Methodologies in Transmission Systems*. Tech. rep. IEEE Power & Energy Society, May 2023. URL: https://resourcecenter.ieee-pes.org/publications/technical-reports/PES_TP_TR109_PSDP_52223.html.
- [7] W. C. Taylor. *Power System Voltage Stability*. McGraw-Hill, 1994.
- [8] J. Matevosyan et al. “A Future With Inverter-Based Resources”. In: *IEEE Power&Energy Society: The Future Balancing Act - High VRE Penetration and Energy System Integration* (Nov. 2021). URL: https://resourcecenter.ieee-pes.org/publications/power-and-energy-magazine/PES_TP_MAG_PE_V19_N6.html.
- [9] National Grid ESO. *Operability Strategy Report*. Tech. rep. Dec. 2022. URL: <https://www.nationalgrideso.com/research-and-publications/system-operability-framework-sof>.
- [10] T. Cutsem and C. Vournas. *Voltage Stability of Electric Power Systems*. Boston, MA: Springer US, 1998. ISBN: 978-0-387-75535-9. DOI: [10.1007/978-0-387-75536-6](https://doi.org/10.1007/978-0-387-75536-6).
- [11] A. Boričić, J. L. R. Torres, and M. Popov. “Comprehensive Review of Short-Term Voltage Stability Evaluation Methods in Modern Power Systems”. In: *Energies* 14.14 (July 2021), p. 4076. ISSN: 1996-1073. DOI: [10.3390/en14144076](https://doi.org/10.3390/en14144076).
- [12] S. Adhikari, J. Schoene, N. Gurung, and A. Mogilevsky. “Fault Induced Delayed Voltage Recovery (FIDVR): Modeling and Guidelines”. In: *2019 IEEE Power & Energy Society General Meeting (PESGM)*. IEEE, Aug. 2019, pp. 1–5. ISBN: 978-1-7281-1981-6. DOI: [10.1109/PESGM40551.2019.8973440](https://doi.org/10.1109/PESGM40551.2019.8973440).
- [13] A. Boričić, J. L. R. Torres, and M. Popov. “Fundamental study on the influence of dynamic load and distributed energy resources on power system short-term voltage stability”. In: *International Journal of Electrical Power & Energy Systems* 131 (Oct. 2021), p. 107141. ISSN: 01420615. DOI: [10.1016/j.ijepes.2021.107141](https://doi.org/10.1016/j.ijepes.2021.107141).

- [14] R. Venkatraman, S. K. Khaitan, and V. Ajarapu. "Impact of Distribution Generation Penetration on Power System Dynamics considering Voltage Ride-Through Requirements". In: *2018 IEEE Power & Energy Society General Meeting (PESGM)*. IEEE, Aug. 2018, pp. 1–5. ISBN: 978-1-5386-7703-2. DOI: [10.1109/PESGM.2018.8585776](https://doi.org/10.1109/PESGM.2018.8585776).
- [15] Y. Cheng, L. Fan, J. Rose, S.-H. Huang, J. Schmall, X. Wang, X. Xie, J. Shair, J. R. Ramamurthy, N. Modi, C. Li, C. Wang, S. Shah, B. Pal, Z. Miao, A. Isaacs, J. Mahseredjian, and J. Zhou. "Real-World Subsynchronous Oscillation Events in Power Grids With High Penetrations of Inverter-Based Resources". In: *IEEE Transactions on Power Systems* 38.1 (Jan. 2023), pp. 316–330. ISSN: 0885-8950. DOI: [10.1109/TPWRS.2022.3161418](https://doi.org/10.1109/TPWRS.2022.3161418).
- [16] A. Boricic, J. L. R. Torres, and M. Popov. "Quantifying the Severity of Short-term Instability Voltage Deviations". In: *2022 International Conference on Smart Energy Systems and Technologies (SEST)*. IEEE, Sept. 2022, pp. 1–6. ISBN: 978-1-6654-0557-7. DOI: [10.1109/SEST53650.2022.9898503](https://doi.org/10.1109/SEST53650.2022.9898503).
- [17] H. Ge, Q. Guo, H. Sun, B. Wang, B. Zhang, J. Liu, Y. Yang, and F. Qian. "An Improved Real-Time Short-Term Voltage Stability Monitoring Method Based on Phase Rectification". In: *IEEE Transactions on Power Systems* 33.1 (Jan. 2018), pp. 1068–1070. ISSN: 0885-8950. DOI: [10.1109/TPWRS.2017.2688129](https://doi.org/10.1109/TPWRS.2017.2688129).
- [18] S. Dasgupta, M. Paramasivam, U. Vaidya, and V. Ajarapu. "Real-Time Monitoring of Short-Term Voltage Stability Using PMU Data". In: *IEEE Transactions on Power Systems* 28.4 (Nov. 2013), pp. 3702–3711. ISSN: 0885-8950. DOI: [10.1109/TPWRS.2013.2258946](https://doi.org/10.1109/TPWRS.2013.2258946).
- [19] S. Dasgupta, M. Paramasivam, U. Vaidya, and V. Ajarapu. "PMU-Based Model-Free Approach for Real-Time Rotor Angle Monitoring". In: *IEEE Transactions on Power Systems* 30.5 (Sept. 2015), pp. 2818–2819. ISSN: 0885-8950. DOI: [10.1109/TPWRS.2014.2357212](https://doi.org/10.1109/TPWRS.2014.2357212).
- [20] S. Wei, M. Yang, J. Qi, J. Wang, S. Ma, and X. Han. "Model-Free MLE Estimation for Online Rotor Angle Stability Assessment With PMU Data". In: *IEEE Transactions on Power Systems* 33.3 (May 2018), pp. 2463–2476. ISSN: 0885-8950. DOI: [10.1109/TPWRS.2017.2761598](https://doi.org/10.1109/TPWRS.2017.2761598).
- [21] S. K. Khaitan. "THRUST: A Lyapunov exponents based robust stability analysis method for power systems". In: *2017 North American Power Symposium (NAPS)*. IEEE, Sept. 2017, pp. 1–6. ISBN: 978-1-5386-2699-3. DOI: [10.1109/NAPS.2017.8107395](https://doi.org/10.1109/NAPS.2017.8107395).
- [22] A. Safavizadeh, M. Kordi, F. Eghtedarnia, R. Torkzadeh, and H. Marzooghi. "Framework for real-time short-term stability assessment of power systems using PMU measurements". In: *IET Generation, Transmission & Distribution* 13.15 (Aug. 2019), pp. 3433–3442. ISSN: 1751-8695. DOI: [10.1049/iet-gtd.2018.5579](https://doi.org/10.1049/iet-gtd.2018.5579).
- [23] Y. Xu, Z. Y. Dong, K. Meng, W. F. Yao, R. Zhang, and K. P. Wong. "Multi-Objective Dynamic VAR Planning Against Short-Term Voltage Instability Using a Decomposition-Based Evolutionary Algorithm". In: *IEEE Transactions on Power Systems* 29.6 (Nov. 2014), pp. 2813–2822. ISSN: 0885-8950. DOI: [10.1109/TPWRS.2014.2310733](https://doi.org/10.1109/TPWRS.2014.2310733).
- [24] Y. Xu, R. Zhang, J. Zhao, Z. Y. Dong, D. Wang, H. Yang, and K. P. Wong. "Assessing Short-Term Voltage Stability of Electric Power Systems by a Hierarchical Intelligent System". In: *IEEE Transactions on Neural Networks and Learning Systems* 27.8 (Aug. 2016), pp. 1686–1696. ISSN: 2162-237X. DOI: [10.1109/TNNLS.2015.2441706](https://doi.org/10.1109/TNNLS.2015.2441706).
- [25] S. Wildenhues, J. L. Rueda, and I. Erlich. "Optimal Allocation and Sizing of Dynamic Var Sources Using Heuristic Optimization". In: *IEEE Transactions on Power Systems* 30.5 (Sept. 2015), pp. 2538–2546. ISSN: 0885-8950. DOI: [10.1109/TPWRS.2014.2361153](https://doi.org/10.1109/TPWRS.2014.2361153).
- [26] M. Glavic, D. Novosel, E. Heredia, D. Kosterev, A. Salazar, F. Habibi-Ashrafi, and M. Donnelly. "See It Fast to Keep Calm: Real-Time Voltage Control Under Stressed Conditions". In: *IEEE Power and Energy Magazine* 10.4 (July 2012), pp. 43–55. ISSN: 1540-7977. DOI: [10.1109/MPE.2012.2196332](https://doi.org/10.1109/MPE.2012.2196332).
- [27] C. D. Vournas, C. Lambrou, and M. Kanatas. "Application of Local Autonomous Protection Against Voltage Instability to IEEE Test System". In: *IEEE Transactions on Power Systems* 31.4 (July 2016), pp. 3300–3308. ISSN: 0885-8950. DOI: [10.1109/TPWRS.2015.2489764](https://doi.org/10.1109/TPWRS.2015.2489764).
- [28] C. D. Vournas, C. Lambrou, and P. Mandoulidis. "Voltage Stability Monitoring From a Transmission Bus PMU". In: *IEEE Transactions on Power Systems* 32.4 (July 2017), pp. 3266–3274. ISSN: 0885-8950. DOI: [10.1109/TPWRS.2016.2629495](https://doi.org/10.1109/TPWRS.2016.2629495).

- [29] P. Mandoulidis and C. Vournas. "A PMU-based real-time estimation of voltage stability and margin". In: *Electric Power Systems Research* 178 (Jan. 2020), p. 106008. ISSN: 03787796. DOI: [10.1016/j.epsr.2019.106008](https://doi.org/10.1016/j.epsr.2019.106008).
- [30] M. Glavic and T. Van Cutsem. "A short survey of methods for voltage instability detection". In: *2011 IEEE Power and Energy Society General Meeting*. IEEE, July 2011, pp. 1–8. ISBN: 978-1-4577-1000-1. DOI: [10.1109/PES.2011.6039311](https://doi.org/10.1109/PES.2011.6039311).
- [31] A. Tiwari and V. Ajarapu. "Optimal Allocation of Dynamic VAR Support Using Mixed Integer Dynamic Optimization". In: *IEEE Transactions on Power Systems* 26.1 (Feb. 2011), pp. 305–314. ISSN: 0885-8950. DOI: [10.1109/TPWRS.2010.2051342](https://doi.org/10.1109/TPWRS.2010.2051342).
- [32] K. Seethalekshmi, S. N. Singh, and S. C. Srivastava. "A Synchrophasor Assisted Frequency and Voltage Stability Based Load Shedding Scheme for Self-Healing of Power System". In: *IEEE Transactions on Smart Grid* 2.2 (June 2011), pp. 221–230. ISSN: 1949-3053. DOI: [10.1109/TSG.2011.2113361](https://doi.org/10.1109/TSG.2011.2113361).
- [33] M. Aslanian, M. E. Hamedani-Golshan, H. Haes Alhelou, and P. Siano. "Analyzing Six Indices for Online Short-Term Voltage Stability Monitoring in Power Systems". In: *Applied Sciences* 10.12 (June 2020), p. 4200. ISSN: 2076-3417. DOI: [10.3390/app10124200](https://doi.org/10.3390/app10124200).
- [34] L. Zhu, C. Lu, and Y. Sun. "Time Series Shapelet Classification Based Online Short-Term Voltage Stability Assessment". In: *IEEE Transactions on Power Systems* 31.2 (Mar. 2016), pp. 1430–1439. ISSN: 0885-8950. DOI: [10.1109/TPWRS.2015.2413895](https://doi.org/10.1109/TPWRS.2015.2413895).
- [35] A. Joseph, M. Cvetkovic, and P. Palensky. "Predictive Mitigation of Short Term Voltage Instability Using a Faster Than Real-Time Digital Replica". In: *2018 IEEE PES Innovative Smart Grid Technologies Conference Europe (ISGT-Europe)*. IEEE, Oct. 2018, pp. 1–6. ISBN: 978-1-5386-4505-5. DOI: [10.1109/ISGTEurope.2018.8571803](https://doi.org/10.1109/ISGTEurope.2018.8571803).
- [36] L. Zhu, C. Lu, and Y. Luo. "Time Series Data-Driven Batch Assessment of Power System Short-Term Voltage Security". In: *IEEE Transactions on Industrial Informatics* 16.12 (Dec. 2020), pp. 7306–7317. ISSN: 1551-3203. DOI: [10.1109/TII.2020.2977456](https://doi.org/10.1109/TII.2020.2977456).
- [37] Y. Zhang, Y. Xu, R. Zhang, and Z. Y. Dong. "A Missing-Data Tolerant Method for Data-Driven Short-Term Voltage Stability Assessment of Power Systems". In: *IEEE Transactions on Smart Grid* 10.5 (Sept. 2019), pp. 5663–5674. ISSN: 1949-3053. DOI: [10.1109/TSG.2018.2889788](https://doi.org/10.1109/TSG.2018.2889788).
- [38] Y. Zhang, Y. Xu, Z. Y. Dong, and R. Zhang. "A Hierarchical Self-Adaptive Data-Analytics Method for Real-Time Power System Short-Term Voltage Stability Assessment". In: *IEEE Transactions on Industrial Informatics* 15.1 (Jan. 2019), pp. 74–84. ISSN: 1551-3203. DOI: [10.1109/TII.2018.2829818](https://doi.org/10.1109/TII.2018.2829818).
- [39] L. Zhu, C. Lu, Z. Y. Dong, and C. Hong. "Imbalance Learning Machine-Based Power System Short-Term Voltage Stability Assessment". In: *IEEE Transactions on Industrial Informatics* 13.5 (Oct. 2017), pp. 2533–2543. ISSN: 1551-3203. DOI: [10.1109/TII.2017.2696534](https://doi.org/10.1109/TII.2017.2696534).
- [40] L. Zhu, C. Lu, I. Kamwa, and H. Zeng. "Spatial-Temporal Feature Learning in Smart Grids: A Case Study on Short-Term Voltage Stability Assessment". In: *IEEE Transactions on Industrial Informatics* 16.3 (Mar. 2020), pp. 1470–1482. ISSN: 1551-3203. DOI: [10.1109/TII.2018.2873605](https://doi.org/10.1109/TII.2018.2873605).
- [41] Y. Luo, C. Lu, and L. Zhu. "Short-Term Voltage Stability Assessment Based on Local Autopattern Discovery". In: *2019 IEEE Sustainable Power and Energy Conference (ISPEC)*. IEEE, Nov. 2019, pp. 2072–2077. ISBN: 978-1-7281-4930-1. DOI: [10.1109/ISPEC48194.2019.8975090](https://doi.org/10.1109/ISPEC48194.2019.8975090).
- [42] J. Liu, S. Wu, F. Qian, Y. Yang, G. Luo, Y. Lou, Z. Zhang, and L. Tang. "Rapid evaluation of short-term voltage stability considering integration of renewable power generations". In: *2017 IEEE Conference on Energy Internet and Energy System Integration (EI2)*. IEEE, Nov. 2017, pp. 1–4. ISBN: 978-1-5386-1427-3. DOI: [10.1109/EI2.2017.8245762](https://doi.org/10.1109/EI2.2017.8245762).
- [43] J. Tianxia, G. Zhuoyuan, S. Huadong, G. Pengfei, Y. Jun, X. Shiyun, and Z. Bing. "Data-driven Research Method For Power System Stability Detection". In: *2018 International Conference on Power System Technology (POWERCON)*. IEEE, Nov. 2018, pp. 3061–3069. ISBN: 978-1-5386-6461-2. DOI: [10.1109/POWERCON.2018.8601601](https://doi.org/10.1109/POWERCON.2018.8601601).

3

SYSTEM STRENGTH AND GRID WEAKNESS

Everything should be made as simple as possible, but not simpler.

- Albert Einstein, Theoretical Physicist (1879-1955)

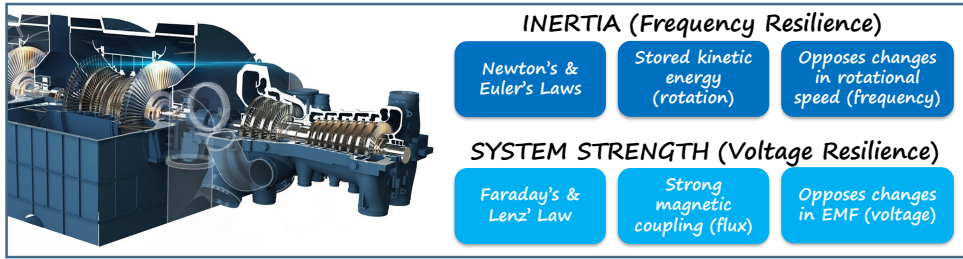
System strength has been receiving more attention as the phase-out of fossil-based synchronous generation advances further. Grids or grid sections are more frequently referred to as weak, especially in remote locations without synchronous generation proximity. Conversely, due to weather conditions and land availability, such remote grid locations often turn out to be very compelling for renewable generation. This makes grid strength evaluation highly important to ensure secure system operation and avoid system instabilities discussed in the previous chapter.

However, as more renewable generation is integrated into power systems through power-electronics converters, the system strength concept of conventional power systems is supposed to evolve as it is becoming less applicable and inaccurate in modern IBR-rich power systems. This chapter explores what system strength is in both conventional and modern power systems, and how it can be evaluated in both steady- and dynamic-state operations. Furthermore, its close relation to system stability and vulnerability is thoroughly investigated.

3.1. SYSTEM STRENGTH FUNDAMENTALS

As discussed in [Chapter 1](#), two main parameters crucial for the power system operation are the frequency and the voltage. Both are conventionally provided to the systems by synchronous generators. Furthermore, synchronous generators also provide natural system resilience by opposing the changes in frequency and voltage; the two effects known as *inertia* and *system strength*, respectively. This resilience is illustrated and described further in [Figure 3.1](#).

Parts of this chapter have been published in peer-reviewed articles and/or conference proceedings. See [The List of Publications](#) section for more details.



3

Figure 3.1.: Synchronous machines powered by turbines (left, courtesy of GE) provide resilience in terms of inertia and system strength (right).

Synchronous generators and turbines form a large rotating mass that weighs tens to hundreds of tons. Such rotating mass contains enormous amounts of kinetic energy. Once an electrical disturbance occurs in the grid, it also manifests electromechanically, attempting to accelerate (or decelerate) the rotation of the machine. The stored kinetic energy is hereby released, opposing the change of motion. Therefore, the rotational speed, and consequently electrical frequency, tend to resist changes and limit disturbances. This effect is known as (*rotational*) *inertia*.

A body remains at rest, or in motion at a constant speed in a straight line¹, unless acted upon by a force.

- Isaac Newton, Newton's first law (of inertia) [1]

Unlike inertia, system strength has nothing to do with the massive rotating machinery and the kinetic energy of a synchronous generator. To provide system strength, a synchronous generator does not even have to produce any active power or be connected to the turbine. The only requirement is that it is *synchronized* (electromagnetically coupled) with the grid. The effect of system strength is purely electromagnetic and comes from the magnetic flux between the stator and the rotor of a generator. When a voltage disturbance occurs, the change in voltage is electromagnetically resisted and limited in size by the windings of a synchronous generator. This process, while analogous, is completely distinct from how the rotational inertia resists changes in power system frequency.

Nature abhors a change in flux...

Faraday induction is a kind of "inertial" phenomenon: A conducting loop "likes" to maintain a constant flux through it; if you try to change the flux, the loop responds by sending a current around in such a direction as to frustrate your efforts...

Lenz's law tells you the direction of this flow.

- David J. Griffiths, Introduction to Electrodynamics [2]

As synchronous machines in fossil fuel-based power plants are phased out and replaced by renewable energy sources (RES), the natural resilience described in

¹Newton's first law is extended by Leonhard Euler to consider rotational rigid bodies and their *moment of inertia* (*rotational inertia*). Since synchronous machines spin, rotational inertia is of interest.

Figure 3.1 is reduced as well. This occurs since RES do not have a large rotating mass (inertia) nor strong electromagnetic coupling with the grid (system strength), as shown in Figures 1.7 and 3.1. This chapter focuses on the reduced system strength, i.e. the consequentially lower voltage resilience (higher vulnerability).

To better describe system strength, an analogy is shown in Figure 3.2 [3]. Two objects with different levels of resilience (robustness), a rock and a jelly, are shown. Assuming a small disturbance, i.e., if someone gently touches the rock, very little happens, and other objects in contact with the rock barely notice the disturbance. However, when the same disturbance is applied to the jelly, it will begin to wobble as vibrations propagate through it. Jelly is thus less resilient (more vulnerable) to disturbances and experiences more consequences from them. Relating this analogy to power systems, rock (jelly) would be a system with many (few) synchronous machines to provide system strength. The voltage of such a system is more sensitive and vulnerable, and the system itself has lower voltage stability margins. This is the main symptom of low system strength.



Figure 3.2.: Rock and jelly analogy for system strength.

There is another interesting consequence of lower resilience (i.e., the jelly). Imagine a situation where one person touches the jelly (applies a disturbance) while others are in contact with it. As the jelly begins to wobble, others may try to counter the wobbles (try to stabilize the jelly). However, as all of them try to do the same simultaneously, they may in fact *worsen* the situation and cause further wobbles unless their actions are perfectly synchronized. Translating this illustration to power systems, when a disturbance occurs, various inverter-based resources may react to it in an attempt to stabilize the system. Just as in the example of a jelly, unless perfectly coordinated and synchronized, such reactions may result in exacerbation of the situation which often reflects in undesired control interactions and oscillations. This is essentially why converter-driven interactions, oscillations, and instabilities become *more likely* in weak grids, as described in Chapter 2 and discussed further in this section. This is the second common symptom of low system strength.

Another analogy is shown in Figure 3.3 [4, 5]. In this example, a strong (weak) system is illustrated as a trampoline with many (few) springs. If one jumps on the trampoline (analogy to a grid disturbance such as a generator trip or short-circuit), the trampoline (grid) is relatively stiff and pushes back (recovers). If some springs are disconnected from the frame (fewer synchronous machines), the trampoline (grid) strength is reduced. While the trampoline still appears flat (i.e. the grid will continue to operate normally in the steady state), if one jumps on the trampoline (a large disturbance occurs) it may no longer push back and could collapse.

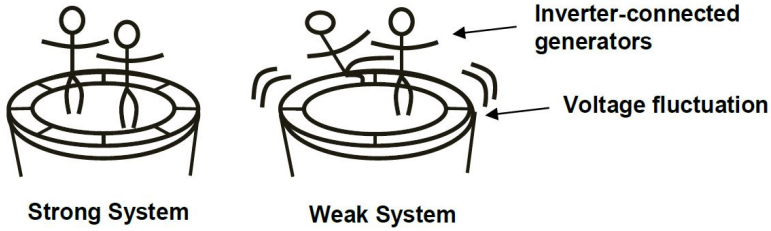


Figure 3.3.: Trampoline analogy for system strength.

Furthermore, in a stronger (weaker) system, the trampoline movements will be slight (severe), and it will be easy (difficult) to keep balance. Therefore, a disturbance in a weaker trampoline (with fewer springs) has more chance of causing one to lose balance, fall off, and cause more (cascading) disturbances. Translating this analogy to power systems, weaker systems are vulnerable to voltage fluctuations that may lead to cascading disturbances and loss of generators and loads, resulting in further cascading and blackout risks. Additionally, weaker systems are more prone to control interactions and oscillations as discussed in [Chapter 2](#), and further in this chapter.

3.1.1. SYSTEM STRENGTH DEFINITION

Various definitions of system strength are available. In conventional power systems, it was a synonym for short-circuit capacity (S_{sc}), which is discussed in the next section. Presently, the commonly used definitions express system strength as the sensitivity of voltage to variations in the current injection [6]. In other words, system strength is understood as voltage *stiffness* [7], analogous to inertia and frequency deviations. Others define system strength as a broader term comprising both inertia and voltage stiffness [8]. Finally, system strength is discussed both in terms of steady-state operation [9], as well as in the dynamic state as the size of the change in voltage following a disturbance [10]. Such a wide dispersion of definitions indicates that classification and understanding of system strength are still maturing.

In an attempt to accurately and concisely reflect all the relevant dimensions of system strength as seen in this thesis, a new definition is proposed as follows:

System strength refers to the ability of a power system to maintain stable voltages in both steady- and dynamic-state and to avoid related instabilities and cascading. Symptoms of low system strength include reduced voltage stability limits and maximum power transfer, higher voltage sensitivity, as well as elevated susceptibility to converter-driven interactions, oscillations, desynchronization, and instabilities.

It is important to highlight that besides the defined aspects, low system strength also introduces challenges for power system protection due to lower and non-conventional fault currents². Moreover, lower system strength is known to result in amplified and more widespread voltage dips, increased harmonic distortions,

²I spent some time on this very interesting and important topic during my Master thesis research, in cooperation with my former colleagues at ABB (Hitachi), KTH, and TU/e [11, 12].

flickers, and other power quality aspects [10, 13]. The aspects of power quality and protection are not directly related to the system stability and vulnerability and are therefore out of the scope of the system strength discussion in this thesis.

3.1.2. SYSTEM STRENGTH CLASSIFICATION

As power systems transition from conventional to modern and incorporate more inverter-based resources, the system strength concept evolves and brings distinctive operational and stability challenges. These may consequently require different considerations for modelling, evaluation, and mitigation. Bearing this in mind, this subsection proposes a new classification of system strength: (i) *Steady-State System Strength*; and (ii) *Dynamic-State System Strength*, described in Figure 3.4. The classification is proposed in a way that closely corresponds to the most recent system stability classification presented in Chapter 2 and Figure 2.2.

Proposed System Strength Classification	
Steady-state System Strength	Dynamic-state System Strength
Mainly deals with:	
<ul style="list-style-type: none"> • Steady state system operation • Long-term stability and slow interactions • Stability when subjected to small disturbances • Linear operation around nominal voltage 	<ul style="list-style-type: none"> • Dynamic state system operation • Short-term (transient) stability and fast interactions • Stability when subjected to large disturbances • Non-linear operation with large voltage deviations
Factors that should be considered:	
<ul style="list-style-type: none"> • Short-circuit capacity (Thevenin impedance) • Impact of loads, grid X/R ratio, Q-support, and PLL in weak grids • Influence of (multiple) IBR(s) and respective transfer impedances • Secondary short-circuit support (e.g. synchronous condensers) • RMS modelling often sufficient (except in very weak grids) 	<ul style="list-style-type: none"> • Impedances' non-linearity (converter saturation) • IBRs' FRT and interactions with post-fault voltage dynamics • Large-signal stability and interactions of control loops • Possible protection maloperation and unintentional IBR tripping • Advanced RMS models needed (often supported by EMT models)

Figure 3.4.: The proposed system strength classification, the scope of the two sub-classes, and the relevant factors to be considered [14].

The following sections extensively discuss the need for the proposed classification and differentiation between steady- and dynamic-state aspects. Furthermore, the implications for understanding and evaluation of system strength are presented. Finally, the consequent challenges in weak grids with a high penetration of IBRs are discussed.

3.2. STEADY-STATE SYSTEM STRENGTH

Steady-state system strength deals with the steady-state operation around nominal voltage, assuming only small disturbances subjected to model linearization. Therefore, it deals with the maximum power transfer during steady-state operation and stable long-term voltages. Several important factors play a role in evaluating steady-state system strength, as listed in Figure 3.4. These are discussed next, followed by the analytical evaluation of their impact on system strength in the following subsections.

- Short-circuit capacity / Thevenin impedance

Since the topic of steady-state system strength deals with small disturbances, it can be analyzed by linearizing the model with Thevenin equivalents. Therefore, concepts such as short-circuit capacity and grid impedance play a central role in steady-state system strength and maximum power transfer (as illustrated in [Chapter 2](#)). However, contrary to the conventional systems dominated by synchronous generation, short-circuit capacity cannot be directly equated with system strength in modern systems. Instead, it only provides one dimension of system strength. This will be explored in more detail for modern power systems in the following subsection.

- Presence of a load

The presence of local load at a bus implies that less power is transferred towards the rest of the system. This meaningfully changes the effective steady-state system strength, maximum power transfer, and voltage stability limits of the system. With renewables adopted in both load-free and load-rich areas in modern power systems, consequent system strength differences ought to be considered. This will be explored in more detail in the following subsection.

- Grid X/R ratio

While it is common to assume that the equivalent system impedance is predominantly reactive, it is not always accurate. IBRs are frequently integrated into grid locations where not only system strength is low, but also the X/R ratio³ of the grid. As the X/R ratio drops, voltage sensitivity to active power ($\partial V/\partial P$) increases, while $\partial V/\partial Q$ decreases, with all else equal. This implies that for buses in low-X/R grid sections, the common $P-\theta$ and $Q-V$ dependence⁴ changes. The (change of) active power affects the voltage magnitude more, and reactive power becomes less capable of controlling the bus voltage. The simplification of ignoring grid resistance may affect the accuracy of system strength evaluation, particularly in weaker grids where the X/R ratio plays a larger role in system strength. This will be explored in more detail in the following subsection.

- Operating voltage and secondary voltage support

System strength is typically calculated with nominal voltage values. However, operating voltage varies across the grid and over time. Higher (lower) operating voltage results in a higher (lower) maximum active power transfer within the voltage stability limits. Furthermore, the impact of various voltage-supporting elements such as capacitors, FACTS devices, and synchronous condensers (SC) on system strength is often neglected. Such devices can, however, introduce a meaningful improvement in system strength, and are common solutions applied in the industry. This will also be explored in more detail in the following subsection.

³The ratio of reactance and resistance in the grid impedance.

⁴See [Chapter 2](#).

- Type of generator and its controls

Weak system operation can typically manifest itself in one of two possible stability concerns: voltage instability or converter interactions/instability.

Voltage instability is closely related to maximum power transfer. While synchronous generators have a strong electromagnetic coupling with the grid, IBRs are inherently different, as illustrated in [Figures 1.7](#) and [3.1](#). The main difference is due to the use of a Phase-Locked Loop (PLL). PLL is a control loop that synchronizes an IBR with the grid by relying on the evaluation of voltage angle and frequency. Therefore, IBRs (unlike SGs) fundamentally rely on the strength of the voltage waveform at the point of connection (PoC). This affects the inherent voltage stability limitations, which will be extensively discussed in the next sections.

Furthermore, even when the voltage stability margin of an IBR is positive, oscillations or instability may occur. This has to do with the voltage sensitivity (vulnerability) of weak grids (high $\partial V/\partial I$), where IBRs' current injection has a high impact on the PoC voltage. In a weak grid, this current injection notably affects the same voltage the PLL is trying to measure, which may result in oscillations and/or controller instability⁵. Therefore, in weak grids, before the static voltage stability limit is reached, oscillations and/or controller instability (also known as small-signal instability) become a common symptom of weak grids [[15](#), [16](#)]. It is important to note that such a symptom is not necessarily mitigated by grid strengthening; an often better and more direct approach is to tune the IBR controls for more optimal weak-grid operation⁶. This may allow for the operation closer to the steady-state voltage stability limit and avoid the need for expensive grid strengthening.

- Impact of multiple IBRs

If multiple IBRs "share" the same (or electrically close) point of connection, they are all relying on (approximately) the same grid voltage, injecting current accordingly. In the case of a weak grid (high voltage sensitivity), these current injections notably affect the voltage. Since the IBRs will often have slightly different control parameters (e.g., gains, time constants), and transfer impedances, the result can be undesired control interactions and potentially small-signal instability.

Suppose the goal is to pinpoint the likelihood of converter-driven interactions. In that case, the voltage stability margin is only one of the aspects, directly related to grid vulnerability (think of the fewer springs in [Figure 3.3](#)). The other aspects need to be related to the number of IBRs sharing the same network bus (or area), as well as their control parameters (i.e., characteristics and actions of individuals sharing the trampoline). This aspect will be briefly discussed, however, it is not the main focus of steady-state system strength evaluation in this thesis. Instead, the focus lies on accurate grid vulnerability evaluation in terms of voltage resilience and stability. These two aspects, while related, are fundamentally different from the underlying physics perspective, and are therefore treated separately in this thesis.

⁵An analogy to this phenomenon is the speaker/microphone positive-feedback loop, which can result in an amplified high-pitch noise we're all familiar with.

⁶A common solution is to slow down IBR controls in weak grids and reduce PLL gains. Furthermore, the parameters of the inner current and DC-link voltage control loops can also be adjusted [[15–19](#)].

3.2.1. EXISTING EVALUATION METHODS

When generation or load needs to be connected to the grid, one must ensure that the point of connection (PoC) is strong enough for such a connection. This strength at the PoC is typically evaluated from the perspective of *Short-Circuit Capacity* (or power), S_{sc} [20]. To understand S_{sc} and its relation to system strength in conventional and modern power systems, a simple but illustrative system in [Figure 3.5](#) is shown. The system depicts a source (in this case an IBR) connected to the bus i , while a Thevenin source represents the rest of the system.

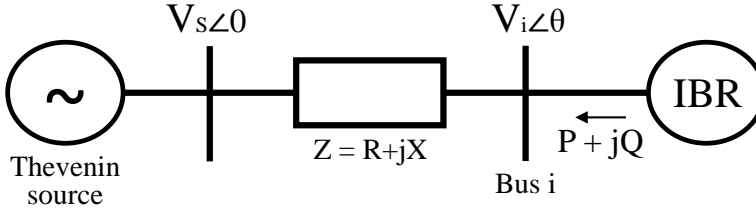


Figure 3.5.: IBR connected to a grid represented by Thevenin's equivalent.

The voltage at the point of the IBR connection can be expressed as a function of Thevenin's voltage and the voltage drop across the impedance.

$$\underline{V}_i = \underline{V}_s - \underline{Z}\underline{I}_i \quad (3.1)$$

For a small change in IBR current $\Delta \underline{I}_i$, the consequent change in voltage can be calculated as follows:

$$\Delta \underline{V}_i + \underline{V}_i = \underline{V}_s - \underline{Z}(\underline{I}_i + \Delta \underline{I}_i) \quad (3.2)$$

$$\Delta \underline{V}_i = -\underline{Z}\Delta \underline{I}_i \quad \rightarrow \quad \underline{Z} = -\frac{\Delta \underline{V}_i}{\Delta \underline{I}_i} \quad (3.3)$$

From [Equation \(3.3\)](#), it can be seen that Thevenin's impedance is directly linked to the relative change of voltage per change of current, which is often described as *voltage sensitivity*. Voltage sensitivity provides information on system strength; when $\Delta V/\Delta I$ is high, it means that the bus voltage is very sensitive (susceptible) to the changes in infeed current (power), often called a “weak bus”. In other words, the current (power) injected by the IBR in [Figure 3.5](#) will have a big impact on the bus i voltage V_i . If this is not the case, the grid can be described as strong.

Voltage sensitivity can be further expressed from the perspective of S_{sc} , as shown in [Equations \(3.4\) and \(3.5\)](#), where I_{sc_i} is the short-circuit current that would flow through the bus in the case of a zero-impedance three-phase short-circuit fault.

$$S_{sc_i} = V_i I_{sc_i} = \frac{V_i^2}{Z} \quad (3.4)$$

$$S_{sc_i} \sim \frac{1}{Z} \sim \frac{\Delta I_i}{\Delta V_i} \quad (3.5)$$

These two expressions reveal a very clear relation between S_{sc} , voltage sensitivity, and consequently system strength. Equation (3.5) depicts the inverse (direct) proportionality between S_{sc} and voltage sensitivity (system strength), and the inverse proportionality between Thevenin's impedance and S_{sc} and system strength. Therefore, buses with relatively high (low) S_{sc} are generally called strong (weak) buses. However, this strength needs to be put into perspective relative to the size of the generating unit requiring connection (e.g., IBR in Figure 3.5). For this purpose, various ratios are defined in the industry and academia, of which the most common ones are discussed further.

SHORT-CIRCUIT RATIO

The S_{sc} concept is hereby expanded further to derive the commonly used *Short-Circuit Ratio* (SCR) [20]. The ratio is defined by Equation (3.6).

$$SCR_i = \frac{S_{sc_i}}{P_{IBR_i}} \quad (3.6)$$

SCR of a bus i is calculated by dividing the short-circuit power at the bus i (S_{sc_i}) with the nominal power of the generating unit connected (P_{IBR} , see Figure 3.5). Such a ratio is very intuitive, relatively easy to calculate, and with a strong physical relation to the maximum power transfer⁷. It is therefore extensively used in power systems to determine system strength value utilized for voltage stability evaluation, renewables or large demand integration, protection coordination, and power quality.

However, the applicability and accuracy of SCR as a measure of modern power systems' strength is questionable. This occurs due to the ongoing shift in generation from dominantly synchronous to inverter-based. Consequently, many new metrics are proposed to attempt to expand SCR applicability to modern grids.

EFFECTIVE SHORT-CIRCUIT RATIO

To expand SCR applicability so that it can also consider shunt capacitance, authors in [21] proposed the *Effective Short-Circuit Ratio* (ESCR). The ratio is shown in Equation (3.7),

$$ESCR_i = \frac{|S_{sc_i} - jQ_{c,i}|}{P_{IBR_i}} \quad (3.7)$$

where S_{sc_i} is the short-circuit capacity of bus i , $Q_{c,i}$ the reactive compensation of the shunt capacitor at PoC, and P_{IBR_i} the active power injected by the IBR.

⁷At least in conventional power systems dominated by synchronous generation. The implications of the increasing share of IBRs on SCR accuracy are discussed in the next section.

WEIGHTED SHORT-CIRCUIT RATIO

Another new metric for system strength quantification of modern grids is the Weighted Short-Circuit Ratio (WSCR) [22]. The ratio is defined in Equation (3.8), where S_{sc_i} is the short-circuit capacity at bus i , P_{IBR_i} is the active power output of the i_{th} IBR and N is the number of IBRs considered to interact fully with each other.

$$WSCR_i = \frac{\sum_{n=i}^N S_{sc_i} P_{IBR_i}}{(\sum_{n=i}^N P_{IBR_i})^2} \quad (3.8)$$

WSCR is an attempt to consider the impact of multiple IBRs in an area and provide a screening method for weak grid symptoms. It is currently being applied by ERCOT⁸ in the Texas grid for the Panhandle region, where $WSCR < 1.5$ is used as an operational threshold value. If the value is lower, RES generation is curtailed to avoid operating the grid too close to the voltage and converter-driven stability limits [23]. The value is determined and validated by performing Electromagnetic Transient (EMT) studies for representative grid scenarios [24]. It is important to note that such a threshold is therefore very system- and scenario-dependent and requires continuous EMT validation [25].

COMPOSITE SHORT-CIRCUIT RATIO

Another similar method that accounts for multiple IBRs is the Composite Short-Circuit Ratio (CSCR) shown in Equation (3.9),

$$CSCR_i = \frac{S_{sc_{comm}}}{\sum_{n=i}^N P_{IBR_i}} \quad (3.9)$$

where $S_{sc_{comm}}$ is the short-circuit power of a fictitious common bus shared by all nearby IBRs, and P_{IBR_i} is the rated power of all IBRs being considered.

CSCR method, originally developed in [4, 26], assumes a composite IBRs' bus by merging together low-voltage sides of plants' transformers. $S_{sc_{comm}}$ is then calculated for such a common composite bus, without considering the contribution from IBRs.

SITE-DEPENDENT SHORT-CIRCUIT RATIO

To evaluate interactions between nearby IBRs and their impact on system strength, the authors of [27] introduced Site-Dependent Short-Circuit Ratio (SDSCR), building up on the original idea of SCR. SDSCR is defined by Equation (3.10).

$$SDSCR_i = \frac{V_{R,i}^2}{(P_{R,i} + \sum_{j \in R, j \neq i} P_{R,j} w_{i,j}) Z_{RR,ii}} \quad ; \quad w_{i,j} = \frac{Z_{RR,ij}}{Z_{RR,ii}} \left(\frac{V_{R,i}}{V_{R,j}} \right)^* \quad (3.10)$$

$V_{R,i}$ is the voltage of the i_{th} busbar with IBR connection, $P_{R,i}$ is the IBRs' active power infeed at the i_{th} bus, and $Z_{RR,ij}$ the corresponding (i, j) element of the system impedance matrix. SDSCR is able to quantify the level of IBRs' interactions

⁸The Electric Reliability Council of Texas, an American organization that operates Texas's electrical grid.

by utilizing information on the actual transfer impedances and active power of IBRs. In [27], it is shown mathematically that SDSCR is a large-grid generalization of SCR, and that it has the same stability thresholds as SCR.

Since the metric can be time-demanding to calculate for large systems, a simplification is introduced in [28], where it was shown that transfer impedances are the most impactful variable in SDSCR calculation. Implementation of the renewable generation uncertainty into the method is explored in [29].

EQUIVALENT SHORT-CIRCUIT RATIO

Another proposed approach is Equivalent Short-Circuit Ratio (E_qSCR)⁹, initially introduced in [20], and sometimes mentioned with different names (e.g. SCRIF¹⁰ [6]).

$$E_qSCR_i = \frac{S_{sc_i}}{(P_i + \sum_{j,i} WPIF_{ji} * P_j)} ; \quad WPIF_{ji} = \frac{\Delta V_j}{\Delta V_i} \quad (3.11)$$

P_i represents the maximum active power of the studied IBR, P_j is the maximum active power of other IBR units, and S_{sc_i} is the network short-circuit contribution to the connection point of the studied converter-connected unit. $WPIF_{ji}$ is the interaction factor between converters j and i , where values represent the electric proximity of other IBRs to the studied IBR bus. A value closer to zero (one) indicates further (closer) electrical connection and thus lower (higher) interactions.

E_qSCR is mathematically and conceptually very similar to SDSCR. However, its implementation is typically based on numerical simulation results rather than using the impedance matrix of the system. $WPIF_{ji}$ can be calculated with power flow simulations by creating a voltage step in the studied bus i . The value is derived by dividing the observed voltage change in the other IBR bus ΔV_j by the voltage change in the studied IBR bus ΔV_i .

VOLTAGE SENSITIVITY

A very different approach is taken in [17, 30], where a voltage sensitivity metric $\partial Q/\partial V$ is mathematically derived based on the voltage and angle stability limitations of IBRs connected to the grid. The final expression is shown in Equation (3.12),

$$\partial Q/\partial V = SCR * \left(2V - \frac{V_{th}}{\sqrt{(1 - \sin^2 \theta)}} \right) \quad (3.12)$$

where V is the voltage of the PoC, V_{th} voltage of the grid Thevenin equivalent, and θ voltage angle at the PoC. $\partial Q/\partial V$ can be also understood as a first derivative of the Q-V curve mentioned in Chapter 2. Theoretically, $\partial Q/\partial V > 0$ is the necessary condition for voltage stability [31, 32]. To apply this method, the authors of [17] suggest plotting P - Q and P - $\partial Q/\partial V$ curves together to locate the maximum power transfer and voltage stability limit, as exemplified in [7, 17].

⁹Sometimes also abbreviated as ESCR, but hereby not to avoid confusion with Effective SCR.

¹⁰Short Circuit Ratio with Interaction Factors.

AVAILABLE FAULT LEVEL

Lastly, another novel approach is currently applied in the AEMO¹¹ grid. The method is termed Available Fault Level (AFL) [33]. To calculate AFL, one first needs to determine the difference between the Synchronous Fault Level (SFL) and the Proxy Fault Level (PFL) [34]. SFL is the short-circuit capacity provided by synchronous machines, i.e. S_{sc} , without considering IBR fault contributions. PFL is a fictive short-circuit value calculated numerically in a power system analysis software, where every IBR has been replaced by a proxy Thevenin equivalence. The impedance of the equivalence is calculated as shown in Equation (3.13), while the voltage source equivalent is set at the nominal level.

$$Z_{IBR} = \frac{1}{|\Delta AFL|} ; \Delta AFL = (-SCR_{withstand} + \alpha) * P_{IBR} \quad (3.13)$$

$SCR_{withstand}$ is the SCR ratio for which the specific IBR is able to operate in a stable manner (it is assumed to have a value of 3 when no better information is available), and α is the stability coefficient (assumed 1.2 as most IBRs have issues operating below $SCR = 1.2$ [34]).

Once SFL and PFL have been determined, AFL is calculated according to Equation (3.14), as illustrated in an example in [34].

$$AFL_{MVA} = SFL - (PFL - SFL) = 2SFL - PFL \quad (3.14)$$

AFL is therefore fundamentally based on SCR and S_{sc} , and is designed so that it takes into account the supply and demand of system strength. Supply is what synchronous machines provide (S_{sc}), while demand is what IBRs "require" to operate in a stable manner (approximated by ΔAFL). With multiple IBRs in proximity, the demand increases, and the "available" grid strength (AFL) is perceived to be lower, limiting further nearby IBR connections.

3.2.2. SUMMARY OF THE EXISTING METHODS AND THEIR LIMITATIONS

Several different methods are introduced in the previous subsections. Here, they are summarized and evaluated based on four important qualitative characteristics that determine the method's suitability for the operation and planning of modern power systems:

- Simplicity of calculation,
- Accuracy when applied in modern grids with IBRs,
- Consideration of loads, capacitors, and X/R ratio,
- Consideration of the impact of multiple nearby IBRs.

Starting with SCR, the most common and broadly applied metric, it is the simplest method in the list. However, as discussed in Chapter 2 and further in the next section, SCR is fundamentally related to the angle stability limits of synchronous

¹¹The Australian Energy Market Operator, operator of a transmission grid in Australia.

machines. This limits its capability in modern grids with an increasing share of IBRs, where voltage stability limits become more stringent. Furthermore, SCR is an approximation that does not account for shunt elements (loads, capacitors) or grid resistance. Finally, the impact of nearby IBRs is ignored. Hence, other metrics are introduced in an attempt to tackle (some of) these limitations.

Regarding ESCR, the only difference compared to SCR is an attempt to include the impact of shunt capacitors. While this makes the metric more accurate in such scenarios, it is found in the next section that ESCR is also a rough approximation without accurate voltage stability limit evaluation. Furthermore, other limitations that apply to SCR are also applicable to ESCR.

Both WSCR and the CSCR methods are slightly more complicated than SCR yet still relatively simple to evaluate. Nevertheless, deciding precisely which IBRs are "interacting" and should be considered when calculating the ratios is a nontrivial and subjective task. Additionally, both methods are in their essence comparable to SCR and focus on synchronous-dominated system stability limitations and fail to consider any shunt elements or grid resistance. Determining the actual stability boundary is therefore difficult and not accurately bound to the underlying physics of voltage stability limits. Nevertheless, the two methods are mainly derived in an attempt to approximate the impact of multiple IBRs on system strength. Both are based on the assumption of strong electrical coupling between IBRs. Hence, this is effectively an assumption that all IBRs share the same fictitious PoC. In practice, however, the IBRs typically do not fully interact with each other due to some existing electrical distance between them. Finally, these two metrics attempt to merge the two conceptually very different system strength aspects: voltage stability limitations and the likelihood of converter-driven interactions. However, such an attempt is effectively an approximation of both and is bound to be inaccurate. The method should be therefore used only as a simple screening method for grids that are not highly meshed. In systems with clustered IBR areas, the methods will typically give a more operationally useful system strength estimate when compared to SCR.

A slightly more accurate (albeit more complicated) approach is the SDSCR method. The method generalizes SCR for larger grids with multiple IBRs, with stability limitations equivalent to those of SCR. It provides, therefore, a more accurate system strength evaluation compared to approximations of WSCR and CSCR. However, the underlying stability limitations are still based on the same conventional concepts as for SCR, i.e. angle stability limits of synchronous machines. Hence, SDSCR is not entirely applicable to IBR-dominated grids and will not accurately determine the steady-state voltage stability limits. Furthermore, the shunt elements and X/R ratio of the grid are not considered by the metric. Finally, depending on the grid size, data quality, and software being used, the complete system impedance matrix may sometimes be complicated to obtain accurately in practice.

Similar to the previous metrics, EqSCR effectively attempts to combine two aspects: voltage stability limitations (implied by the S_{Sc_i}) and susceptibility to IBRs' control interactions (implied by the $WPIF_{j_i}$ factor). Such an attempt, however, is an approximation, as it has no underlying physical foundations in either of the two aspects. In terms of voltage stability limits, EqSCR faces the same issue

as SCR since the calculation is based on the analytical evaluation of synchronous generators' power transfer limits. Furthermore, the effects of grid resistance, shunt capacitance, and loads are not considered. Additionally, the new term $WPIF_{ji}$ affects the calculation even though it has no impact on the underlying voltage stability limit. This term instead attempts to approximate the likelihood of control interactions of multiple IBRs. However, it is very difficult to evaluate such a risk without accurately considering the transfer impedances and control parameters of all the involved converters. Hence, inaccuracy is guaranteed by design. While such a method may prove useful in meshed grids where other methods such as WSCR become inapplicable, its disconnection from the physical concepts that drive voltage instability and converter interactions makes it bound to be inaccurate and suboptimal. Finally, the $WPIF_{ji}$ factors need to be calculated numerically by performing a large number of power flow simulations with voltage variations, which notably increases its complexity, particularly when applied in larger grids.

The voltage sensitivity metric $\partial Q/\partial V$ is also proposed. What makes this metric different compared to the previous ones is that it is derived by considering both angle and voltage stability limits, accurately relating them to the maximum power transfer. This makes it applicable for IBRs as well, and therefore much more accurate in modern power systems compared to SCR-based methods. While shunt elements and the X/R factor are discussed and possible to add to the method, this increases its complexity compared to the existing metrics. Finally, the $\partial Q/\partial V$ calculation does not consider the impact of multiple IBRs in any manner.

And lastly, the AFL method was briefly introduced. In terms of complexity, the method requires several calculations to determine fault levels with and without IBRs, where $SCR_{withstand}$ and α factors also need to be utilized. The method aims to approximate the impact of multiple IBRs that act as a "sink" for system strength. However, there are a couple of concerns with such an approach. Firstly, in order to merge the evaluation of voltage stability limits and the likelihood of converter interactions, the approach moves very far from fundamental physical processes that define both of these phenomena. IBRs are modelled as proxy Thevenin sources, assumed to reduce the total "available" fault level. This is, of course, technically impossible, and is only an artificial numerical construct. The second concern is that the approach completely disregards the impact of shunt elements and grid resistance on system strength. Finally, as the method relies on utilizing fault levels and SCR for system strength evaluation, it is still fundamentally more related to synchronous generators' limitations rather than to IBRs. In other words, while these approximations may provide acceptable screening in some cases and might provide more information relative to simple S_{sc} values, there is a big question about their accuracy as systems evolve and the method becomes even more disconnected from the underlying physics of voltage instability and converter interactions. As RES developers need to manufacture renewable plants and their controls to comply with such a fictitious metric and policy, the effects on overall system stability and system strength are at risk of becoming much different than desired.

Table 3.1.: Overview of the common system strength evaluation methods.

Method	Abbreviation	Advantages and Limitations	Sources
Short-Circuit Ratio	SCR	+ Simple, easy to calculate - Derived for SGs, not IBRs - Ignores X/R, load, C - Ignores nearby IBRs	[6, 20]
Effective Short-Circuit Ratio	ESCR	+ Simple, easy to calculate - Derived for SGs, not IBRs +- Ignores X/R, load, considers C - Ignores nearby IBRs	[21]
Weighted Short-Circuit Ratio	WSCR	+- Relatively simple, easy to calculate - Derived for SGs, not IBRs - Ignores X/R, load, C +- Approximates nearby IBRs	[22–24]
Composite Short-Circuit Ratio	CSCR	+- Relatively simple, easy to calculate - Derived for SGs, not IBRs - Ignores X/R, load, C +- Approximates nearby IBRs	[4, 26]
Site-Dependent Short-Circuit Ratio	SDSCR	- Complex to calculate - Derived for SGs, not IBRs - Ignores X/R, load, C +- Approximates nearby IBRs	[27, 28]
Equivalent Short-Circuit Ratio	EqSCR	- Complex to calculate - Derived for SGs, not IBRs - Ignores X/R, load, C +- Approximates nearby IBRs	[6, 20]
Voltage Sensitivity	$\partial Q/\partial V $	+- Moderately complex to calculate + Derived for any source +- Somewhat considers X/R, load, C - Ignores nearby IBRs	[7, 17, 30]
Available Fault Level	AFL	- Complex to calculate - Derived for SGs, not IBRs - Ignores X/R, load, C +- Approximates nearby IBRs	[33, 34]

Table 3.1 provides a concise overview of the discussed system strength methods¹², evaluated on the basis of the four qualitative aspects introduced at the beginning of this section. It is clear that neither of the methods is very suitable for the challenges of modern power systems. Most of the methods are fundamentally derived from conventional power systems dominated by synchronous generation. Furthermore, various simplifications are often used that may not be accurate in modern systems.

To overcome some of the discussed limitations, the next chapter introduces a novel method for system strength evaluation in modern power systems.

¹²Of course, this overview cannot include every proposed method in the literature. Nevertheless, it is the author's view that the presented methods are the most important and most common ones. Other methods are typically minor variations or combinations of these.

3.3. EXCESS SYSTEM STRENGTH (ESS) METHOD

As previously discussed, system weakness manifests itself in voltage instability or converter interactions and instability. The existing and commonly-applied methods are unable to assess either accurately. Instead, various approximations are used to try to derive a *single* metric for system strength that will describe the susceptibility to *both* voltage instability and converter-driven interactions or instability.

While this may result in an acceptable rule-of-thumb screening in cases where accurate system strength evaluation is not critical and RES penetration is not particularly high, the disconnection from the physical concepts that drive voltage instability and converter interactions makes them bound to become (more) inaccurate and sub-optimal. As power systems evolve and system strength scarcity increases, it will become increasingly important to have an accurate system strength evaluation and consequent stability limitations. Naturally, the principle behind the methods should be bound in the laws of physics, and only then can the evaluation methods be engineered to be *as simple as possible, but not simpler*.

This subsection introduces a new method that provides a very precise yet simple quantification of system strength in terms of voltage stability and maximum power transfer boundary. Furthermore, all the relevant qualitative aspects discussed previously are taken into consideration. The goal is to give an accurate representation of voltage resilience and sensitivity, the core vulnerability aspects discussed in previous chapters. Afterwards, the related issue of converter interactions is discussed.

ANALYTICAL DERIVATION

For the derivation of the new method and demonstration of the performed analysis [35], a single-IBR-infinite-bus system is used, as shown in Figure 3.6.

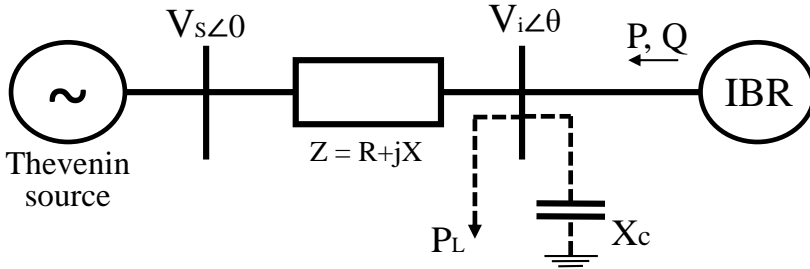


Figure 3.6.: IBR connected to a grid represented by Thevenin's equivalent.

For this system (ignoring P_L and X_C for now), the following equations are written.

$$\frac{V_i - V_s}{Z} = \underline{I} = \left(\frac{\underline{S}}{V_i} \right)^* \rightarrow \underline{S} = \underline{V}_i \frac{V_i^* - V_s^*}{Z^*} = P + jQ \quad (3.15)$$

$$\underline{S} = (V_i \cos \theta + j V_i \sin \theta) \frac{V_i \cos \theta - j V_i \sin \theta - V_s}{R - jX} \quad (3.16)$$

$$\alpha = \frac{R}{Z^2} ; \beta = \frac{X}{Z^2} \quad (3.17)$$

By separating real and imaginary parts of Equation (3.16) and combining those with Equation (3.17), the expressions for active and reactive power are derived.

$$P = \alpha(V_i^2 - V_i V_s \cos\theta) + \beta V_i V_s \sin\theta \quad (3.18)$$

$$Q = \beta(V_i^2 - V_i V_s \cos\theta) - \alpha V_i V_s \sin\theta \quad (3.19)$$

If $R \approx 0$ is assumed, this simplifies to the expressions in Equation (3.20), which is equivalent to the derivation in Chapter 2. The impact of $R > 0$ is investigated later in the chapter.

$$P = \frac{V_i V_s \sin\theta}{X} ; Q = \frac{V_i^2 - V_i V_s \cos\theta}{X} \quad (3.20)$$

This expression for P dictates the maximum active power transfer with respect to the angle stability, and the necessary reactive power to sustain that transfer. However, these P and Q expressions do not consider static voltage stability. To derive voltage stability limits, Equation (3.15) can be rewritten as:

$$\underline{ZS}^* = V_i^2 - \underline{V_s V_i}^* \quad (3.21)$$

If $\underline{Z} = a - jb$, where a and b are real numbers, real and imaginary parts of Equation (3.21) can be separated as follows.

$$a = V_i^2 - V_s V_i \cos\theta = f_1(V_i, \theta) \quad (3.22)$$

$$b = V_s V_i \sin\theta = f_2(V_i, \theta) \quad (3.23)$$

The Jacobian matrix of $\mathbf{f} = [f_1, f_2]^T$ is further derived.

$$J = \begin{bmatrix} \frac{\partial f_1}{\partial V_i} & \frac{\partial f_1}{\partial \theta} \\ \frac{\partial f_2}{\partial V_i} & \frac{\partial f_2}{\partial \theta} \end{bmatrix} = \begin{bmatrix} 2V_i - V_s \cos\theta & V_s V_i \sin\theta \\ V_s \sin\theta & V_s V_i \cos\theta \end{bmatrix} \quad (3.24)$$

A singular Jacobian matrix indicates a static voltage instability condition of the system [31, 36]. The stability boundary is therefore found by solving the $\det(J) = 0$ expression. The solution is shown below.

$$\cos\theta = \frac{1}{2} \frac{V_s}{V_i} \longrightarrow \theta_{max} = \arccos\left(\frac{1}{2} \frac{V_s}{V_i}\right) \quad (3.25)$$

For a base scenario $V_i = V_s = 1 pu$, the maximum angle equals 60° . This is lower than the angle stability limitation of 90° implied by the active power computed by Equation (3.20) and discussed in Chapter 2. Therefore, this approach is extended further by incorporating the voltage stability boundary from Equation (3.25) into the active power transfer from Equation (3.20).

$$P_{max} = \frac{V_i V_s \sin(\theta_{max})}{X} = \frac{V_i V_s \sin\left[\arccos\left(\frac{1}{2} \frac{V_s}{V_i}\right)\right]}{X} \quad (3.26)$$

By using a known trigonometric identity¹³, a novel expression for static voltage stability limit in terms of maximum power transfer is derived in Equation (3.27).

$$P_{max} = \frac{1}{X} V_i V_s \sqrt{1 - \left(\frac{1}{2} \frac{V_s}{V_i}\right)^2} \quad (3.27)$$

For transferring $P = P_{max}$, the reactive power required to maintain the voltage can be computed by combining Equations (3.20) and (3.25).

$$Q_{P=P_{max}} = \frac{V_i^2 - V_i V_s \cos(\theta_{max})}{X} = \frac{1}{X} \left(V_i^2 - \frac{V_s^2}{2} \right) \quad (3.28)$$

For an illustrative case with parameters $S_{sc} = V_i = V_s = 1 pu$, P_{max} is computed for the boundary stability condition based on the SCR metric introduced in the previous section and compared to Equation (3.27).

$$SCR = 1 = \frac{S_{sc}}{P_{max}} = \frac{V_{i,nom}^2 / X}{P_{max}} \rightarrow P_{max} = 1 pu \quad (3.29)$$

$$P_{max} = \frac{1}{X} V_i V_s \sqrt{1 - \left(\frac{1}{2} \frac{V_s}{V_i}\right)^2} = \frac{\sqrt{3}}{2} = 0.866 pu \quad (3.30)$$

One can observe that the maximum power transfer is *lower* than what the SCR ratio would imply. This is due to the fact that a grid-following¹⁴ IBR is a PQ source, rather than a PV source. In other words, IBR does not behave as a voltage source but is instead perceived as a current source from the bulk power system perspective. This fundamentally differs from a synchronous generator electromagnetically coupled to the grid, which would be able to operate at $P_{max} \approx 1 pu$ in a similar case.

SCR is therefore an over-optimistic measure of system strength and the voltage collapse boundary with common IBRs. Furthermore, SCR does not consider the actual operating voltage V_i . Meanwhile, expression Equation (3.27) does. The relation is depicted in Figure 3.7, by plotting the function $P_{max} = f(V_i)$ for a per-unit system with base $S_{sc} = X = V_s = 1$.

For $V_i = 1 pu$, a maximum of $P = 0.866 pu$ can be transferred, as per Equation (3.30). Furthermore, transferring $P = S_{sc} = 1 pu$ (as implied by SCR) would result in a voltage collapse for $V_i = 1 pu$. Instead, the voltage would need to be higher ($V_i = 1.118 pu$) for such a transfer to be feasible from a voltage stability perspective. Therefore, in a lossless system with a PQ source supplying power to the grid, the SCR method is an over-optimistic system strength measure. In contrast, the derived approach shows high accuracy, which will be substantiated further in this section.

¹³ $\sin(\arccos(x)) = \sqrt{1 - x^2}$.

¹⁴New developments such as grid-forming control would theoretically allow IBRs to exhibit behaviour more similar to PV sources, at least in the steady-state operation within converter thermal limits.

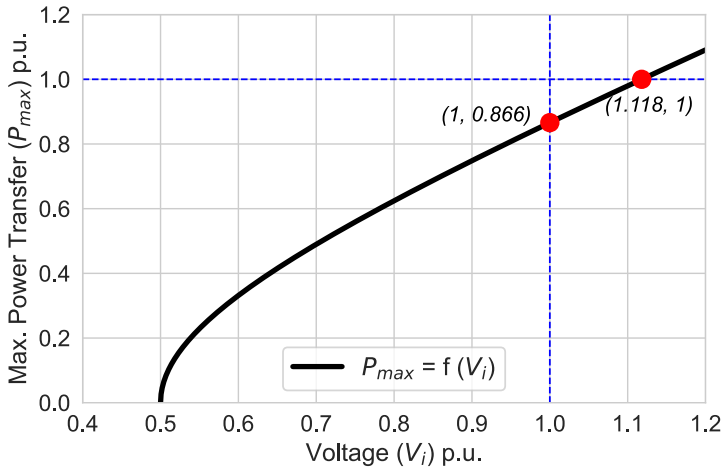


Figure 3.7.: Maximum power transfer as a function of operating voltage.

So far, all the analysis and derivation assumed no load, shunt capacitance, or resistive losses in the grid. As these assumptions do not perfectly reflect the reality of modern power systems, the following subsections expand the analysis to consider these more accurately.

IMPACT OF LOCAL LOAD ON SYSTEM STRENGTH

The system shown in Figure 3.6 is altered by adding a local load at bus i ($P_L > 0$). Deriving the boundary condition for such a case is relatively simple. What matters for the voltage stability is the power transfer towards the system, from the system perspective. In other words, the *net* maximum active power transfer. This can be calculated as proposed below.

$$P_{net_{max}} = P_{max} + P_L \quad (3.31)$$

The maximum power transfer with a load included is evaluated analytically for an illustrative load of $P_L = 0.2 pu$. The results are shown in Figure 3.8. For nominal voltage, voltage collapse occurs at power transfer $P_{net_{max}}$ (dashed line), which is precisely in line with Equations (3.30) and (3.31). Furthermore, it can be seen that the entire plot from Figure 3.7 is shifted upwards by the value of P_L , in line with the mentioned analytical expressions.

It is important to note that a constant active power load is assumed in this analysis. If there is a voltage dependence, it should be reflected as $P_L = f(V_i)$ relation. In such a case, the difference would also appear in the upward shift in Figure 3.8, however, this would not be distributed equally along the curve. Additional analysis for different and more detailed load types remains a future work consideration.

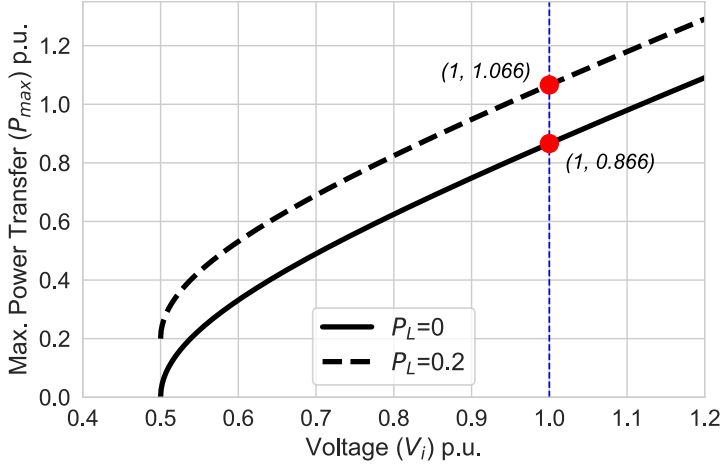


Figure 3.8.: Maximum power transfer as a function of operating voltage V_i with the presence of a local load.

IMPACT OF CAPACITORS ON SYSTEM STRENGTH

The impact of shunt capacitance is evaluated now, assuming a capacitor X_C connected in parallel at the bus i in Figure 3.6. The reactive power of the capacitor can be expressed as $Q_C = V_i^2 / X_C$, where X_C is the capacitive reactance. To derive the boundary voltage stability condition, the impedance equivalent is derived first, as shown below.

$$\underline{Z}' = \underline{Z}_L \parallel \underline{Z}_C = \frac{jX_L(-jX_C)}{jX_L + (-jX_C)} = j \frac{X_L X_C}{X_C - X_L} \quad (3.32)$$

Alternatively, with the nominal reactive power of the capacitor $Q_{C_{nom}} = V_{i_{nom}}^2 / X_C$, the expression for the magnitude of the impedance can be rewritten as follows.

$$Z' = \frac{X_L X_C}{X_C - X_L} = \frac{X_L}{1 - X_L / X_C} = \frac{X_L}{1 - \frac{X_L Q_{C_{nom}}}{V_{i_{nom}}^2}} \quad (3.33)$$

The new Thevenin's source voltage equivalent is derived utilizing the voltage divider principle.

$$V'_s = V_s \frac{Z'}{Z} = V_s \frac{1}{1 - \frac{X_L Q_{C_{nom}}}{V_{i_{nom}}^2}} = \frac{V_s}{1 - f_c} \quad (3.34)$$

$$f_c = \frac{X_L}{X_C} = \frac{X_L Q_{C_{nom}}}{V_{i_{nom}}^2} \quad (3.35)$$

By inserting Equations (3.33) and (3.34) into Equation (3.27), the analytical expression of the maximum active power transfer in the presence of a shunt capacitor is derived.

$$P_{max} = \frac{1}{X} V_i V_s \sqrt{1 - \left(\frac{1}{2} \frac{V_s}{V_i(1-f_c)} \right)^2} \quad (3.36)$$

The necessary reactive power provided at the bus i is calculated by combining Equations (3.33) and (3.34) with Equation (3.28).

$$Q_{P=P_{max}} = \frac{1-f_c}{X} \left[V_i^2 - \frac{1}{2} \left(\frac{V_s}{1-f_c} \right)^2 \right] \quad (3.37)$$

This dependence is visualized in Figure 3.9 ($S_{sc} = V_i = 1 pu$). The Y-axis depicts the maximum power transfer, while the X-axis shows reactive power compensation. For no compensation, the maximum power transfer equals $0.866 pu$, as expected based on Equation (3.30). However, with additional reactive power compensation, the maximum power transfer drops. For illustrative cases with capacitor's reactive power $Q_{Cnom} = 0.1(0.25) pu$, the maximum power drops to $0.8315 (0.7454) pu$, respectively.

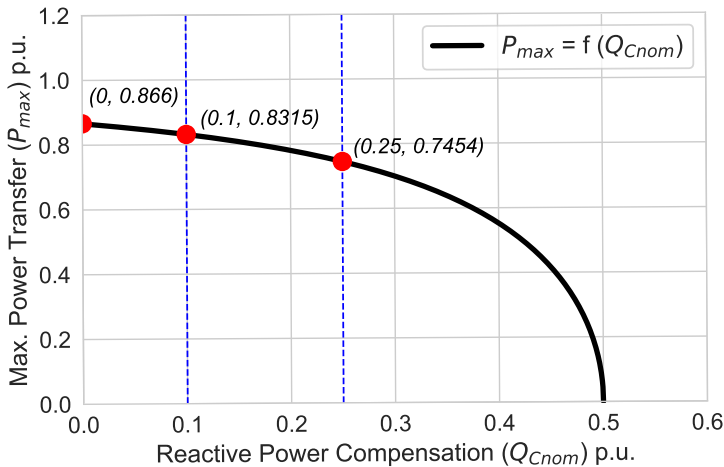


Figure 3.9.: Maximum power transfer as a function of shunt compensation normalized by the short-circuit capacity ($S_{sc} = V_i = 1 pu$).

To understand these effects, two aspects are important. Firstly, capacitors increase system impedance, as per Equation (3.33). This reduces system strength. However, they also boost the voltage by injecting reactive power, which increases system strength. Figure 3.9 shows the comparison for the *same* voltage level, i.e. given the same voltage, the bus with less compensation needed to achieve that voltage is the stronger bus. If it is, however, assumed that adding a capacitor would increase the voltage, the maximum power transfer could increase. To showcase this, two cases are considered and visualized using Equation (3.36). The first case is with a nominal voltage $V_i = 1 pu$, and the second one is with an assumption that the shunt capacitor boosts the voltage to $V_i = 1.1 pu$. The results are shown in Figure 3.10.

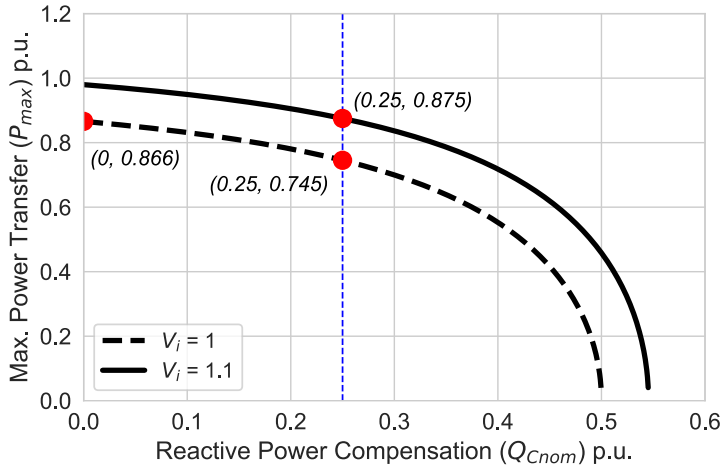


Figure 3.10: Maximum power transfer as a function of shunt compensation. Impact of a different operating voltage.

In this case, adding a capacitor increased the maximum power transfer from 0.866 to 0.875 pu. However, to maintain voltage stability, the operating voltage had to be increased from $V_i = 1$ to $V_i = 1.1$ pu. If the voltage remains the same, the maximum power transfer would decrease to 0.745 pu

Therefore, shunt capacitors have *two opposing effects* on system strength. Firstly, they increase system impedance, as per Equation (3.33), which has a negative effect on system strength. However, they also increase the operating voltage by providing reactive power, which has a positive effect on system strength. Which effect would be dominant depends on the system parameters. This can be accurately evaluated using Equation (3.36). Simplified approximation methods such as ESCR ignore these intricacies and may therefore over- (under-) estimate system strength.

This analytical approach can be expanded to include other shunt-connected reactive power elements such as reactors, Static VAR Compensators (SVCs), and Static Synchronous Compensators (STATCOMs). This remains a topic for future work.

IMPACT OF THE X/R RATIO ON SYSTEM STRENGTH

Lastly, it is hereby explored how the X/R ratio affects maximum power transfer and associated system strength. If $R \neq 0$, Equation (3.20) is no longer valid, and Equations (3.18) and (3.19) should be used. However, the boundary condition defined by Equation (3.25) is still applicable, as it is derived for any R . Therefore, Equation (3.25) is integrated into Equations (3.18) and (3.19). For simplicity, M and N are defined, keeping in mind the θ_{max} derived in Equation (3.25), as well as the mentioned trigonometric identity.

$$M = V_i^2 - V_i V_s \cos(\theta_{max}) = V_i^2 - \frac{V_s^2}{2} \quad (3.38)$$

$$N = V_i V_s \sin(\theta_{max}) = V_i V_s \sqrt{1 - \left(\frac{1}{2} \frac{V_s}{V_i}\right)^2} \quad (3.39)$$

Boundary active power transfer and its corresponding necessary reactive power can now be expressed as follows.

$$P_{max(R \neq 0)} = \alpha M + \beta N \quad (3.40)$$

$$P_{max(R \neq 0)} = \frac{R}{Z^2} \left(V_i^2 - \frac{V_s^2}{2} \right) + \frac{X}{Z^2} V_i V_s \sqrt{1 - \left(\frac{1}{2} \frac{V_s}{V_i}\right)^2} \quad (3.41)$$

$$Q_{P=P_{max(R \neq 0)}} = \beta M - \alpha N \quad (3.42)$$

$$Q_{P=P_{max(R \neq 0)}} = \frac{X}{Z^2} \left(V_i^2 - \frac{V_s^2}{2} \right) - \frac{R}{Z^2} V_i V_s \sqrt{1 - \left(\frac{1}{2} \frac{V_s}{V_i}\right)^2} \quad (3.43)$$

From Equation (3.40), the boundary transfer is increased by αM , implying that system strength increases with $R > 0$. However, careful observation reveals that the expression βN is not the same as Equation (3.27) due to $X \neq |Z|$. The impact of resistance, therefore, becomes more intricate. To shed light on this, Figure 3.11 plots the dependence $P_{max(R \neq 0)} = f(X, X/R)$, with the X-axes depicting the system reactance X and the X/R ratio. For $X \approx 1$ and $R \approx 0$ ($X/R \rightarrow \infty$), the maximum power transfer equals 0.866, in line with Equation (3.27). However, the function $P_{max(R \neq 0)} = f(X)$ reaches a maximum for $X = 0.866$ ($X/R = 1.7321$). Hence, decreasing the X/R ratio from a high value to 1.7321 increases the maximum power transfer from 0.866 to 1 per unit (from right to left red dot in Figure 3.11).

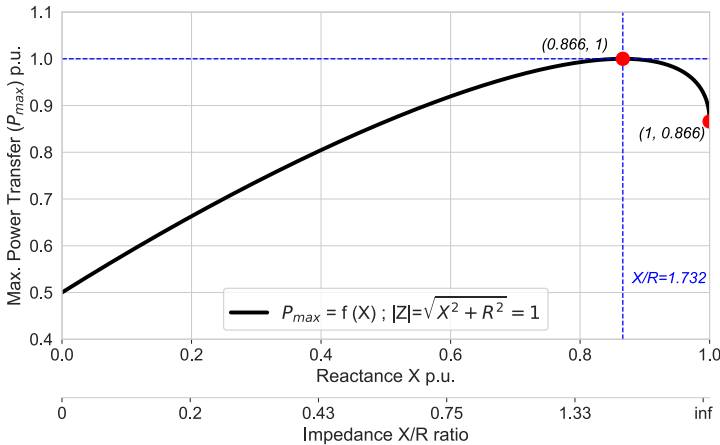


Figure 3.11.: Maximum power transfer as a function of the X/R ratio.

However, the relationship is concave, with a peak. In other words, $P_{max(R \neq 0)}$ drops with a further decrease of the X/R ratio. In a fully resistive system, maximum power transfer drops to only $0.5 pu$. The derived analytical expressions for $P_{max(R \neq 0)}$ and $Q_{P=P_{max(R \neq 0)}}$ are validated with numerical simulations in the next section.

The question arises whether the ratio $X/R = 1.7321$ is a constant parameter that allows for peak maximum power transfer in every case. The answer is no, as the peak ratio will depend on the operating voltage V_i . This is demonstrated in Figure 3.12, by plotting the $P_{max(R \neq 0)} = f(X, X/R)$ dependence for typical operating voltage range $V_i = [0.9 - 1.1] pu$.

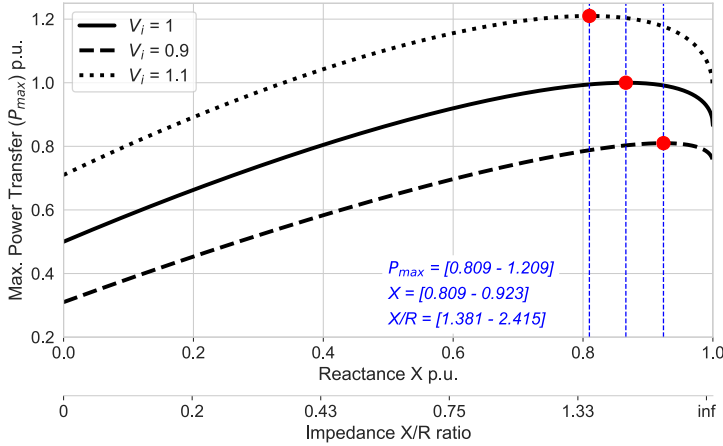


Figure 3.12.: Maximum power transfer as a function of the X/R ratio and the operating voltage V_i .

From Figure 3.12, the maximum active power transfer occurs at $X/R = 1.381(2.415)$ for $V_i = 0.9(1.1) pu$. Therefore, the optimal X/R ratio for peak maximum active power transfer takes a value in the range $X/R = [1.381 - 2.415]$, depending on the steady-state operating voltage. The commonly made assumption that a relatively larger resistance increases maximum power transfer capability is hence only valid up to a point, after which the opposite occurs.

DEFINITION OF THE EXCESS SYSTEM STRENGTH (ESS) METHOD

In Chapters 2 and 3, it is shown that SCR and SCR-based methods are incomplete and may significantly overestimate system strength. In this section, a new method for system strength evaluation is introduced, based on the analytical description of the voltage collapse boundary obtained in the previous section. The *Excess System Strength (ESS)* method is hereby introduced. It is defined in Equation (3.44), based on the perceived balance of system strength supply and demand, normalized by the bus short-circuit capacity S_{sc} , as per Equation (3.4), calculated for $V = V_{nom}$.

$$ESS = \frac{SS_{supply} - SS_{demand}}{S_{sc}} \quad (3.44)$$

ESS directly quantifies steady-state system strength. For the bus to maintain voltage stability, there should be an excess of system strength available.

$$ESS > 0 \rightarrow SS_{supply} > SS_{demand} \quad (3.45)$$

The supply of system strength is defined as the maximum possible power transfer at the bus, considering impedance, capacitors, and X/R ratio. Therefore, equations Equations (3.27), (3.36) and (3.41) are to be used for P_{max} . Equation (3.47) exemplifies this for conditions assumed in Equation (3.27).

$$SS_{supply} = P_{max} ; SS_{demand} = P_{IBR} - P_L \quad (3.46)$$

$$ESS = \frac{1}{S_{sc}} \left[\frac{1}{X} V_i V_s \sqrt{1 - \left(\frac{1}{2} \frac{V_s}{V_i} \right)^2} - P_{IBR} - P_L \right] \quad (3.47)$$

System operators can use the normal operating range of voltages V_i (e.g. 0.95 - 1.05 per unit) and expected load and generation profiles to derive the operating system strength values for each IBR bus of interest. This information can be used to determine the maximum renewable generation that can be injected into a bus and transported to the rest of the system in a (steady-state) stable and secure manner. Furthermore, the impact of the RES collector network, filters, and selected N-1 (N-2) contingencies can be easily incorporated into the impedance value.

ESS NUMERICAL SIMULATIONS

The ESS method is hereby tested against two common single-IBR system strength evaluation methods, SCR and ESCR. A simple model as shown in Figure 3.13 is simulated in Digsilent PowerFactory 2022. The IBR is modelled using the standard IEC Wind Generator Type 4B model [37].

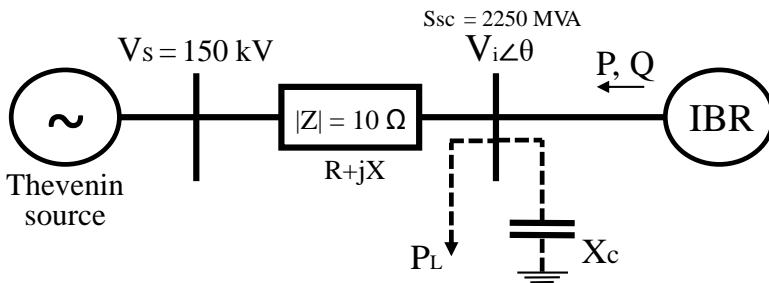


Figure 3.13.: IBR connected to a grid represented by Thevenin's equivalent.

Figure 3.14 shows 20 scenarios selected to reflect various operating conditions. In cases A1-A3, methods are compared on a system with $P_L = 0$, $X_C = 0$, and $R \approx 0$. For case A1, 1000MW is transferred. Both SCR and ESS indicate voltage stability, which is validated by simulations. Note that the ESS value indicates that an extra 948.5MW

can be transferred (42.16% of S_{sc}) which is also the boundary voltage stability condition in simulations. When the power increases to the boundary (1948.5MW) SCR remains larger than 1, incorrectly indicating that more power can be transferred. Meanwhile, ESS is near 0, correctly indicating the boundary condition. If the power increases further by only 1.5MW (A3), the voltage collapses. This is accurately predicted by a negative ESS, while SCR is still larger than 1, overestimating system strength. SCR implies that 2250MW can be transferred, equal to S_{sc} . However, as per derivations in Section II, this is technically unfeasible due to voltage instability.

Simulations B1-B4 explore the impacts of the operating voltage. For case B1, which is the same as A1 with 1000MW, but now with $V_i = 0.95pu$, SCR has the same value as in A1. Thus, SCR is insensitive to the change in voltage as it is typically calculated with nominal values. In contrast, ESS is 0.3633, indicating an extra 817.5MW of capacity available (36.33% of S_{sc}). By increasing power to the boundary condition, it is found that precisely 1817.5MW is the maximum power transfer (MPT) at $V_i = 0.95pu$, as predicted by ESS. Meanwhile, SCR is still larger than 1 (1.238), wrongly indicating that the system is far from a voltage collapse. If the power experiences further increase (B3), a voltage collapse occurs, as predicted by negative ESS. SCR is, however, still positive, overestimating system strength. In case B4, the operating voltage is increased to $V_i = 1.15pu$. Here, simulations show that the MPT is 2330MW i.e. more than what SCR suggests. Therefore, SCR can also underestimate system strength by not taking into account the operating voltage. ESS is conversely able to pinpoint the MPT, correctly considering the impact of V_i .

In cases C1 (C2), a 400MW (600MW) load is introduced. Based on the boundary voltage stability results, the MPT is 2348.5MW (2548.5MW), respectively. This is equal to case A2 with the addition of load, as predicted by Equation (3.31). Therefore, while SCR labels these cases as unstable, ESS correctly characterizes them as boundary cases. In other words, ESS is, unlike SCR, able to accurately consider the positive impact of load on steady-state system strength and stability limits.

Simulations D1-D3 show how capacitance impacts system strength. A shunt capacitor with $Q_{C_{nom}} = 250MVar$ is added, and system strength is evaluated for three different voltages. In case D1, the MPT for $V_i = 1pu$ is found in simulations. In this case, SCR overestimates system strength, while ESCR, designed to consider capacitors, performs better. However, it still inaccurately indicates that there is some power transfer margin left. ESS locates the boundary condition accurately, as per Equation (3.36), perfectly matching simulations. In cases D2 and D3, simulations are repeated for $V_i = 0.9(1.1)pu$, respectively. ESCR is unable to accurately find the boundary condition, overestimating (underestimating) system strength in D2 (D3). On the other hand, ESS is again able to precisely match the boundary condition, and thus perform much better in the presence of a shunt capacitance.

Finally, cases E1-E8 show the impact of resistance on system strength. Cases E1-E3 show the operation for the ratio $X/R = 10$. For case E1, one already sees a problem for SCR, as it is equal to case A1, where $R \approx 0$. Meanwhile, ESS predicts that an extra 1050.75MW (46.7% of S_{sc}) of transfer is possible before voltage collapse (note the difference with case A1). Indeed, simulations confirm that 2050.8MW is the boundary condition for voltage stability, as seen from case E2. If power is increased

Operating scenario	P_{IBR} [MW]	Q_{IBR} [MVAr]	V_i [kV]	θ [deg]	P_L [MW]	$Q_{c_{nom}}$ [MVAr]	X/R	SCR	ESCR	ESS	Voltage collapse
A1	1000.0	234.5	150.0	26.39	0	0	inf.	2.250	-	0.4216	No
A2	1948.5	1124.9	150.0	59.99	0	0	inf.	1.154	-	≈ 0.001	Boundary
A3	1950.0	-	150.0	-	0	0	inf.	1.153	-	-0.0006	Yes
B1	1000.0	142.5	142.5	27.89	0	0	inf.	2.250	-	0.3633	No
B2	1817.5	905.6	142.5	58.23	0	0	inf.	1.238	-	≈ 0.001	Boundary
B3	1850.0	-	142.5	-	0	0	inf.	1.216	-	-0.0144	Yes
B4	2330.0	1850.3	172.6	64.15	0	0	inf.	0.965	-	≈ 0.001	Boundary
C1	2348.5	1124.9	150.0	59.86	400	0	inf.	0.958	-	≈ 0.001	Boundary
C2	2548.5	1124.9	150.1	59.87	600	0	inf.	0.882	-	≈ 0.001	Boundary
D1	1860.3	734.3	150.1	55.71	0	250	inf.	1.209	1.075	≈ 0.001	Boundary
D2	1722.5	539.37	142.5	53.68	0	250	inf.	1.306	1.161	≈ 0.001	Boundary
D3	2126.9	1154.3	165.0	59.21	0	250	Inf.	1.057	0.940	≈ 0.001	Boundary
E1	1000.0	126.9	150.0	25.89	0	0	10	2.250	-	0.4670	No
E2	2050.8	925.5	150.0	59.93	0	0	10	1.097	-	≈ 0.001	Boundary
E3	2055	-	150.0	-	0	0	10	1.094	-	-0.0018	Yes
E4	2131.3	721.0	150.0	59.99	0	0	5	1.056	-	≈ 0.001	Boundary
E5	2245.9	134.8	150.0	59.95	0	0	2	1.002	-	≈ 0.001	Boundary
E6	2173.3	-582.3	150.0	59.91	0	0	1	1.035	-	≈ 0.001	Boundary
E7	1683.8	-697.4	135.1	56.19	0	0	1	1.336	-	≈ 0.001	Boundary
E8	3188.4	-429.2	165.0	62.91	500	0	1	0.706	-	≈ 0.001	Boundary

Figure 3.14.: Simulation results for the system in Figure 3.13 comparing different system strength metrics over various operating scenarios.

further (E3), a voltage collapse occurs. SCR fails in evaluating this, while ESS predicts the voltage collapse point accurately. Simulations E4-E6 evaluate the impact of the X/R ratio on power transfer. When the ratio decreases from 10 to 5 (E2 to E4), the MPT is increased. The same occurs when the X/R ratio is decreased to 2 (E5). However, when the X/R ratio further decreases to 1 (E6), the MPT in simulations decreases, as predicted in Figure 3.12. Therefore, the expressions for ESS correctly evaluate the intricate impact of the X/R ratio on system strength, as per E1-E6. Meanwhile, SCR falls short in determining the MPT as it does not consider the X/R ratio. This is emphasized further in cases E7 (E8), where $V_i = 0.9(1.1)pu$, with a 500MW load P_L in the latter case. SCR significantly over- (under-) estimates system strength in these two scenarios. Conversely, ESS once again precisely matches the boundary voltage collapse point found in numerical simulations.

These simulations verify the analytical results derived in Section 3.3 and show that ESS is a much more accurate measure of the steady-state system strength. SCR (ESCR) can significantly over- or under-estimate system strength, as they are designed for synchronous generation, and are also unable to accurately take into account impacts of voltage, loads, capacitors, and X/R ratio. Meanwhile, the accuracy of ESS is numerically demonstrated, in line with the detailed analytical expressions for maximum power transfer. Therefore, it can be concluded that ESS is a more accurate and more suitable measure of steady-state system strength to be used in modern power systems in terms of voltage stability limitations.

IMPACT OF MULTIPLE IBRS ON THE ESS METHOD

The analysis shown in the previous subsection deals with a single-IBR-system scenario. ESS does not directly consider the impact of multiple IBRs. However, it does so *indirectly*. Since the goal of ESS is to locate the steady-state voltage stability boundary, any nearby IBR (replacing SG) will be reflected in system impedance and

operating voltage, both of which are considered by ESS. Moreover, in case another IBR is directly (or very closely) connected to the busbar being analyzed, it will be reflected in SS_{demand} considered in Equation (3.44).

Nevertheless, more nearby IBRs will result in more chance of converter interactions. This is not something that ESS can evaluate in its current form, and it is not designed to do so. If an approximation is needed, combining ESS (as an accurate voltage sensitivity metric) with a number that quantifies the local penetration of IBRs in an area (e.g. PER or SNSP)¹⁵ may be a useful screening method for converter interaction issues. Furthermore, control parameters with a dominant role in converter interactions (e.g. of PLL and inner current control loop) could be incorporated into the screening method. This remains a topic of future work.

Instead, this thesis tackles oscillations and converter interactions analysis and predictions from a different data-driven perspective, discussed in Chapter 5.

3.4. DYNAMIC-STATE SYSTEM STRENGTH

All the analyses so far dealt with the steady-state operation of power systems, i.e. small disturbances. Dynamic-state system strength deals with the dynamic state operation of power systems, i.e., once the system is subjected to large disturbances. This means the operation can be highly non-linear, and short-term (transient) stability and faster voltage interactions play an important role.

While all the factors relevant to steady-state system strength also apply to dynamic-state system strength, several additional factors are fundamentally different, as listed in Figure 3.4.

- Non-linearity of modern grids

For conventional systems, the Thevenin impedance derived in steady-state conditions is not meaningfully affected by the intensity of the disturbance. The impedance is instead primarily related to the inherent physical characteristics of synchronous machines and passive grid components. Therefore, the assumed grid linearity holds true for both small and large disturbances.

This situation is different in IBR-dominated grids. Instead of underlying physics, IBR response is primarily driven by the applied controls and power electronics thermal limitations. The system can no longer be linearized, as impedances change with the controls (often discretely), which respond differently to various changes in voltage, especially if the converter's thermal limits are reached [39]. This is mathematically explored in [40], where impedance mapping is introduced. The analysis shows that the system impedance of modern systems is not a single value, but a non-linear spectrum of values based on the operating point. Moreover, this non-linearity leads to non-differentiability in the complex space, i.e. V/I relationship is not analytical (holomorphic). Therefore, a deterministic analytical method does not seem to be derivable. This is a challenge that requires further research to describe grid non-linearity and its impact on dynamic-state system strength. The

¹⁵PER - Power Electronics Ratio [5], SNSP - System Non-Synchronous Penetration [38].

system linearization applied in the steady-state analysis is therefore inaccurate in the (post-)disturbance operation of modern systems, more so as the share of IBRs rises.

Instead of using an analytical approach, an alternative is to evaluate dynamic-state system strength numerically via dynamic simulations. This is explored in [Chapter 5](#).

- Large-signal stability of control loops

Weak grid operation during and after large disturbances is a major and distinctive challenge for IBRs. During faults, the voltage waveform, which the control loops of IBRs rely upon, can be notably disrupted. In IBR-dominated systems, faults induce larger voltage angle jumps and rate of change of frequency (RoCoF), due to the reduction of system strength and inertia, respectively (see [Chapters 2](#) and [3](#)). This poses risks to the transient stability of IBR control loops¹⁶ and may lead to oscillations, disconnections, and converter-driven instability [41]. Such events stress a grid further, inducing vulnerability to fault cascading. This is explored in [Chapter 4](#). Finally, with more IBRs in a grid, the likelihood of post-disturbance interactions increases, especially in weaker grids. To evaluate the large-signal stability of IBR control loops, steady-state methods are often insufficient¹⁷, and more advanced methods (e.g. see [44–46]) or dynamic simulations are typically required.

- Maloperation and unintentional disconnections

It is common that some IBRs may exhibit undesired fault-ride-through (FRT) behaviour and enter momentary cessation mode or even disconnect during (or following) a disturbance. As grids weaken, voltage deviations are amplified, which makes FRT compliance more difficult. Furthermore, IBRs may also be (incorrectly) disconnected due to protection maloperation, which is much more likely in IBR-dominated grids [12, 47]. Inverter blocking or disconnection is particularly concerning as it tends to happen during severe disturbances, where a power system is already very vulnerable, exacerbating the issue. The recent experience with massive IBR disconnections in the (post-)fault period stresses the importance of this (see [Table 1.1](#)). AEMO showed that there is a strong correlation between fault intensity and the amount of distributed IBRs likely to trip [48]. The MIGRATE project demonstrates that the loss of devices in the FRT period is one of the key stability challenges for European TSOs [9]. Furthermore, dynamic load (post-)fault behaviour may contribute to the probability of nearby IBR disconnection by introducing FIDVR or other complex voltage deviations. This will be explored more in [Chapter 4](#). Therefore, it is prudent to assume that *some* IBRs will not operate as expected, particularly in weaker grids, which effectively reduces dynamic-state system strength.

- Modelling considerations

In comparison to steady-state system strength which can be generally evaluated analytically or by performing power flow and RMS simulations, dynamic-state

¹⁶Note that IBR transient stability is fundamentally very different than the transient stability of synchronous machines, which is an electromechanical phenomenon related to rotor angles.

¹⁷Nevertheless, a promising approximation/screening method is suggested by EPRI in [42, 43].

system strength is much more difficult to evaluate. It requires advanced models of generators and their control parameters for operation during and after disturbance, as well as more detailed (dynamic) load models. Consequently, it is necessary to use advanced RMS models [49] and support the analysis with more detailed EMT models when necessary [50].

3.5. CONCLUDING REMARKS

The main sources of system strength, synchronous generators, become more scarce. As systems evolve to include more renewable generation, the importance of accurate system strength evaluation in progressively weaker grids is only increasing. Failure to properly quantify system strength may result in voltage instability or converter-driven interactions, or alternatively, in sub-optimal and expensive decisions in grid operation and planning. These can include unnecessary and expensive curtailments of renewable generation or sub-optimal placement of grid-strengthening equipment (e.g., synchronous condensers, FACTS devices, grid-forming controls).

This chapter presented a comprehensive discussion and analysis of system strength in conventional and modern power systems. The underlying concept of system strength and the fundamental physical principles that describe it are explained. A new definition and a new classification are proposed that carefully reflect the multilayered complexity of system strength. Furthermore, the existing system strength methods are rigorously examined and their limitations in modern power systems are revealed and highlighted.

To overcome some of the discovered limitations, a new steady-state system strength method is proposed, based on a rigorous analytical derivation of IBR maximum active power transfer. Unlike the existing SCR-based methods that rely on equations describing synchronous machines, the proposed method is derived to be also applicable to IBRs. Furthermore, the method accurately takes into consideration operating voltage, loads, capacitors, and X/R ratio. Simulation results confirm superior performance in identifying the power transfer margin and the static voltage collapse point. The method can be used as a replacement or a complement to SCR-based methods for a more accurate evaluation of system strength and voltage stability limits in a variety of operating scenarios. This ultimately allows for more robust renewables integration planning, as well as operational screening for weak buses with potential voltage instability risks where mitigation measures may be necessary. For future work, the new method can be expanded to consider the topic of small-signal stability limits and converter-driven interactions.

The challenges of steady- and dynamic-state system strength presented in this section are fundamentally different. Consequently, the system may be strong in the steady state, but simultaneously exhibit dynamic-state weakness, further justifying the need for the new classification. This requires a tailored evaluation approach and a need for innovative solutions to tackle all the present and emerging challenges. Some of the aspects not covered in steady-state system strength and voltage stability evaluation are extensively explored in the following two chapters that focus on the dynamic behaviour of modern power systems during and after large disturbances.

REFERENCES

- [1] Isaac Newton. *Philosophiæ Naturalis Principia Mathematica*. 1687.
- [2] D. J. Griffiths. *Introduction to Electrodynamics*. 4th. Cambridge University Press, June 2017. ISBN: 9781108333511. DOI: [10.1017/9781108333511](https://doi.org/10.1017/9781108333511).
- [3] GHD Advisory. *Managing system strength during the transition to renewables*. Tech. rep. May 2020. URL: <https://arena.gov.au/assets/2020/05/managing-system-strength-during-the-transition-to-renewables.pdf>.
- [4] R. Fernandes, S. Achilles, and J. MacDowell. *Report to NERC ERSTF for Composite Short Circuit Ratio (CSCR) Estimation Guideline*. Tech. rep. Schenectady, NY, USA: GE Energy Consulting, Jan. 2015.
- [5] Hawai'i Natural Energy Institute School of Ocean and Earth Science and Technology University of Hawai'i. *Oahu Distributed PV Grid Stability Study Part 3: Grid Strength*. Tech. rep. GE Energy Consulting, July 2016.
- [6] NERC. *Integrating Inverter-Based Resources into Low Short Circuit Strength Systems - Reliability Guideline*. Tech. rep. North American Electric Reliability Corporation, Dec. 2017. URL: https://www.nerc.com/comm/RSTC_Reliability_Guidelines/Item_4a._Integrating%20Inverter-Based_Resources_into_Low_Short_Circuit_Strength_Systems_-_2017-11-08-FINAL.pdf.
- [7] B. Badrzadeh, Z. Emin, S. Goyal, and et al. "System Strength". In: *CIGRE Science&Engineering Journal* 20 (2021).
- [8] National Grid. *System Operability Framework*. Tech. rep. Sept. 2014. URL: <https://www.nationalgrideso.com/document/63446/download>.
- [9] MIGRATE Project. *Massive Integration of Power Electronic Devices*. Tech. rep. 2019.
- [10] AEMO. *System Strength in the NEM Explained*. Tech. rep. Australian Energy Market Operator, Mar. 2020. URL: <https://aemo.com.au/-/media/files/electricity/nem/system-strength-explained.pdf>.
- [11] A. Boričić. *Impact on Power System Protection by a Large Penetration of Renewable Energy Sources (Master Thesis)*. Aug. 2019. URL: <http://dx.doi.org/10.13140/RG.2.2.10226.58561>.
- [12] A. Boričić, J. Wang, Y. Li, S. Zubic, and N. Johansson. "Impact on Power System Protection by a Large Penetration of Renewable Energy Sources". In: *18th Wind Integration Workshop*. Dublin, Ireland, Oct. 2019.
- [13] R.Torkzadeh, J. Waes, G. Mulder, V. Čuk, and S. Cobben. "An Estimation for Short-Circuit Power Changes in the Dutch Grid to Analyze the Impacts of Energy Transition on Voltage Dips". In: *CIGRE 2022*. Paris.
- [14] A. Boricic, J. L. R. Torres, and M. Popov. "System Strength: Classification, Evaluation Methods, and Emerging Challenges in IBR-dominated Grids". In: *2022 IEEE PES Innovative Smart Grid Technologies - Asia (ISGT Asia)*. IEEE, Nov. 2022, pp. 185–189. ISBN: 979-8-3503-9966-0. DOI: [10.1109/ISGTAsia54193.2022.10003499](https://doi.org/10.1109/ISGTAsia54193.2022.10003499).
- [15] L. Huang, H. Xin, W. Dong, and F. Dörfler. "Impacts of Grid Structure on PLL-Synchronization Stability of Converter-Integrated Power Systems". In: *IFAC-PapersOnLine* 55.13 (2022), pp. 264–269. ISSN: 24058963. DOI: [10.1016/j.ifacol.2022.07.270](https://doi.org/10.1016/j.ifacol.2022.07.270).
- [16] J. Z. Zhou, H. Ding, S. Fan, Y. Zhang, and A. M. Gole. "Impact of Short-Circuit Ratio and Phase-Locked-Loop Parameters on the Small-Signal Behavior of a VSC-HVDC Converter". In: *IEEE Transactions on Power Delivery* 29.5 (Oct. 2014), pp. 2287–2296. ISSN: 0885-8977. DOI: [10.1109/TPWRD.2014.2330518](https://doi.org/10.1109/TPWRD.2014.2330518).

- [17] T. Lund, H. Wu, H. Soltani, J. G. Nielsen, G. K. Andersen, and X. Wang. “Operating Wind Power Plants Under Weak Grid Conditions Considering Voltage Stability Constraints”. In: *IEEE Transactions on Power Electronics* 37.12 (Dec. 2022), pp. 15482–15492. ISSN: 0885-8993. DOI: [10.1109/TPEL.2022.3197308](https://doi.org/10.1109/TPEL.2022.3197308).
- [18] L. Meegahapola, S. Bu, and M. Gu. “Low Short-Circuit Strength and Converter Associated Stability Issues”. In: 2022, pp. 189–231. DOI: [10.1007/978-3-031-06384-8_{_}7](https://doi.org/10.1007/978-3-031-06384-8_{_}7).
- [19] M. Zhang. “Modeling, Identification, and Stability Analysis of Inverter-Based Resources Integrated Systems”. PhD thesis. Nov. 2021. URL: <https://digitalcommons.usf.edu/etd/9735/>.
- [20] CIGRE WG B4.62 671. *Connection of wind farms to weak AC networks*. Tech. rep. CIGRE, Dec. 2016.
- [21] A. Ekic, B. Strombeck, D. Wu, and G. Ji. “Assessment of Grid Strength Considering Interactions between Inverter-based Resources and Shunt Capacitors”. In: *2020 IEEE Power & Energy Society General Meeting (PESGM)*. IEEE, Aug. 2020, pp. 1–5. ISBN: 978-1-7281-5508-1. DOI: [10.1109/PESGM41954.2020.9281633](https://doi.org/10.1109/PESGM41954.2020.9281633).
- [22] Y. Zhang, S.-H. F. Huang, J. Schmall, J. Conto, J. Billo, and E. Rehman. “Evaluating system strength for large-scale wind plant integration”. In: *2014 IEEE PES General Meeting | Conference & Exposition*. IEEE, July 2014, pp. 1–5. ISBN: 978-1-4799-6415-4. DOI: [10.1109/PESGM.2014.6939043](https://doi.org/10.1109/PESGM.2014.6939043).
- [23] J. Matevosyan. *ERCOT’s Experience Integrating High Shares of IBR*. June 2021. URL: <https://www.wingrid.org/wp-content/uploads/2021/08/13-Julia-Matevosyan-ERCOT-Integrating-high-shares-of-IBR.pdf>.
- [24] Electronix Corporation. *System Strength Assessment of the Panhandle System*. Tech. rep. Feb. 2016.
- [25] S. Nuthalapati, ed. *Use of Voltage Stability Assessment and Transient Stability Assessment Tools in Grid Operations*. Springer International Publishing, 2021. ISBN: 978-3-030-67481-6. DOI: [10.1007/978-3-030-67482-3](https://doi.org/10.1007/978-3-030-67482-3).
- [26] *Minnesota Renewable Energy Integration and Transmission Study - Final Report*. Tech. rep. GE Energy Consulting, in Collaboration with MISO, Oct. 2014.
- [27] D. Wu, G. Li, M. Javadi, A. M. Malyscheff, M. Hong, and J. N. Jiang. “Assessing Impact of Renewable Energy Integration on System Strength Using Site-Dependent Short Circuit Ratio”. In: *IEEE Transactions on Sustainable Energy* 9.3 (July 2018), pp. 1072–1080. ISSN: 1949-3029. DOI: [10.1109/TSTE.2017.2764871](https://doi.org/10.1109/TSTE.2017.2764871).
- [28] D. Wu, A. M. Aldaoudeyeh, M. Javadi, F. Ma, J. Tan, and J. N. Jiang. “A method to identify weak points of interconnection of renewable energy resources”. In: *International Journal of Electrical Power & Energy Systems* 110 (Sept. 2019), pp. 72–82. ISSN: 01420615. DOI: [10.1016/j.ijepes.2019.03.003](https://doi.org/10.1016/j.ijepes.2019.03.003).
- [29] M. Maharjan, A. Ekic, M. Beedle, J. Tan, and D. Wu. “Evaluating grid strength under uncertain renewable generation”. In: *International Journal of Electrical Power & Energy Systems* 146 (Mar. 2023), p. 108737. ISSN: 01420615. DOI: [10.1016/j.ijepes.2022.108737](https://doi.org/10.1016/j.ijepes.2022.108737).
- [30] T. Lund, B. Yin, G. K. Andersen, and M. Gupta. “Challenges and solutions for integration of wind power in weak grid areas with high inverter penetration”. In: *19th Wind Integration Workshop*. Ljubljana, Slovenia, Nov. 2020.
- [31] T. Cutsem and C. Vournas. *Voltage Stability of Electric Power Systems*. Boston, MA: Springer US, 1998. ISBN: 978-0-387-75535-9. DOI: [10.1007/978-0-387-75536-6](https://doi.org/10.1007/978-0-387-75536-6).
- [32] W. C. Taylor. *Power System Voltage Stability*. McGraw-Hill, 1994.
- [33] AEMC. *Investigation Into System Strength Framework in the NEM - Final Report*. Tech. rep. Australian Energy Market Commission, Oct. 2020.
- [34] AEMO. *System Strength Impact Assessment Guidelines*. Tech. rep. Australian Energy Market Operator, Mar. 2023. URL: https://aemo.com.au/-/media/files/stakeholder_consultation/consultations/nem-consultations/2022/ssrmiag/final-report/system-strength-impact-assessment-guideline_v2.pdf?la=en.

- [35] A. Boričić, J. L. R. Torres, and M. Popov. “Beyond SCR in Weak Grids: Analytical Evaluation of Voltage Stability and Excess System Strength”. In: *2023 International Conference on Future Energy Solutions (FES)*. IEEE, June 2023, pp. 1–6. ISBN: 979-8-3503-3230-8. DOI: [10.1109/FES57669.2023.10183286](https://doi.org/10.1109/FES57669.2023.10183286).
- [36] Y. Tang. *Voltage Stability Analysis of Power System*. Singapore: Springer Singapore, 2021. ISBN: 978-981-16-1070-7. DOI: [10.1007/978-981-16-1071-4](https://doi.org/10.1007/978-981-16-1071-4).
- [37] International Electrotechnical Commission. *IEC 61400-27-1, Electrical Simulation Models for Wind Power Generation*. 2020.
- [38] EirGrid. *System Non-Synchronous Penetration Definition and Formulation*. Tech. rep. EirGrid, the Transmission System Operator (TSO) of Ireland., Aug. 2018. URL: <https://www.eirgridgroup.com/site-files/library/EirGrid/SNSP-Formula-External-Publication.pdf>.
- [39] K. V. Kkuni, M. Nuhic, and G. Yang. “Power System Stability Impact Assessment for the Current Limits of Grid Supporting Voltage-Source Converters”. In: *2021 IEEE Power & Energy Society General Meeting (PESGM)*. IEEE, July 2021, pp. 1–5. ISBN: 978-1-6654-0507-2. DOI: [10.1109/PESGM46819.2021.9637902](https://doi.org/10.1109/PESGM46819.2021.9637902).
- [40] O. Gomis-Bellmunt, J. Song, M. Cheah-Mane, and E. Prieto-Araujo. “Steady-state impedance mapping in grids with power electronics: What is grid strength in modern power systems?” In: *International Journal of Electrical Power & Energy Systems* 136 (Mar. 2022), p. 107635. ISSN: 01420615. DOI: [10.1016/j.ijepes.2021.107635](https://doi.org/10.1016/j.ijepes.2021.107635).
- [41] IEEE PES-TR77. *Stability definitions and characterization of dynamic behavior in systems with high penetration of power electronic interfaced technologies*. Tech. rep. IEEE Power & Energy Society, May 2020. URL: https://resourcecenter.ieee-pes.org/publications/technical-reports/PES_TP_TR77_PSDP_STABILITY_051320.html.
- [42] D. Ramasubramanian, J. Ruddy, P. Dattaray, E. Farantatos, and A. Gaikwad. “A Positive Sequence Screening Tool to Identify Areas of Potential Inverter Instability in Inverter Dominated Systems”. In: *18th Wind Integration Workshop*. Dublin, Ireland, Oct. 2019.
- [43] D. Bowman, D. Ramasubramanian, R. McCann, E. Farantatos, A. Gaikwad, and J. Caspary. “SPP Grid Strength Study with High Inverter-Based Resource Penetration”. In: *2019 North American Power Symposium (NAPS)*. IEEE, Oct. 2019, pp. 1–6. ISBN: 978-1-7281-0407-2. DOI: [10.1109/NAPS46351.2019.9000309](https://doi.org/10.1109/NAPS46351.2019.9000309).
- [44] W. Wang, G. M. Huang, D. Ramasubramanian, and E. Farantatos. “Transient stability analysis and stability margin evaluation of phase-locked loop synchronised converter-based generators”. In: *IET Generation, Transmission & Distribution* 14.22 (Nov. 2020), pp. 5000–5010. ISSN: 1751-8687. DOI: [10.1049/iet-gtd.2020.0620](https://doi.org/10.1049/iet-gtd.2020.0620).
- [45] M. Zarif Mansour, S. P. Me, S. Hadavi, B. Badrzadeh, A. Karimi, and B. Bahrani. “Nonlinear Transient Stability Analysis of Phased-Locked Loop-Based Grid-Following Voltage-Source Converters Using Lyapunov’s Direct Method”. In: *IEEE Journal of Emerging and Selected Topics in Power Electronics* 10.3 (June 2022), pp. 2699–2709. ISSN: 2168-6777. DOI: [10.1109/JESTPE.2021.3057639](https://doi.org/10.1109/JESTPE.2021.3057639).
- [46] M. G. Taul, X. Wang, P. Davari, and F. Blaabjerg. “Systematic Approach for Transient Stability Evaluation of Grid-Tied Converters during Power System Faults”. In: *2019 IEEE Energy Conversion Congress and Exposition (ECCE)*. IEEE, Sept. 2019, pp. 5191–5198. ISBN: 978-1-7281-0395-2. DOI: [10.1109/ECCE.2019.8912571](https://doi.org/10.1109/ECCE.2019.8912571).
- [47] A. Haddadi, E. Farantatos, I. Kocar, and U. Karaagac. “Impact of Inverter Based Resources on System Protection”. In: *Energies* 14.4 (Feb. 2021), p. 1050. ISSN: 1996-1073. DOI: [10.3390/en14041050](https://doi.org/10.3390/en14041050).
- [48] AEMO. *Behaviour of distributed resources during power system disturbances: Overview of key findings*. Tech. rep. Australian Energy Market Operator, May 2021.
- [49] D. Ramasubramanian, P. Pourbeik, E. Farantatos, and A. Gaikwad. “Simulation of 100% Inverter-Based Resource Grids With Positive Sequence Modeling”. In: *IEEE Electrification Magazine* 9.2 (June 2021), pp. 62–71. ISSN: 2325-5897. DOI: [10.1109/MELE.2021.3070938](https://doi.org/10.1109/MELE.2021.3070938).

- [50] CIGRE WG C4.56. *Electromagnetic transient simulation models for large-scale system impact studies in power systems having a high penetration of inverter-connected generation*. Tech. rep. CIGRE, Sept. 2022. URL: <https://e-cigre.org/publication/881-electromagnetic-transient-simulation-models-for-large-scale-system-impact-studies-in-power-systems-having-a-high-penetration-of-inverter-connected-generation>.

4

SHORT-TERM STABILITY WITH DER AND DYNAMIC LOADS

Great things are done by a series of small things brought together.

- Vincent Van Gogh, Dutch Painter (1853-1890)

The number of Distributed Energy Resources (DER) and dynamic loads is increasing rapidly in modern power systems. Their aggregated effects on power system dynamics are, however, still insufficiently explored. Consequently, such effects are typically not appropriately considered when evaluating overall system stability, strength, or (voltage) resilience. Nevertheless, it is expected that the further proliferation of DERs and dynamic loads will lead to more pronounced distribution-transmission grid interactions in the future. This results in a stronger need to model and analyze distribution systems when evaluating the stability, resilience, and strength of modern power systems, discussed in previous chapters.

This chapter aims to improve the understanding of modern distribution-transmission interactions related to short-term stability. Moreover, it emphasizes the importance of a more accurate representation of DERs and dynamic loads when performing stability analyses and dynamic-state system strength evaluations. Following a short introduction to modern distribution systems, a comprehensive fundamental analysis is performed to reveal the impacts of DER and dynamic loads on short-term instability, with a particular focus on voltage stability. Based on generated big data by performing a substantial number of dynamic simulations automatically, the instability effects are extensively explored from several perspectives: i) the type and amount of dynamic load, ii) the penetration of DERs, and iii) DER control strategies. Finally, the key aspects and parameters of distributed generation and dynamic load affecting the overall system stability and strength are revealed.

Parts of this chapter have been published in peer-reviewed articles and/or conference proceedings. See [The List of Publications](#) section for more details.

4.1. MODERN DISTRIBUTION NETWORKS

DERs are spreading rapidly in power systems worldwide. This trend, discussed in [Chapter 1](#), is primarily initiated by the small- and mid-scale solar PV and wind generation, scattered across the system and typically connected to the distribution grid. As a consequence, transmission grid operators, responsible for power system stability and resilience, have very little observability or control over such units. As their number and generation capacity rise relative to the controllable and observable synchronous generation, so does their impact on the overall system dynamics and stability. This impact is further amplified if system strength is low.

Some cases of DER impact on stability have been exemplified in [Table 1.1](#), where a simultaneous (mal)operation or disconnection of a large number of DERs notably impacts the severity of the disturbance and the ability of the system to recover. For instance, the Australian blackout event became more severe due to the failure of wind farms to ride through [1]. Moreover, the recent event that led to a blackout in the United Kingdom was negatively impacted by more than half a gigawatt of DER loss [2]. Another known example occurred in Germany, the so-called *flapping* (also known as the 50.2 Hz problem), where numerous DERs would simultaneously connect and disconnect due to their shared overfrequency disconnection settings, resulting in frequency oscillations [3]. Further studies and examples of DERs' impact on stability can be found in [4–11]. In general, as DER penetration rises, their impact on system stability is expected to rise accordingly. [Figure 4.1](#) illustrates this further.

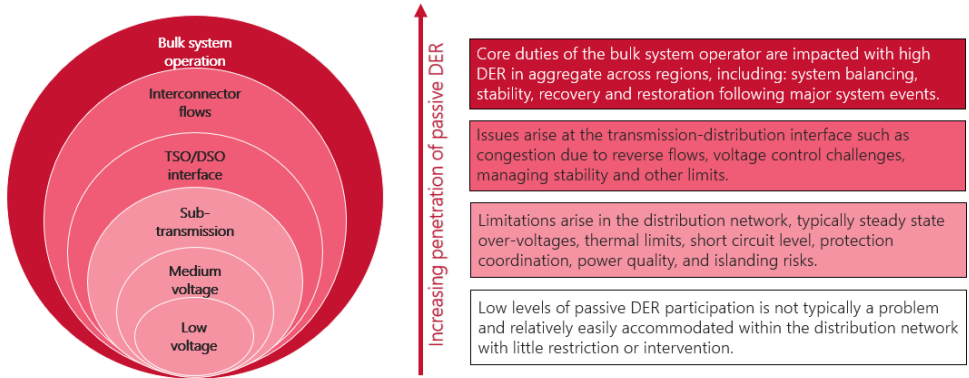


Figure 4.1.: Trajectory of system challenges with an increasing share of DERs [12].

When the penetration of DERs is small, this is generally not a problem, and any effects are limited to the surrounding low- and medium-voltage networks. Typical challenges at this stage are related to local protection coordination, power quality, and steady-state overvoltages [13, 14]. However, as DER penetration rises, as illustrated by moving up in [Figure 4.1](#), issues begin to arise further in the grid, for instance in the distribution-transmission interface. Finally, once systems begin to reach high DER penetration levels, the bulk power system stability is also directly impacted by the commonly unobservable and uncontrollable DER units' operation.

An important aspect of DERs operation is their Fault Ride Through (FRT) capability. FRT is typically a part of the *grid code*, which describes the operation that each generating unit, including DERs, should exhibit in a steady and dynamic system state. Two common ride-through criteria are voltage ride-through (VRT) and frequency ride-through. As this thesis primarily focuses on voltage stability and resilience, the VRT concept is of more importance and is described further.

VRT describes the set of demands for the capability of electric generators to stay connected to the grid in short periods of voltage deviations. VRT typically comprises low-voltage ride-through (LVRT) and high-voltage ride-through (HVRT). A typical VRT voltage-time characteristic is illustrated in Figure 4.2. Depending on the intensity of the voltage drop and its duration, generating units are either obliged to stay connected (yellow region)¹ or allowed to disconnect (pink region). As countries (regions) have their specific grid codes, the exact characteristics can differ [15–19].

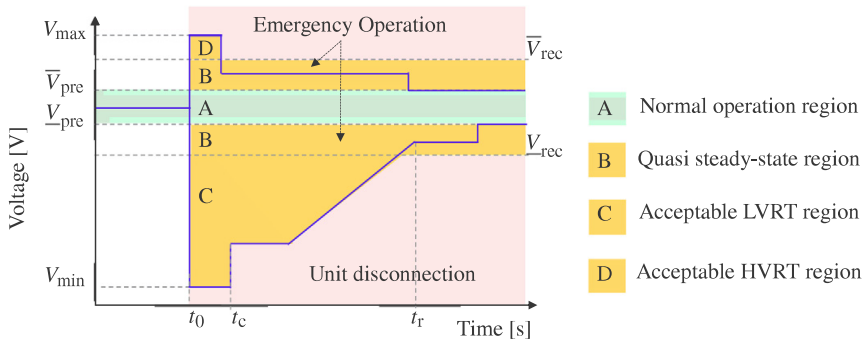


Figure 4.2.: Typical Voltage Ride Through (VRT) characteristic [20].

Coincidentally with the proliferation of DER, the number and complexity of dynamic loads are also growing. As discussed in Chapter 1, the small and large industries are shifting from fossil-powered to electrified, resulting in many complex and power-intensive motors. Furthermore, with the improvements in power electronics, the number of variable frequency drives and electronic loads is also increasing. The power system demand behaviour hereby changes, resulting in a higher impact on system dynamics and stability [21–23]. Additionally, as both dynamic loads and DERs are located in distribution grids, their interactions and mutual impact on grid stability increase in complexity and importance as well [24].

The two described trends of DER and dynamic load rise lead to increasingly intricate and relevant impacts of modern distribution systems on the overall system dynamics and stability. Short-term stability, discussed in Chapter 2, consequently becomes one of the major issues that modern power systems face. It is therefore of the uttermost importance to comprehensively analyze the impacts of DERs and dynamic loads on short-term stability, while also considering the large number of components and possible control parameters that define their operation. The following sections present a comprehensive analysis in this direction.

¹And possibly support the grid with (re)active current injection, depending on grid codes.

4.2. IMPACT ANALYSIS ON SHORT-TERM STABILITY

To shed more light on the impact of dynamic loads and DERs on the short-term stability of a bulk power system, with a specific focus on voltage behaviour and stability, a comprehensive analysis is performed with the results depicted in this chapter [24]. The test system description and the methodology are described first, followed by the numerical results and comprehensive discussion.

4.2.1. TEST SYSTEM DESCRIPTION

Various test grids for stability studies are available in the literature. Nevertheless, the IEEE Test System for Voltage Stability Analysis and Security Assessment [25] represents one of the most comprehensive generic test grids for voltage stability studies. The grid model contains all the necessary specifications for a realistic dynamic response representation. Furthermore, the dynamic constraints this system experiences during simulations are precisely in terms of voltage stability [26]. Hence, this model is, at present, extensively used for voltage stability research. The main characteristics of the system are listed in Table 4.1, with more details shown in the Appendix A and further in [25–27].

Table 4.1.: Characteristics of the system in Figure 4.3 [26].

Nominal frequency (Hz)	50
Number of buses	74
Number of lines	50
Number of transformers	52
Number of generators	19
Number of sync. condensers	1
Number of loads	22
Number of shunt elements	11
Total Generation (MW)	11506
Total Load (MW)	11060

The basic system is enhanced for this study by introducing advanced load models in the central area of the system, the WECC Composite Load models. The part of the grid is chosen due to the fact that a great amount of the load is located in this area, and the dynamics of the area itself are the most prone to trigger voltage instability, as explained in [25–27]. Furthermore, DER units based on the advanced DER-A model are introduced in the central area as well. These two load and DER models are described in more detail further in the chapter.

This enhanced grid model creates conditions to comprehensively analyze the effects and mutual interactions of DER penetration and dynamic load presence on the short-term stability of the bulk power system. The system's diagram and the locations where load and DER models are introduced are shown in Figure 4.3, while the details of the changes are enlisted further in the chapter.

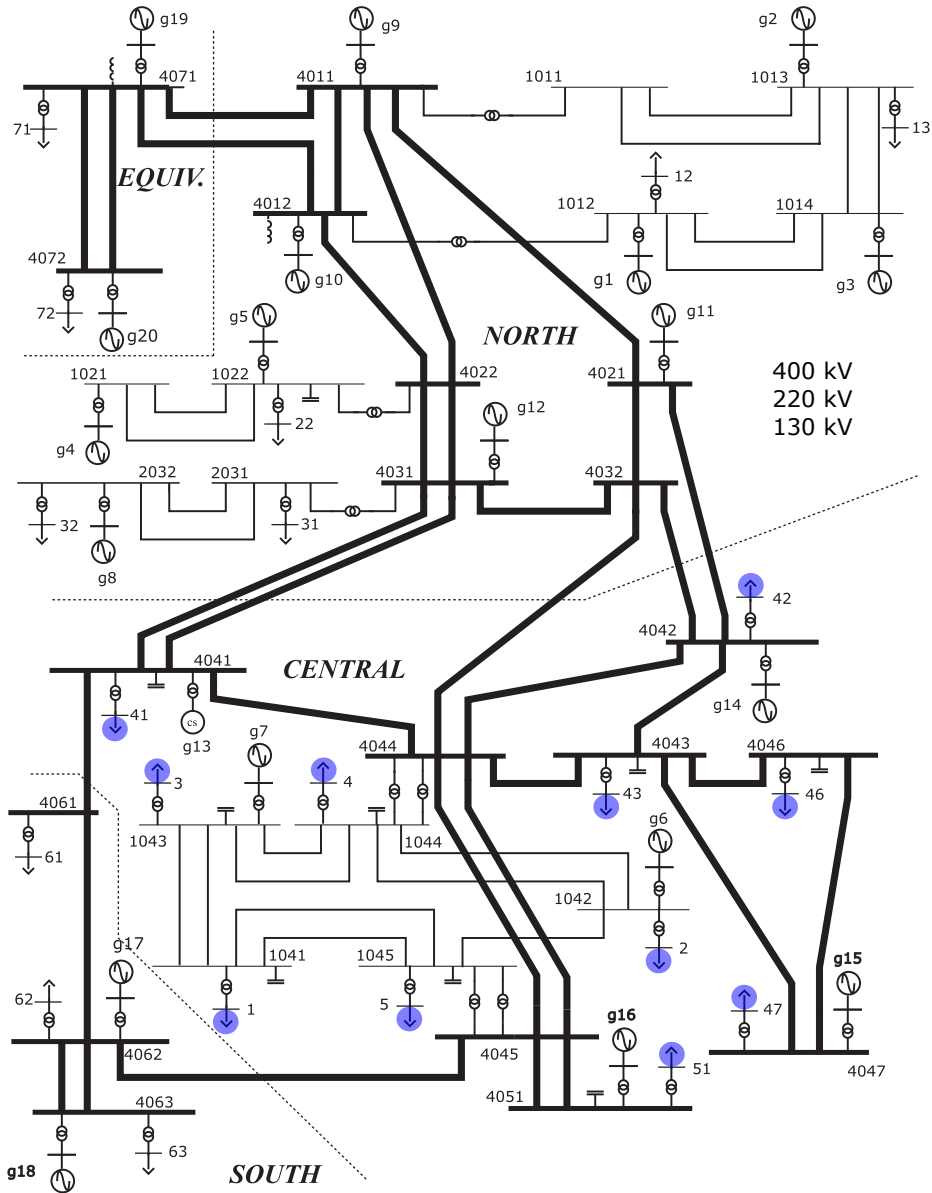


Figure 4.3.: IEEE Test System for Voltage Stability Analysis and Security Assessment. Blue circles indicate the locations of the WECC composite load and DER-A models additions.

The dynamic load and DER additions and their dynamic models are introduced further in the following subchapters, with more details in [Appendix B](#).

DYNAMIC LOAD MODELLING

Load modelling is an important part of power system studies and it attracts a lot of research attention. It is impractical to model every load accurately, as this will impose two issues. Firstly, the low feasibility due to the data uncertainty and unavailability, and secondly, even if the loads are accurately modelled, the complexity and size of the whole model would be unmanageable for any practical bulk power system simulations. Hence, a trade-off should be found in having enough precision for the study in question, but with a limited level of complexity.

Modern distribution systems contain an increased number of complex dynamic loads such as induction motors and electronic loads. However, at present, the models used for analyses are often still very basic, even for dynamic studies [21, 22]. Hence, the path of lower complexity and therefore lower precision is often chosen. These simplifications often neglect major dynamic interactions occurring in modern distribution systems, which can significantly affect the bulk power system and its stability, as will be demonstrated in this chapter.

To achieve both high fidelity for dynamic studies and a relatively low level of complexity, aggregated load models are used. One of them is the Western Electricity Coordinating Council (WECC) Composite Load Model, which is presently one of the best models for such a task. The model was initially developed in 2012 and since then it has been repeatedly updated and validated [28, 29]. The simplified schematic structure of the model is shown in Figure 4.4.

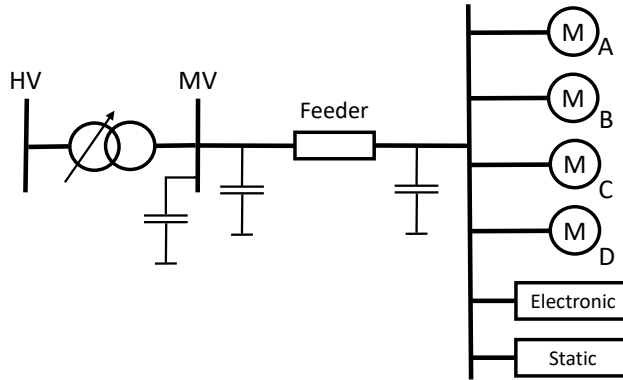


Figure 4.4.: WECC Composite Load model diagram with various types of load.

Its ability to take into account various compositions of the load, allowing more precise dynamic response modelling, makes this model very attractive. Furthermore, its complexity is kept at a reasonable level, resulting in great interest from both academia and industry. The system contains a feeder representation, several types of motors, an electronic load, and a static load. More information about this can be found in [28–30]. The share of different load types is adjustable to any particular case or system. The model used in this thesis is the WECC Load Model from DIGSILENT PowerFactory 2020 SP2A [31], described further in the Appendix B. The

analysis utilizes default parameter values, whilst the share and penetration of each of the motor types are varied throughout the simulations, as will be demonstrated in the results section. More information about parametrization and uncertainty can be found in [32, 33], as this falls beyond the scope of this work.

The motors of types A, B, and C are utilized in the model to represent different types of three-phase motors. Model A represents low inertia induction motors driving constant torque load, e.g. compressor motors. Model B represents induction motors with high inertia, driving quadratic torque loads, e.g. ventilation systems. Model C represents low inertia induction motors driving quadratic torque loads, such as centrifugal pumps. Finally, Model D represents single-phase induction motors, e.g. A/C units. More information about the motor types can be found in [28–30].

DER DYNAMIC MODELLING

Except for the load effects on short-term stability, a strong impact on modern grids is caused by the integration of distributed generation in distribution grids [5]. Since most DERs are coupled with the grid using an inverter, their dynamic behaviour is largely dominated by the control strategy rather than the generation unit specifics. DERs come in various types and with several possible control strategies. Furthermore, their distribution all over the network makes them very hard to model and incorporate in analyses. As accurate models are computationally time-consuming and difficult to develop, the use of aggregated models is the viable way to take into account the DER effects in a larger system study [34]. One of the most advanced aggregated DER models to date is the DER-A model. In comparison to its predecessor, the PVD1 model, DER-A has enhanced abilities to represent various control strategies and LVRT operation, while exhibiting a lower overall complexity. The detailed model diagram of the DER-A model is given in Figure 4.5. Further information can be found in the Appendix B and in [30, 35–38].

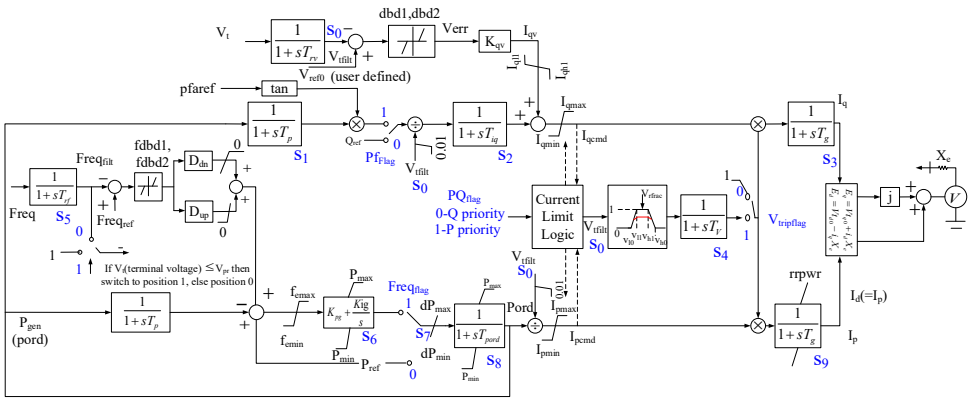


Figure 4.5.: Diagram of the DER-A model [30].

The parameterization of the model for the purposes of this thesis is shown further in the chapter and in Appendix B.

4.2.2. METHODOLOGY

Short-term stability and its evaluation are described extensively in Chapter 2. The flowchart in Figure 4.6 describes the methodology developed as a basis of the performed analysis in this chapter. The algorithm begins with the scenario selection and simulation initiation, shortly followed by the fault inception and fault clearing. The scenarios are described further in the results section.

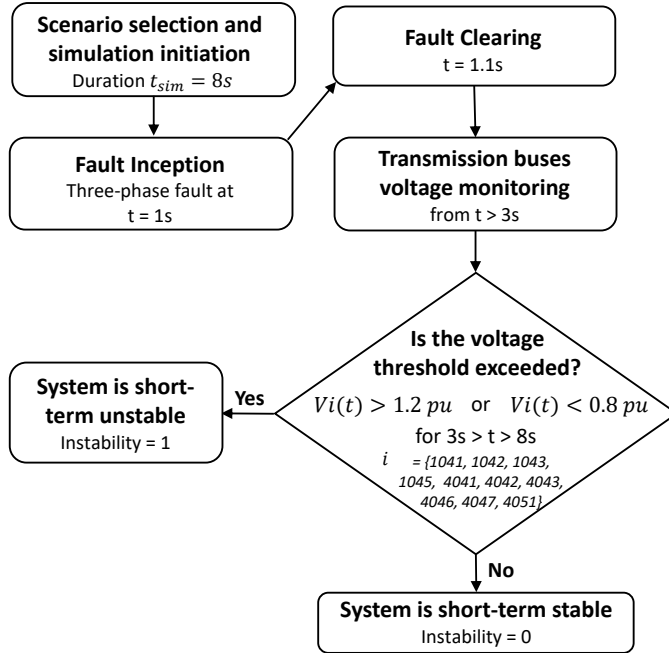


Figure 4.6.: A flowchart of the methodology for short-term stability evaluation of transmission buses from the central area of the system in Figure 4.3.

Throughout this process, the transmission bus voltages are monitored continuously. Once the voltage values are obtained for the full simulation time (8 s), their values are analyzed to check whether they surpassed the upper or lower set thresholds (1.2 and 0.8 per unit, respectively). If at least one of the monitored voltage values is outside of the defined thresholds at any moment after 3 s ($t_f + 2$), the system is considered unstable. The value of 3 s is chosen to avoid initial fault-induced voltage variations, which could lead to incorrect categorization of the results. The buses in vector i selected for analysis are taken as major transmission buses in the central area of the grid, which allows capturing most of the central region dynamics.

To clarify this methodology further, Figure 4.7 shows examples of short-term stable and unstable cases, respectively.

Black horizontal lines represent the utilized thresholds, which should not be surpassed. In other words, all voltages should stay in the zone in between the black lines for short-term stability to be preserved. The left plot in Figure 4.7 shows a case

of stable operation, whilst the right plot shows a case where the system is short-term unstable. As extensively discussed in [Chapter 2](#), the short-term instability can be experienced either as a sharp drop in voltages, unsustainably low post-fault voltages, or as undamped voltage oscillations that eventually lead to a voltage collapse (see [Figures 2.11](#) and [2.12](#)). The shown plots in [Figure 4.7](#) are two exemplifying cases of low (left) and high (right) amounts of dynamic load present in the grid and its influence on short-term instability. Extensive analysis in this regard will be demonstrated and explained in the next section.

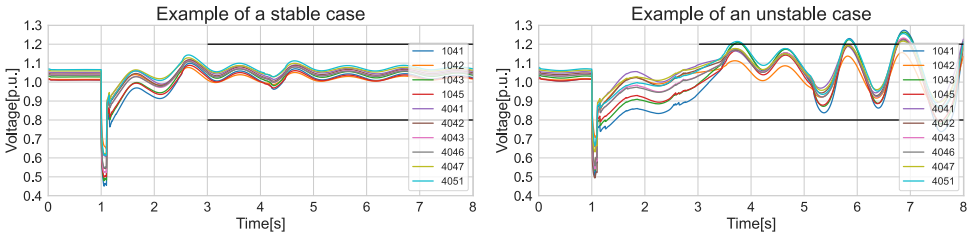


Figure 4.7.: Examples of the methodology applied in the study. The left figure represents a stable case, and the right figure is an unstable one.

It should be noted that these thresholds are not perfect and that some events will be incorrectly categorized. These conditions should instead be thought of not as a definite short-term instability evaluation, but as an approximation framework that will allow automatic risk-of-instability check. Failure to fulfil the presented conditions can be also thought of as an imminent threat to short-term stability, i.e. a system being in severe danger of short-term instability. Nevertheless, most of the events will indeed be properly categorized since the majority of grids would not be able to recover from such high- or low-voltage situations in the HV grid without severe consequences. Slight differences for specific systems are, of course, plausible.

This process is applied recursively, following the methodology shown in the flowchart in [Figure 4.8](#), conducted in Python 3.8.3 and DIgSILENT PowerFactory 2020 SP2A operated in parallel.

[Figure 4.8](#) describes this recursive Python-PowerFactory process. Firstly, the scenario is selected, after which it is checked whether all the scenarios are already analyzed. If that is not the case, the flowchart connects to the algorithm in [Figure 4.6](#), and the process repeats itself until all the scenarios are analyzed. Once this is completed, the resulting instability data is presented on a heatmap, as illustrated later in this chapter.

The created heatmaps are based on the Python Seaborn library [39] and will be used throughout the chapter to visualize the results effectively. Different parameters will be varied on X and Y-axes, while the Z-axis will be used for twelve different short-circuit scenarios in the grid. The numbers in the heatmap blocks demonstrate how many of those short-circuit scenarios are unstable, as per the previously introduced methodology.

The numbers are also shown in a coloured box for clearer visualization, in a

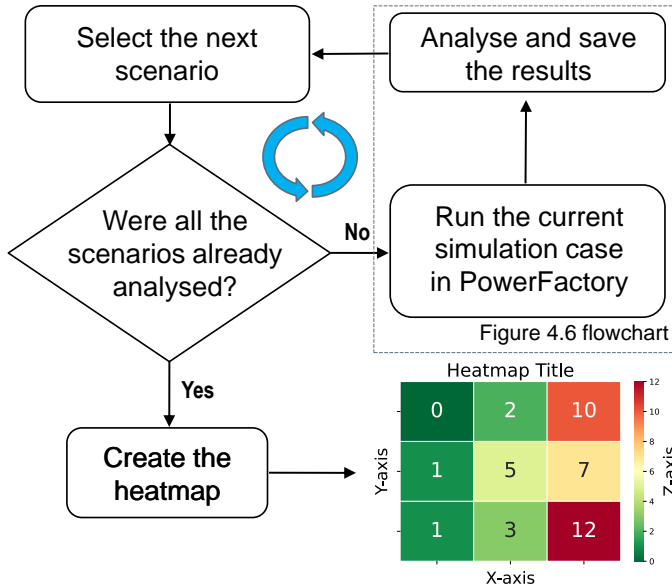


Figure 4.8.: Flowchart of the entire Python-PowerFactory methodology, with the heatmap example as a result.

colour spectrum from green (low number of instabilities), yellow (medium number of instabilities), to red (high number of instabilities).

This methodology allows the automatized analysis of a vast number of grid scenarios to derive conclusions on which dynamic load and DER specifics of interest are most correlated with the short-term instability, and in what amount they contribute to its inception or suppression.

4.3. RESULTS AND DISCUSSION

The analysis comprises two main directions. The first is the influence of the dynamic load models on short-term stability without any DER penetration in the grid. The second direction of the analysis follows up on the first one, by introducing DER penetration in the distribution grids as well, to evaluate the overall effects and interactions of dynamic loads and DERs together in terms of short-term stability.

4.3.1. IMPACT OF DYNAMIC LOADS ON SHORT-TERM STABILITY

The first part of the analysis deals with the influence of the dynamic load on short-term stability. While it is known that dynamic loads are the common culprits for short-term voltage instability, the amounts of their penetration in the grid that could cause system-wide instability are less known. Furthermore, how different induction motors in the grid relate to short-term stability is unclear as well since the

existing research is mainly theoretical or focused on a specific smaller-system case study. Hence, the research questions this section aims to answer are as follows:

1. *What is the amount of dynamic load in a grid that may cause a significant impact on short-term stability?*
2. *How does each type of dynamic load affect short-term stability, and which types are the most dangerous for the bulk power system stability?*

To give comprehensive answers to these questions, the IEEE system presented in Figure 4.3 is adopted. The system is utilized in its operating point "A", introduced in [25] as an operating scenario where the system is close to voltage stability limits. The model is further extended and enhanced by introducing 11 identical WECC Composite Load models to the central region, replacing the existing simplistic static load models, as shown in Figure 4.3. The parameters of these dynamic loads are initially kept at their default PowerFactory values, except for the voltage level and base power adaptations to match the IEEE test system. The parameters related to the share of each load type in the analysis are presented further in the text. The Active Distribution Network (ADN) busbars where the WECC Composite Load models are introduced are listed in Table 4.2. Furthermore, the same table shows the location of twelve different 3-phase short circuit scenarios used in the analysis.

Table 4.2.: Location of WECC Dynamic Load models (left) and fault scenarios (right).

MV busbars with ADNs	Fault location busbars
1	1041
2	1042
3	1043
4	1044
5	1045
41	4031
42	4032
43	4041
46	4042
47	4043
51	4044
-	4062

The fault buses are chosen to be dominantly in the central region, as this will likely lead to further voltage-related stress and potential instabilities in the grid due to two reasons. Firstly, the IEEE system is susceptible to voltage instability in the case of North-Central corridor faults [25, 26]. Secondly, due to the addition of dynamic loads and DER units in the central area, such nearby faults are expected to aggravate more severe dynamic events. Nevertheless, a few faults in the proximity to the central area are also analyzed, so that a larger variety of faults are taken into account. A three-phase short circuit is chosen, as its severity is most likely to initiate severe voltage deviations and instabilities.

The amount of composite load is varied by replacing the static load, in a range between 0 and 50% of the total system demand, in 5% steps. Cases above 50% are not shown, as such penetrations are uncommon in large power systems. The steps of 5% are selected as a compromise between desired sensitivity, computational complexity, and the clarity of results being presented.

Moreover, 10 different load compositions are used to evaluate how different types of motors affect short-term stability. [Table 4.3](#) summarizes this methodology.

Table 4.3.: Ten load composition scenarios and their respective parameters.

Load scenario abbreviation	Description of the scenario	Share of motors A/B/C/D (per unit)
0	Static load	0.00 / 0.00 / 0.00 / 0.00
N	Equal share	0.15 / 0.15 / 0.15 / 0.15
A	More A-type	0.30 / 0.10 / 0.10 / 0.10
AA	Majority A-type	0.45 / 0.05 / 0.05 / 0.05
B	More B-type	0.10 / 0.30 / 0.10 / 0.10
BB	Majority B-type	0.05 / 0.45 / 0.05 / 0.05
C	More C-type	0.10 / 0.10 / 0.30 / 0.10
CC	Majority C-type	0.05 / 0.05 / 0.45 / 0.05
D	More D-type	0.10 / 0.10 / 0.10 / 0.30
DD	Majority D-type	0.05 / 0.05 / 0.05 / 0.45

The rest of the dynamic load composition not mentioned in [Table 4.3](#) (40%), is kept in electronic load (15%) and static load (25%) in all the scenarios.

The presented analysis framework results in a total of 1320 dynamic time-domain simulations of 8 s duration each, ran via a Python script connected through DIGSILENT PowerFactory 2020 SP2A. In each simulation, central bus voltages are monitored to determine if the short-term stability is preserved. An example of such a measurement is already shown in [Figure 4.7](#). The heatmap resulting from this comprehensive analysis is shown in [Figure 4.9](#).

The X-axis in [Figure 4.9](#) represents an increasing share of WECC Composite Load models replacing static loads. The Y-axis takes all the scenarios from [Table 4.3](#) for analysis. Finally, the color bar (Z-axis) shows the number of unstable scenarios, based on the 12 analyzed faults enlisted in the second column of [Table 4.2](#). As previously explained, the numbers in the heatmap blocks represent how many fault cases, out of the total of 12, are short-term unstable for the corresponding parameters on the X- and Y-axis. Larger (smaller) numbers, visualized with the colour spectrum for further clarity, effectively indicate a stronger (weaker) correlation of those parameter values with the short-term instability inception.

From the heatmap, it can be seen that the dynamic load percentage below 20% does not affect short-term stability for any of the given scenarios. With percentages of dynamic load between 20 and 35%, some instability is observed, while for 40–50% values most scenarios exhibit an inability to cope with the majority of the faults in terms of short-term stability. For even higher percentages, which are not shown, it is found that the large majority of the cases are unstable. For the sake of comparison,

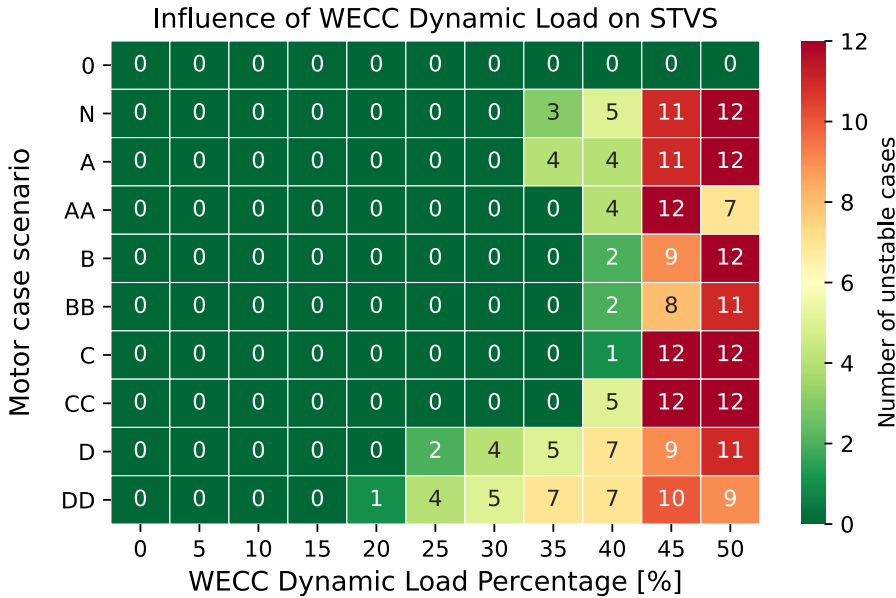


Figure 4.9.: Heatmap visualization of the WECC Dynamic load influence on short-term stability with a varying presence and type of dynamic loads.

a basic model with only static load is shown in the first row of the heatmap, where all the cases are evaluated to be stable. Clearly, dynamic load plays a large role in short-term instability inception.

Hence, in terms of maximum penetration of dynamic load, approximately 25–30% is predominantly related to instability in the studied grid, with shown differences depending on the type of load. This number also depends on how constrained the analyzed operating state of a system is, with emphasis on the available voltage/reactive power support, fault type/intensity, fault clearing time, power flows/contingencies, and the available Q-reserves and/or emergency control possibilities.

In terms of the second research question of this subchapter, by analyzing responses for different load compositions, several patterns are seen. Firstly, scenario *N* with an equal share of dynamic load types (see Table 4.3) begins to show an increasing number of instability scenarios starting from 35% dynamic load share. Moreover, motors *A* and *C*, seen from scenarios *A/AA/C/CC* (see Table 4.3), show worse results in Figure 4.9 in comparison to the motor *B/BB* scenarios. This can be theoretically explained by the fact that motors *A* and *C* are low-inertia motors, unlike motors of type *B* [30]. More inertia is known to be related to less severe oscillations and instabilities (e.g. see [40]), even when provided from the consumption side [41, 42]. Furthermore, the deceleration of induction motors causes them to draw higher

currents, which leads to further voltage drops. This affects short-term stability negatively [40]. Hence, all else equal, lower inertia amplifies oscillatory peaks of motors after faults, which reflects on system voltage deviations and ultimately short-term stability of the system as a whole.

Regarding motor type D, after 25% of the dynamic load share, they start to increasingly trigger instabilities. This occurs due to the initiation of the FIDVR event, leading to a depressed voltage profile with a duration of several seconds, followed by an overvoltage spike. This severe voltage deviation is categorized as instability by the presented methodology, in line with the discussion in [Chapter 2](#).

Overall, it can be concluded from this section that dynamic loads play a significant role in short-term stability, confirming theoretical expectations. The additional novel contribution is the insight into what percentages of dynamic load are expected to lead to short-term stability, as well as which types of induction motors are more strongly correlated with the likelihood of short-term stability.

4.3.2. IMPACT OF DYNAMIC LOADS AND DER ON SHORT-TERM STABILITY

For the second part of the analysis, the system from the previous section is taken as a basis. Hence, all 11 WECC Composite Loads are kept in the grid, with a fixed share of 50% relative to the static load. This corresponds to the central part of the last column of the heatmap in [Figure 4.9](#).

The research questions addressed in this section are as follows:

1. ***How do DERs interact with dynamic load and the grid in terms of short-term stability?***
2. ***Are DERs beneficial or detrimental to short-term stability? What penetration amounts make a difference?***
3. ***How do different DER control strategies affect the results?***

Six different load composition scenarios are analyzed, i.e. cases A, AA, B, BB, C, and CC from [Table 4.3](#). DERs have been added to the same 11 busbars where dynamic loads are located (see [Table 4.2](#) and [Figure 4.3](#)). The amount of DER penetration is varied in the range of 0 to 10% of the total generation of the system, with 1.25% incremental steps. This allows an evaluation of how different grid penetration scenarios affect short-term stability. DER generation is effectively replacing synchronous generation, not complementing it, making it more realistic and more voltage stability-constrained. Hence, for instance, the maximum of 10% penetration results in 936 MW of DER infeed spread out in the central region, considering the total sum of synchronous generation in operating point A [25] and the characteristics of the system in [Figure 4.3](#). More details about the system itself can be found in [Appendices A](#) and [B](#).

Furthermore, to address the third research question of this section and pinpoint the impact of various DER control strategies on system stability, four different DER fault control strategies are analyzed. The strategies are selected as the most common ones seen in the DER grid codes and operational requirements in power systems all around the world [4, 15].

- DER disconnects shortly after a fault ($\Delta t = 0.05$ s)
- Ride-through with Q-priority
- Ride-through with P-priority
- Momentary Cessation

The fault responses of a single DER unit with each of the fault control strategies are shown in Figure 4.10.

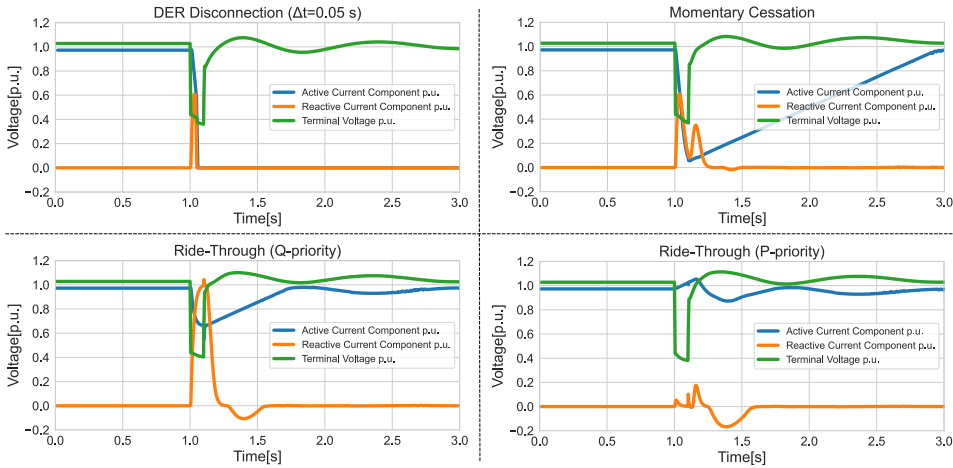


Figure 4.10.: Four fault control strategies of the DER-A model used in the analysis and their active/reactive current components after being subjected to a voltage drop at the point of connection [24].

The upper left plot shows the DER disconnection strategy. Many DER units (especially smaller ones) in grids exhibit this kind of behaviour for a severe voltage drop, although more recent regulations, such as the latest IEEE standards [16, 43], introduce more strict regulations for the DER and IBR ride through. However, the problem remains since a vast majority of DER were installed and are still operated based on the older standards that do not have such requirements. Furthermore, as discussed previously, it is common that some DER units will not operate properly and disconnect during severe faults. In the analyzed setup, the DER units are set to trip 50 ms after the fault inception and the consequent large voltage drop.

In the lower plots of Figure 4.10, Q-priority and P-priority fault ride-through control strategies are shown, respectively. After the fault inception, the DER provides voltage support to the grid either by prioritizing reactive (left plot) or active (right plot) current, with differences seen in the graphs. In the lower right plot, due to the P-priority setting, the active current component is kept near the maximum converter current (1.2 per unit), hence almost no reactive current can be provided. On the contrary, in the lower left plot, the reactive current component is prioritized, which results in its sharp increase following the disturbance. After the fault is cleared,

the operation is continued with pre-fault settings. As distribution systems generally contain cables rather than overhead lines, it is theoretically expected that purely reactive power support would be sub-optimal in terms of voltage improvements, due to the lower X/R ratio of the grid². However, some studies show that this is not always the case [34, 44], hence both strategies are analyzed in this study independently to shed more light on this phenomenon.

Finally, the upper right plot in Figure 4.10 shows another fault control strategy used in modern DER units, momentary cessation. As soon as the voltage drop is detected, the unit drops its active power output to zero in a steep ramp decline. After the fault is cleared and the voltage recovers, the unit ramps up the power output to its pre-fault value. This control strategy is hence a compromise between disconnection and ride-through with support, as the DER will remain connected, but will not actively provide grid support during the fault.

Detailed DER parameters for all four control strategies are listed in the Appendix B.

The same 12 fault scenarios from Table 4.2 are used, with heatmaps for result visualization. The results are shown in Figure 4.11. The results contain over 2500 dynamic time-domain RMS simulations, each of 8 s duration, performed and analyzed through the presented Python-PowerFactory framework.

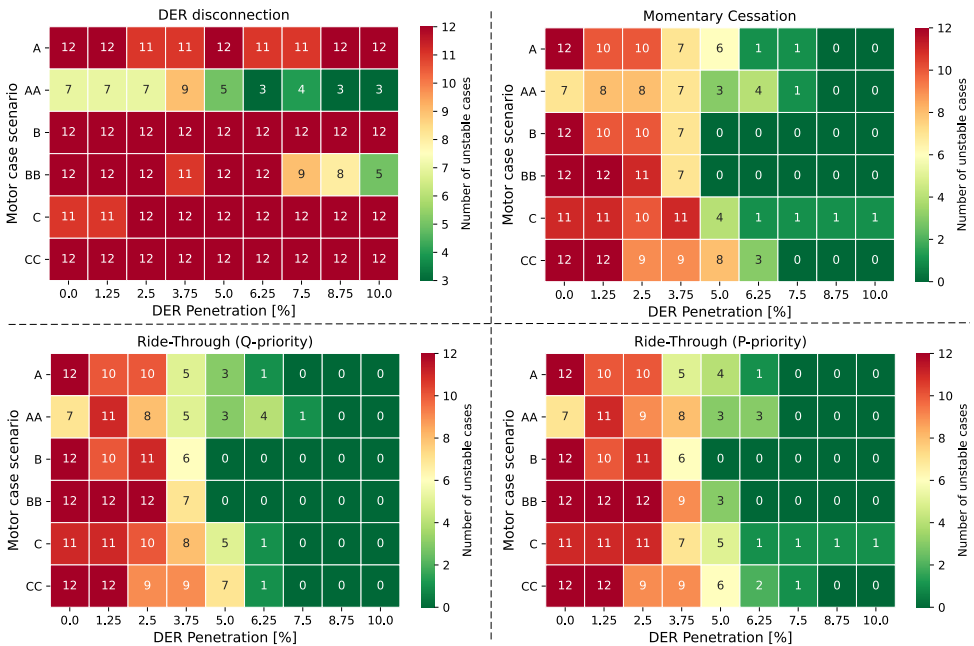


Figure 4.11.: Heatmap visualizations of the influence of DER control strategies on short-term voltage stability. a) DER disconnection; b) Momentary Cessation; c) Ride-Through (Q-priority); d) Ride-Through (P-priority).

²See previous two chapters for more details about the impact of X/R ratio.

The first column of all four heatmaps is effectively the same as the (middle part of the) last column of [Figure 4.9](#). For the upper left heatmap shown in [Figure 4.11](#), units are set to trip 50 ms after the fault inception. By introducing more penetration of renewable energy, overall, it can be seen that the short-term stability of the system does not improve. Furthermore, since this amount of lost generation would cause other issues (e.g. power imbalance, frequency deviations), the effect can be described as detrimental to short-term stability and overall grid resilience. This is explored further in the next set of simulations.

If a ride-through fault control strategy is used, different effects are seen, shown in the two lower heatmaps in [Figure 4.11](#). Firstly, differences in P-priority and Q-priority heatmaps are very subtle, hence the same conclusions can be derived for each. For penetrations of 0 to 2.5% of the total system generation, slight improvements in short-term stability are spotted. However, starting from 3.75% penetration, the effects are more clearly visible, with most of the scenarios being stable for 6.25% or more of DER penetration.

For the momentary cessation control, results shown in the upper right heatmap are slightly worse than with the ride-through, however still similarly beneficial relative to the DER disconnection due to quick ramp-up and power recovery. While not explicitly explored in depth, some preliminary results indicate that the faster the ramp-up is, the better the overall grid stability will be³. This is expected as a faster ramp-up effectively approaches the ride-through operation. Nevertheless, a more detailed study on different ramp-up speed parameters and their impact on system-wide short-term stability is an interesting future work topic.

The beneficial effects of these three strategies can be theoretically understood by considering that DERs provide local voltage support, effectively reducing voltage excursions in grid areas where the dynamic load is connected. By doing so, they support short-term stability. The more such voltage support exists, the more resilient the system is to short-term instabilities. In terms of obtained values, it can be concluded that roughly about 5% of local DER generation (relative to the total system generation) is already enough to mitigate most of the possible short-term stability issues in the analyzed system, *if* ride-through or momentary cessation is used and *if* the units are able to properly apply the intended controls. Furthermore, scenarios with more A and/or C types of motor are once again shown to be more correlated with short-term instability, i.e. being harder for DERs' voltage support to mitigate. This aligns with the results obtained in the previous section, which can be physically understood due to the lower inertia of such induction motors (e.g. compressor motors, centrifugal pumps). This results in higher voltage oscillatory peaks, and consequently, amplified voltage excursions and higher susceptibility to short-term instabilities that are harder for DERs' voltage support to mitigate.

Nevertheless, one should note that many older (or smaller) DERs in the grid do not have ride-through or momentary cessation control strategies, or fail to implement them successfully during/after severe faults. Hence, this percentage effectively increases in practical scenarios. To evaluate to what extent DER disconnection correlates with short-term instability, in comparison to the units that ride through,

³A trade-off exists though: fast ramp-up may affect the converter's weak-grid stability (see [Chapter 3](#)).

another analysis is conducted. Figure 4.12 shows a heatmap with an increasing (decreasing) number of the trip (ride-through, Q-priority) DER units on the Y-axis, while the X-axis varies the total penetration of DERs in the system. The effects are evaluated for the 12 mentioned fault scenarios once again, with a 50% share of WECC Composite Load compared to the static load. The equal-share load composition scenario N (see Table 4.3) is chosen for all the simulations since individual motor type effects have already been evaluated. The numerous dynamic simulations are conducted using the same automation setup as previously described.

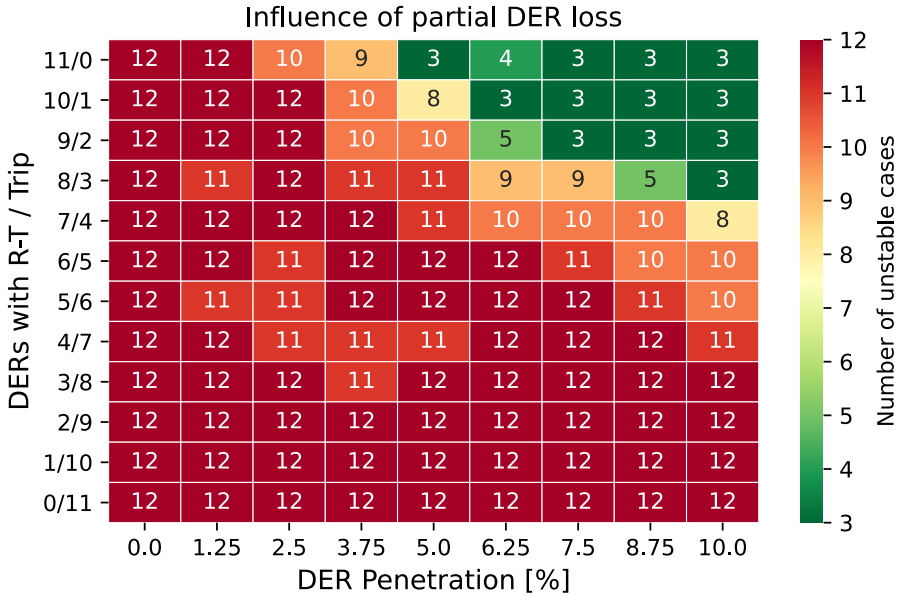


Figure 4.12.: Heatmap visualization of the influence of combined DER disconnection (Trip) and DER Ride-Through (R-T) on short-term stability.

As previously shown, these results confirm that a high amount of dynamic load causes instability in the large majority of cases, and low amounts of DER penetration are unable to mitigate this. Furthermore, with higher DER penetration, less instability is seen across the two analyzed scenarios. However, there is a clear difference between a trip and a ride-through correlation with short-term stability. If the majority of DER units disconnect (bottom part of the heatmap in Figure 4.12), even high amounts of penetration do not provide any benefits to short-term stability. On the other hand, a high number of Ride-Through (R-T) DER units (top part of the heatmap) shows clear improvements. The most impactful finding of this analysis is how overwhelming the influence of disconnecting DERs is in comparison to the R-T units. By observing cases with a similar number of trips and R-T units (middle rows of the heatmap), the system remains unstable in the majority of cases. The stability

improvements are observed only when the number of R-T units is approximately double compared to the number of trip units. This provides a clear insight into how strongly DER disconnection is correlated to short-term instability, being about twice as detrimental to short-term stability in comparison to the benefits of R-T units' voltage support in this analysis. Practically, this implies that in a voltage stability stressed system, for each MVA of DER lost, the studied system needs roughly 2 MVA of voltage-supporting DER which rides through the fault so that the overall effect of distributed generation on bulk power system short-term stability is neutral. While this ratio is not a precise rule, as it depends on the specific system, it is still likely that the general takeaway holds. On a positive note, the overpowering of DER disconnection's detrimental effect over DER R-T beneficial effect diminishes for higher DER penetration (top-right part of the heatmap), suggesting that in very high DER penetration scenarios the discussed instability risks become less severe.

It should be noted that the entire analysis is established on the IEEE system from Figure 4.3, which is dominantly based on synchronous generation. While a decrease (increase) of synchronous generation (renewable generation) in terms of large units is not addressed in the study, it can be expected that most of the obtained results would be further emphasized in a modern grid with overall lower inertia and system strength, as well as less voltage (reactive power) support, as discussed in previous chapters. Therefore, the results are rather conservative from such a perspective.

Finally, simulations also uncovered another important effect, often referred to as a *Voltage Dip-Induced Frequency Excursion* [24]. Following a large disturbance, voltage dip propagates further away from the fault location in modern (i.e. weaker) power systems. If many DERs simultaneously disconnect or reduce their active power output due to voltage perturbations, this may affect the overall frequency of the grid as well, causing a potentially significant drop. This risk is increased in networks where DERs form a large percentage of the total instantaneous active power supply, which is more frequently seen in, for instance, systems with a significant amount of distributed wind or PV. The situation is particularly dangerous if a large disturbance occurs during low-demand parts of the day when (distributed) solar generation is high, sometimes even supplying close to 100% of the demand with a very low amount of rotating inertia present in the system⁴. The consequent frequency excursions may further aggravate the disturbance and increase the risks of cascading. As frequency resilience is not the topic of this work, these effects are highlighted as interesting future research recommendations.

4.4. CONCLUDING REMARKS

The impact of dynamic loads and DERs on the short-term stability of power systems is investigated in terms of different penetrations, types, and control strategies. Extensive simulation results reveal which dynamic load and distributed generation specifications contribute positively and negatively to short-term instability.

Regarding dynamic loads, it has been shown that the increase in the share of

⁴Padraig Buckley, a master's student I supervised during my PhD, researched this topic and its impacts on under-frequency load shedding (UFLS) within the scope of his master's thesis [45].

motors in the grid relative to the static load leads to more pronounced voltage deviations. Once those penetrations reach higher values, larger voltage deviations, and consequently short-term instabilities, begin to emerge more frequently.

With the amounts starting from 30% dynamic load share in the framework of this study, the bulk power system starts experiencing short-term instabilities. With the dynamic load share approaching 50%, most analyzed cases become unstable following a fault. Furthermore, it has been shown that low-inertia motor types are more detrimental to short-term stability, as they tend to have overall lower robustness and thus amplify voltage oscillations further during and after disturbances. Particular dangers also arise with a high share of stalling-prone motors (e.g. A/C units), which may draw significantly higher reactive currents during and after faults. If this occurs, voltage sags in the system are deeper, FIDVR events occur, and the system stability may be jeopardized as the cascading risks increase.

When a system contains a significant share of DER units, this can be either detrimental or beneficial for short-term stability, as shown in this chapter. The two determining factors uncovered in this chapter are the penetration amount of DER and their respective control strategy. It is shown that DER disconnection shortly after the fault is very detrimental to short-term stability in almost all scenarios. On the contrary, grid-supporting ride-through strategies can suppress voltage oscillations and excursions initiated (or amplified) by the fault response of the dynamic load. In terms of the penetration amounts, it has been shown that about 3–5% of DER penetration relative to the total system generation is already providing visible benefits to short-term stability. More than 5% of local grid-supporting DER is strongly correlated with the preservation of short-term stability. Moreover, the negative impact of DER disconnection is demonstrated to be only partly offset by a comparable ride-through grid-supporting share of DER, indicating the importance of avoiding massive DER disconnection during and after faults.

The chapter concludes with a clear verdict that dynamic load and DER units play a very important role in distribution-transmission interactions and short-term stability, particularly related to voltage stability. The adverse impact of dynamic loads on short-term voltage stability has been illustrated concerning both their amount and composition. Additionally, DER units are shown to be either beneficial or detrimental, depending on their penetration and control parameters. Consequently, an enhanced understanding of the short-term stability phenomena and their driving forces in modern power grids is provided.

With the current strategic direction of power systems towards the low-emission of greenhouse gases, it is expected that dynamic load presence and DER penetration will keep increasing. This leads to a potentially compromised short-term stability. Furthermore, with the overall system generation shift towards low inertia and low system strength operation, these effects will be further emphasized in the future. Modeling and analysis of such phenomena become crucial, so the impacts on short-term stability and dynamic-state system strength can be properly evaluated. Novel data-driven methods to evaluate these effects and put them into the perspective of dynamic-state system strength are proposed in the next chapter.

REFERENCES

- [1] R. Yan, N.-A. Masood, T. Kumar Saha, F. Bai, and H. Gu. “The Anatomy of the 2016 South Australia Blackout: A Catastrophic Event in a High Renewable Network”. In: *IEEE Transactions on Power Systems* 33.5 (Sept. 2018), pp. 5374–5388. ISSN: 0885-8950. DOI: [10.1109/TPWRS.2018.2820150](https://doi.org/10.1109/TPWRS.2018.2820150).
- [2] National Grid. *2019 Hornsea Offshore Windfarm Incident Report*. Tech. rep. Sept. 2019. URL: <https://www.nationalgrideso.com/document/152346/download>.
- [3] H. Hermanns and H. Wiechmann. “Demand-Response Management for Dependable Power Grids”. In: 2013, pp. 1–22. DOI: [10.1007/978-1-4419-8795-2_1](https://doi.org/10.1007/978-1-4419-8795-2_1).
- [4] R. Bhattarai, A. Levitt, D. Ramasubramanian, J. C. Boemer, and N. Kang. “Impact of Distributed Energy Resource’s Ride-through and Trip Settings on PJM’s Footprint”. In: *2020 IEEE Power & Energy Society General Meeting (PESGM)*. IEEE, Aug. 2020, pp. 1–5. ISBN: 978-1-7281-5508-1. DOI: [10.1109/PESGM41954.2020.9281948](https://doi.org/10.1109/PESGM41954.2020.9281948).
- [5] IEEE PES. *Contribution to Bulk System Control and Stability by Distributed Energy Resources connected at Distribution Network*. Tech. rep. IEEE Power & Energy Society, Jan. 2017. URL: <https://resourcecenter.ieee-pes.org/publications/technical-reports/PESTRPDFMRH0022.html>.
- [6] R. Shah, N. Mithulananthan, R. Bansal, and V. Ramachandaramurthy. “A review of key power system stability challenges for large-scale PV integration”. In: *Renewable and Sustainable Energy Reviews* 41 (Jan. 2015), pp. 1423–1436. ISSN: 13640321. DOI: [10.1016/j.rser.2014.09.027](https://doi.org/10.1016/j.rser.2014.09.027).
- [7] S. Eftekharijad, V. Vittal, Heydt, B. Keel, and J. Loehr. “Impact of increased penetration of photovoltaic generation on power systems”. In: *IEEE Transactions on Power Systems* 28.2 (May 2013), pp. 893–901. ISSN: 0885-8950. DOI: [10.1109/TPWRS.2012.2216294](https://doi.org/10.1109/TPWRS.2012.2216294).
- [8] D. Lew, M. Asano, J. Boemer, C. Ching, U. Focken, R. Hydzik, M. Lange, and A. Motley. “The Power of Small: The Effects of Distributed Energy Resources on System Reliability”. In: *IEEE Power and Energy Magazine* 15.6 (Nov. 2017), pp. 50–60. ISSN: 1540-7977. DOI: [10.1109/MPE.2017.2729104](https://doi.org/10.1109/MPE.2017.2729104).
- [9] D. Ramasubramanian, P. Mitra, P. Dattaray, M. Bello, J. C. Boemer, and A. Gaikwad. “Analyzing impact of DER on FIDVR - comparison of EMT simulation of a combined transmission and distribution grid with aggregated positive sequence models”. In: *Electric Power Systems Research* 201 (Dec. 2021), p. 107534. ISSN: 03787796. DOI: [10.1016/j.epsr.2021.107534](https://doi.org/10.1016/j.epsr.2021.107534).
- [10] T. Sadamoto, A. Chakraborty, T. Ishizaki, and J.-i. Imura. “Dynamic Modeling, Stability, and Control of Power Systems With Distributed Energy Resources: Handling Faults Using Two Control Methods in Tandem”. In: *IEEE Control Systems* 39.2 (Apr. 2019), pp. 34–65. ISSN: 1066-033X. DOI: [10.1109/MCS.2018.2888680](https://doi.org/10.1109/MCS.2018.2888680).
- [11] A. Schinke and I. Erlich. “Impact of Distributed Photovoltaic Generation on Power System Dynamics”. In: *2018 IEEE Power & Energy Society General Meeting (PESGM)*. IEEE, Aug. 2018, pp. 1–5. ISBN: 978-1-5386-7703-2. DOI: [10.1109/PESGM.2018.8586241](https://doi.org/10.1109/PESGM.2018.8586241).
- [12] AEMO. *Maintaining Power System Security with High Penetrations of Wind and Solar Generation*. Tech. rep. Australian Energy Market Operator, Oct. 2019. URL: https://www.aemo.com.au/-/media/Files/Electricity/NEM/Security_and_Reliability/Future-Energy-Systems/2019/AEMO-RIS-International-Review-Oct-19.pdf.

- [13] E. Coster. “Distribution grid operation including distributed generation: impact on grid protection and the consequences of fault ride-through behavior”. PhD thesis. Eindhoven University of Technology, 2010. URL: <https://research.tue.nl/en/publications/distribution-grid-operation-including-distributed-generation-impa>.
- [14] J. Morren. “Grid support by power electronic converters of distributed generation units”. PhD thesis. 2006. URL: <https://repository.tudelft.nl/islandora/object/uuid%3Aef7c350e-9292-4064-b1c9-81ed15e7cfc1>.
- [15] IRENA. *Grid codes for renewable powered systems*, International Renewable Energy Agency. Tech. rep. Abu Dhabi: International Renewable Energy Agency, 2022. URL: <https://www.irena.org/publications/2022/Apr/Grid-codes-for-renewable-powered-systems>.
- [16] IEEE. *IEEE Std 2800-2022: IEEE Standard for Interconnection and Interoperability of Inverter-Based Resources (IBRs) Interconnecting with Associated Transmission Electric Power Systems*. Tech. rep. IEEE, Apr. 2022. DOI: [10.1109/IEEESTD.2022.9762253](https://doi.org/10.1109/IEEESTD.2022.9762253).
- [17] ENTSO-e. *ENTSO-e Requirements for Generators*. URL: https://www.entsoe.eu/network_codes/rfg/.
- [18] B. Schowe-von der Brelie, S. Mansoor Ali, Y. Ayadi, and E. Makki. “RfG NC implementation in Europe - The whole picture”. In: *20th International Workshop on Large-Scale Integration of Wind Power into Power Systems as well as on Transmission Networks for Offshore Wind Power Plants (WIW 2021)*. Institution of Engineering and Technology, 2021, pp. 367–373. ISBN: 978-1-83953-681-6. DOI: [10.1049/icp.2021.2637](https://doi.org/10.1049/icp.2021.2637).
- [19] Netbeheer Nederland. *Power-Generating Modules compliance verification: Power-Generating Modules type B, C and D according to NC RfG and Netcode elektriciteit*. Tech. rep. Nov. 2022. URL: https://www.netbeheernederland.nl/_upload/Files/Regulering_20_5f2166cdb4.pdf.
- [20] S. Chatzivasileiadis, P. Aristidou, I. Dassios, T. Dragicevic, D. Gebbran, F. Milano, C. Rahmann, and D. Ramasubramanian. “Micro-flexibility: Challenges for power system modeling and control”. In: *Electric Power Systems Research* 216 (Mar. 2023), p. 109002. ISSN: 03787796. DOI: [10.1016/j.epsr.2022.109002](https://doi.org/10.1016/j.epsr.2022.109002).
- [21] J. V. Milanovic, K. Yamashita, S. Martinez Villanueva, S. Z. Djokic, and L. M. Korunovic. “International Industry Practice on Power System Load Modeling”. In: *IEEE Transactions on Power Systems* 28.3 (Aug. 2013), pp. 3038–3046. ISSN: 0885-8950. DOI: [10.1109/TPWRS.2012.2231969](https://doi.org/10.1109/TPWRS.2012.2231969).
- [22] A. Arif, Z. Wang, J. Wang, B. Mather, H. Bashualdo, and D. Zhao. “Load Modeling—A Review”. In: *IEEE Transactions on Smart Grid* 9.6 (Nov. 2018), pp. 5986–5999. ISSN: 1949-3053. DOI: [10.1109/TSG.2017.2700436](https://doi.org/10.1109/TSG.2017.2700436).
- [23] L. Sundaresh, P. Mitra, and D. Ramasubramanian. “The impact of adoption of variable frequency drives on the bulk power system”. In: *CIGRE Science & Engineering* (Mar. 2023). URL: <https://cse.cigre.org/cse-n028/the-impact-of-adoption-of-variable-frequency-drives-on-the-bulk-power-system>.
- [24] A. Boričić, J. L. R. Torres, and M. Popov. “Fundamental study on the influence of dynamic load and distributed energy resources on power system short-term voltage stability”. In: *International Journal of Electrical Power & Energy Systems* 131 (Oct. 2021), p. 107141. ISSN: 01420615. DOI: [10.1016/j.ijepes.2021.107141](https://doi.org/10.1016/j.ijepes.2021.107141).
- [25] IEEE PES. *IEEE PES-TR19: Test Systems for Voltage Stability Analysis and Security Assessment*. Tech. rep. IEEE Power & Energy Society, Aug. 2015. URL: <https://resourcecenter.ieee-pes.org/publications/technical-reports/PESTR19.html>.
- [26] T. Van Cutsem, M. Glavic, W. Rosehart, C. Canizares, M. Kanatas, L. Lima, F. Milano, L. Papangelis, R. A. Ramos, J. A. d. Santos, B. Tamimi, G. Taranto, and C. Vournas. “Test Systems for Voltage Stability Studies”. In: *IEEE Transactions on Power Systems* 35.5 (Sept. 2020), pp. 4078–4087. ISSN: 0885-8950. DOI: [10.1109/TPWRS.2020.2976834](https://doi.org/10.1109/TPWRS.2020.2976834).
- [27] T. Van Cutsem and L. Papangelis. *Description, Modeling and Simulation Results of a Test System for Voltage Stability Analysis*. Tech. rep. University of Liege, Nov. 2013. URL: https://orbi.uliege.be/bitstream/2268/141234/1/Nordic_test_system_V6.pdf.

- [28] WECC Modelling Group: *Composite Load Model for Dynamic Simulations - Report 1.0*. Tech. rep. Western Electricity Coordinating Council, 2012.
- [29] *WECC Dynamic Composite Load Model (CMPLDW) Specifications*. Tech. rep. Iowa State University, Jan. 2015. URL: <https://home.engineering.iastate.edu/~jdm/ee554/WECC%20Composite%20Load%20Model%20Specifications%2001-27-2015.pdf>.
- [30] Z. Ma, Z. Wang, Y. Wang, R. Diao, and D. Shi. "Mathematical Representation of WECC Composite Load Model". In: *Journal of Modern Power Systems and Clean Energy* 8.5 (2020), pp. 1015–1023. ISSN: 2196-5625. DOI: [10.35833/MPCE.2019.000296](https://doi.org/10.35833/MPCE.2019.000296).
- [31] *DigSILENT PowerFactory Version 2020 "Technical Reference – WECC Dynamic Composite Load Model Template*. Tech. rep.
- [32] G. Chaspierre, G. Denis, P. Panciatici, and T. Van Cutsem. "An Active Distribution Network Equivalent Derived From Large-Disturbance Simulations With Uncertainty". In: *IEEE Transactions on Smart Grid* 11.6 (Nov. 2020), pp. 4749–4759. ISSN: 1949-3053. DOI: [10.1109/TSG.2020.2999114](https://doi.org/10.1109/TSG.2020.2999114).
- [33] R. Venkatraman, S. K. Khaitan, and V. Ajarapu. "Application of Combined Transmission-Distribution System Modeling to WECC Composite Load Model". In: *2018 IEEE Power & Energy Society General Meeting (PESGM)*. IEEE, Aug. 2018, pp. 1–5. ISBN: 978-1-5386-7703-2. DOI: [10.1109/PESGM.2018.8585910](https://doi.org/10.1109/PESGM.2018.8585910).
- [34] J. Boemer. "On Stability of Sustainable Power Systems: Network Fault Response of Transmission Systems with Very High Penetration of Distributed Generation". PhD thesis. Delft University of Technology, June 2016. URL: <https://doi.org/10.4233/uuid:78bffb19-01ed-48f9-baf6-ffb395be68a0>.
- [35] NERC. *1200 MW Fault Induced Solar Photovoltaic Resource Interruption Disturbance Report*. Tech. rep. North American Electric Reliability Corporation, June 2017.
- [36] NERC. *Reliability Guideline Modelling Distributed Energy Resources in Dynamic Load Models*. Tech. rep. North American Electric Reliability Corporation, Dec. 2016. URL: https://www.nerc.com/comm/RSTC_Reliability_Guidelines/Reliability_Guideline_-_Modeling_DER_in_Dynamic_Load_Models_-_FINAL.pdf.
- [37] NERC. *Distributed Energy Resources Connection Modelling and Reliability Considerations*. Tech. rep. North American Electric Reliability Corporation, Feb. 2017. URL: https://www.nerc.com/comm/Other/essntlr1rlbltysrvctskfrcDL/Distributed_Energy_Resources_Report.pdf.
- [38] NERC. *Reliability Guideline Parameterization of the DER_A Model*. Tech. rep. North American Electric Reliability Corporation, Sept. 2019. URL: https://www.nerc.com/comm/RSTC_Reliability_Guidelines/Reliability_Guideline_DER_A_Parameterization.pdf.
- [39] *Python - Seaborn: statistical data visualization*.
- [40] IEEE PES-TR77. *Stability definitions and characterization of dynamic behavior in systems with high penetration of power electronic interfaced technologies*. Tech. rep. IEEE Power & Energy Society, May 2020. URL: https://resourcecenter.ieee-pes.org/publications/technical-reports/PES_TP_TR77_PSDP_STABILITY_051320.html.
- [41] L. Chen, X. Wang, Y. Min, G. Li, L. Wang, J. Qi, and F. Xu. "Modelling and investigating the impact of asynchronous inertia of induction motor on power system frequency response". In: *International Journal of Electrical Power & Energy Systems* 117 (May 2020), p. 105708. ISSN: 01420615. DOI: [10.1016/j.ijepes.2019.105708](https://doi.org/10.1016/j.ijepes.2019.105708).
- [42] H. Thiesen and C. Jauch. "Determining the Load Inertia Contribution from Different Power Consumer Groups". In: *Energies* 13.7 (Apr. 2020), p. 1588. ISSN: 1996-1073. DOI: [10.3390/en13071588](https://doi.org/10.3390/en13071588).
- [43] IEEE. *IEEE 1547-2018: IEEE Standard for Interconnection and Interoperability of Distributed Energy Resources with Associated Electric Power Systems Interfaces*. Tech. rep. IEEE, 2018. URL: <https://standards.ieee.org/ieee/1547/5915/>.

- [44] M. Coumont, F. Bennewitz, and J. Hanson. “Influence of Different Fault Ride-Through Strategies of Converter-Interfaced Distributed Generation on Short-Term Voltage Stability”. In: *2019 IEEE PES Innovative Smart Grid Technologies Europe (ISGT-Europe)*. IEEE, Sept. 2019, pp. 1–5. ISBN: 978-1-5386-8218-0. DOI: [10.1109/ISGTEurope.2019.8905465](https://doi.org/10.1109/ISGTEurope.2019.8905465).
- [45] P. Buckley, A. Boričić, and M. Popov. *Improving Load Shedding Schemes for Critical System Conditions (Master Thesis)*. Aug. 2023. URL: <https://repository.tudelft.nl/islandora/object/uuid:3ef30f70-f533-4f41-b47f-5af4b2499221?collection=education>.

5

DATA-DRIVEN STABILITY AND STRENGTH EVALUATION METHODS

Theory will only take you so far.¹

The dynamics of conventional power systems are largely defined by dominant electromechanical and electromagnetic aspects originating from synchronous machines. Therefore, analytical methods that describe their physical behaviour achieve high accuracy in representing the overall grid dynamics. However, as extensively explored in previous chapters, power systems are evolving. With fewer synchronous generators to define the core grid dynamics, the tasks of system stability and system strength evaluation become increasingly complex. The evaluation faces a large number of scattered IBRs with discrete control-driven behaviour which often invalidates conventional analytical and deterministic stability and strength evaluation methods. Additionally, a detailed analytical evaluation becomes computationally intensive, as the number of models and their parameter count increases. In other words, the order of the problem needs to be reduced to manageable levels so that important stability and strength analyses can be performed more efficiently.

This is where data-based methods may offer large benefits. While system operators gain access to big data with the advances in grid sensors and time-efficient simulation automation, the insights of such data are yet to be efficiently utilized. This chapter introduces novel vulnerability evaluation methods for risk-based and probabilistic instability quantification and classification. The methods are aimed to cut through the complexity noise and highlight the weakest and most instability-prone grid sections and operating scenarios that require a more detailed stability analysis. Finally, the increasingly important topic of model parameter uncertainty in vulnerability assessment is also addressed.

Parts of this chapter have been published in peer-reviewed articles and/or conference proceedings.

See [The List of Publications](#) section for more details.

¹From the biography of American scientist J. Robert Oppenheimer, portrayed in Christopher Nolan's film *Oppenheimer* (2023). As complexity increases, deterministic mathematical expressions may no longer reflect the intricacies of the reality with sufficient fidelity. Probability slowly replaces certainty.

5.1. DATA OPPORTUNITIES IN MODERN POWER SYSTEMS

As illustrated in previous chapters, energy transition and rapid proliferation of renewable energy sources lead to technical challenges related to power system resilience, strength, and stability. This is reflected in more complex, amplified, and faster grid dynamics that require more comprehensive modelling and analysis.

Concurrently to these developments, computational power grows exponentially as well, following Moore's law². This allows engineers to perform complex simulations faster, utilizing larger and more advanced models in the process.

Furthermore, the rise in the usage of programming and automation in society is also unprecedented and is only expected to rise, as seen from the recent AI advancements³. This is also embraced by power systems simulation software, such as DiGSILENT, PSCAD, and PSS/e, to name a few, which all have capable and easy-to-use Python Application Programming Interfaces (APIs). This enables relatively easy and extremely time-efficient automation of complex power system simulations, where grid dynamics can be seamlessly evaluated for a large variety of study scenarios and parameters. Such an approach is also utilized here, particularly in [Chapters 4 and 5](#). The framework used in this thesis is illustrated in [Figure 5.1](#).

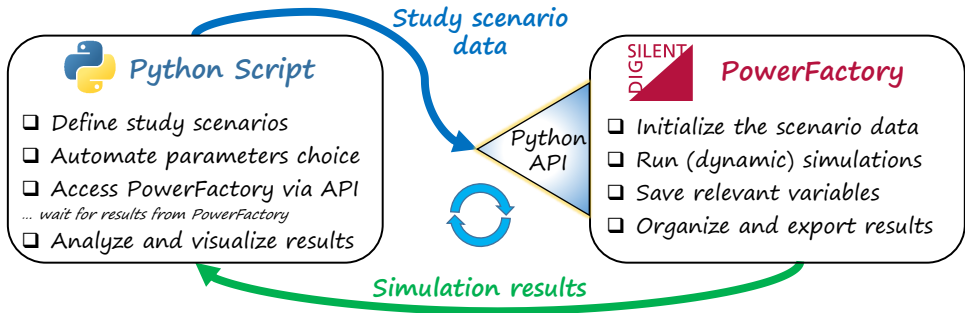


Figure 5.1.: Automation framework utilizing Python scripting and DiGSILENT PowerFactory dynamic simulations used in this thesis.

This kind of framework is hereby utilized to perform a large number (hundreds to thousands) of dynamic simulations automatically across a wide range of operating scenarios and parameters. Furthermore, the results are also automatically processed, analyzed, and quantified with the goal of providing insights into grid resilience, stability, and strength. The ultimate goal is to obtain unique insights about grid dynamics and resilience that would otherwise remain largely hidden from grid operators who have a limited amount of time to perform complex and time-consuming analyses across a vast power grid with numerous operating scenarios and parameters.

²The observation that the number of transistors in integrated circuits roughly doubles every two years. Gordon E. Moore was one of the most influential people in the field of electronics and electrical engineering. He sadly passed away in March 2023 at the age of 94, as I started drafting this chapter.

³Automation of tasks becomes easier every day. One does not even need to understand programming code and syntax that much anymore with the recent advancements in AI and NLP algorithms.

Another important development in power grids is the rise in observability. This is a direct consequence of advanced monitoring sensors in the grids, known as synchrophasors or phasor measurement units (PMUs). Synchrophasors are advanced power system measurement devices that provide precise and time-synchronized measurements of power system variables such as voltages, currents, and frequency, with a much higher resolution than the existing SCADA monitoring. A further important benefit is, as their name implies, the ability to provide not only amplitude but also phase measurements of these complex variables. PMUs are often pooled together as building blocks of Wide-Area Monitoring Systems (WAMS), as illustrated in Figure 5.2. These monitoring systems are far more capable than conventional SCADA systems. An excellent source of information on this topic can be found in [1], one of the work packages of this project (see Section 1.5).

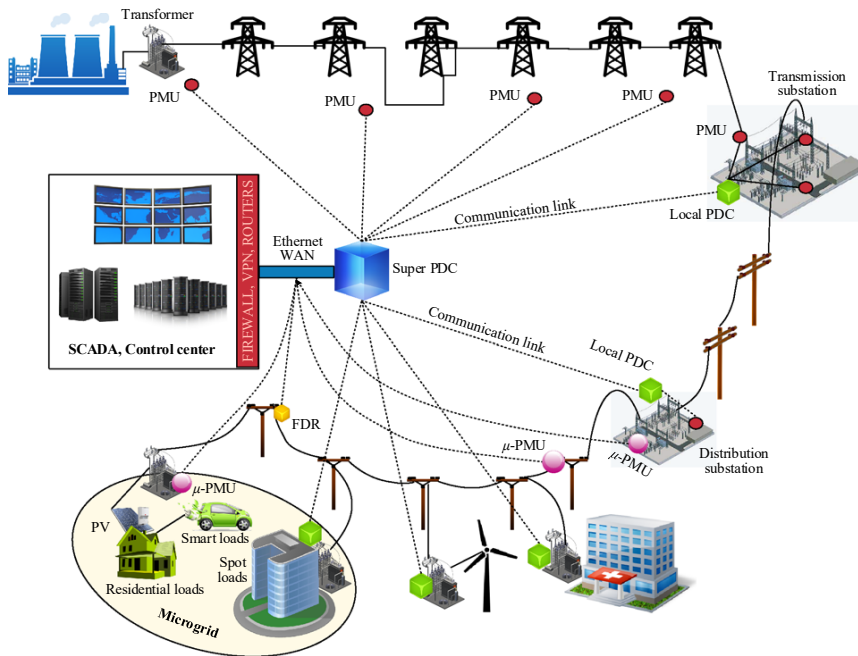


Figure 5.2.: Wide-area monitoring system impression in modern and future grids [2].

The number of PMUs in grids is rising worldwide to allow grid operators to observe and analyze increasingly complex and faster dynamic phenomena [3].

Besides monitoring, these systems enable the rise of other advanced applications. As relevant variables are monitored in real-time, suitable control and protection actions can be performed, forming the Wide-Area Protection and Control (WAMPAC) Systems [4–10]. One of the numerous potential utilizations of such real-time data is for online quantification and classification of grid disturbances, which will be explored further in this chapter [11].

5.2. QUANTIFICATION: CUMULATIVE VOLTAGE DEVIATION (CVD) METHOD

With the power systems evolution, voltage perturbations become faster and highly variable, exposing systems to much larger risks of cascading faults (see [Chapters 1 and 2](#)). Therefore, assessing the severity and cascading potential of voltage deviations becomes a critical step in risk-based vulnerability analysis of modern power systems. In this section, a novel approach that evaluates rapid post-fault voltage deviations for both online and offline short-term instability quantification is proposed and evaluated on a comprehensive set of numerical simulations [11, 12]. The method is designed to enable grid operators to predict and prioritize potential high-risk events and act with suitable preventive and/or corrective actions.

5.2.1. METHODOLOGY

As inertia and system strength of power systems decrease (see also [Chapter 3](#)), system dynamics become faster and more severe. Furthermore, inverter-based resources, in contrast to synchronous generators, are much more voltage-sensitive and at a higher risk of maloperation or disconnections that may lead to cascading events. The complex dynamics resulting from the rising share of dynamic load affect this further (see [Chapter 4](#)). Therefore, evaluating and quantifying short-term voltage deviations and their threat to grid resilience becomes highly relevant.

Concurrently, the accelerating application of PMUs drastically changes the real-time monitoring and control landscape, as discussed in the previous section. What used to be impossible due to the slow SCADA sampling (typically one unsynchronized measurement per 2-10 seconds), is now much more feasible with time-synchronized and fast wide-area measurements (typically 50 or more measurements per second). This opens a completely new range of possibilities for monitoring and vulnerability assessment analysis in modern power systems.

The existing short-term stability evaluation and quantification methods are analyzed in [Chapter 2](#), including their shortcomings when applied to modern power systems. It was concluded that a new quantitative metric is necessary for modern and IBR-rich systems, which should meet the following conditions:

- able to detect and quantify the severity of various post-fault short-term voltage deviations,
- useful in both conventional and modern power systems,
- intuitive for practical on- and off-line applications,
- adaptable to any system and operational scenario,
- as simple and computationally efficient as possible,
- can provide real-time stability insights, for instance by relying on PMU data.

To address these challenges, the Cumulative Voltage Deviation (CVD) method is hereby introduced, visualized in [Figure 5.3](#), and mathematically described by [Equations \(5.1\) to \(5.3\)](#).

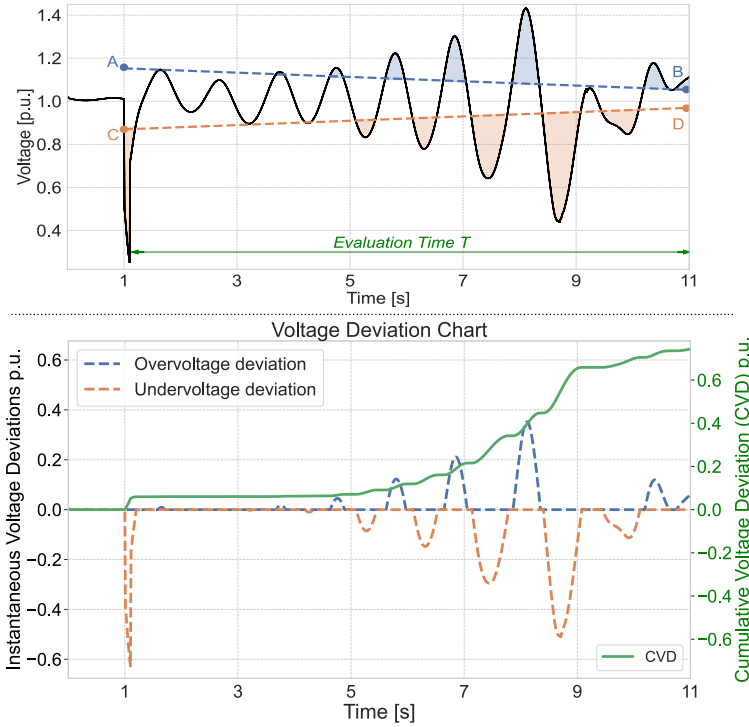


Figure 5.3.: Visualization of the CVD method for an illustrative case of oscillatory voltage deviations.

$$V_U(t) = (1 + a)V_0 - t/b \quad (5.1)$$

$$V_D(t) = (1 - a)V_0 + t/b \quad (5.2)$$

$$CVD = \sum_{t=t_f}^{t=t_f+T} \begin{cases} V(t) - V_U(t), & \text{if } V(t) > V_U(t) \\ V_D(t) - V(t), & \text{if } V(t) < V_D(t) \\ 0, & \text{otherwise} \end{cases} \quad (5.3)$$

In Equation (5.3), t_f is the fault inception time, and T is the evaluation time window. $V_U(t)$ is the upper threshold (blue dashed line in the upper graph in Figure 5.3), whereas $V_D(t)$ is the lower threshold (the orange dashed line). Equations (5.1) and (5.2) define the envelope of permissible voltage levels.

The CVD evaluation starts once the voltage overshoots the initial threshold (shown as points A or C in Figure 5.3), indicating a disturbance that may potentially lead to instability. The linear envelope threshold is then applied to quantify the severity and duration of the detected voltage deviations. Based on this threshold,

the post-disturbance voltage deviations are disentangled into undervoltages (orange areas in Figure 5.3) and overvoltages (blue areas), and extracted onto a voltage deviation chart (the lower plot of Figure 5.3). The green line of the lower plot represents CVD, i.e. the cumulative sum of over- (blue) and under-voltage (orange) deviations. Therefore, the final CVD value reflects the total amplitude and time of the voltage deviations outside the predefined limits. The larger this value is, the more perturbed the system is, indicating a higher risk of cascading and instabilities.

The linear threshold is chosen as it exploits the fact that voltage deviations in the late (early) post-disturbance phase are more (less) indicative of instabilities. In other words, initial large post-fault voltage transients are to be expected, however, when the voltage deviations do not decrease sufficiently fast during the post-fault period, it indicates a larger probability of instability. Furthermore, the method is straightforward, computationally fast, and valid for any system or short-term instability scenario addressed in Figure 2.12, to be demonstrated in the following sections. Finally, as it relies solely on voltage measurements, it is applicable to both automated offline studies as well as online analyses by utilizing PMU measurements.

A short-term instability monitoring method should be easy to parameterize and apply to arbitrary systems [13]. The CVD method requires selecting only three simple parameters. The first is the evaluation time denoted with T . As described in Chapter 2, the majority of the short-term phenomena occur within a ten-second period, therefore chosen as a T value. Such a value is also commonly used for short-term studies [14]. The other two parameters are a and b . They define the initial points (A and C in Figure 5.3), and the final points (B and D in Figure 5.3), including the slopes of $V_U(t)$ and $V_D(t)$. To detect and quantify severe voltage deviations of the four types introduced in Figure 2.12, $a = 0.15$ and $b = 100$ are proposed. Practically, this means that the evaluation starts when the voltage overshoots $\pm 15\%$ from the pre-fault voltage ($t = t_f$) moving towards $\pm 5\%$ ($t = t_f + T$), with a slope of $1\%/s$. Such values are chosen as they represent common thresholds for large voltage disturbances and recovery values, respectively, and at the same time efficiently capture various short-term phenomena. Finally, V_0 is the pre-fault voltage, calculated as an average value prior to the fault. To ensure that the pre-fault voltage value is not impacted by the fault transients or initial model transients, a half-a-second pre-fault window ($0.4 - 0.9s$, for $t_f = 1s$) is hereby used.

The effectiveness and the applicability of CVD to detect and quantify the severity of various short-term voltage deviations with the selected parameters are analyzed in the following sections.

5.2.2. NUMERICAL SIMULATIONS

In this section, the CVD method efficacy is evaluated on a large number of dynamic simulations utilizing DigSILENT PowerFactory supported by Python scripting. The method is assessed for various short-term instability phenomena and compared to an existing commonly used metric for the quantification of voltage deviations. For a comprehensive analysis and comparison, many dynamic post-fault voltage trajectories are needed. For this task, the IEEE Test System for Voltage Stability Analysis and Security Assessment is used [15]. This test grid is one of the most

advanced large grids for dynamic voltage stability simulations and is extensively used in research on related topics. The system is hereby further enhanced by introducing many WECC Composite Load models to improve the representativeness of modern load dynamics, in a similar way as in Chapter 4. The model is depicted in Figure 5.4.

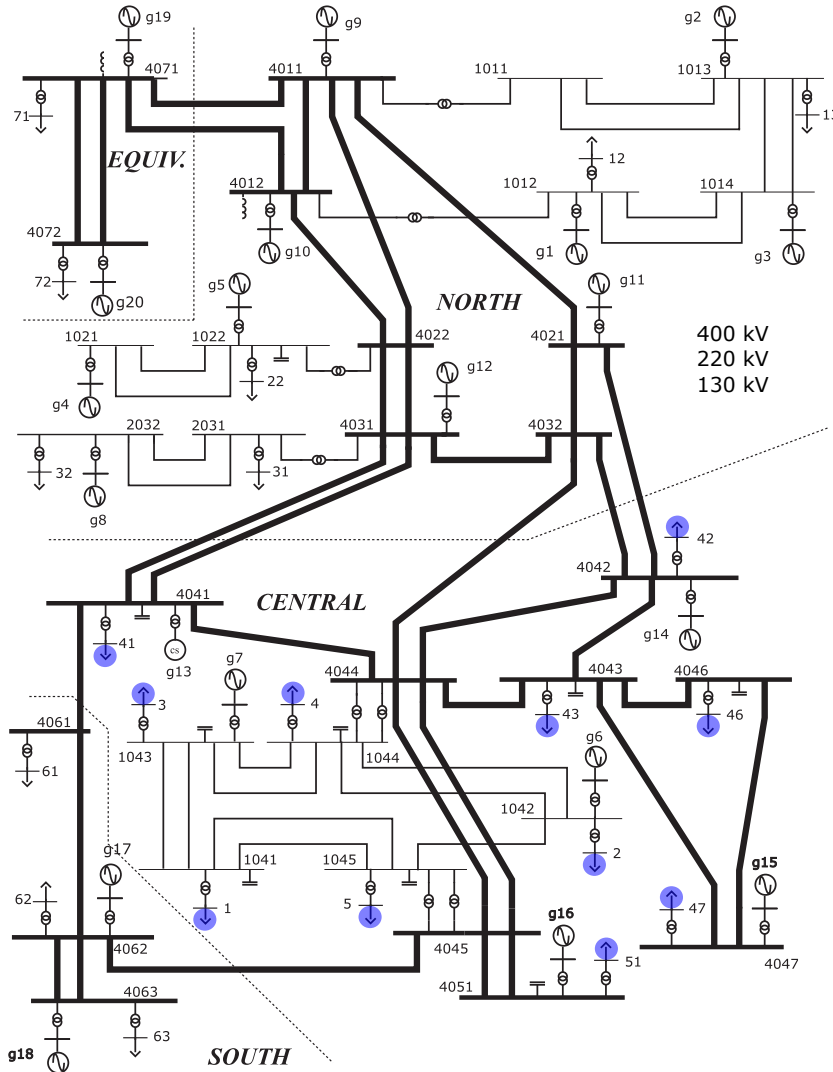


Figure 5.4.: IEEE Test System for Voltage Stability Analysis and Security Assessment. Blue circles indicate WECC composite load and DER-A models additions.

To illustrate the method, all the simulations are performed for 100ms three-phase faults on bus 4044 with a fault impedance of 2.5Ω unless stated differently. A large number of scenarios are selected based on the analysis in Chapter 4, demonstrating

the system conditions and parameters that lead to relevant instabilities in this grid. The voltage responses are reported for bus 1041, with comparable results to other buses susceptible to voltage instability in the surrounding central area [15, 16].

The CVD method, as introduced in the previous section, is compared to the Transient Voltage Severity Index (TVSI), which is commonly used in the literature for quantifying post-fault transient voltage deviations [17] (see Chapter 2). The TVSI method for a specific bus is mathematically straightforward and is described in Equations (5.4) and (5.5), where T is the analyzed transient time frame, T_c is the fault clearing time, TVDI is the Transient Voltage Deviation Index, $V_{i,t}$ is the voltage magnitude of the bus i at time t , and μ is the threshold used to define the unacceptable voltage deviation level. According to [17], a threshold of $\mu = 20\%$ is hereby adopted for numerical analysis and comparison purposes.

$$TVSI = \frac{\sum_{t=T_c}^T TVDI_{i,t}}{T - T_c} \quad (5.4)$$

$$TVDI_{i,t} = \begin{cases} \frac{|V_{i,t} - V_{i,o}|}{V_{i,o}}, & \text{if } \frac{|V_{i,t} - V_{i,o}|}{V_{i,o}} > \mu \\ 0, & \text{otherwise} \end{cases} \quad \forall t \in [T_c, T] \quad \text{and} \quad V_{i,t} < V_{i,o} \quad (5.5)$$

The next subsections in this chapter deal with modelling a comprehensive number of increasingly severe voltage deviations and instabilities of different types, on which the two methods (CVD and TVSI) are compared. An ideal method should be able to quantitatively indicate the increase in severity accurately, regardless of the event type. In other words, it should be able to accurately sort the events by their severity, indicating which of them pose an increased risk of cascading and instabilities.

FAULT-INDUCED DELAYED VOLTAGE RECOVERY (FIDVR)

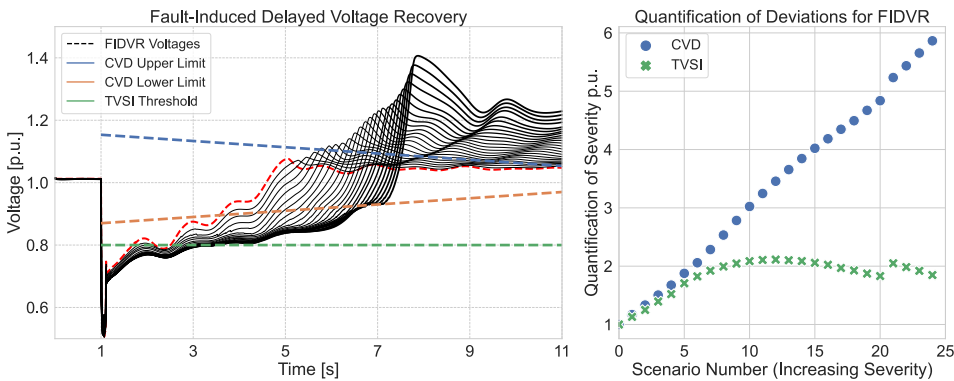
The analysis commences with FIDVR simulations. Based on the experience from Chapter 4, the best way to simulate FIDVR events is to introduce a large number of stalling-prone dynamic loads, particularly single-phase A/C units; the more loads, the more severe the FIDVR event is. By taking this into account, a range of 25 dynamic simulations is conducted with increasing severity, by controlling two parameters: (i) the overall dynamic load percentage in the grid; and (ii) the percentage of motor type D (single-phase A/C units) in the WECC composite loads. The varying FIDVR simulation parameters are listed in Table 5.1, and sorted from the least to the most severe. The share of A/B/C-type motors in the dynamic loads is set to 10% for all simulations to represent realistically diverse system loads (see Chapter 4).

The results are shown in two adjacent graphs in Figure 5.5. The left graph shows the increasingly severe FIDVR voltage events, with a darker colour indicating a more severe simulation scenario. The corresponding CVD and TVSI thresholds are also depicted in the plots with dashed lines.

The right graph shows a scatterplot that quantifies the total severity events (normalized to event 0), for CVD and TVSI. The events are reported on the X-axis from the least severe (leftmost, simulation number 0), to the most severe (rightmost, simulation number 24), as per Table 5.1.

Table 5.1.: Parameters used for modelling FIDVR events.

Simulation number	Dynamic load penetration	Share of motor type D
0	16 %	36 %
1	17 %	37 %
2	18 %	38 %
...
24	40 %	60 %

**Figure 5.5.:** FIDVR events: Comparison of CVD and TVSI methods in quantifying the increasingly severe voltage deviations. *Left:* Simulation results. *Right:* Corresponding quantification scatterplots.

It can be seen that TVSI reaches a peak at event number 12, inaccurately indicating that the events that follow are less (not more) severe. Meanwhile, CVD successfully quantifies the increasing severity, presenting a linear rise. This can be explained by a few key differences between the two approaches: (i) TVSI is, unlike CVD, unable to take into account the time-increasing voltage characteristics of FIDVR; (ii) the overvoltage deviations in the late FIDVR phase, which can be detrimental to the system's ability to recover, are much better evaluated by CVD; and (iii) CVD adaptive linear threshold helps to evaluate the specific events more accurately.

Overall, it can be concluded that FIDVR events of increasing severities are adequately quantified and sorted by the CVD approach, which shows much better performance than TVSI.

TRANSIENT ROTOR ANGLE INSTABILITY (TRAI)

To simulate TRAI events, the system needs to be stressed electromechanically so that electrical machine(s) begin to oscillate against each other. For the system shown in Figure 5.4, this can be achieved by applying a fault at bus 4062, which

results in oscillations of generators g_{17} and g_{18} against the rest of the system. To model increasingly severe post-fault electromechanical oscillations, parameters shown in Table 5.2 are utilized, where dynamic load penetration is continuously increased. The share of A/B/C-type motors in the WECC dynamic load model is set to 0.3/0.2/0.3 to emphasize their impact on post-fault voltage deviations, based on analysis from Chapter 4. The results are illustrated in Figure 5.6.

Table 5.2.: Parameters used for modeling TRAI events.

Simulation number	Dynamic load penetration	Fault clearing time [ms]
0	36 %	200
1	37 %	200
2	38 %	200
...
24	60 %	200

In Figure 5.6, post-disturbance TRAI events are plotted, with increasing severity as more dynamic loads are introduced. The simulated system eventually reaches a stable equilibrium, however with a rising severity of voltage deviations, indicating a higher risk of cascading and potential instability in practice. For completeness, another case with an unstable long-term equilibrium is studied in the later section. The rising severity of responses in Figure 5.6 is reflected by CVD and TVSI values, with a visualized comparison in the right plot.

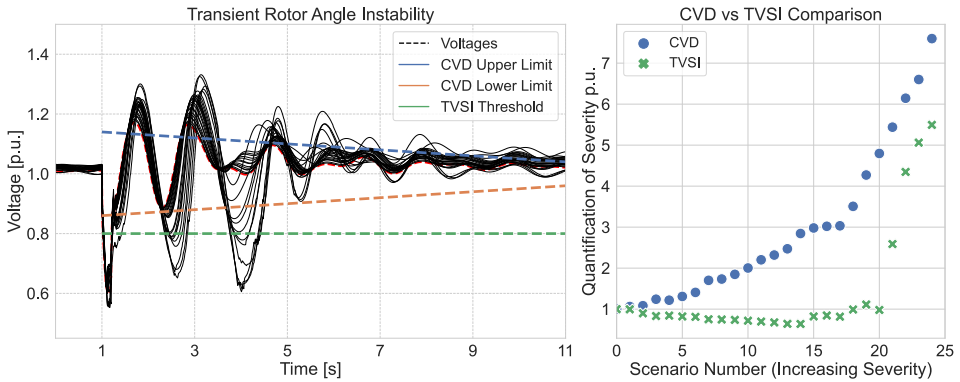


Figure 5.6.: TRAI events: Comparison of CVD and TVSI methods in quantifying the increasingly severe voltage deviations. *Left:* Simulation results. *Right:* Corresponding quantification scatterplots.

By observing the trends in Figure 5.6 (right plot), it can be seen that TVSI has a downward trend up until simulation number 15, wrongly indicating that events are getting less (not more) severe. This is despite oscillations becoming

more pronounced with a potentially higher impact on system stability. Only after simulation number 20 is the increased severity correctly picked up by TVSI. Meanwhile, CVD correctly evaluates that the system experiences more severe voltage deviations throughout all simulations, with no issues in describing the rising severity trend in simulations. Hence, CVD performance is much better for TRAI events. The improvement is achieved since CVD, unlike TVSI, evaluates both over- and undervoltages, while it also applies a time-adaptive linear threshold which tracks and quantifies the voltage response more accurately, as previously explained.

CONVERTER-DRIVEN SLOW INTERACTIONS INSTABILITY (CSII)

To model a large number of severe CSII events, electromagnetic transient (EMT) simulations would be necessary, as any RMS-modelled events above ~ 5 Hz are unlikely to be accurately captured [18]⁴. Furthermore, realistic CSII voltage deviations are generally difficult to model, as they are often a consequence of complex control interactions in weak grids (see Chapter 3). As RMS simulations on the system from Figure 5.4 are performed in this thesis, a different approach to derive suitable voltage profiles is used. Relying on the current understanding of CSII phenomena (see Chapter 2), and according to the recent CSII events from Texas, Australia, and Scotland [21] and other events discussed in Table 1.1, synthetic events are created analytically, with the voltage after the fault clearing defined by Equation (5.6).

$$V(t) = Ae^{\beta t} \cos(2\pi f t) + 1 \quad ; \quad \forall t > t_{cl} \quad (5.6)$$

The two parameters, initial amplitude A and exponential coefficient β are defined in Table 5.3. The values are chosen to replicate possible CSII voltage waveforms based on real grid events, while at the same time providing varying and increasing severity in terms of the post-fault amplitude and exponential rise. This allows testing the CVD method on a comprehensive number and variety of events.

Table 5.3.: Parameters used for modelling CSII events.

Simulation number	Amplitude A	Exponential coefficient β
0	0.052	0.050
1	0.054	0.054
2	0.056	0.058
...
24	0.100	0.150

The derived voltages are shown in the left graph of Figure 5.7. The synthetic voltage profiles conceptually match the CSII voltage profiles commonly seen in EMT analyses or field measurements [21, 22]. The least severe voltage profile is plotted in dashed red for clearer visualization, whereas every following event has a higher amplitude and exponential rise, as described in Table 5.3.

⁴New generation of positive sequence IBR models could partly mitigate this challenge [19, 20].

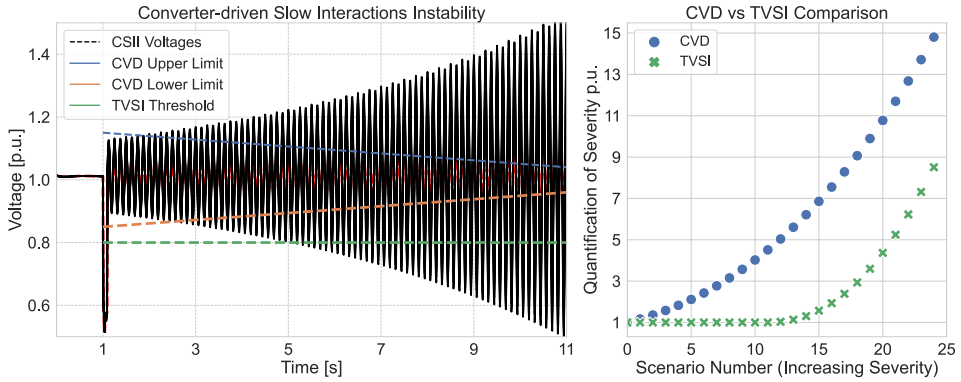


Figure 5.7.: CSII events: Comparison of CVD and TVSI methods in quantifying the increasingly severe voltage deviations. *Left:* Simulation results. *Right:* Corresponding quantification scatterplots.

5

In the lower middle scatterplot, the quantification of these events is shown for CVD and TVSI. Starting with TVSI, one can see that the increasing severity is accurately quantified only from event number 13. Before this event, the sensitivity of TVSI is insufficient to differentiate among the events of various severities, resulting in an inaccurately flat trend. On the other hand, CVD is sensitive enough to pick up the differences even amongst the first few events and continues to quantify increasing severity for all the events. These improvements in CVD relative to TVSI are, similarly to FIDVR, a consequence of analogous reasons as described in previous subsections dealing with FIDVR and TRAI.

Furthermore, the ability to put more weight on voltage deviations that come later in time relative to the fault inception benefits CVD over TVSI. This is shown to be very important in exponentially growing oscillatory voltage behaviour, being the main stability risk of CSII.

The frequency of the oscillations f is chosen to be 8Hz, as the frequency range of observed CSII events is typically 7 - 10Hz (see [Chapter 2](#)). Nevertheless, the results are not sensitive to this assumption and hold equally for other CSII event frequencies, which is another benefit of the method. From the overall results, it can be seen that CVD is very suitable for quantifying the severity of dangerous CSII-related post-fault voltage deviations.

COMBINED INSTABILITY (FIDVR + TRAI)

For the last round of simulations, a case of intertwined instabilities is considered. As discussed in [Chapter 2](#), the structural changes of the power systems lead to more interactions among different instability phenomena, resulting in a risk of combined instability events, which is illustrated here.

The simulations in this subsection are, once again, performed on the IEEE test system from [Figure 5.4](#). To produce cases of entangled instabilities, two changes

are introduced in the model: (i) a high and increasing amount of dynamic load is added; and (ii) the fault clearing time is increased. Table 5.4 shows the parameters for the scenarios taken into consideration.

Table 5.4.: Parameters used for modelling combined events.

Simulation number	Dynamic load penetration	Fault clearing time [ms]
0	38 %	125
1	38.5 %	125
2	39 %	125
...
24	50 %	125

The share of A/B/C/D-type motors in the dynamic loads is set to 0.1/0.1/0.3/0.1, respectively, for all simulations. The values are chosen in a way to produce the combined instability scenarios as per experience from Chapter 4.

The results are shown in Figure 5.8. All the events show an initial short-lasting FIDVR event (up to ~3-4 seconds), followed by electromechanical oscillations which indicate a risk of TRAI. The simulations are sorted in an increasing severity order, as shown in Table 5.4. This can be seen in the progressively more severe FIDVR, as well as stronger voltage oscillations, starting from the least severe case (dashed red). These sorts of complex grid instability phenomena are more likely to emerge in modern grids, such as low inertia grids with a high share of dynamic load.

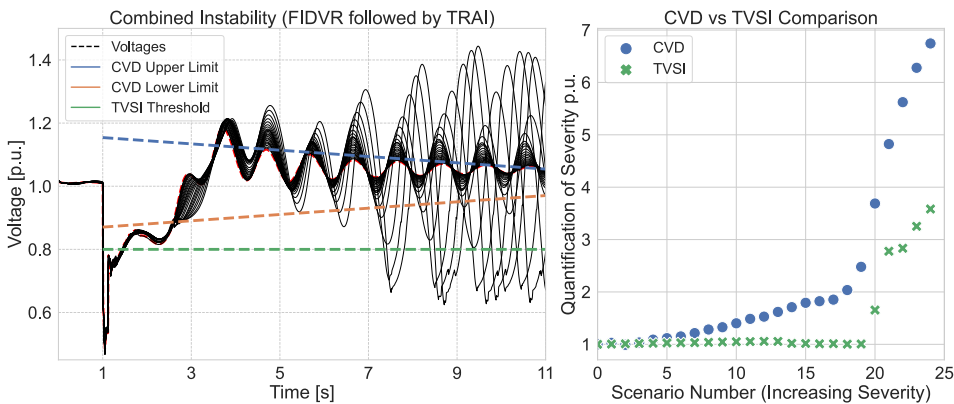


Figure 5.8.: Combined events: Comparison of CVD and TVSI methods in quantifying the increasingly severe voltage deviations. *Left:* Simulation results. *Right:* Corresponding quantification scatterplots.

From the scatterplot in Figure 5.8, one can again note that CVD is performing much better than TVSI in quantifying the severity of these voltage deviations. TVSI

shows almost no sensitivity to the increasing severity up to event number 20, which is already a very severe one. It even shows a slight downward trend, wrongly indicating a reduction in severity. The last five events are the most severe as TRAI rapidly unfolds, followed by low-frequency but extremely high-amplitude voltage deviations that are followed by out-of-step conditions and expected system splitting and/or instability. CVD is again able to correctly distinguish between various events of different severity by utilizing the proposed time-adaptive linear voltage thresholds.

QUANTIFICATION: CONCLUDING REMARKS

The results from the four analyzed instability mechanisms show unanimously how the Cumulative Voltage Deviation (CVD) method is an efficient numerical approach for quantifying voltage deviations. The voltage deviations are correctly sorted based on their severity, with a quantifiable value that can be understood as pu-sec (or kV-sec) voltage deviation outside of the predefined dynamically secure voltage boundaries. The larger the value is, the more likely the system is to experience cascading and instability. The method is shown to perform notably better than the commonly used severity index TVSI, with much less risk of underestimating an event, irrespective of the instability type. These results hold for all four short-term instability mechanisms discussed in [Chapter 2](#), even in combined and intertwined instability scenarios, demonstrating the flexibility and versatility of the method in both conventional and modern power systems.

The value of such a method is the fact that grid engineers do not have to manually and qualitatively determine which simulation results are more or less severe. As the number of relevant operating and fault scenarios increases, the number of relevant large-grid simulations that need to be studied rises exponentially. This is emphasized by the reduced system inertia and system strength aspects discussed in [Chapters 2](#) and [3](#). Hence, a quantification method such as the CVD allows for risk-based automation of grid vulnerability assessment, where thousands of scenarios can be reduced to a much lower number deemed to have the potential to cause short-term instability. These severe scenarios can be then studied in more detail so that suitable mitigation techniques can be taken proactively. Finally, with the increasing application of PMUs and WAMPAC systems, the method can be also incorporated into online and real-time algorithms, as well as risk-based decision-making.

5.3. SHORT-TERM INSTABILITY CLASSIFICATION ALGORITHM

In [Section 5.2](#), quantification of various disturbances based on the voltage deviation severity is introduced. However, such an approach addresses only the voltage event severity, without providing insights into the type of event taking place. Such information can be valuable in analyses and is hence explored here further.

The theoretical classification and characterization of disturbances and instabilities is an important topic in academia and industry. However, approaches that focus on short-term instabilities are rarely investigated [[23](#)], and are emerging as major challenges for the resilient operation of IBR-dominated power systems, as discussed in previous chapters. Some existing data-based classification approaches rely on

statistics, clustering, regressions, and other machine learning (ML) techniques to rapidly detect and classify disturbances [8, 24–26]. Moreover, oscillation detection algorithms based on approaches such as the Prony method, the Hankel Total Least Square method, the Matrix Pencil method, and the Wavelet transform have been proposed in [27–30]. Non-oscillatory instability events such as FIDVR are typically detected based on voltage or admittance monitoring [31, 32]. STVI detection is discussed extensively in [13] and Chapter 2.

Most of the short-term instability classification methods, therefore, focus on detecting a specific type of disturbance or instability, rather than on classifying various disturbances in simulation results or in real-time.

This section introduces a novel classification algorithm for short-term instabilities that complements the CVD quantification method presented in the previous section. Similarly to the CVD quantification algorithm, the classification algorithm is designed to be robust and perform based on voltage inputs only. This makes it applicable not only for rapid automated risk-based stability studies by applying tools such as DiGSILENT PowerFactory and Python, but also for real-time applications with synchrophasors. The algorithm is designed to distinguish between the four types of short-term instabilities described in Figure 2.12 with high accuracy.

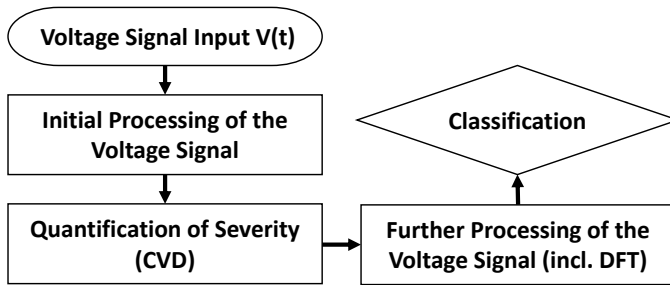


Figure 5.9.: Overview of the relation of quantification and classification algorithms.

The high-level overview of the entire quantification and classification algorithm process is shown in Figure 5.9. The first three steps are already explained in the previous sections. The implementation of steps 4 and 5 is hereby discussed in detail.

5.3.1. METHODOLOGY AND IMPLEMENTATION

There are four distinctive short-term instabilities: Short-Term Voltage Instability (STVI), Transient Rotor Angle Instability (TRAI), Fault-Induced Delayed Voltage Recovery (FIDVR), and Converter-driven Slow Interactions Instability (CSII) (see Chapter 2 and Figure 2.12). All these phenomena have unique characteristics that can be exploited to differentiate between them in the classification algorithm. The four types are hereby initially split into two groups: *oscillatory* and *non-oscillatory* phenomena. TRAI and CSII fall into the former category, while STVI and FIDVR fall into the latter. These two categories are discussed further.

For the classification of the two oscillatory phenomena (TRAI and CSII), the suggested algorithm pre-processes and transforms the time-series signal into the frequency domain. This is achieved by using Discrete Fourier Transform (DFT), based on the well-known algorithm from [33], hereby implemented in Python. The pre-processing involves three steps: i) extracting the post-fault voltage deviation signal; ii) removing the first 300ms to avoid the initial fault transients' impact on DFT accuracy; and iii) removing the DC offset by deducting the mean from the signal. The last step is also implemented to improve the DFT accuracy, as the DC offset is not of interest for classification.

With the frequency domain signal derived, two classification variables are calculated: Peak Frequency Magnitude (PFM) and Energy Spectral Density (ESD), shown in Equations (5.7) to (5.10) for TRAI and CSII, respectively. PFM is the magnitude of the oscillations in the relevant frequency band, while ESD is based on Parseval's unitary Fourier transform theorem, representing the energy of a signal in a frequency band. $X[k]$ is the frequency domain signal, calculated as the DFT of $V(t)$.

$$PFM_{TRAI} = \max(X[k]); \quad k \in [0.75-3\text{Hz}] \quad (5.7)$$

$$PFM_{CSII} = \max(X[k]); \quad k > 3\text{Hz} \quad (5.8)$$

$$ESD_{TRAI} = \sum_{k=0.75}^3 |X[k]|^2 \quad (5.9)$$

$$ESD_{CSII} = \sum_{k=3}^{\max(k)} |X[k]|^2 \quad (5.10)$$

These two variables are calculated inside two frequency bands: 0.75Hz to 3Hz, and $> 3\text{Hz}$. The choice of such bands is directly related to the inherent differences between TRAI and CSII phenomena. As described in Chapter 2, TRAI voltage deviations are *electromechanical* by nature, and therefore much slower, typically appearing in the mentioned frequency interval. These oscillatory dynamics are known as modes [34], and are mathematically described in Equations (5.11) and (5.12).

$$y_i(t) = A_i^{\sigma_i t} \sin(\omega_i t + \phi_i) \quad (5.11)$$

where ω_i is the imaginary part of the complex eigenvalues λ_i , related to the oscillation frequency f_i :

$$\lambda_i = \sigma_i + j\omega_i \quad ; \quad f_i = \omega_i/2\pi \quad (5.12)$$

There are three types of electromechanical oscillation modes related to rotor angle instability: i) local-area, ii) intra-station, and iii) inter-area modes [35]. These modes commonly exhibit natural frequencies f_i below 3 Hz due to inherent structural characteristics of power systems and synchronous machines [36]. This is typically evaluated with a modal (eigenvalues) analysis.

Meanwhile, CSII is generally a sub-synchronous oscillation phenomenon, and by nature, it is almost exclusively electromagnetic. As such, it often appears in the 7-10 Hz frequency range (see [Chapter 2](#)), however, it can also take other (typically larger) values in the sub-synchronous range [14, 21]. These oscillations are often a consequence of control interactions or PLL performance, particularly in weak grids, and are fundamentally different from TRAI oscillations (see [Chapters 2 and 3](#)). This is reflected in their higher frequency, hereby utilized for classification.

For this analysis, the threshold used for both PFM and ESD is set to 0.175 per unit, based on extensive simulation results of the analysed system in [Figure 5.4](#). The frequency bands and thresholds can be fine-tuned for the system in question for better performance – for instance by knowing the size of the system and expected electromechanical oscillation modes [14, 35]. When the dominant modes of interest in the analysed (large) system are low-frequency inter-area modes, the lower frequency threshold can be reduced for improved classification accuracy. The entire classification process is exemplified in [Figure 5.10](#) for scenario number 15 dealing with combined instability from [Table 5.4](#) (left) and CSII scenario number 5 from [Table 5.3](#) (right), both from [Section 5.2](#). These scenarios are taken as illustrative examples; similar analyses and conclusions hold for other scenarios. In [Figure 5.10](#), for both left and right-side graphs, black plots are in the time domain, while blue plots are in the frequency domain.

In [Figure 5.10](#) right side plots, it can be seen how the voltage signal (upper plot) is firstly processed to remove initial transients and correct for DC offset (middle plot), and then transformed to the frequency domain (lower plot). The DFT graph (blue) shows that the PFM of the oscillations is at 8 Hz with amplitude above the threshold. Furthermore, the ESD value as per [Equation \(5.12\)](#) is also above the threshold (not shown in graphs), which results in a unanimous decision to classify this event as CSII. On the left side of [Figure 5.10](#), a combined instability plot is depicted, which contains a TRAI event. From the DFT, it can be seen that the PFM and ESD are both concentrated inside the 0.75Hz to 3Hz frequency band, with PFM crossing the threshold at around 1 Hz. There is also a peak in the disregarded < 0.75 Hz range, however, it is not of interest as it originates from the initial FIDVR recovery of the combined instability scenario. In this case, the ESD value is below the threshold, however, as the algorithm only needs one value over the threshold (PFM or ESD), it is correctly classified as a TRAI event. This is a good example to show the benefit of using both PFM and ESD since a signal in the frequency domain could have high PFM but low ESD (high kurtosis), or low PFM but still high ESD (low kurtosis). The latter may occur when the frequency of oscillations is changing over the duration of the event, or if the data acquisition is less precise, or with a lower sampling frequency. By utilizing both values in the classification algorithm, the accuracy of detecting oscillatory events such as TRAI and CSII can be notably increased.

For non-oscillatory events (FIDVR and STVI), a different approach is used, as DFT would not provide a useful differentiator due to the non-oscillatory nature of the events. Instead, these events can be detected and classified in the time domain, by taking advantage of the CVD algorithm introduced in [Section 5.2](#). Firstly, the algorithm is used to determine whether a prolonged undervoltage condition takes

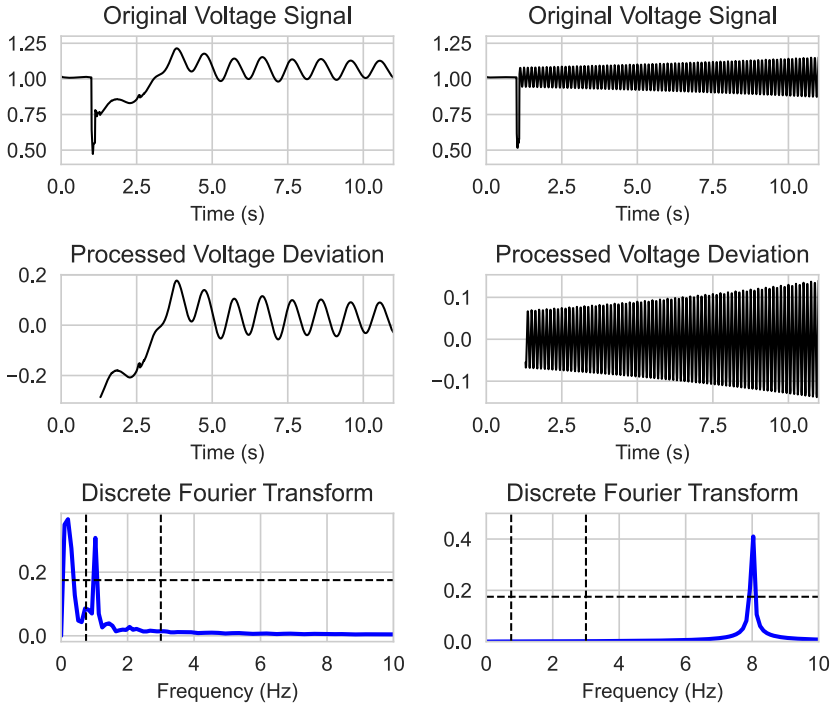


Figure 5.10.: Example of the DFT-based classification. Scenarios *Combined Instability no. 15* (left), and *CSII Instability no. 5* (right) (see Section 5.2). Dashed lines depict PFM thresholds (horizontal) and frequency bands (vertical).

place. This is achieved by using the two following conditions: i) when undervoltage CVD (CVD_{UV}) is larger than 75% of the total CVD value; and ii) when CVD_{UV} is larger than 0.03 per unit. Both conditions are applied only to the first 3 seconds of the post-fault signal and are described in Equations (5.13) and (5.14).

$$\sum_{t=t_f}^{t_f+3} CVD_{UV} > 75\% * CVD \quad (5.13)$$

$$\sum_{t=t_f}^{t_f+3} CVD_{UV} > 0.03 p.u. \quad (5.14)$$

The reasoning behind the two utilized conditions has both theoretical and experimental bases. The first condition, shown in Equation (5.13), is used to differentiate between oscillatory and non-oscillatory events. In the first few seconds of STVI and FIDVR, the undervoltage deviation is the dominant type relative to the overvoltage deviation (see Figure 2.11). When a significant overvoltage also exists, the event is likely of an oscillatory nature instead (TRAI or CSII). Furthermore, the

event needs to be sufficiently severe so that it is considered a FIDVR or an STVI event. This is ensured by the second condition shown in Equation (5.14), i.e. the voltage being at least 1% below the $V_D(t)$ curve for 3 seconds. The proposed thresholds are based on extensive simulations in Chapters 4 and 5 and fundamental characteristics of typical FIDVR and STVI dynamics in various system conditions.

The methodology is illustrated in Figure 5.11, once again on the combined instability scenario number 15 (see Table 5.4). The FIDVR event that takes place in the first few seconds after the fault is of interest. The upper plot in Figure 5.11 depicts the original voltage signal, as well as the $V_U(t)$ and $V_D(t)$ curves. The blue dashed vertical line represents the cut-off time for the algorithm evaluation. The lower plots show the initial post-fault voltage of interest (left), and its corresponding voltage deviation chart in per-unit values (right). These types of curves and plots are further explained in Section 5.2.

Once both conditions in Equations (5.13) and (5.14) are met, it can be considered that one of the non-oscillatory events (either STVI or FIDVR) is taking place, i.e. a delayed voltage recovery is present; however, it does not reveal which one.

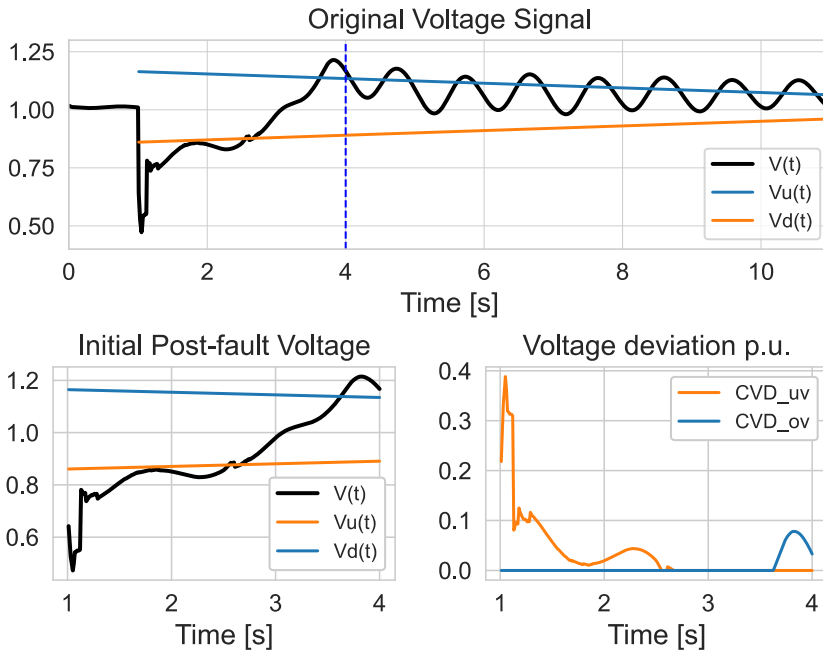


Figure 5.11.: Classification example for non-oscillatory events. The upper plot depicts the original voltage signal and CVD thresholds introduced in Section 5.2. The lower graphs are the extracted signal interval (left) and the corresponding over- and under-voltage CVD (right).

As the main difference between FIDVR and STVI is in the voltage recovery, a simple check of whether the voltage crosses $V_D(t)$ curve throughout the total duration of

the evaluation is employed, as shown in Equation (5.15).

$$V(t) < V_D(t), \quad \forall t \in [t_f + 0.3, t_f + 10] \quad (5.15)$$

If the condition is not true, the voltage has been depressed but it has eventually recovered, indicating FIDVR. If the condition is true, i.e. $V(t)$ is lower than $V_D(t)$ for every t , the prolonged voltage depression is present. This likely results in a partial or total voltage collapse, i.e. STVI. The first 300ms of the signal are again ignored to reduce the impact of the initial (post-)fault transients on the classification accuracy.

The introduced methodologies for oscillatory and non-oscillatory events jointly form the classification algorithm, designed to complement the CVD quantification algorithm presented in the previous section. The accuracy of the classification algorithm is tested in the next subsection.

5

5.3.2. CLASSIFICATION ACCURACY

To test the accuracy of the classification algorithm, the 100 scenarios from Section 5.2 are analysed. The classification accuracy is calculated using Equation (5.16), where TP and TN are the numbers of True Positive and True Negative classifications, respectively, and FP and FN are False Positives and False Negatives, respectively [37].

$$Acc(\%) = \frac{TP + TN}{TP + TN + FP + FN} * 100 \quad (5.16)$$

Furthermore, to evaluate the robustness of the classification methodology for shorter simulation times, tests are conducted not only for a 10-second duration, but also for 8, 6, 4, and 2 seconds. These tests are conducted for all 100 scenarios from Section 5.2, resulting in a total of 500 classification tasks. The benefits of a potentially faster classification are twofold. For offline simulations, a shorter dynamic simulation time reduces the computational demand and allows faster analysis. For online applications, classifying events promptly is crucial for fast detection and decision-making. The classification accuracy of the algorithm is shown in Figure 5.12.

For the original signal duration of 10 seconds, the classification algorithm performs very well, achieving 96.2% accuracy over the analysed scenarios. Reducing the available interval to 8 or 6 seconds barely affects the accuracy, which remains higher than 91.5%. However, when even shorter time intervals are used (e.g. <5 seconds), the classification accuracy drops rapidly, as shown in Figure 5.12. This is expected as some events need several seconds to advance enough to be detectable and classifiable, especially in the case of FIDVR and STVI. A promising approach to address this reduced accuracy is to apply time-series extrapolation of the voltage to detect the likely future trend of the voltage deviation. Unreported preliminary results show that this may improve accuracy notably for shorter time intervals, and is, therefore, a promising topic for future research. As this thesis deals with the existing data only, relevant extrapolation techniques and their application are out of scope.

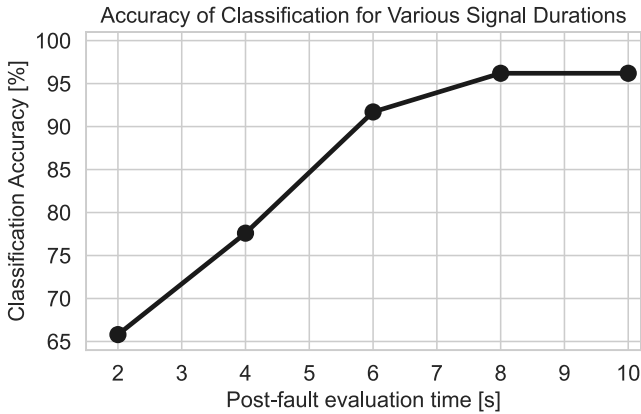


Figure 5.12.: Classification accuracy for a large set of post-fault deviations with varying evaluation times provided to the algorithm.

CLASSIFICATION: CONCLUDING REMARKS

This section introduced a novel algorithm to classify short-term instability events automatically and rapidly based on their voltage curve. The presented results confirm that the proposed classification algorithm shows a high level of accuracy. Furthermore, the efficacy remains high even for shorter post-fault voltage signals, albeit with an expected reduction in accuracy. The classification algorithm, therefore, complements the quantification algorithm well, allowing for a combined automatic evaluation of severity and type of short-term instability, regardless of the type and nature of the event taking place.

5.4. VOLTAGE VULNERABILITY CURVES AND DYNAMIC-STATE SYSTEM STRENGTH

With faster and more severe voltage dynamics and related instabilities, modern power systems are more vulnerable to widespread cascading. To ensure system resilience and stability, power system operators need to be aware of any vulnerable grid sections and dangerous operating scenarios so that these can be planned for and addressed. Nevertheless, as discussed extensively in previous chapters, the rising complexity of system modelling and analysis of dynamical processes in modern power systems makes the evaluation task increasingly intricate. The large number of grid locations and operating scenarios with complex inverter-based generation and load, paired with parameter uncertainty, make deterministic analytical analyses increasingly difficult and time-consuming.

This section proposes a new method designed to simplify this problem. Voltage Vulnerability Curves (VVCs) are proposed and created by relying on the already-introduced CVD method and a novel data-based interpolation algorithm. The

method aims to quantify the dynamic-state aspect of system strength, which is largely overlooked by the steady-state methods discussed in [Chapter 3](#). The section commences by exploring the important relation between short-circuit capacity and voltage deviations, uncovering a fundamental problem of currently available methods. To address these limitations, the VVC method is proposed and exemplified on several rounds of numerical simulations, exhibiting very good performance.

5.4.1. SHORT-CIRCUIT CAPACITY AND VOLTAGE DEVIATIONS

Short-circuit capacity (S_{sc}) is one of the most common metrics used to describe system strength at a certain bus. S_{sc} is used for numerous steady-state system strength evaluation methods, as discussed extensively in [Chapter 3](#). For convenience, its analytical definition is repeated here, as shown in [Equation \(5.17\)](#),

$$S_{sc} = \frac{V^2}{Z_{sc}} \quad (5.17)$$

The higher the S_{sc} , the stronger the bus is assumed to be. This conclusion has strong theoretical support in conventional power systems, as described analytically in [Equation \(3.3\)](#) and discussed extensively in [Chapter 3](#).

To demonstrate this conclusion numerically on the same test system as before ([Figure 5.4](#)), S_{sc} of each 130kV busbar is calculated based on the IEC 60909-2016 standard. The results are shown in [Figure 5.13](#).

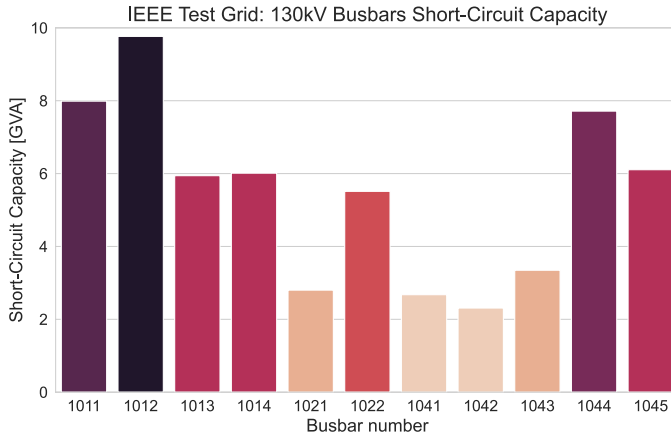


Figure 5.13.: Short-circuit capacity of every 130kV busbar in the test system based on the IEC 60909-2016 standard.

There is clearly a large variation in S_{sc} across the system. This is a consequence of several factors, mainly the proximity to synchronous generators and the (E)HV grid, impedances and lengths of the lines, and how meshed the surrounding grid is. Based on the S_{sc} values, an engineer could, for instance, conclude that buses such as 1041 or 1043 are much weaker than bus 1045. The accuracy of such a common conclusion in modern grids will be challenged and nuanced further in this chapter.

To demonstrate how S_{sc} relates to the severity of voltage dips, 3-phase short-circuit faults with a fault resistance of $2.5\ \Omega$ are applied to each 130kV bus, and the voltage response is measured. The results are plotted in Figure 5.14, with a colour bar label representing the S_{sc} of the respective busbar, also illustrated in Figure 5.13.

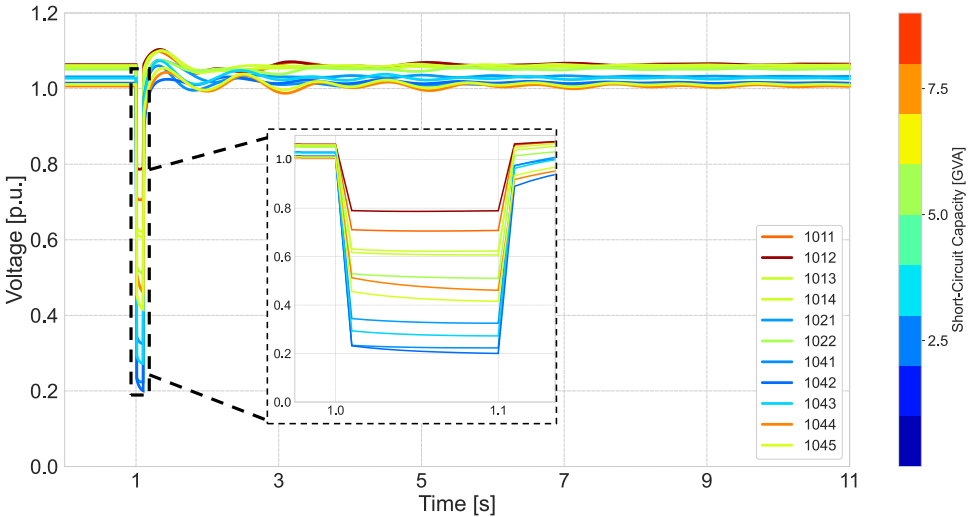


Figure 5.14.: Dynamic simulations illustrating the inverse relation between fault voltage drop (ΔU_f) and short-circuit capacity of a bus (S_{sc}).

It can be seen from the voltage plots that S_{sc} and the severity of voltage dips exhibit a strong inverse relation. Busbars with a higher (lower) S_{sc} experience a lower (higher) fault-induced voltage dip. This is the primary reason why S_{sc} is generally used as a system strength indicator. Buses with higher (lower) S_{sc} will therefore experience lower (higher) voltage sensitivity to disturbances in general, often described as stronger (weaker) buses. This has been also demonstrated analytically in Equations (3.1) to (3.3).

However, such an analytical analysis contains a few important assumptions. The first assumption is that the system can be replicated well with a Thevenin equivalence. For a modern power system with an increasing share of inverter-based resources, this assumption becomes less and less accurate, as discussed in Chapter 3.

The other important assumption in this analysis is that the demand is static and passive. As such, these loads do not have a major impact on fault and post-fault voltage dynamics. While this assumption used to be reasonably accurate in conventional power systems whose dynamics were dominated by the operation of synchronous machines, it becomes progressively more inaccurate in modern power systems. The first reason for this inaccuracy is the increasing penetration of DERs throughout the medium- and low-voltage networks. What used to be a passive distribution system (PDN) is nowadays much more often an active distribution system (ADN), with a bidirectional power flow and a potentially big impact on

grid dynamics (see Chapter 4). Moreover, the second reason is that dynamic loads are becoming much more common in distribution systems, as electrification is realized in sectors that were previously powered by fossil fuels, such as the heating sector, transportation, and industry, as discussed in Chapter 1. Furthermore, the composition of distribution systems is shown to play a major role in grid dynamics in Chapter 4 and can be particularly relevant when short-term voltage deviations and stability are concerned. The proliferation of RES and the transition from conventional to modern distribution systems therefore invalidates the assumption that S_{sc} can be used to directly evaluate dynamic-state system strength (see Chapter 3). Instead, the situation becomes significantly more complex.

Voltage dynamics with IBRs and dynamic loads occur not only during the fault period but also in the several seconds after the fault, i.e. in the post-fault period. These variations play a key role in vulnerability as they may lead to cascading. Therefore, in order to capture the full scope of voltage deviations related to dynamic-state system strength, evaluating only the voltage dip during the fault provides an incomplete picture of the voltage deviations resulting from a disturbance.

The newly developed cumulative voltage deviation (CVD) method, introduced in Section 5.2, is hereby used to quantify both fault and post-fault voltage deviations. Utilizing the results obtained in Figure 5.14, maximum voltage drop ΔU_f and CVD are calculated for each 130 kV bus with various S_{sc} . The relation between the short-circuit capacity and voltage deviations is shown in Figure 5.15 with a scatterplot. The trend is visualized with a simple best-fit linear regression.

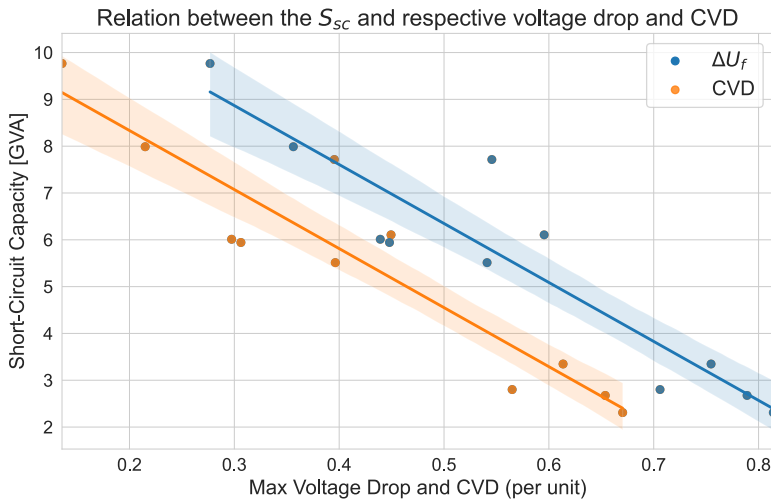


Figure 5.15.: Relationship between S_{sc} and voltage deviations measured by voltage drop ΔU_f and CVD , for each 130 kV bus in the IEEE test system.

What can be deduced from the plot is that both ΔU_f and CVD have a very strong and similar inverse linear relationship with S_{sc} . This is expected as both metrics numerically evaluate voltage deviations. Therefore, even simple methods such as S_{sc}

can often be used to quantify and describe system strength in *conventional* power systems with *passive* distribution systems.

In the next sections, the assumptions of static load and conventional generation will be relaxed to show how S_{sc} becomes progressively less accurate in modern power systems. In other words, it will be shown how it loses relevance as a dynamic-state system strength metric in a modern power system. A new method derived to tackle this problem is presented in the next section.

5.4.2. VVC METHODOLOGY

The impact of load and DER response on grid resilience, as discussed in [Chapter 4](#), is shown to be very important to model and consider when analyzing grid stability and strength. However, system strength, as one of the main aspects of grid resilience and vulnerability, is typically evaluated only from the steady-state perspective, as described in [Chapter 3](#). This evaluation, while important for the steady-state operation, completely misses the intricate dynamical response of dynamic load and DER, and its impact on dynamic-state system strength explored in [Chapter 4](#).

As discussed at the beginning of this chapter, scripting and automation offer the possibility to rapidly and efficiently simulate the dynamic response of a system for a wide range of operating scenarios and parameters. However, the big data set originating from such an analysis can be very time-consuming to analyze manually. It is therefore also necessary to have a scalable and fast approach that can quantify the severity of voltage deviations automatically. This is what the CVD method, introduced in [Section 5.2](#), is able to do. This section expands on the CVD method by applying it to not only evaluate voltage deviations of various operating scenarios but to efficiently provide insights into the intricate aspects of dynamic-state system strength, as introduced and discussed in [Chapter 3](#).

A new method is developed for this purpose, named *Voltage Vulnerability Curves* (VVCs). The method is exemplified and described in [Figure 5.16](#).

The right part of the figure shows an example of a VVC plot. The Y-axis of the plot is designed to quantify the severity of a disturbance, relying on the already-introduced CVD method. Meanwhile, the X-axis depicts the increasing duration of the fault. The Y-axis can be expressed in kV.sec or per-unit.sec, while the X-axis is in milliseconds or seconds. By utilizing the algorithm shown on the left-hand side, a series of dynamic simulations are performed, where Δt_f is increased until a predefined Δt_f^{max} value. This value can be chosen as a maximum expected total⁵ fault-clearing time, based on protection coordination.

The resulting CVD values are collected for each discrete simulation scenario and are scatter-plotted on the VVC plot on the right (black circles). Once all the simulations are completed, an interpolated⁶ curve is created, depicted in blue in the example in [Figure 5.16](#). The most suitable way to perform the interpolation will be discussed later in this chapter.

⁵This includes relay operation, circuit breaker opening time, and arc quenching. It may also include protection/breaker malfunction assumptions.

⁶Interpolation is a method of constructing new data points based on the range of a discrete set of known data points. In this case, known points are simulation-based CVD values for respective Δt_f .

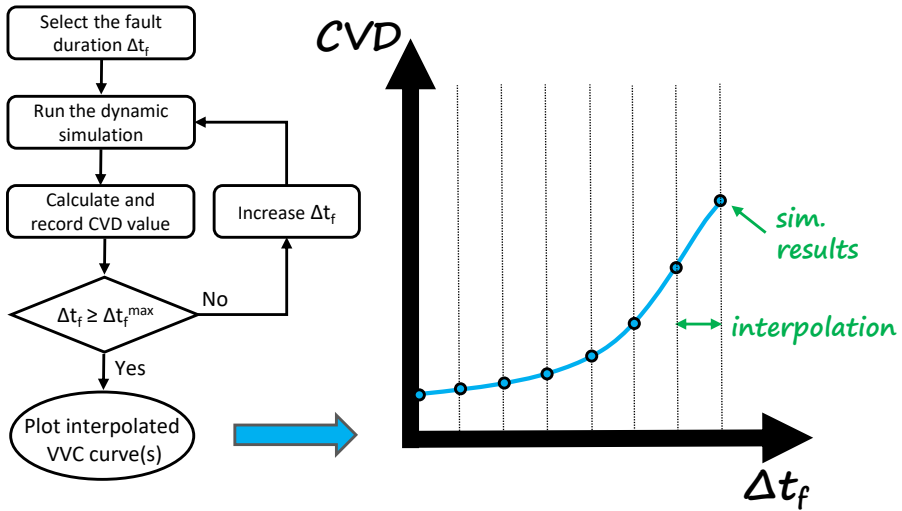


Figure 5.16.: The methodology of the VVC method (left) and the example of the resulting VVC plot and curve (right).

The resulting VVC curve can be understood as follows. For a certain simulation scenario, the CVD value is calculated, indicating the severity of a disturbance. This severity will naturally depend on the fault duration. The longer the fault lasts, the more severe the voltage deviation is, as illustrated in Figure 5.16. However, this severity will also depend on other relevant factors, such as the composition of the load and the distributed generation presence, as well as their contribution to voltage dynamics, as discussed in Chapters 3 and 4.

In the next two sections, the assumptions of static load and conventional generation will be relaxed in order to show how S_{sc} and ΔU_f become progressively less accurate as dynamic-state system strength metrics of a modern power system. Instead, the newly developed VVC method is proposed and benchmarked against S_{sc} , providing much broader insights about dynamic-state system strength.

5.4.3. NUMERICAL SIMULATIONS AND RESULTS

In this section, voltage vulnerability curves will be utilized to evaluate the dynamic-state system strength of buses with various distribution system compositions. The analysis commences with static load models, followed by an introduction of dynamic load models with a potential for stalling, and DERs with partial LVRT disconnection (see Figure 4.2). Finally, in the last part of this section, the analysis will demonstrate the suitability of VVC for evaluating the dynamic-state system strength of various buses, as well as its superiority compared to the commonly used short-circuit capacity as a measure of system strength.

STATIC LOAD SIMULATIONS WITH VVC

The first set of simulations is performed on the unaltered system from [38], also shown in Appendix A. The loads are kept as default static loads, with original system parameters as per operating point A from [38]. For each busbar, a VVC is plotted by running a series of dynamic simulations in DiGSILENT PowerFactory assisted with Python scripting (see Figure 5.1). In every consecutive simulation, fault duration is increased, to increase the severity of the disturbance, as described in Figure 5.16. The results are plotted in Figure 5.17.

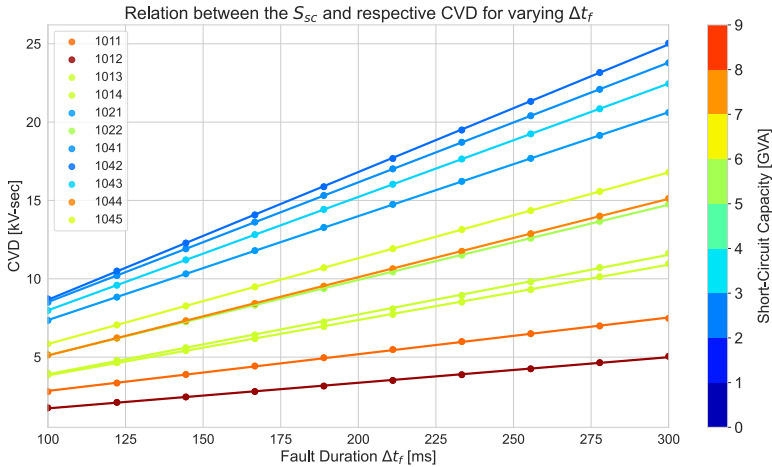


Figure 5.17.: Voltage vulnerability curves for 130kV buses in the IEEE test system.

For each busbar, a voltage vulnerability curve is plotted by linearly interpolating the obtained simulation results. Furthermore, the results are colour-coded to show how S_{sc} relates to the results. From the plots, it can be seen that each VVC is linear. Furthermore, the colour coding clearly shows that buses with larger S_{sc} generally experience lower voltage deviations, and this conclusion holds regardless of the fault duration or intensity. Therefore, for the case of static loads and conventional power systems, the VVC method arrives at the same conclusions as simpler methods like S_{sc} . It is therefore often sufficient to calculate S_{sc} and use this information as a suitable steady- and dynamic-state system strength measure in such cases.

DYNAMIC LOADS AND DELAYED VOLTAGE RECOVERY EVALUATION WITH VVC

In this subsection, the static load at busbar 1041 in the IEEE Test system is replaced by two WECC dynamic loads with an overall increasing share of stalling single-phase A/C units. This change is introduced to synthetically replicate the effects of a larger amount of motor load stalling as voltage dips become more severe [39], leading to Fault-Induced Delayed Voltage Recovery (FIDVR), as discussed in Chapter 4.

A series of faults are simulated on busbar 1041 with varying fault duration. Details of the simulation parameters are listed in the Appendix B. The resulting voltage

responses are plotted in [Figure 5.18](#), with a green (red) highlight for the least (most) severe scenario in terms of fault duration and the consequent voltage deviation.

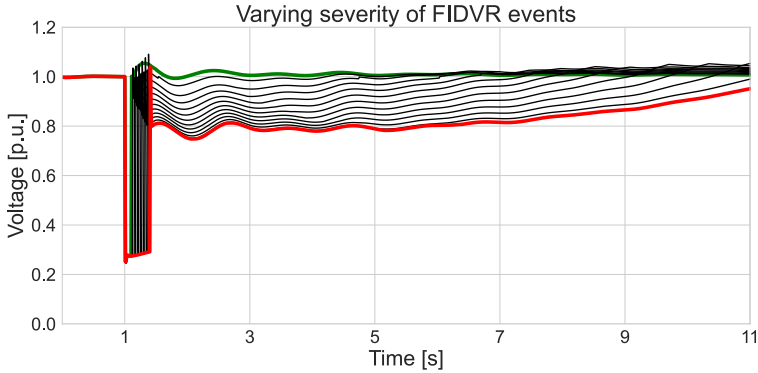


Figure 5.18.: Voltage responses of bus 1041 for a variety of fault scenarios.

It can be seen that a FIDVR event occurs, with progressively deeper voltage sag, in line with previous simulations. To quantify the FIDVR effect, voltage vulnerability curves are used based on the CVD metric, as described in [Section 5.4.2](#). The VVCs for the cases of static load versus the discussed dynamic case are plotted in [Figure 5.19](#).

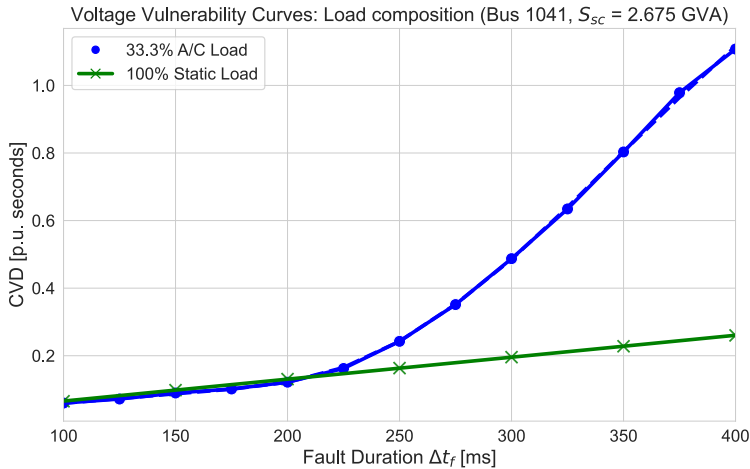


Figure 5.19.: Voltage Vulnerability Curves (VVC) for the case in [Figure 5.18](#), compared with a base case with only static load.

A clear benefit of VVCs is revealed here. The green line indicates the static load VVC, as per the previous section, while the blue line indicates a VVC for the case of dynamic load with A/C units. For fault duration below 200ms, there is almost no difference between the curves. However, as fault severity increases with a larger fault

duration, some motors start to stall, resulting in higher reactive power demand. This reduces the voltage further, leading to larger voltage deviations. The VVC shown in blue captures this effect, as it starts diverging from the green curve, indicating higher voltage deviation, and thus lower dynamic-state system strength.

If S_{sc} would be used as a dynamic-state system strength and voltage sensitivity metric in this case, the bus strength would be significantly overestimated for longer-duration faults with dynamic loads. The intricate effects of dynamic load would not be captured as they are only seen by means of dynamic simulations. Meanwhile, VVC demonstrates how longer fault duration and severity affect the post-fault voltage response. Therefore, based on the VVC curve, an engineer could conclude that the blue case busbar is much weaker than the green one if fault clearing time is expected to be higher than 200 ms. Consequently, further and more detailed stability analysis can be performed if deemed necessary or if a new load or generation is to be connected to this bus or in its proximity.

DISTRIBUTED ENERGY RESOURCES AND LOW-VOLTAGE TRIPPING WITH VVC

Apart from dynamic loads, modern distribution systems comprise a variety of distributed energy resources (DERs). These can be located on both low- and/or medium-voltage levels. Based on the voltage level and nominal power, DERs have different low-voltage ride-through (LVRT) settings, and consequently, a different impact on short-term voltage deviations and stability, as discussed in [Chapter 4](#). Furthermore, DERs increasingly fail to ride through disturbances and disconnect the longer and more severe the disturbance is, as seen in [Table 1.1](#) and in [Chapter 4](#). This is hereby synthetically replicated and analyzed, to see how partial LV-DER and MV-DER disconnection affects post-fault voltage response and stability, and particularly show how this can be evaluated with VVCs. Simulations are performed with varying fault duration, comparable to previous sections. The parameters are listed in the [Appendix B](#). The voltage responses are shown in [Figure 5.20](#).

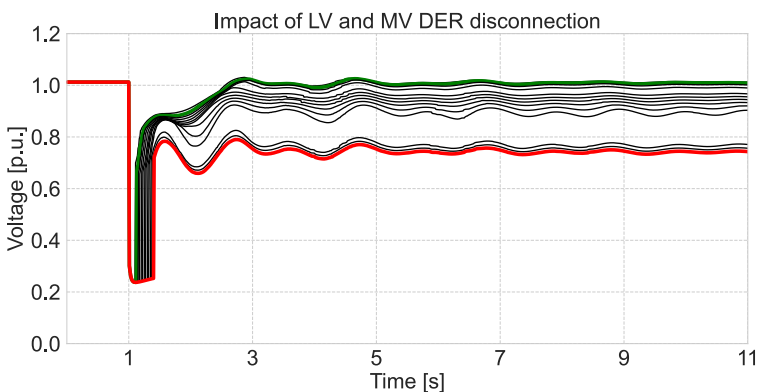


Figure 5.20.: Voltage response of bus 1041 with increasing fault duration which leads to partial DER disconnections.

As seen in the figure, an increasingly severe post-fault voltage sag occurs due to the partial disconnection of DER units. Furthermore, the last few simulations show an even larger voltage drop with a risk of potential voltage collapse. This occurs as MV-DER also disconnects for a larger fault duration in this illustrative example.

The corresponding VVC is plotted in Figure 5.21. Furthermore, to illustrate the effect of disconnections, it is indicated in the figure how much LV-DER has disconnected for each simulation, as well as when the larger MV-DER unit has disconnected. Similarly to previous results with dynamic load, for short fault duration Δt_f , the VVC with only static load is very similar to the VVC with DERs. This implies that voltage deviations and dynamic-state system strength are comparable. However, as the fault duration and severity increase, LV-DERs begin to partially trip, as indicated in Figure 5.21. Furthermore, for cases above 325 ms, MV-DER also trips, exposing the system to an even higher post-fault voltage drop. For a very long fault duration, almost all LV-DER and MV-DER have tripped, leading to a severely depressed post-disturbance voltage.

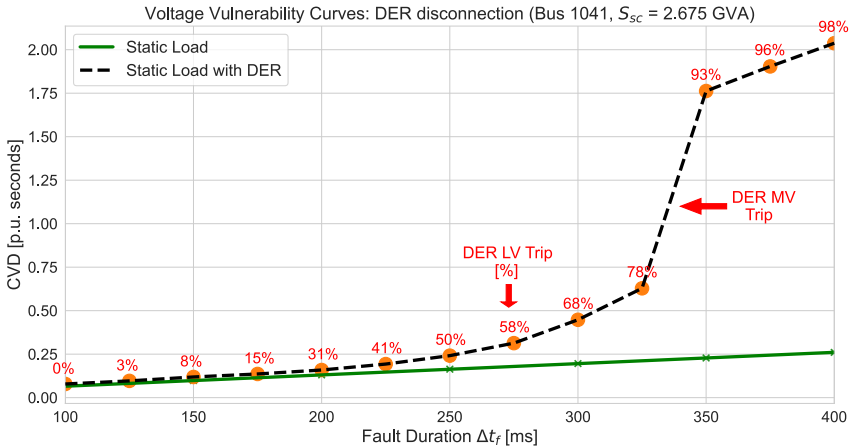


Figure 5.21.: Voltage Vulnerability Curves for the case in Figure 5.20, compared with a base case with only static load.

These simulations demonstrate a few important points. Firstly, DERs can have a large impact on post-fault voltage deviations, and therefore dynamic-state system strength, which is in line with the results presented in Chapter 4. Secondly, if the dynamic-state system strength of a busbar with DER was evaluated using only S_{sc} , it could be severely misestimated. Finally, using VVC, grid engineers can see how partial and total disconnections of various DERs may affect system response, and in that sense obtain more information about the dynamic-state system strength of their system and its resilience considering the rising fault-clearing time and/or further penetration of DERs at the bus of interest.

COMPARISON OF DIFFERENT DISTRIBUTION NETWORK COMPOSITIONS WITH VVC

In this subsection, a few changes are implemented in the unaltered network from Figure 5.4. The static loads connected to busbars 1041, 1043, and 1045 are replaced with dynamic loads, with the presence of DER, as shown in Figure 5.22. The details and parameters not shown in the text and figure are listed in the Appendix B.

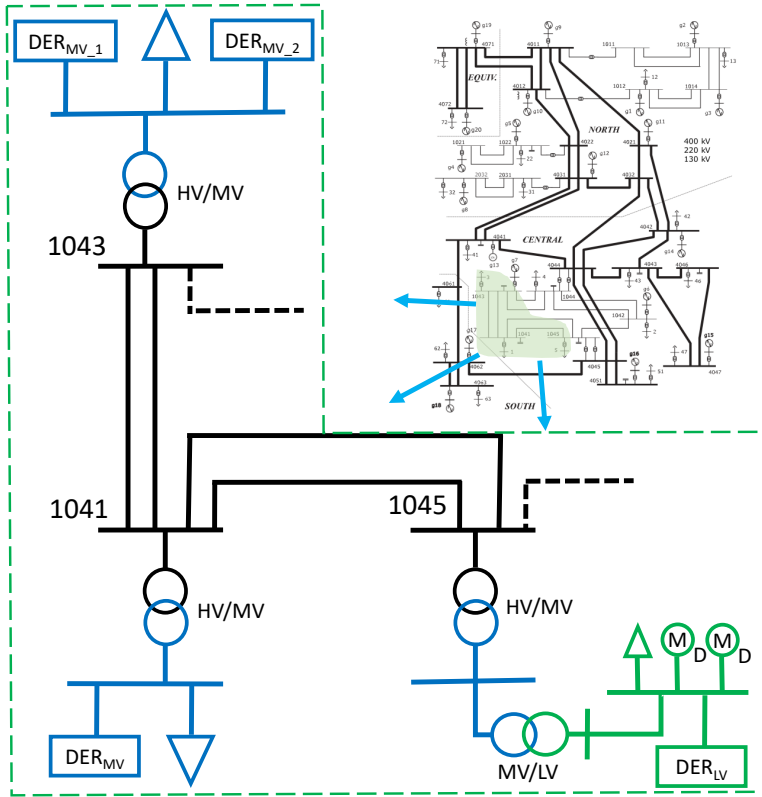


Figure 5.22.: Zoom-in on the altered part of the IEEE Test System. Three 130 kV buses (1041, 1043, 1045) with different demand compositions.

Each of the three busbars is exposed to a fault with an increasing fault duration, as per Section 5.4.2. The results are plotted in Figure 5.23 for all three busbars separately, with the least (most) severe events highlighted in green (red).

The voltage responses of busbar 1041 are depicted in the upper left plots of Figure 5.23. One can note that bus 1041 has the lowest short-circuit capacity of the three, $S_{sc} = 2.67 \text{ GVA}$. As depicted in Figure 5.22, bus 1041 contains a static load and a DER unit connected to the medium voltage level. When subjected to a fault, a voltage drop occurs, followed by an increasingly large post-fault voltage deviation. In the most severe case, voltage experiences slight oscillations and delayed recovery, but manages to recover successfully without severe voltage deviations.

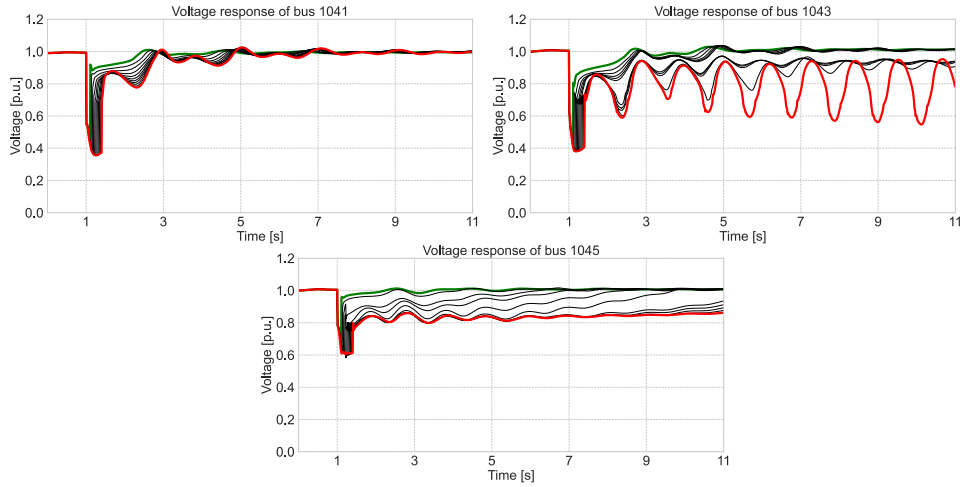


Figure 5.23.: Voltage responses of buses 1041 (top-left, $S_{sc} = 2.67$ GVA), 1043 (top-right, $S_{sc} = 3.34$ GVA), and 1045 (bottom, $S_{sc} = 6.10$ GVA) for a varying fault duration Δt_f .

The voltage response of bus 1043 is depicted in the top-right curves in the [Figure 5.23](#). Bus 1043 has a somewhat higher short-circuit capacity than bus 1041, $S_{sc} = 3.34$ GVA. Its demand composition is similar to the one of bus 1041, however, with two DER units connected to the MV grid. One of them is assumed to be able to withstand a low-voltage condition of up to 200 ms, while the other one up to 325 ms. Details can be found in the [Appendix B](#). As seen from the curves, voltage responses vary a lot as Δt_f increases. For the least severe fault duration, the response highlighted in green is similar to the one of bus 1041. However, as fault duration increases, voltage deviations intensify, eventually resulting in DER disconnections and severe voltage oscillations which would likely lead to short-term instability.

Finally, the voltage response of bus 1045 is shown in the lower plot of [Figure 5.23](#). Bus 1045 is much stronger than the other two in terms of short-circuit capacity, with $S_{sc} = 6.10$ GVA. This bus contains two dynamic loads of D-type, with one of them more prone to stalling, as well as an aggregated LV-DER unit representing a large number of PV panels and/or other small generating units. As fault duration in this example increases, so does the amount of stalled dynamic load and partial LV-DER disconnections, resulting in a post-fault low-voltage event.

Based on the voltage responses of the three buses, respective voltage vulnerability curves (VVCs) are created and plotted in [Figure 5.24](#) for comparison.

There are several important insights to draw from these simulations and VVC plots. Firstly, one can note the difference in the S_{sc} of each busbar. For faults with a very short duration, depicted on the left part of the curves, S_{sc} is indeed correctly indicating that 1045 is the strongest bus with the least severe voltage deviations, followed by 1043 and 1041. However, as fault duration increases, changes are quickly

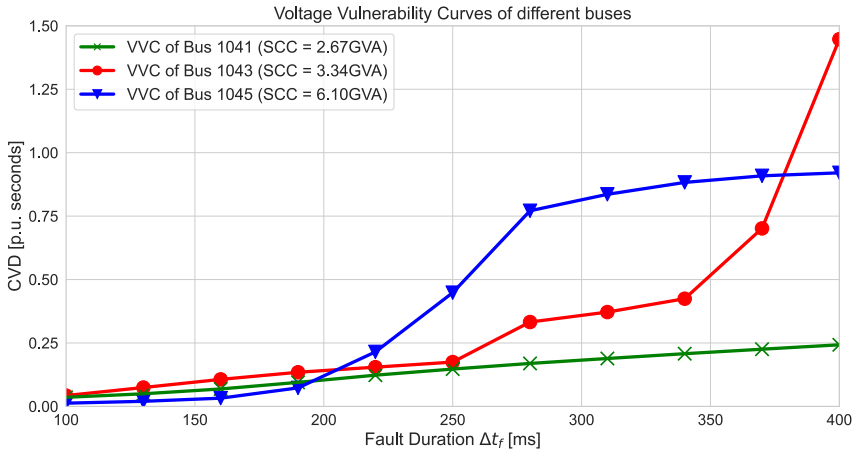


Figure 5.24.: Voltage Vulnerability Curves of buses 1041, 1043, and 1045 as per the model in Figure 5.22 and responses in Figure 5.23.

observed. From approximately $\Delta t_f = 200$ ms, bus 1045 (blue) begins to experience FIDVR events, and quickly becomes effectively the weakest bus. Meanwhile, bus 1043 (red) sees an increase in voltage deviations starting from 250 ms, as some of the LV-DER units begin to disconnect. Therefore, in the range of 200 to 350 ms fault duration, busbar 1045 is the weakest bus, while 1041 (green) is the strongest bus. This is completely opposite compared to what S_{sc} would indicate.

When fault duration increases further towards 400 ms, bus 1043 (red) begins to experience severe voltage deviations and oscillations. Therefore, its VVC quickly rises, reaching a CVD value of almost 1.5 pu-seconds. Therefore, in the >350 ms range, busbar 1043 (red) is the weakest bus, followed by 1045 (blue), and finally 1041 (green). Once again, S_{sc} would imply a completely different evaluation of system strength. In this sense, VVC is far superior in providing more extensive information about dynamic-state system strength and voltage sensitivity with modern distribution systems and their contribution to voltage dynamics.

The next section demonstrates how to incorporate parameter uncertainty into VVC analysis by utilizing an advanced interpolation method.

5.4.4. VVC WITH PARAMETER UNCERTAINTY

For the VVC analysis to be as informative as possible, dynamic DER and load models should be parameterized as accurately as possible to replicate the dynamics of the studied system well. This can be a difficult task, particularly for medium- and low-voltage grids where data availability and quality are limited. To tackle this challenge, the VVC method is expanded to consider parameter uncertainty as well.

As presented in Section 5.4.2, the interpolation technique is used to derive voltage vulnerability curves. So far in the analysis, it was assumed that all the parameters

are known, and simple linear interpolation was used. As parameter uncertainty may be an issue, an advanced interpolation method is hereby introduced. The interpolation is utilized in voltage vulnerability curves to tackle the parameter uncertainty challenges.

METHODOLOGY: LOCALLY WEIGHTED SCATTERPLOT SMOOTHING (LOWESS)

Locally Weighted Scatterplot Smoothing (LOWESS) is a statistical non-parametric regression method designed to combine multiple regression models in one based on the k -closest samples. It falls into the broader category of predictive analytics methods designed for extrapolation or interpolation of data, as well as local regressions for robustly fitting smoothing curves without prior assumptions about the curve shape. LOWESS fundamentally relies on classical methods such as linear and nonlinear least squares regressions. However, it differs from those methods as it uses only subsets of data for each weighted least squares fit. In other words, it combines the results of multiple local regressions over different regions of the data domain and combines them based on weightings linked to the distance between the prediction point and the data used to fit each of the local regressions.

Figure 5.25 illustrates the LOWESS concept [40, 41]. A regression is performed using a polynomial function on a local data subset centred around a particular point in the data series. The procedure is typically repeated multiple times to minimize or ignore the impact of outliers and obtain a more accurate result.

LOWESS: 1st-order weighted local regression key parameter: **fraction**

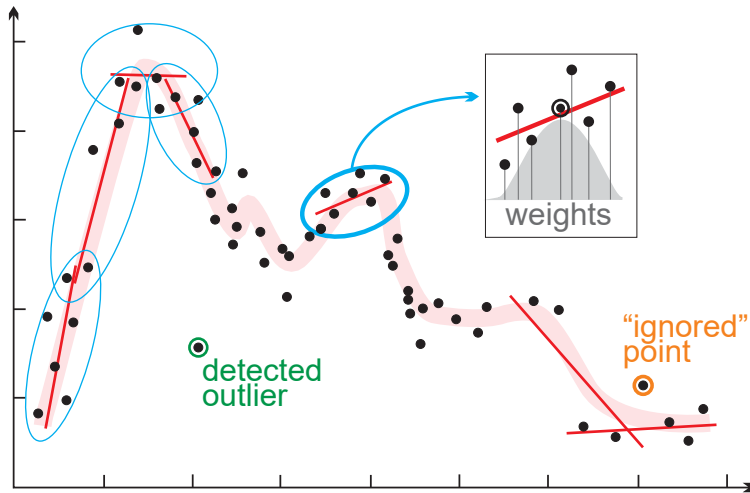


Figure 5.25.: Principles of LOWESS method for a 1st-order polynomial. Black points are the source data; red narrow lines are the local regression solutions; the thick rose line is a final LOWESS solution. The gray area on the sub-panel represents a weight-defining function.

LOWESS is a non-parametric regression method, which means no analytical response function will be produced by the algorithm. Instead, the predictor curve is completely data-driven, i.e. it is directly constructed according to the information derived from the data. It is therefore a very useful method for cases where the data does not closely follow any clear analytical pattern, such as with noisier and scattered data that exhibits a more complex relationship, and where the analytical response function is not suitable or necessary.

Further and more detailed discussions on the LOWESS algorithm, its applications, limitations, and parametrization are out of the scope of this thesis, and can be found in [40–42]. Once all the local regressions are derived using a moving localized regression approach, the final LOWESS curve is created, as depicted in the thick pink line as shown in Figure 5.25.

This final curve, however, only indicates the mean prediction value of the algorithm. To include uncertainty prediction intervals around it, MOE-Py implementation of the LOWESS method is utilized in Python [42]. This is hereby discussed further.

VVC INTERPOLATION WITH LOWESS

Voltage Vulnerability Curves (VVC), as introduced in Figure 5.16, are fundamentally data-driven curves. A series of scattered data points are derived from simulations, with a discrete fault time step between them. Therefore, to produce a continuous curve, an interpolation technique needs to be applied.

In the analysis so far, linear interpolation was used (e.g. see Figure 5.24). This is naturally an approximation and such interpolation is not able to consider parameter uncertainty. To expand on this, LOWESS interpolation is hereby utilized to enhance the VVC method. To demonstrate this, the system from Figure 5.4 is adjusted to incorporate dynamic loads in bus 1041 only. The D-type motors are used, which stall for larger fault duration and initiate FIDVR events.

Two parameters chosen to represent the uncertainty are the penetration of the D-type motor in the WECC composite load model (F_{md}) and the thermal time constant of the motors (T_{th}) which affects the stalling characteristics. These parameters are selected due to their large impact on FIDVR intensity, as found in Chapter 4, and similarly in [43, 44]. Furthermore, fault duration is increased in steps of 25 ms from 100 ms to 400 ms, with an additional small uncertainty band.

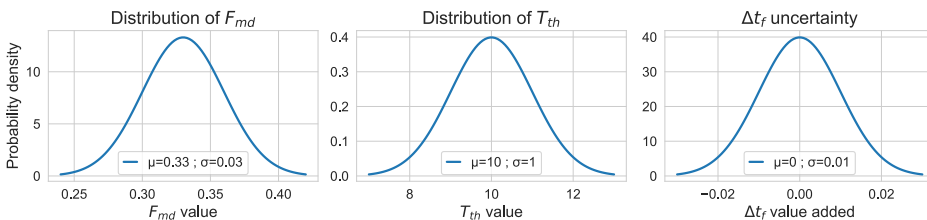


Figure 5.26.: Uncertainty modelling of the three selected parameters using a normal distribution with mean value (μ) and standard deviation (σ).

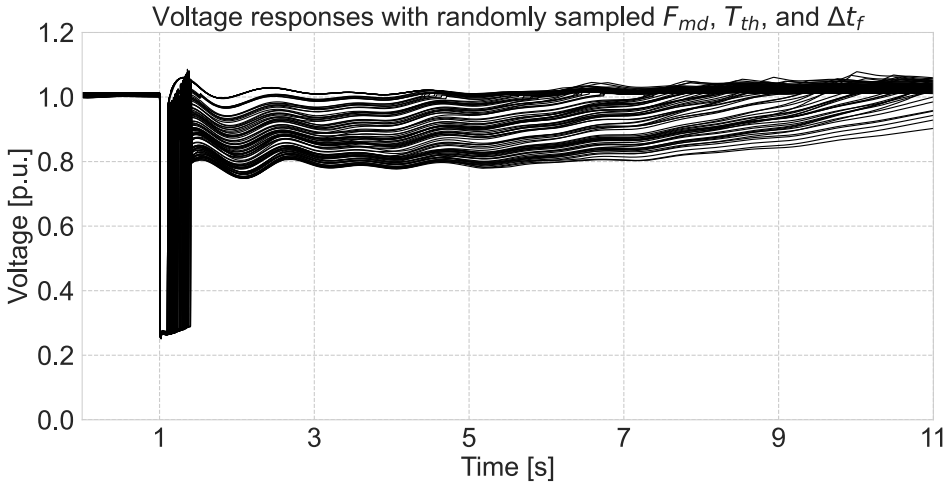


Figure 5.27.: Voltage responses of bus 1041 with considering parameter uncertainty.

5

The uncertainty of all three parameters is modelled by randomly sampling from a normal distribution in each simulation, as shown in Figure 5.26. There are, of course, many ways to model parameter uncertainty depending on the application and goal, which is beyond the scope of this work. Instead, the goal here is to demonstrate how uncertainty can be incorporated into the VVC methodology.

The resulting family of 90 curves showing voltage responses with parameter uncertainty are plotted in Figure 5.27. As seen from the figure, the wide parameter uncertainty reflects itself in a wide dispersion of voltage deviations with varying severity. In other words, the selected parameters and their wide range have a large impact on the voltage deviations of this busbar.

VVC curve is created based on the simulation results and plotted in Figure 5.28, relative to the static load scenario. The simulation results are shown in blue dots, based on their respective CVD and Δt_f values. Afterwards, the simulation results are used for regression and interpolation using the described LOWESS method. The mean value is plotted, alongside two prediction intervals to capture the uncertainty of the parameters and illustrate their impact on voltage vulnerability curves.

As seen from Figure 5.28, the results for <200 ms fault duration are very much in line with the linear static load curve. Hence, the bus strength is not influenced by the demand composition and its parameter uncertainty for shorter-duration faults. However, as fault duration increases, voltage deviations become more severe. Furthermore, the uncertainty intervals also widen, as indicated by the two shaded areas. This is expected, as more severe faults reveal the impact of parameters more strongly. The information provided by such a curve can help grid engineers to evaluate the dynamic-state system strength, and determine the risk of short-term instabilities for not just varying fault duration, but also for varying parameters of relevance considering their uncertainty.

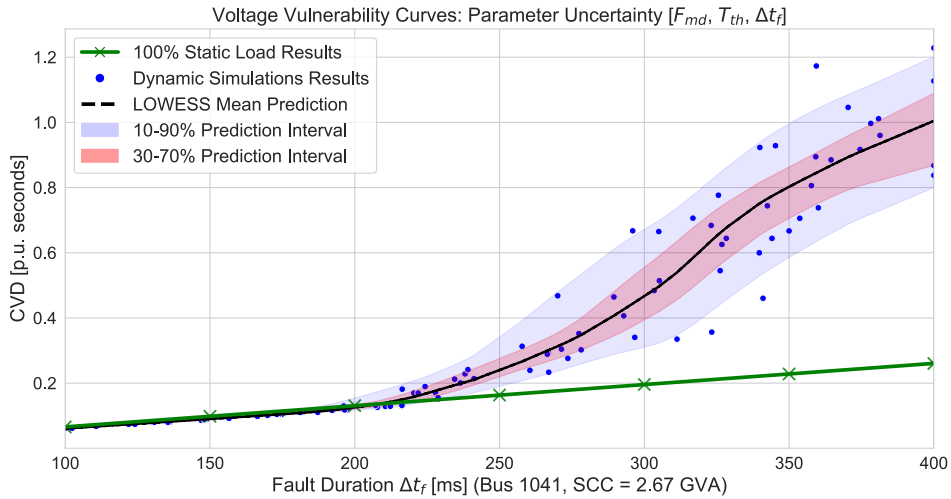


Figure 5.28.: VVC with parameter uncertainty by using the LOWESS method.

VOLTAGE VULNERABILITY CURVES: CONCLUDING REMARKS

To quantify the dynamic-state system strength of various buses, steady-state methods based on short-circuit capacity are shown to be insufficient in modern power systems. To tackle this limitation, the numerically-derived VVC method is proposed, as an extension of the previously introduced Cumulative Voltage Deviation (CVD) method. This subsection showcased that VVC is an efficient method to numerically quantify how severe a certain short-term system disturbance is, and whether it may lead to a high risk of cascading or any of the four types of short-term instability. The analysis is conducted on several exemplifying scenarios, where the benefits of the method are comprehensively demonstrated. Furthermore, the method is extended with an advanced interpolation approach for analyses with parameter uncertainty, which are reflected in prediction intervals.

The implementation of the method can be a part of the probabilistic dynamic stability/security assessment, with a focus on short-term instabilities and the risk of cascading events. In this way, grid operators can get advanced insights into not only static grid limitations but also dynamic system limits in terms of the likelihood of short-term instabilities. For each grid location of interest, a quantifiable steady-state system strength value (i.e. ESS, see [Chapter 3](#)) can be complemented by a respective VVC, representing a dynamic-state system strength quantification for the selected disturbances and parameters. The result is an automated vulnerability assessment across both steady- and dynamic-state operations, indicating which grid locations exhibit relative weakness and risk of instability. Once detected, such buses and operational scenarios can be explored further with detailed analysis and possible mitigation measures in a much more time-efficient manner.

5.5. CONCLUDING REMARKS

Existing grid vulnerability and stability evaluation approaches typically focus on key performance metrics of conventional systems, such as rotor angles and frequency of synchronous machines. However, as systems rapidly shift from synchronous to inverter-based generation, the dynamics will be dominantly driven by voltage- and control-related behaviour. With system strength reduced, such dynamics and voltage deviations will also become faster and more severe. Consequently, the importance of accurate voltage stability and system strength evaluation rises.

Furthermore, this and previous chapters show that the intricate challenges of modern power systems often transcend the possibilities of steady-state evaluation methods. The dynamic-state quantification therefore becomes a crucial task for evaluating grid vulnerability and maintaining the short-term stability and resilience of modern power systems.

This section presented the concurrent data-driven opportunities in modern power grids, enabled by the continuous increase in computational power and automation, as well as better grid observability with the usage of synchrophasors and wide-area systems. Three novel data-driven evaluation methods are developed and introduced in order to tackle the challenges of modern grids' stability and strength: quantification (CVD), classification, and dynamic strength evaluation (VVC). These are comprehensively introduced and tested, showing very good performance across a variety of complex dynamic phenomena in modern grids.

The methods are very suitable for probabilistic grid vulnerability as well as dynamic security and stability assessment. They can complement the existing conventional approaches by introducing risk-based voltage instability and system strength aspects, particularly useful in grids with high parameter and operational uncertainty. Ultimately, the goal is to provide grid operators with more advanced insights about their grid vulnerability and stability margins, both across steady- and dynamic-state operations. Weak grid areas and stability-constrained operating scenarios can be revealed in advance, providing time for more detailed studies and suitable mitigation measures. Finally, with the fast advancements of the WAMPAC technology, the methods can be used to improve both the grid dynamics observability and the decision-making process for advanced wide-area instability detection and mitigation techniques.

REFERENCES

- [1] M. Naglič. “On power system automation: Synchronised measurement technology supported power system situational awareness”. PhD thesis. Delft University of Technology, 2020. URL: <https://research.tudelft.nl/en/publications/on-power-system-automation-synchronised-measurement-technology-su>.
- [2] A. Sundararajan, T. Khan, A. Moghadasi, and A. I. Sarwat. “Survey on synchrophasor data quality and cybersecurity challenges, and evaluation of their interdependencies”. In: *Journal of Modern Power Systems and Clean Energy* 7.3 (May 2019), pp. 449–467. ISSN: 2196-5625. DOI: [10.1007/s40565-018-0473-6](https://doi.org/10.1007/s40565-018-0473-6).
- [3] F. R. Segundo Sevilla, Y. Liu, E. Barocio, P. Korba, M. Andrade, F. Bellizio, J. Bos, B. Chaudhuri, H. Chavez, J. Cremer, R. Eriksson, C. Hamon, M. Herrera, M. Huijsman, M. Ingram, D. Klaar, V. Krishnan, J. Mola, M. Netto, M. Paolone, P. Papadopoulos, M. Ramirez, J. Rueda, W. Sattinger, V. Terzija, S. Tindemans, A. Trigueros, Y. Wang, and J. Zhao. “State-of-the-art of data collection, analytics, and future needs of transmission utilities worldwide to account for the continuous growth of sensing data”. In: *International Journal of Electrical Power & Energy Systems* 137 (May 2022), p. 107772. ISSN: 01420615. DOI: [10.1016/j.ijepes.2021.107772](https://doi.org/10.1016/j.ijepes.2021.107772).
- [4] V. Terzija, G. Valverde, Deyu Cai, P. Regulski, V. Madani, J. Fitch, S. Skok, M. M. Begovic, and A. Phadke. “Wide-Area Monitoring, Protection, and Control of Future Electric Power Networks”. In: *Proceedings of the IEEE* 99.1 (Jan. 2011), pp. 80–93. ISSN: 0018-9219. DOI: [10.1109/JPROC.2010.2060450](https://doi.org/10.1109/JPROC.2010.2060450).
- [5] D. Novosel, V. Madani, B. Bhargava, Khoi Vu, and J. Cole. “Dawn of the grid synchronization: Benefits, Practical Applications, and Deployment Strategies for WAMPAC”. In: *IEEE Power and Energy Magazine* 6.1 (2008), pp. 49–60. ISSN: 1540-7977. DOI: [10.1109/MPAE.2008.4412940](https://doi.org/10.1109/MPAE.2008.4412940).
- [6] A. Phadke, H. Volskis, R. M. de Moraes, T. Bi, R. Nayak, Y. Sehgal, S. Sen, W. Sattinger, E. Martinez, O. Samuelsson, D. Novosel, V. Madani, and Y. A. Kulikov. “The Wide World of Wide-area Measurement”. In: *IEEE Power and Energy Magazine* 6.5 (Sept. 2008), pp. 52–65. ISSN: 1540-7977. DOI: [10.1109/MPE.2008.927476](https://doi.org/10.1109/MPE.2008.927476).
- [7] PES-TR 94. *Enabling Computing Techniques for Wide-Area Power System Applications*. Tech. rep. IEEE Power & Energy Society, Jan. 2022.
- [8] M. Popov, A. Boričić, N. Kumar, and et al. “Synchrophasor-based Applications to Enhance Electrical System Performance in the Netherlands”. In: *CIGRE*. Paris: CIGRE, Aug. 2022.
- [9] M. U. Usman and M. O. Faruque. “Applications of synchrophasor technologies in power systems”. In: *Journal of Modern Power Systems and Clean Energy* 7.2 (Mar. 2019), pp. 211–226. ISSN: 2196-5625. DOI: [10.1007/s40565-018-0455-8](https://doi.org/10.1007/s40565-018-0455-8).
- [10] VISOR Project SP Energy Networks. *VISOR: Visualisation of Real-Time System Dynamics using Enhanced Monitoring (Booklet)*. July 2016. URL: https://www.spenergynetworks.co.uk/userfiles/file/VISOR_Booklet_July_2016.pdf.
- [11] A. Boričić, J. L. R. Torres, and M. Popov. “Quantification and Classification of Short-term Instability Voltage Deviations”. In: *IEEE Transactions on Industry Applications* (2023), pp. 1–11. ISSN: 0093-9994. DOI: [10.1109/TIA.2023.3289931](https://doi.org/10.1109/TIA.2023.3289931).
- [12] A. Boricic, J. L. R. Torres, and M. Popov. “Quantifying the Severity of Short-term Instability Voltage Deviations”. In: *2022 International Conference on Smart Energy Systems and Technologies (SEST)*. IEEE, Sept. 2022, pp. 1–6. ISBN: 978-1-6654-0557-7. DOI: [10.1109/SEST53650.2022.9898503](https://doi.org/10.1109/SEST53650.2022.9898503).

- [13] A. Boričić, J. L. R. Torres, and M. Popov. “Comprehensive Review of Short-Term Voltage Stability Evaluation Methods in Modern Power Systems”. In: *Energies* 14.14 (July 2021), p. 4076. ISSN: 1996-1073. DOI: [10.3390/en14144076](https://doi.org/10.3390/en14144076).
- [14] IEEE PES-TR77. *Stability definitions and characterization of dynamic behavior in systems with high penetration of power electronic interfaced technologies*. Tech. rep. IEEE Power & Energy Society, May 2020. URL: https://resourcecenter.ieee-pes.org/publications/technical-reports/PES_TP_TR77_PSDP_STABILITY_051320.html.
- [15] T. Van Cutsem, M. Glavic, W. Rosehart, C. Canizares, M. Kanatas, L. Lima, F. Milano, L. Papangelis, R. A. Ramos, J. A. d. Santos, B. Tamimi, G. Taranto, and C. Vournas. “Test Systems for Voltage Stability Studies”. In: *IEEE Transactions on Power Systems* 35.5 (Sept. 2020), pp. 4078–4087. ISSN: 0885-8950. DOI: [10.1109/TPWRS.2020.2976834](https://doi.org/10.1109/TPWRS.2020.2976834).
- [16] A. Boričić, J. L. R. Torres, and M. Popov. “Fundamental study on the influence of dynamic load and distributed energy resources on power system short-term voltage stability”. In: *International Journal of Electrical Power & Energy Systems* 131 (Oct. 2021), p. 107141. ISSN: 01420615. DOI: [10.1016/j.ijepes.2021.107141](https://doi.org/10.1016/j.ijepes.2021.107141).
- [17] Y. Xu, Z. Y. Dong, K. Meng, W. F. Yao, R. Zhang, and K. P. Wong. “Multi-Objective Dynamic VAR Planning Against Short-Term Voltage Instability Using a Decomposition-Based Evolutionary Algorithm”. In: *IEEE Transactions on Power Systems* 29.6 (Nov. 2014), pp. 2813–2822. ISSN: 0885-8950. DOI: [10.1109/TPWRS.2014.2310733](https://doi.org/10.1109/TPWRS.2014.2310733).
- [18] CIGRE WG B4.62 671. *Connection of wind farms to weak AC networks*. Tech. rep. CIGRE, Dec. 2016.
- [19] D. Ramasubramanian, W. Wang, P. Pourbeik, E. Farantatos, A. Gaikwad, S. Soni, and V. Chadliev. “Positive sequence voltage source converter mathematical model for use in low short circuit systems”. In: *IET Generation, Transmission & Distribution* 14.1 (Jan. 2020), pp. 87–97. ISSN: 1751-8695. DOI: [10.1049/iet-gtd.2019.0346](https://doi.org/10.1049/iet-gtd.2019.0346).
- [20] D. Ramasubramanian, P. Pourbeik, E. Farantatos, and A. Gaikwad. “Simulation of 100% Inverter-Based Resource Grids With Positive Sequence Modeling”. In: *IEEE Electrification Magazine* 9.2 (June 2021), pp. 62–71. ISSN: 2325-5897. DOI: [10.1109/MELE.2021.3070938](https://doi.org/10.1109/MELE.2021.3070938).
- [21] Y. Cheng, L. Fan, J. Rose, S.-H. Huang, J. Schmall, X. Wang, X. Xie, J. Shair, J. R. Ramamurthy, N. Modi, C. Li, C. Wang, S. Shah, B. Pal, Z. Miao, A. Isaacs, J. Mahseredjian, and J. Zhou. “Real-World Subsynchronous Oscillation Events in Power Grids With High Penetrations of Inverter-Based Resources”. In: *IEEE Transactions on Power Systems* 38.1 (Jan. 2023), pp. 316–330. ISSN: 0885-8950. DOI: [10.1109/TPWRS.2022.3161418](https://doi.org/10.1109/TPWRS.2022.3161418).
- [22] B. Badrzadeh, Z. Emin, S. Goyal, and et al. “System Strength”. In: *CIGRE Science&Engineering Journal* 20 (2021).
- [23] M. Glavic and T. Van Cutsem. “A short survey of methods for voltage instability detection”. In: *2011 IEEE Power and Energy Society General Meeting*. IEEE, July 2011, pp. 1–8. ISBN: 978-1-4577-1000-1. DOI: [10.1109/PES.2011.6039311](https://doi.org/10.1109/PES.2011.6039311).
- [24] S. Pandey, A. K. Srivastava, and B. G. Amidan. “A Real Time Event Detection, Classification and Localization Using Synchrophasor Data”. In: *IEEE Transactions on Power Systems* 35.6 (Nov. 2020), pp. 4421–4431. ISSN: 0885-8950. DOI: [10.1109/TPWRS.2020.2986019](https://doi.org/10.1109/TPWRS.2020.2986019).
- [25] R. Igual and C. Medrano. “Research challenges in real-time classification of power quality disturbances applicable to microgrids: A systematic review”. In: *Renewable and Sustainable Energy Reviews* 132 (Oct. 2020), p. 110050. ISSN: 13640321. DOI: [10.1016/j.rser.2020.110050](https://doi.org/10.1016/j.rser.2020.110050).
- [26] M. Sun, I. Konstantelos, and G. Strbac. “A Deep Learning-Based Feature Extraction Framework for System Security Assessment”. In: *IEEE Transactions on Smart Grid* 10.5 (Sept. 2019), pp. 5007–5020. ISSN: 1949-3053. DOI: [10.1109/TSG.2018.2873001](https://doi.org/10.1109/TSG.2018.2873001).
- [27] A. Almunif and L. Fan. “PMU Measurements for Oscillation Monitoring: Connecting Prony Analysis with Observability”. In: *2019 IEEE Power & Energy Society General Meeting (PESGM)*. IEEE, Aug. 2019, pp. 1–5. ISBN: 978-1-7281-1981-6. DOI: [10.1109/PESGM40551.2019.8973910](https://doi.org/10.1109/PESGM40551.2019.8973910).

- [28] M. Golshani, D. Wilson, S. Norris, I. Cowan, M. H. Rahman, and B. Marshall. “Application of Phasor-based Functionality to HVDC Control in Reduced System Strength”. In: *The 17th International Conference on AC and DC Power Transmission (ACDC 2021)*. Institution of Engineering and Technology, 2021, pp. 44–49. ISBN: 978-1-83953-574-1. DOI: [10.1049/icp.2021.2442](https://doi.org/10.1049/icp.2021.2442).
- [29] J. D. Follum. *Detection of forced oscillations in power systems with multichannel methods*. Tech. rep. Richland, WA (United States): Pacific Northwest National Laboratory (PNNL), Sept. 2015. DOI: [10.2172/1222904](https://doi.org/10.2172/1222904).
- [30] D. P. Wadduwage and U. D. Annakkage. “Improving Matrix Pencil and Hankel Total Least Squares algorithms for identifying dominant oscillations in power systems”. In: *2015 IEEE 10th International Conference on Industrial and Information Systems (ICIIS)*. IEEE, Dec. 2015, pp. 13–18. ISBN: 978-1-5090-1741-6. DOI: [10.1109/ICIINFS.2015.7398978](https://doi.org/10.1109/ICIINFS.2015.7398978).
- [31] S. Halpin, R. Jones, and L. Taylor. “The MVA-Volt Index: A Screening Tool for Predicting Fault-Induced Low Voltage Problems on Bulk Transmission Systems”. In: *IEEE Transactions on Power Systems* 23.3 (Aug. 2008), pp. 1205–1210. ISSN: 0885-8950. DOI: [10.1109/TPWRS.2008.926405](https://doi.org/10.1109/TPWRS.2008.926405).
- [32] A. R. R. Matavalam and V. Ajarapu. “PMU-Based Monitoring and Mitigation of Delayed Voltage Recovery Using Admittances”. In: *IEEE Transactions on Power Systems* 34.6 (Nov. 2019), pp. 4451–4463. ISSN: 0885-8950. DOI: [10.1109/TPWRS.2019.2913742](https://doi.org/10.1109/TPWRS.2019.2913742).
- [33] J. W. T. J. W. Cooley. “An algorithm for the machine calculation of complex Fourier series”. In: *Math. Comput.* (1965).
- [34] P. Kundur. *Power System Stability & Control*. McGraw-Hill, 1994.
- [35] G. Rogers. *Power System Oscillations*. Boston, MA: Springer US, 2000. ISBN: 978-1-4613-7059-8. DOI: [10.1007/978-1-4615-4561-3](https://doi.org/10.1007/978-1-4615-4561-3).
- [36] M. Gibbard, P. Pourbeik, and D. Vowles. *Small-signal stability, control and dynamic performance of power systems*. University of Adelaide Press, July 2015. ISBN: 9781925261035. DOI: [10.20851/small-signal](https://doi.org/10.20851/small-signal).
- [37] Grandini M, Bagli E, and Visani G. *Metrics for Multi-Class Classification: an Overview*.
- [38] IEEE PES. *IEEE PES-TR19: Test Systems for Voltage Stability Analysis and Security Assessment*. Tech. rep. IEEE Power & Energy Society, Aug. 2015. URL: <https://resourcecenter.ieee-pes.org/publications/technical-reports/PESTR19.html>.
- [39] E. Hajipour, H. Saber, N. Farzin, M. R. Karimi, S. M. Hashemi, A. Agheli, H. Ayoubzadeh, and M. Ehsan. “An Improved Aggregated Model of Residential Air Conditioners for FIDVR Studies”. In: *IEEE Transactions on Power Systems* 35.2 (Mar. 2020), pp. 909–919. ISSN: 0885-8950. DOI: [10.1109/TPWRS.2019.2940596](https://doi.org/10.1109/TPWRS.2019.2940596).
- [40] W. S. Cleveland. “Robust Locally Weighted Regression and Smoothing Scatterplots”. In: *Journal of the American Statistical Association* 74.368 (Dec. 1979), pp. 829–836. ISSN: 0162-1459. DOI: [10.1080/01621459.1979.10481038](https://doi.org/10.1080/01621459.1979.10481038).
- [41] A. Derkacheva, J. Mouginot, R. Millan, N. Maier, and F. Gillet-Chaulet. “Data Reduction Using Statistical and Regression Approaches for Ice Velocity Derived by Landsat-8, Sentinel-1 and Sentinel-2”. In: *Remote Sensing* 12.12 (June 2020), p. 1935. ISSN: 2072-4292. DOI: [10.3390/rs12121935](https://doi.org/10.3390/rs12121935).
- [42] A. Bourn. *Merit-Order-Effect (MOE-Py) Python Library*. Mar. 2021. URL: <https://ayrtonb.github.io/Merit-Order-Effect>.
- [43] M.W. Tenza and S. Ghiocel. *An Analysis of the Sensitivity of WECC Grid Planning Models to Assumptions Regarding the Composition of Loads*. Tech. rep. Mitsubishi Electric Power Products, Nov. 2016. URL: <https://eta-publications.lbl.gov/sites/default/files/meppi-wecc-grid-planning-models-nov2016.pdf>.
- [44] S. Nuthalapati, ed. *Use of Voltage Stability Assessment and Transient Stability Assessment Tools in Grid Operations*. Springer International Publishing, 2021. ISBN: 978-3-030-67481-6. DOI: [10.1007/978-3-030-67482-3](https://doi.org/10.1007/978-3-030-67482-3).

6

CONCLUSIONS

Learning is the only thing the mind never exhausts, never fears, and never regrets.

- Leonardo da Vinci, Renaissance polymath (1452 - 1519)

This thesis explores the evolution of power systems and the technical challenges that arise. In this context, the main focus is on the aspects of grid vulnerability, stability, and strength. The impacts of IBR proliferation on voltage stability are analyzed, particularly in short-term aspects. Additionally, the multifaceted concept of system strength is explored, and new evaluation methods for modern grids are developed. Moreover, the dynamic aspects of a modern system's response to disturbances are extensively investigated. Finally, advanced data-driven methods are developed for the dynamic response evaluation and probabilistic vulnerability assessment. This final chapter comprises key scientific contributions, practical recommendations, and future research suggestions.

6.1. SCIENTIFIC CONTRIBUTIONS

The thesis is structured around five main research questions and objectives, introduced in [Chapter 1](#). Each research question is extensively explored in its corresponding chapter. The conclusions and scientific contributions are hereby summarized.

1. ***How does the energy transition lead to a higher vulnerability of electric power systems? What are the possible consequences?*** ([Chapter 1](#))
2. ***Why is securing voltage stability (particularly short-term) a progressively more critical and challenging task in modern power systems? Why are the existing evaluation methods insufficient?*** ([Chapter 2](#))
3. ***How should system strength be understood and evaluated in modern power systems, and how does it relate to vulnerability and stability?*** ([Chapter 3](#))
4. ***What kind of effects do dynamic loads and distributed generation have on the short-term stability and resilience of modern power systems?*** ([Chapter 4](#))
5. ***How can novel data- and simulation-driven approaches and methods help in alleviating the challenges highlighted in this thesis?*** ([Chapter 5](#))

1. ***How does the energy transition lead to a higher vulnerability of electric power systems? What are the possible consequences? (Chapter 1)***

Humanity has indisputable evidence that our current way of living, if left unchanged, leads to a climate catastrophe with far-reaching and largely irreversible consequences. The only feasible way forward is to combat climate change at its very source: to globally reduce our emission of greenhouse gases.

As one of the largest pollutants, the energy sector needs to dramatically evolve. This ongoing process is often referred to as the energy transition. The most viable path towards decarbonization is twofold. On one side, the electricity supply needs to shift from conventional fossil-based to renewable wind and solar power. On the other side, consumption needs to be electrified to a high degree so it can utilize clean carbon-free electricity and significantly reduce the usage of fossil fuels across sectors.

Both directions strongly impact electric power systems. On the supply side, the conventional dominantly fossil-based generation is increasingly phased out and replaced by the power-electronics interfaced renewables. On the demand side, the need for stable and reliable electricity is ever-growing, with rapid electrification of various energy-heavy sectors such as transportation, heating/cooling, and industry.

This revolution also inevitably changes the very fundamentals of system resilience, often resulting in higher vulnerability and higher susceptibility to instabilities. The higher vulnerability has two central technical causes. Firstly, as fossil fuels are being decommissioned, so are the majority of synchronous generators in conventional power plants. Synchronous generators are the backbone of the power system as we know it, providing stable frequency and voltage. Besides this, they also provide significant resilience to disturbances in the form of inertia and system strength. The energy transition therefore inevitably leads to fewer such generators. This results in a natural drop in resilience, which reflects itself in higher vulnerability to cascading faults, more severe and faster grid dynamics, and emphasized stability challenges.

The electricity sector is evolving, with synchronous fossil-fuel generation being replaced by inverter-based renewables. Furthermore, the demand becomes increasingly electrified, impacting grid dynamics. The combined effect is elevated vulnerability and more complex instability phenomena, threatening the resilience of modern power systems.

Secondly, synchronous generators are replaced by a very large number of renewable energy sources, also known as inverter-based resources (IBRs). Not only that IBRs exhibit fundamentally different dynamic performance, but are also often integrated in remote (weak) grid sections or scattered across largely unobservable and uncontrollable distribution systems. Since most IBRs require a strong grid connection, particularly in terms of voltage resilience, this results in a higher probability of maloperation, especially during and after large disturbances. The consequences are undesired IBR behavior which may lead to more severe dynamics, oscillations, or even widespread disconnections and cascading events. These effects are emphasized as more IBRs enter the system while phasing out synchronous generation.

The consequences of these vulnerability trends are far-reaching. Power system dynamics and stability become not only physics-based, but increasingly control-based, where resilience is not a given, but must be actively provided. This results in the acceleration of system dynamics, leaving less time for remedial protection and control actions. Furthermore, the complexity of dynamics also increases, shifting from dominantly electromechanical to electromagnetic. Similar trends are seen in terms of system stability, which becomes harder to maintain and guarantee. The mechanisms behind instabilities become more intricate, faster, amplified, and often intertwined with each other, having both electromechanical and electromagnetic dimensions.

Overall, it can be concluded that power systems are indeed becoming more vulnerable and more prone to instabilities. This thesis particularly explores the key challenges that the energy transition and consequent power system evolution bring in terms of voltage stability deterioration and system strength reduction. These two challenges are expected to be major bottlenecks for the widespread proliferation of renewable energy on a larger scale. As reaching climate goals directly depends on a successful energy transition and electricity supply decarbonization, these bottlenecks need to be mitigated.

2. Why is securing voltage stability (particularly short-term) a progressively more critical and challenging task in modern power systems? Why are the existing evaluation methods insufficient? (Chapter 2)

In conventional power systems, stability has been closely related to the operation of synchronous generators (SGs). By their very design and fundamental physics behind it, generators provide high robustness to both the frequency and voltage of the grid. In conventional systems, events that would cause instability were largely related to severe disturbances and the loss of synchronism amongst the SGs (or groups of SGs). Alternatively, voltage collapses would occasionally arise in cases of very high active power transfers and insufficient or suboptimally-placed reactive power support.

In modern power systems, with far less robustness provided by SGs, the situation drastically changes. The conventional types of system instability remain relevant but are often amplified and accelerated due to the lower inertia and lower system strength. This thesis largely focuses on the latter and its important effect on voltage stability and other types of short-term instabilities.

As IBRs replace SGs, voltage vulnerability and stability become key aspects of grid resilience. Unlike SGs, IBRs are more voltage-sensitive and often require resilient voltage at their connection point. As grid resilience reduces, voltage disturbances are not only amplified but also accelerated, stressing the importance of short-term dynamics.

The rapid proliferation of inverter-based generation (IBR) inevitably changes the way power system instability manifests itself. This is illustrated by the most recent classification of stability, which introduces two new types of stability (i.e., resonance and converter-driven stability) to account for the newly observed dynamics in the system. Another effect that the new classification does not show explicitly is the rising interrelation between different types of instability. An example of these intertwined effects studied in this thesis is the close connection between some types of voltage instability and

converter-driven instability. The way IBR converters operate in a steady and dynamic state directly relates to the voltage stability of the grid. On the other hand, the measures of voltage stability resilience, such as short-circuit capacity and system strength, directly relate back to the higher risk of converter-driven instability. In its essence, system stability largely becomes a joint problem of both the inherent physical response of the system and the imposed control of renewable sources. As more renewable IBRs are connected to the grid, replacing synchronous generation, dynamics are accelerated and more severe, often described by an important voltage-related dimension.

These changes are particularly seen in the way system instabilities manifest themselves, which is explored in this thesis extensively. Two major trends dictate this: the proliferation of IBRs and their connection in remote and relatively weaker grid sections, subject to weather conditions and land availability. This thesis provides insight into how these two effects relate to maximum power transfer and voltage stability. Furthermore, it is shown that the very understanding of short-term instabilities, particularly related to voltage, requires an update. The conventional methods developed to evaluate short-term voltage stability are shown to be largely outdated and often not suited to deal with amplified and accelerated dynamics and intricacies of IBR-dominated grids.

3. *How should system strength be understood and evaluated in modern power systems, and how does it relate to vulnerability and stability?* (Chapter 3)

6

As systems evolve, so should our understanding of system strength and grid weakness. For conventional power systems, system strength and short-circuit capacity were almost interchangeable terms. Thanks to their direct and strong electromagnetic coupling to the grid, synchronous generators intrinsically provide almost instantaneous and high reactive current support proportional to the size of the disturbance. This is very convenient for secure grid design and operation, as these high currents are not only suitable for fault recognition and consequent protection coordination but also support voltage resilience and recovery. By evaluating short-circuit capacity (or grid impedance) with relatively straightforward calculations, system operators were able to easily and rapidly evaluate grid resilience in terms of voltage stability, protection reliability, and power quality. Any change in the system, operational or expansional, would be easily quantifiable by simple and very intuitive metrics such as the Short-Circuit Ratio (SCR). In other words, system strength was simple and abundant.

In modern power systems, however, inverter-based generation progressively replaces synchronous generation. This increasingly invalidates the fundamental interchangeability of short-circuit capacity and system strength for several reasons. Firstly, IBRs are not directly coupled to the grid, but are, as their name implies, interfaced through power-electronics converters. This is necessary as the electricity produced by renewables is not suitable for the grid as is, both in terms of frequency and voltage characteristics. The converters, therefore, play an important role in transforming these variables so that synchronization and efficient power exchange with the grid are achieved. However, the converters effectively "break" the direct electromagnetic coupling between the renewable energy source and the grid. Hence, the inherent voltage resilience such as the one offered by synchronous generators is simply not present.

Secondly, the converters in IBRs are designed using power electronics made from semi-conducting materials. While this provides very good and fast controllability of operation, such materials are not able to withstand large and long-lasting overloads. In other words, unless the converters get significantly oversized (which would be economically inefficient), inverter-based resources are unable to provide high fault currents during and after disturbances. Instead, their controls must be utilized to limit the current output during disturbances to protect the converter itself from overheating. This is fundamentally different from synchronous generators which provide (reactive) current support almost instantaneously, with values up to several times higher than the nominal current. Therefore, the operation of IBRs can be very different in steady- and dynamic-state aspects.

System strength is a complex umbrella term¹. In conventional power systems, it can be easily evaluated by simple metrics such as SCR. However, in modern power systems, such an approach becomes increasingly inaccurate due to the way IBRs are integrated and operated in a grid. As system strength directly affects susceptibility to various types of voltage-related instabilities, understanding its intricate dimensions and accurately evaluating them is crucial for the vulnerability assessment of modern power systems.

To evaluate the system strength of modern power systems, the conventional approach of utilizing short-circuit capacity and related metrics is often far from sufficient. To improve the evaluation, the first question must be which of the three effects is being studied; (short-term) voltage stability and resilience, protection reliability, or power quality. The second question that should follow is whether the static or dynamic operation is of interest. Without providing this context, the system strength evaluation of a modern grid is set to fall short even before it begins.

This thesis largely focuses on the voltage stability and resilience aspects of system strength, across both steady and dynamic states. To evaluate the steady-state system strength and voltage stability margin of modern power systems, it is shown that common metrics such as SCR are often oversimplified quantification measures that ignore several important aspects of voltage resilience. A novel analytical method is designed to overcome these limitations, termed Excess System Strength. The method relies on rigorous fundamental analysis of maximum power transfer with IBRs to determine the effective strength of the analyzed point in the grid. In this process, the grid resistance and operating voltage are not neglected, and capacitors and loads are also taken into account. The method is tested extensively, showing significant improvement in pinpointing steady-state system strength margins and conditions that lead to voltage collapse.

Nevertheless, it is important to recognize that even the newly introduced and improved method is only applicable to one dimension of system strength, i.e. steady-state operation. To evaluate dynamic-state system strength, deterministic analytical models quickly reach their limits due to the complexity and non-linearity of IBR and dynamic load (control) parameters during and after disturbances. This makes the task of defining simple and accurate quantification metrics of dynamic-state system strength very challenging. In this thesis, this task is tackled from a very different data-driven perspective, which is discussed in the last two chapters.

¹See definition and discussion in [Chapter 3](#).

4. *What kind of effects do dynamic loads and distributed generation have on the short-term stability and voltage resilience of modern power systems? (Chapter 4)*

While large-scale inverter-based resources get a lot of attention in academia and industry in terms of their grid impact, a relatively under-researched area is the (combined) impact of smaller distributed energy resources (DERs). Naturally, a small number of such units will only have limited and local impacts; however, as their number increases significantly, their impact on the bulk power system rises accordingly. Furthermore, with the ongoing demand electrification, the overall impact of active distribution systems comprising both DERs and dynamic loads becomes crucial to understand and evaluate. This thesis presents a comprehensive and fundamental study of the individual and joint effects of DERs and dynamic loads on short-term instability and voltage resilience. A large test grid enhanced with advanced dynamic load and DER models has been utilized to automatically perform thousands of dynamic simulations and uncover these effects.

The main findings can be summarized in three broad points. Firstly, the rising electrification of consumption will inevitably lead to a larger presence of dynamic loads, such as motors and converter-interfaced loads. This has a significant impact on short-term stability, as more complex and amplified dynamics begin to appear in medium- and low-voltage grids. The load is therefore transitioning from dominantly passive to dynamically (very) active, often significantly contributing to system dynamics. This is explored extensively, showing that an increase in the share of dynamic loads leads to more severe voltage deviations and higher risks of short-term instability. Furthermore, a different composition of the dynamic load is also shown to differently affect the risk of instability. Motor loads that provide more (less) inertia and system strength contribute less (more) to short-term instability. Additionally, stalling-prone motors negatively affect short-term stability as the risks of fault-induced delayed voltage recovery rise.

Dynamic loads and DERs affect grid dynamics and short-term instability proportionally to their relative presence. Since their proliferation is expected to rise, system impacts are expected to progressively become more significant, and thus important to consider. While dynamic loads mostly bring negative effects, DERs can either worsen or improve the short-term stability of a grid, depending on their control strategies defined by grid codes.

Secondly, the proliferation of DERs across medium- and low-voltage grids also plays a large role in short-term grid stability. An extensive set of simulations is performed utilizing advanced DER models to uncover these effects. The results show that the increasing penetration of DERs in distribution systems could have either positive or negative effects on short-term stability and voltage resilience. The key factor that determines this is the applied control strategy. If DERs are operated in such a manner as to support the grid as much as possible during- and post-disturbances, for instance by supplying active or reactive current support, short-term stability can be effectively improved. In contrast, if DER units massively disconnect or temporarily seize their operation during or after disturbances, this can effectively amplify the disturbance and result in widespread voltage deviations. This consequently leads to reduced voltage resilience and higher risks of short-term instabilities. Another interesting observation from simulations is that the

DER disconnection has a higher negative effect on stability relative to the positive effect of grid-supporting DERs. In other words, the consequences of widespread disconnection of DERs may be difficult to counter with controlled post-disturbance system support. This emphasizes the need for suitable and strict grid codes for DER operation during and after disturbances in modern power systems, especially as their number and relative share (and thus impact) in systems rise.

Lastly, not only voltage but also frequency may become affected by the aggregated response of many DERs. The effect known as voltage dip-induced frequency excursion is likely to become more prevalent as the relative impact of aggregated DER response increases. This poses a risk of cascading, as one event may initiate another one, emphasizing the risks of intertwined instability events. Such developments, unless mitigated by suitable actions, may significantly increase the risks of widespread blackouts.

5. *How can novel data- and simulation-driven approaches and methods help in alleviating the challenges highlighted in this thesis? (Chapter 5)*

As synchronous generators are phased out, power systems inevitably become weaker. Disturbances will therefore result in intensified and faster voltage deviations. Such deviations are more likely to overshoot safe voltage stability thresholds in the system during and after disturbances, particularly in the shorter-term time scale. Since the system operators already face time constraints in reacting to fast system dynamics, the resulting impact on system vulnerability can be severe.

Deterministic and detailed stability evaluation methods are a powerful and indispensable part of the power system engineer's toolbox. However, as the energy transition progresses, and the size and complexity of power systems ever increase with the trends described in this thesis, utilizing this tool turns into a very time- and knowledge-demanding task. The question begins to arise of how to better prioritize stability and vulnerability analyses in terms of not only grid section but also operational conditions and control parameters, often accompanied by a dose of uncertainty. This is particularly challenging for dynamic analyses, where deterministic analytical approaches face the increasing complexity of grid response which becomes extremely difficult to evaluate without conducting complex and time-consuming dynamic simulations.

Nevertheless, two promising and enabling technological trends occur concurrently. The widespread usage of PMUs improves system observability and provides large data sets that can be utilized for observing and evaluating system resilience in real-time. This also opens possibilities for Wide-Area Monitoring, Protection, and Control (WAMPAC) applications to preserve system resilience and automatically steer the system away from instabilities. Furthermore, automation of power system analysis with programming and scripting approaches is enabled by the advances in modern power system simulation software and programming language interfaces. These two developments enable more advanced and data-driven approaches in power systems.

To tackle some of the short-term stability and dynamic-state system strength challenges, this thesis proposes a few advanced stochastic data- and risk-based methods.

Deterministic stability and strength evaluation methods often fail to consider complex interactions in modern power systems during and after disturbances. These aspects, therefore, remain hidden, and a grid may seem resilient in steady-state but exhibit high dynamic-state weakness and vulnerability. The developed data-driven methods, enabled by advancements in computing power and grid monitoring, provide dynamic grid resilience information in terms of probabilistic security and vulnerability assessments.

Firstly, to efficiently quantify voltage deviations automatically, a novel data-based approach termed the Cumulative Voltage Deviation (CVD) method is proposed. The CVD method is designed to utilize either PMU measurement or data provided by numerous automated simulations and quantify the severity of the voltage disturbance. Such non-binary information can be used to efficiently screen for dangerous and weak grid states which may lead to cascading, short-term instabilities, and voltage instabilities.

Furthermore, as system dynamics become more complex, it is often necessary to not only quantify their severity and the risk they pose to stability but to also classify the type of event taking place. As different instability mechanisms may require different mitigation actions, knowing the type of event taking place may help in designing and performing suitable control mitigation actions. The classification algorithm which relies on voltage trajectory is hereby derived, designed to determine the type of short-term instability event taking place. The algorithm is tested extensively and shown to perform with high classification accuracy.

Finally, the CVD method is utilized further to derive a novel dynamic-state system strength evaluation method termed Voltage Vulnerability Curves (VVC). The method relies on automated dynamic simulations of increasing severity to determine consequent voltage deviations and risk of instabilities. This provides information that analytical methods discussed in steady-state system strength evaluation cannot provide, considering the complex and discrete nature of system operation with many dynamic loads, IBRs, and DERs. Therefore, VVCs provide another dimension of system resilience and vulnerability evaluation, specifically targeted at the increasingly relevant intricate dynamics of modern power systems and their impact on system strength and stability.

The three methods are designed to be used in automatic and probabilistic offline or online dynamic stability and security analysis, cutting through the complexity of modern power systems with a high proliferation of IBRs, DERs, and dynamic loads. By utilizing such data-driven methods jointly, system operators can obtain more information about the operating scenarios and grid locations that exhibit elevated vulnerability. This can be followed by a more detailed and targeted analysis, resulting in suitable mitigation measures to minimize the risks of related instabilities. In this way, the dynamic security analysis of the system could become more time-efficient, while also providing deeper insights into the vulnerability level and the stability risks the system may be facing.

6.2. PRACTICAL RECOMMENDATIONS

Based on the results and insights of this thesis, several practical recommendations for system operation and planning are provided in order to cope with the rising complexity and vulnerability of power systems going forward.

- *Evolving power systems require evolving stability understanding and evaluation.*

As more IBRs are integrated into the grid, replacing synchronous generation, the conventional understanding and evaluation of system stability partly lose their significance. It is therefore crucial to update the concepts and methods so that the evolving dynamics and stability effects are accurately captured. This is particularly relevant for the topic of voltage stability and other short-term stability mechanisms which are rapidly evolving, as discussed in this thesis.

- *Advanced voltage stability and system strength evaluations shall become critical for securing the stable operation of modern power systems. Such evaluations should be an integral part of dynamic stability and security assessment.*

While the current dynamic security and stability evaluation often focuses on frequency and rotor-angle instability analysis, those two aspects are likely going to be overshadowed by voltage stability concerns in IBR-rich grids. As synchronous machines are phased out, grid strength will decrease, and reactive power support will become more scarce. Concurrently, IBRs often require precisely this to be able to operate in a stable manner. As these trends continue, voltage-related instabilities will become faster and more prevalent, stressing the importance of advanced and accurate evaluation.

- *Short-circuit capacity as a system strength metric becomes increasingly inaccurate. As more IBRs replace SGs, using more advanced methods becomes inevitable.*

Short-circuit capacity was inherently related to conventional power systems and synchronous generators. With a high share of inverter-based generation, system strength has multiple dimensions. It is necessary to keep in mind which aspect of system strength is being studied, and in what time frame. Hence, a question should be asked whether the focus is to analyze voltage resilience, protection coordination, or power quality, and whether the steady or dynamic state operation is of interest. Only after this can the right evaluation method be selected. This thesis extensively explored the voltage resilience aspect, across both steady and dynamic states, and proposed novel and more accurate methods for their evaluation in modern power systems with a high share of IBRs.

- *While related, voltage instability and converter-driven instability are fundamentally distinct mechanisms with a different relation to system strength. They should be understood and treated with this in mind.*

The voltage stability limit corresponds to the maximum power transfer limit over a certain grid corridor. These limits are joined and quantified by (steady-state) system strength evaluation. On the other hand, converter-driven instability occurs due to the control instability of converters or their interactions with each other. While this becomes

more likely in weaker grids due to the higher voltage sensitivity, the control parameters of converters are the real culprits in the converter-driven instability phenomenon.

Therefore, unlike with voltage instability, mitigating converter-driven instability should initially not be a question of strengthening the grid, but of designing and (re)tuning the controls for stable operation in the given system strength conditions.

These fundamental differences should be also kept in mind when evaluating the likelihood of either of the two instability mechanisms occurring.

- *Insufficient system strength is on a path to becoming one of the key bottlenecks for stable and secure operation of renewable-rich power systems. Timely planning for this challenge is crucial.*

As synchronous generators, the main sources of system strength, are phased out, system strength and resilience drop. Most IBRs dominantly rely on strong grids for stable operation, which means more grid sections will inevitably reach their voltage stability limits. Since system strength, unlike inertia, is provided locally, the lack of it becomes a major challenge for the high decarbonization of the electricity supply. Grid planners should prepare for this challenge accordingly and proactively explore the optimal ways for grid strengthening amid the further integration of renewables.

- *Ensuring sufficient steady- and dynamic-state system strength may require very different thinking and approaches.*

In steady-state operation, main grid strengthening approaches involve grid reinforcements to reduce the grid impedance. In other words, more parallel lines, transformers, meshed grid topologies, and (fossil-free) synchronous generators. Besides this, synchronous condensers are another effective approach as they can replace the role of synchronous generators in terms of voltage resilience. Care is advised as synchronous condensers can introduce new oscillation modes and possible risks of rotor angle instability. Furthermore, stability and vulnerability risks arise in case of their (un)scheduled outages since their redundancy is typically very costly to provide.

On the other hand, dynamic-state system strength is improved by means of (fast) dynamic voltage support during and after disturbances. Besides synchronous condensers, Flexible AC Transmission System (FACTS) devices and batteries may provide rapid and necessary reactive power support to aid voltage recovery. With the further weakening of the grid, such devices may also need to opt for advanced weak grid operation controls of grid-following and grid-forming types to be able to effectively support the grid.

- *When studying (voltage) stability and resilience of a modern power system, advanced load and DER models are vital.*

Stability analysis of large-scale grids is often performed with simplistic load models. While this may have been sufficiently accurate in conventional power grids where inertia and system strength were abundant, modern grids experience relatively higher vulnerability. Meanwhile, loads are becoming more complex as various energy-intensive sectors are electrified. Therefore, it becomes very important to accurately model (dynamic) loads so that their effects on stability are taken into account during analyses.

Furthermore, simple modelling of DERs during large-grid studies, for instance as negative loads, is unable to capture the intricacies of DER dynamics during and after disturbances. As DERs become widespread in distribution grids, their controls and aggregated impact on grid stability and resilience are shown to be very important to consider. Hence, the utilized models should reflect the static and dynamic characteristics of DERs as accurately as possible.

Advanced aggregated dynamic load and DER models are available and are continuously improved, as discussed in this thesis. These should be increasingly utilized and carefully parameterized for large-grid studies, particularly in terms of voltage stability analysis where distribution grids and their interactions with the bulk power system play a major role.

- *If a grid section has a high share of dynamic load and DER, it should likely receive more attention in terms of short-term and voltage stability studies.*

Simply stated, more complexity yields more chances of things going wrong. Interactions between dynamic loads and DERs play an important role in short-term and voltage stability studies. This cannot be easily evaluated without dynamic time-domain simulations, as steady-state methods are generally unable to capture the dynamic effects of relevance. Furthermore, if the grid itself is already weak, dynamics originating from loads and DERs may aggravate the situation further during and after disturbances.

- *Grid codes should ensure that the combined effect of DERs contributes to the improvement, not worsening, of voltage stability and resilience.*

This can be achieved by designing and enforcing firm low- and high-voltage ride-through characteristics with strict requirements for voltage support during and after disturbances. Careful outline of such grid codes should also take into consideration their effect on protection coordination, to avoid any potential reduction of protection reliability and selectivity in distribution grids.

- *Meten is weten². System dynamics are becoming faster and more severe. Without synchronized wide-area measurements, system operators are "driving" a vulnerable system with a foggy windshield. Avoiding a crash (blackout) becomes harder.*

Power system observability has long relied on Supervisory Control and Data Acquisition (SCADA). However, as synchronous machines are phased out, dynamics are accelerated and are often impossible to capture with slow and unsynchronized SCADA measurements. This is where synchrophasors, with their high sampling frequency of synchronized measurements, offer essential observability for secure system operation. Furthermore, as discussed in the thesis, synchrophasors enable a whole new range of wide-area control and protection applications for improving the resilience of modern power systems. Without synchrophasors, system observability and controllability are set to significantly decrease over the course of the energy transition. Hence, investing in such monitoring equipment now is essential so that suitable WAMPAC applications are developed and ready when the systems will need them the most.

²Dutch proverb that translates to *measuring is knowing*.

- *In light of increasing complexity, system operators should further embrace data-driven stochastic approaches for probabilistic vulnerability and security assessment.*

Deterministic analytical approaches are powerful when the dynamic process is driven by the fundamental physics of electrical machines and equipment. However, as grids become increasingly dominated by numerous control-driven power electronics, the discrete nature of their response and high uncertainty due to their sheer number and parameter count often invalidates deterministic analytical methods.

Meanwhile, the discussed trends of synchrophasor observability and simulation automation can provide enormous amounts of data. Paired with carefully designed stochastic risk-based methods, data-driven approaches can provide an automatic reduction of the order of the problem magnitude. This creates possibilities to cut through the complexity noise and pinpoint the key grid sections and operating scenarios that pose elevated risks to grid stability. These can then be analyzed in detail by experienced grid stability and dynamics experts in a much more time-efficient manner.

6.3. FUTURE RESEARCH RECOMMENDATIONS

- *Grid-forming IBRs and their impact on system strength.*

An observant and knowledgeable reader may notice that this thesis deals with IBRs in general, occasionally focusing on grid-following IBRs in particular. This is intentional, as almost all IBRs in the grids now and in the near future are of this type. Nevertheless, grid-forming control is a promising approach for addressing some challenges of future grids, especially by allowing IBRs to operate in weaker grids. However, grid-forming converters are still evolving. Furthermore, they have inherent power electronics limitations in (fault) current support. This affects their dynamic-state system strength capabilities. Therefore, grid-forming is certainly not the panacea for all strength-related issues. Instead, only some of the discussed challenges are likely to be diminished. How and to what extent can various grid-forming control strategies help to alleviate system weakness challenges is yet to be fully uncovered, and is an important future research path.

- *Optimal selection and placement of grid-strengthening equipment to mitigate low system strength challenges.*

This thesis deals with vulnerability assessment, an important step in evaluating the grid sections and operating scenarios that exhibit weakness and a higher likelihood of instabilities. Nevertheless, following such an assessment, the optimal way to mitigate the uncovered issues likely deserves a thesis of its own. With various grid-strengthening equipment appearing in the market (synchronous condensers, batteries, E-STATCOMS, other grid-forming FACTS devices, and a combination of these), a complex choice needs to be made in selection, sizing, and location of such equipment considering not only technical but also financial and societal aspects. This is an important future work topic that directly follows up on the research presented in this thesis.

- *Operation of large systems with near-100%-IBR generation considering very low inertia and system strength challenges.*

For countries with limited hydro and nuclear generation, continuous system operation close to 100%-IBR will soon become a reality. Research should therefore uncover the expected challenges in such a system, and the measures that should be taken so that the system resilience remains on a sufficiently high level. While such systems are inherently less resilient and weaker, the other side of that coin is that they are also more controllable. Hence, utilizing advanced measurements and designing cutting-edge controls is crucial for maintaining the stable operation of future power systems.

- *Possibilities for system strength and inertia provision as market services.*

Unlike in conventional power systems, inertia and system strength are not abundant in modern power systems but must be actively provided instead. While some market pilots exist, the topic grows in importance as resilience becomes more scarce. Finding the optimal ways to design such ancillary market services is hence an important research task. Moreover, the location where such services are to be provided plays a crucial role, as system strength but also inertia exhibit increasingly localized characteristics.

- *Impact of reduced system strength on protection coordination and power quality.*

System strength is a complex concept that affects several aspects of power systems. While system stability and resilience are the focus of this thesis, protection coordination and power quality are also expected to become more challenging as the energy transition continues. To maintain reliable and selective protection operations, novel algorithms need to be developed, able to operate regardless of low and non-conventional fault currents. Furthermore, susceptibility to power quality issues increases in weaker grids, requiring research on more advanced evaluation and mitigation measures. These are important future work directions that were not directly tackled in this thesis.

- *Further utilization of WAMS and development of advanced WAMPAC methods for ensuring stable system operation.*

With the accelerated system dynamics, lower grid resilience, and rising system complexity, it becomes clear that advanced and faster monitoring is an absolute necessity. However, the utilization of such measurements in advanced wide-area control and protection algorithms is in its early stage, with a massive potential to alleviate many of the discussed challenges in this thesis. More research in this direction is therefore one of the key solutions to stable and secure operation of future power systems.

- *Development of more advanced and computationally efficient IBR, DER, and load models, as well as their easy parametrization and usage in real systems.*

All models are wrong, but some are useful³. A stability evaluation is only as good as its underlying models and data. As complexity in power systems increases, the number of grid elements with numerous control parameters increases accordingly. Since these parameters are often proprietary and subjected to a dose of uncertainty, suitable aggregated models with sufficient dynamic fidelity will be in high demand. Developing such models for utilization in large-scale stability studies is a fine balancing act of fidelity and complexity, requiring more research and development.

³An aphorism typically attributed to George Box, a British statistician.

- *AI and ML approaches for automated probabilistic grid vulnerability evaluation.*

The huge potential of AI in various fields is slowly becoming clear. The intersection of AI and power systems presents a large opportunity for mitigating some of the complexity issues expected in the future. However, a big challenge remains in designing trustworthy AI algorithms to be reliably utilized in controlling critical infrastructure within power systems. The first step for successful utilization of AI in power systems is therefore likely in offline analysis and online monitoring, with a focus on probabilistic rather than deterministic methods that provide support in decision-making. Furthermore, the underlying physics of power systems should be sufficiently represented in AI/ML methods to ensure applicability. All of these challenges are interesting future work considerations.

- *Frequency stability and resilience of low-inertia grids.*

While this thesis dominantly focuses on system strength and voltage stability, the power system evolution brings another major challenge as well: reduced inertia and frequency resilience. Ensuring frequency stability, therefore, also becomes more complex, where novel and more advanced system defence methods will be required. This also remains a very important topic for further research.

Lastly, I will end my thesis with a few general thoughts. Over the years of my PhD journey, I have been repeatedly amazed by how fast the research progresses. We are witnessing an exponential rise in high-quality research in the field of power systems worldwide. I see this as a clear sign that innovation plays a key role in overcoming the challenges I address in my thesis, but also as a sign that any problem humanity faces can be overcome by our combined efforts. We should therefore remain open to new ideas and cooperation across countries and cultures, and channel our combined efforts into resolving the technical challenges and mitigating the effects of climate change in time.

As I write this, 2023 is passing by, and global temperatures have already risen by approximately 1.2 °C on average, with significantly higher local increases in some parts of the world. Natural catastrophes have also started to emerge more frequently and with more impact, with extremes that surprise even the scientists who study this. Meanwhile, the greenhouse gas emissions are still **rising** (!), albeit in a decelerating tempo. Furthermore, as geopolitical tensions are increasing, sustainability trends face significant socio-economic and political frictions that threaten to slow down the energy transition. The challenges are enormous, and strong global cooperation is vital.

European Union strives to be climate-neutral by 2050. This implies that the electricity sector should be emissions-free by as early as 2035. Consequently, we only have about a decade left. Integration of renewables and phase-out of fossil-fuel generation must therefore continue with an even higher tempo. This will not be easy, as reliable grids with very high penetrations of renewables are technically challenging to achieve, as discussed in this thesis. Integration of renewables has been relatively easy while the grids were strong. The main challenges arise when we cannot fall back to the inherent grid's robustness and strength, but must design our system and its components to actively contribute to it. I foresee this as the key technical challenge to be overcome, and I truly hope my work has helped in this direction, and perhaps motivated you, the reader, to contribute to this important and engaging topic as well.

The future, for which we really need to work, can still be ours.

A

IEEE TEST SYSTEM DESCRIPTION

The original system used in [Chapters 4 and 5](#) is shown in [Figure A.1](#), known as the IEEE Test Systems for Voltage Stability Analysis and Security Assessment. It is sometimes also referred to as the Nordic system.

The system consists of four main areas.

- “North”, with hydro generation and some demand,
- “Central”, with thermal generation and high demand,
- “Equiv.”, connected to the “North”, which includes a very simple equivalent of an external system,
- “South” with the thermal generation, loosely connected to the rest of the system.

The system has long 400 kV transmission lines, as well as a regional sub-transmission grid operating at 220 and 130 kV. Each area has a certain amount of generation and load, as listed in [Table A.1](#). It can be seen that the central area contains the most demand, while the bulk of the generation comes from the North. The system has two readily available operating points, A and B, of which A is primarily used in this thesis.

Table A.1.: Active power generation and load for operating point A.

Grid Area	Generated Power [MW]	Consumed Power [MW]
North	4628.5	1180.0
Central	2850.0	6190.0
South	1590.0	1390.0
Equiv.	2437.4	2300.0
Total	11505.0	11060.0

The system is therefore heavily loaded with large transfers from the North to the Central area. Secure system operation is limited by mainly angular and voltage stability, both of which are stressed in case of a loss of an important transmission corridor.

A

The original system is equipped with static loads with an exponential model as shown in Equation (A.1), where $\alpha = 1.0$ and $\beta = 2$.

$$P = P_0 \left(\frac{V}{V_0} \right)^\alpha ; \quad Q = Q_0 \left(\frac{V}{V_0} \right)^\beta \quad (\text{A.1})$$

Throughout the analysis in Chapters 4 and 5, these loads are replaced with more detailed models of modern distribution systems, characterized by complex dynamic load models and distributed energy resources. These details are provided in Appendix B and each section with numerical simulations, respectively.

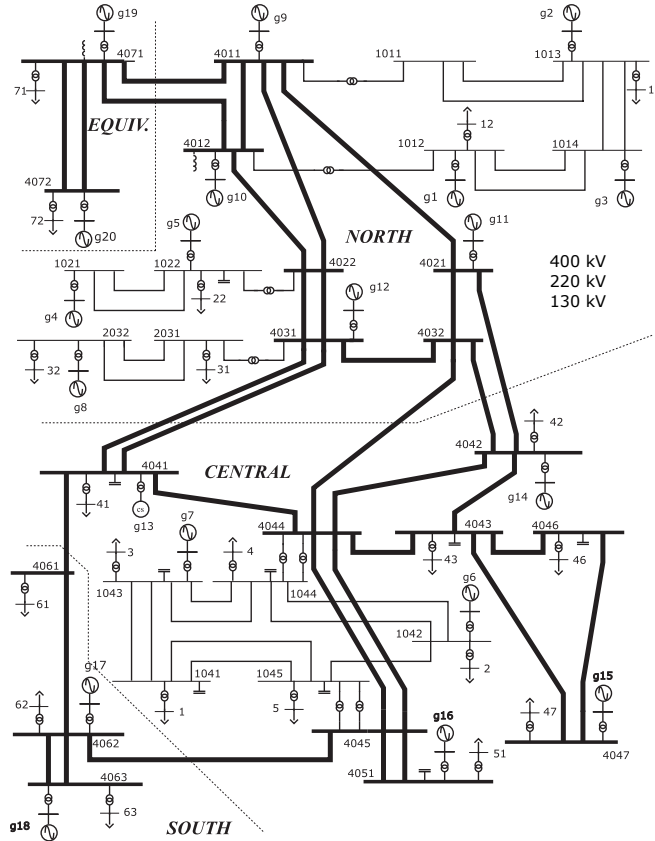


Figure A.1.: IEEE Test System for Voltage Stability Analysis and Security Assessment.

Further details about the system and its parameters, including the model itself in various software packages, can be found on the page of the IEEE Power System Dynamic Performance Committee (Link: <https://cmte.ieee.org/pes-psdp/489-2/>).

B

DER AND LOAD MODELS

DER-A MODEL

Distributed Energy Resources (DER) are modelled in this thesis by utilizing the DER-A model. Its diagram is shown once again in Figure B.1.

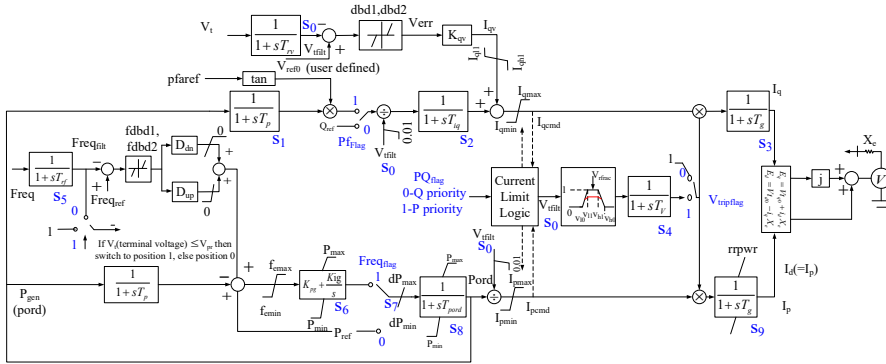


Figure B.1.: Diagram of the DER-A model.

To model four different DER control strategies utilized in Chapter 4, four sets of parameters are used. These are shown in Table B.1.

Table B.1.: DER parameters relevant for simulations in Chapter 4.

Parameter	Description	DER Disconnection	Ride-Through (P-priority)	Ride-Through (Q-priority)	Momentary Cessation
Δt	Trip time (post-fault)	0.05 s	N/A	N/A	N/A
v10	Voltage break-point	0.15	0.15	0.15	0.15
v11	Voltage break-point	0.9	0.9	0.9	0.8
tv10	Timer for v10	0.1 s	0.1 s	0.1 s	1.5 s
tv11	Timer for v11	1.5 s	1.5 s	1.5 s	0.5 s
Vtripflag	Enable voltage trip	0	0	0	1
Pqflag	P/Q-current priority	1	1	0	0

The other parameters and their values as used in this thesis (unless stated differently) are listed in [Table B.2](#). Next to the values, a short description is provided for each of the parameters, corresponding to their role in the model shown in [Figure B.1](#). More details can be found in the numerous references on the DER-A model provided in the main text of [Chapters 4 and 5](#).

Table B.2.: DER-A parameters used in this thesis.

Parameter	Description	Value
Trv	Transducer time constant (volt.) [s]	0.02
Vref0	Voltage ref. set point [pu]	-1
dbd1	Lower voltage deadband [pu]	-0.05
dbd2	Upper voltage deadband [pu]	0.05
Kqv	Prop. Volt. Control gain [pu/pu]	5
Tp	Transducer time constant (power) [s]	0.02
PfFlag	Freq. control flag	1
Tiq	Q control time constant [s]	0.02
Trf	Transducer time constant (freq.) [s]	0.1
Freqflag	Freq. control flag	1
Ddn	Freq. droop gain (down-side) [pu/pu]	20
Dup	Freq. droop gain (up-side) [pu/pu]	0
fdbd1	Lower freq. control deadband [pu]	-0.004
fdbd2	Upper freq. control deadband [pu]	0.004
Kpg	Active power control prop. gain [pu]	0.1
Kiq	Active power control integral gain [up]	10
Tpord	Power order time constant [s]	0.02
Imax	Max. converter current [pu]	1.2
Tg	Current control time constant [s]	0.02
vh0	Voltage break-point for HV cut-out [pu]	2
vh1	Voltage break-point for HV cut-out [pu]	1.1
tvh0	Timer for HV break-point (vh0) [s]	0.1
tvh1	Timer for HV break-point (vh1) [s]	1.5
Vfrac	Fraction of units that recovers (0..1)	0.7
Tv Time	Constant-output volt. cut-out [s]	0.02
Ftripflag	Frequency tripping	1
fl	Freq. break-point for low freq. cut-out [Hz]	47.5
fh	Freq. break-point for high freq. cut out [Hz]	51.5
tfl	Timer for low freq. break-point (fl) [s]	0.3
tfh	Timer for high freq. break-point (fh) [s]	0.3
Vpr	Min. volt. To disable freq. tripping [pu]	0.8
Iql1	Min. limit of reactive current injection [pu]	-1
femin	Frequency control min. error [pu]	-99
Pmin	Minimum power [pu]	0
dPmin	Min. power ramp rate (down) [pu/s]	-0.5
Iqh1	Max. limit of reactive current injection [pu]	1
femax	Frequency control max. error [pu]	99
Pmax	Max. power [pu]	1.1
dPmax	Max. power ramp rate (up) [pu/s]	0.5
rrpwr	Max. power rise ramp post fault [pu/s]	0.5

WECC COMPOSITE DYNAMIC LOAD MODEL

Complex dynamic loads are modelled in this thesis by using the WECC Composite Load Model. Its high-level diagram is shown in Figure B.2.

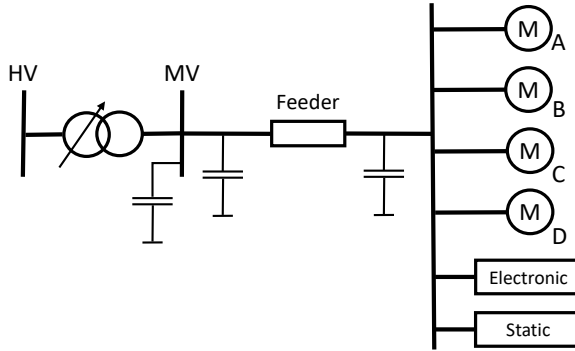


Figure B.2.: WECC Composite Load Model.

In this model, motors A, B, and C are used to represent different types of three-phase motors typically seen in power systems. Motor A represents the performance of three-phase induction motors with low-inertia driving constant torque loads, such as air conditioning compressor motors, refrigerators, and positive displacement pumps. Motor B represents the three-phase induction motors with high-inertia driving variable torque loads such as commercial ventilation fans and air handling systems. Motor C represents the three-phase induction motors with low-inertia driving variable torque loads such as the common centrifugal pumps.

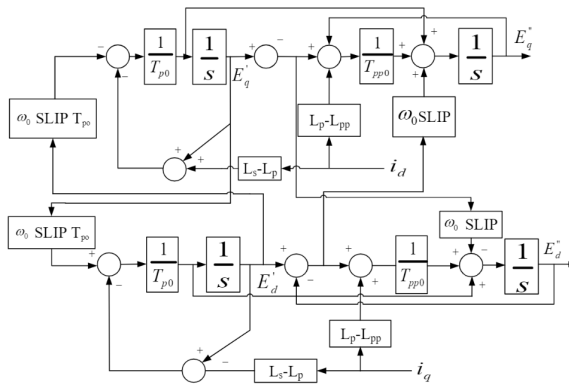


Figure B.3.: The shared schematic of three-phase motors.

These three-phase motors share the same model structure. However, their model parameters are different. Therefore, a fifth-order induction motor model is adopted to represent three-phase motors in WECC CLM. Its block diagram is shown in Figure B.3.

Motor D in Figure B.2 represents a performance-based model of a single-phase motor, designed to capture the behavior of residential A/C units. The model is developed experimentally based on extensive laboratory testing of a large number of A/C units and is intended to represent a composite of many individual single-phase A/C compressors and their protective devices. Its scheme is shown in Figure B.4.

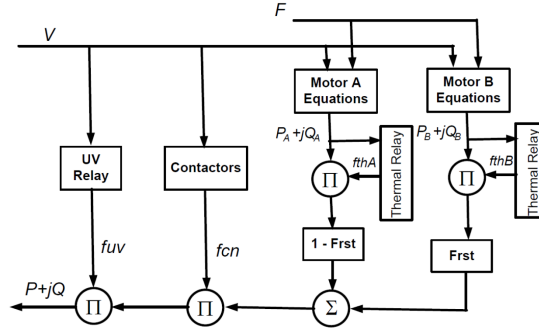


Figure B.4.: Single-phase A/C performance-based model scheme.

Besides the dynamic motor models, which are most relevant for this thesis, the WECC model also contains electronic and static loads, as well as models of a typical distribution feeder and transformer. The details of these are omitted here for brevity and can be found in the references in the main text of Chapter 4.

The dynamic load parameters used in this thesis are introduced in each respective section. The parameters that are not explicitly mentioned are kept at their default values from the WECC Load model in DlgSILENT PowerFactory 2020 SP2A.

OTHER PARAMETERS USED IN CHAPTER 5

Chapter 5 utilizes DER-A and WECC models in the IEEE test system to exemplify novel numerical methods. The relevant models and non-default parameters for 11 fault scenarios per case are listed in Table B.3. Other information can be found in the main text.

Table B.3.: Parameters relevant for simulations in Chapter 5. ($\Delta t_f = [100 - 400]$ ms)

Figure	Load	LV-DER	MV-DER
5.18.	$F_{md} = 0.33, V_{st} = 0.5,$ $T_{st} = 0.1, T_{th} = 10$	-	-
5.20.	Default values	$P = 600, V_{fr} = [1 - 0]$	$P = 200, V_{l0} = 0.5, t_{v/l0} = 0.33$
5.23a.	Default values	$P = 100$	-
5.23b.	Default values	-	$P_{1,2} = 300, V_{(l0)1,2} = 0.5$ $t_{(v/l0)1,2} = 0.325/0.2$
5.23c.	$P_1 = [720 - 144], P_2 = 720 - P_1,$ $F_{md} = 0.3, V_{(st)1/2} = 0.2/0.7,$ $T_{(st)1/2} = 0.5/0.2, T_{(th)1/2} = 10/20$	$P = 500, V_{l0} = 0.6,$ $t_{v/l0} = 0.4, V_{l1} = 0.9,$ $t_{v/l1} = 0.4, V_{fr} = [1-0.5]$	-

LIST OF ABBREVIATIONS

Abbreviation	Explanation
AC	Alternating Current
ADN	Active Distribution Network
AEMO	Australian Energy Market Operator
AFL	Available Fault Level
AI	Artificial Intelligence
API	Application Programming Interface
AU	Australia
A/C	Air Conditioning
CE	Central Europe
CIGRE	Conseil International des Grands Réseaux Electriques
CSCR	Composite Short-Circuit Ratio
CSI	Contingency Severity Index
CSII	Converter-driven Slow-Interactions Instability
CVD	Cumulative Voltage Deviation
DC	Direct Current
DDM	Data-Driven Methods
DER	Distributed Energy Resource
DFT	Discrete Fourier Transform
DG	Distributed Generation
DSO	Distribution System Operator
EMT	Electromagnetic Transient
EqSCR	Equivalent Short-Circuit Ratio
ERCOT	Electric Reliability Council of Texas
ESCR	Effective Short-Circuit Ratio
ESD	Energy Spectral Density
ESS	Excess System Strength
FACTS	Flexible AC Transmission Systems
FIDVR	Fault-Induced Delayed Voltage Recovery
FRT	Fault-Ride Through
GB	Great Britain
HI	Hawaii
HV/MV/LV	High/Medium/Low Voltage
IBR	Inverter-Based Resource
IEA	International Energy Agency
IEEE	Institute of Electrical and Electronics Engineers
IPCC	Intergovernmental Panel on Climate Change
IR	Ireland
LE	Lyapunov Exponent

Abbreviation	Explanation
LOWESS	Locally Weighted Scatterplot Smoothing
LT	Long-Term
LVRT	Low-Voltage Ride-Through
ML	Machine Learning
MPT	Maximum Power Transfer
PDN	Passive Distribution System
PER	Power Electronics Ratio
PFM	Peak Frequency Magnitude
PFL	Proxy Fault Level
PLL	Phase-Locked Loop
PMU	Phasor Measurement Unit
PoC	Point of Connection
PV	PhotoVoltaic
ReSident	Resilient Synchroreasurement-based Grid Protection Platform
RMS	Root Mean Square
RoCoF	Rate of Change of Frequency
SC	Synchronous Condenser
SCADA	Supervisory Control and Data Acquisition
SCC	Short-Circuit Capacity
SCR	Short-Circuit Ratio
SCRIF	Short-Circuit Ratio with Interaction Factors
SDSCR	Site-Dependent Short-Circuit Ratio
SFL	Synchronous Fault Level
SG	Synchronous Generator
SNSP	System Non-Synchronous Penetration
SS	System Strength
ST	Short-Term
STATCOM	Static Synchronous Compensator
STVI	Short-Term Voltage Instability
SVC	Static VAR Compensator
TN/FN	True/False Negative
TP/FP	True/False Positive
TRAI	Transient Rotor Angle Instability
TSO	Transmission System Operator
TVDI	Transient Voltage Deviation Index
TVI	Trajectory Violation Integral
TVSI	Transient Voltage Severity Index
TX	Texas
VVC	Voltage Vulnerability Curves
VIP	Voltage Instability Predictor
VRT	Voltage Ride-Through
VSRI	Voltage Stability Risk Index
WAMPAC	Wide-Area Monitoring Protection And Control
WAMS	Wide-Area Measurement System
WECC	Western Electricity Coordinating Council
WP	Work Package
WSCR	Weighted Short-Circuit Ratio

LIST OF PUBLICATIONS

PEER-REVIEWED JOURNAL ARTICLES:

1. **A. Boričić**, J. L. R. Torres, and M. Popov. “Quantification and Classification of Short-term Instability Voltage Deviations”. In: *IEEE Transactions on Industry Applications* (2023), pp. 1–11. ISSN: 0093-9994. DOI: 10.1109/TIA.2023.3289931.
2. **A. Boričić**, J. L. R. Torres, and M. Popov. “Fundamental study on the influence of dynamic load and distributed energy resources on power system short-term voltage stability”. In: *International Journal of Electrical Power and Energy Systems* 131 (Oct. 2021), p. 107141. ISSN: 01420615. DOI: 10.1016/j.ijepes.2021.107141.
3. **A. Boričić**, J. L. R. Torres, and M. Popov. “Comprehensive Review of Short-Term Voltage Stability Evaluation Methods in Modern Power Systems”. In: *Energies* 14.14 (July 2021), p. 4076. ISSN: 1996-1073. DOI: 10.3390/en14144076.
4. **A. Boričić** and M. Popov. “Voltage Vulnerability Curves: Data-Driven Dynamic Security Assessment Method for Evaluating Instability Risks and System Strength”. [submission in process]

PEER-REVIEWED CONFERENCE ARTICLES:

1. **A. Boričić**, J. L. R. Torres, and M. Popov. “Beyond SCR in Weak Grids: Analytical Evaluation of Voltage Stability and Excess System Strength”. In: *2023 International Conference on Future Energy Solutions (FES)*. Vaasa, Finland. IEEE, June 2023, pp. 1–6. ISBN: 979-8-3503-3230-8. DOI: 10.1109/FES57669.2023.10183286.
2. **A. Boričić**, J. L. R. Torres, and M. Popov. “System Strength: Classification, Evaluation Methods, and Emerging Challenges in IBR-dominated Grids”. In: *2022 IEEE PES Innovative Smart Grid Technologies (ISGT-Asia)*. Singapore. Nov. 2022, pp. 185–189. ISBN: 979-8-3503-9966-0. DOI: 10.1109/ISGTAsia54193.2022.10003499.
3. **A. Boričić**, J. L. R. Torres, and M. Popov. “Quantifying the Severity of Short-term Instability Voltage Deviations”. In: *2022 International Conference on Smart Energy Systems and Technologies (SEST)*. Eindhoven, the Netherlands. IEEE, Sept. 2022, pp. 1–6. ISBN: 978-1-6654-0557-7. DOI: 10.1109/SEST53650.2022.9898503.
4. M. Popov, **A. Boričić**, N. Kumar, et al. “Synchrophasor-based Applications to Enhance Electrical System Performance in the Netherlands”. In: *CIGRE proceedings*. Paris, France. CIGRE, Aug. 2022. Rep: e-cigre.org/publication/c2-10550_2022.
5. **A. Boričić**, J. L. Rueda Torres, and M. Popov. “Impact of Modelling Assumptions on the Voltage Stability Assessment of Active Distribution Grids”. In: *2020 IEEE PES*

Innovative Smart Grid Technologies (ISGT-Europe). The Hague, the Netherlands. IEEE, Oct. 2020, pp. 1040–1044. DOI: 10.1109/ISGT-Europe47291.2020.9248764.

TECHNICAL REPORTS, BOOK CHAPTERS, AND OTHER:

1. IEEE/CIGRE C4-C2 Joint Working Group Technical Brochure, "Evaluation of Voltage Stability Assessment Methodologies in Transmission Systems" (TR 109). URL: resourcecenter.ieee-pes.org/publications/technical-reports/PES_TP_TR109_PSDP_52223.
2. M. Popov, **A. Boričić**, N. Kumar, et al. "Improving Power System Resilience with Enhanced Monitoring, Control, and Protection Algorithms", Commit2Data Research and Innovation Programme [under review].

MASTER THESES SUPERVISED DURING THE PHD:

1. P. Buckley. "Improving Load Shedding Schemes for Critical System Conditions" (*Master Thesis*) mentors: **A. Boričić**, M. Popov. TU Delft, Aug. 2023, Repository Link: <http://resolver.tudelft.nl/uuid:3ef30f70-f533-4f41-b47f-5af4b2499221>.

OTHER PUBLICATIONS NOT INCLUDED IN THE THESIS:

1. P. Palensky, J. L. Rueda, P. P. Vergara, **A. Boričić**, et al. "Oplossingsrichtingen voor congestie in middenspanningsnetten: de casus Buiksloterham-Zuid/Overhoeks Amsterdam". Tech. rep. Amsterdam, the Netherlands: AMS Institute for Advanced Metropolitan Solutions, Mar. 2022. DOI: [dx.doi.org/10.13140/RG.2.2.11476.68481](https://doi.org/10.13140/RG.2.2.11476.68481).
2. **A. Boričić**, J. Wang, Y. Li, S. Zubic, and N. Johansson. "Impact on Power System Protection by a Large Penetration of Renewable Energy Sources". In: *18th Wind Integration Workshop*. Dublin, Ireland, Oct. 2019.
3. **A. Boričić**, P. Westerlund, and D. Bhatt. "Reliability and Cost-Effectiveness Analysis of Various HV Substation Configurations". In: *14e congrès annuel de CIGRE Canada*. Montréal, Québec, Canada, Sept. 2019.
4. **A. Boričić**. "Impact on Power System Protection by a Large Penetration of Renewable Energy Sources" (*Master Thesis*). TU Eindhoven and KTH Royal Institute of Technology, Aug. 2019. DOI: [dx.doi.org/10.13140/RG.2.2.10226.58561](https://doi.org/10.13140/RG.2.2.10226.58561).
5. **A. Boričić**, D. Laban, B. Moedim, A. C. Lopez, B. Molinari, Z. Riaz, and R. Nikjoo. "Dynamic Resistance Measurements and Result Interpretation for Various On-Load Tap Changers". In: *2019 IEEE Milan PowerTech*, Italy. IEEE, June 2019, pp. 1–6. ISBN: 978-1-5386-4722-6. DOI: 10.1109/PTC.2019.8810530.
6. **A. Boričić**. "Enhancement Possibilities of Power System Transient Angle Stability by using UPFC" (*Specialization Thesis*). University of Montenegro, 2017. DOI: [dx.doi.org/10.13140/RG.2.2.10113.53606](https://doi.org/10.13140/RG.2.2.10113.53606).

ACKNOWLEDGEMENTS

The four years of my doctorate research path have been a truly life-changing experience. I have grown not only professionally, but also personally in many different ways. One of them is the realization of just how complex the world we live in is. We often take things for granted, but in reality, there is a complex and fascinating background to many everyday aspects of life. Being able to profoundly understand one of them, namely electricity, and work on improving and decarbonizing electric power systems, has been both intellectually challenging and enjoyable on so many levels.

The other experience I would like to mention is the opportunity to meet and cooperate with people from all around the world. This broadened my perspectives of the world and the amazing people that can be found in every corner of it. Moreover, it helped me grow to be a better person, and for that, I am very grateful.

None of this, however, would have been possible without the support of numerous people around me. I would hereby like to thank some of them, and apologize to others who I had no opportunity to mention here by name.

First and foremost, I would like to express my sincere and deepest gratitude to my promotor, prof. dr. ir. Marjan Popov. Since the very moment we first met, his support was simply extraordinary. Not only did he selflessly guide me through the complexities of scientific research, but he also showed great care for my well-being and success. People sometimes say that you should choose your boss, not your job. I was fortunate enough to work on an exciting research topic, but I was even more lucky to have a person like Marjan to guide me through it. I thank you, Marjan, for all the great moments and inspiring conversations we had over the past years. I am sure this is only the beginning of our long-term cooperation and friendship.

I would also like to wholeheartedly thank em. prof. ir. Mart van der Meijden, who strongly supported me on this journey. Mart has the unique ability to explain both the fine details and the bigger picture, which made the conversations we had intellectually stimulating and enjoyable. Furthermore, his genuine care and interest in people and their work are something we should all aspire to. I also wish to thank dr. Jose L. R. Torres for his support, particularly during the early stage of my research.

My sincere gratitude also goes to the members of my doctoral examination committee, for the effort and time spent reviewing my research and providing invaluable feedback. This helped me improve my thesis further, and it has been a pleasure to have such distinguished experts present at my defense in Delft.

Furthermore, my research would not be as nearly as impactful and relevant if it weren't for the significant support from the industry project committee members. My particular gratitude goes to Jorrit Bos (TenneT), Danny Klaar (TenneT), Jacques van Ammers (GE), Maarten van Riet (Alliander), Ernst Wierenga (Stedin/DNV), Arjen Jongepier (Stedin), Helko van den Brom (VSL), and others involved in the project. Their expertise and

guidance throughout my research term were extremely helpful, and I enjoyed the engaging technical discussions we've had over the years. Additionally, I would like to thank their respective organizations and the Dutch Research Council (NWO) for supporting and funding this project, allowing me to research this timely and interesting topic.

From TU Delft, I would also like to thank prof. dr. Peter Palensky for his vision and leadership of the Intelligent Electrical Power Grids (IEPG) group, as well as for the friendly work atmosphere he encouraged. I always felt welcome to stop by his office for a chat or anything I needed. We also had the opportunity to perform interesting and practical work on grid congestions in Amsterdam, together with Aihui and Pedro, which was a lot of fun! Furthermore, I owe a big thank you to TU Delft/IEPG secretaries Ellen, Sharmila, and Carla, without whom everything stops at our department.

The colleagues I cooperated and shared the office with also deserve a special mention: Matija, Ilya, Arcadio, and later Shengren, Farzad, Mojtaba, and Wouter. Thank you, guys, for the great company, always positive spirits and many fun and memorable conversations and moments. Furthermore, many thanks to my other numerous TU Delft and IEPG colleagues and friends who made my time at the university enjoyable.

Studying and working abroad means one must leave some people behind. However, the distance says nothing about how close you are to someone. I want to thank some of my best friends from Montenegro - Amar, Milena, Uroš, and Luka, for being true friends for many years. Whenever we meet, it feels like I never left. I also wish to thank my international friends from my master's studies in Sweden and the Netherlands, with whom I shared many noteworthy moments and travels.

I consider myself fortunate to have a very warm "schoonfamilie", who make me feel welcome in the Netherlands. Thank you, Ingrid, Jan, and Adriaan.

My family remains in Montenegro, and I wish to tell them a few words in my native language. *Mojim roditeljima, Vesni i Vesku, i mom bratu, Miloradu, želim da se zahvalim na neiscrpnoj podršci i svemu sto su me naučili. Uvijek ste bili tu za mene, vjerovali u mene, i nesebično me motivisali da idem naprijed, gdje god u svijetu to bilo. Neka vas ovo veliko dostignuće u mojoj karijeri i životu učini ponosnim, jer bez vas ne bi bilo moguće!*

Last but surely not least, I want to thank my dear girlfriend, partner, and love, Sylvie, for being by my side throughout all this. Your warm love and endless support fill me with joy and give me motivation and energy to go forward. There is nobody in this world with whom I want to share the happy moments more than with you.

Aleksandar Boričić
Delft, April 2024

BIOGRAPHY



Aleksandar Boričić was born on the 10th of July 1994 in Podgorica, Montenegro. He received his Dipl.Ing. in electrical power engineering from the University of Montenegro in 2017, specializing in power system stability. He further received his double master's degree from the KTH Royal Institute of Technology in Stockholm and the Eindhoven University of Technology in 2019, within the EIT programme Smart Electrical Networks and Systems. He completed his thesis research externally at ABB Corporate Research Center in Sweden, on the topic of power system protection of wind farm connections. Aleksandar temporarily worked for the TSO of Montenegro (CGES), as well as for DNV in the Netherlands. From 2019 to 2023, he was a Ph.D. researcher at the Delft University of Technology, Intelligent Electrical Power Grids group, with main research interest in power system dynamics, stability, system strength, and WAMPAC. He is an active IEEE (PES) and CIGRE member and CIGRE Next Generation Network ambassador and has actively contributed to the IEEE/CIGRE C4/C2.58 Joint Working Group on Evaluation of Voltage Stability Assessment Methodologies in Transmission Systems. In 2023, after completing his Ph.D. research, Aleksandar joined TenneT TSO B.V. in the Netherlands in the role of a Future Grids Operation Developer within the System Operations Development department, as an expert on grid stability, dynamics, and WAMPAC. At TenneT, he will continue to support the energy transition from the perspective of the Dutch and European electric power systems.